ROLE OF THE GPR55 RECEPTOR IN THE MODULATION OF JOINT AFFERENT MECHANOSENSITIVITY

KENNETH A. PATON, BSc. MRes

Thesis submitted to the University of Nottingham

for the degree of Doctor of Philosophy

September 2014

Abstract

Deep somatic pain originating from synovial joints is a major clinical problem as it is the primary reason for loss of joint mobility and function in musculoskeletal disorders. Musculoskeletal disorders, including osteoarthritis (OA), are the most prevalent cause of disability worldwide with an estimated 1 in 3 adults affected. Current therapies for the treatment of joint pain have limited effectiveness and certain drugs produce unwanted side effects, preventing their long-term use. Targeting pain at the level of the joint may have the potential to maximise treatment efficacy, whilst reducing possible non-specific side effects associated with systemic drug treatment. Identification of novel analgesic targets that inhibit peripheral mechanical sensitization during joint pain states will be critical to the development of improved analgesics for these conditions. Based on recent preclinical findings, the orphan G protein-coupled receptor GPR55 has controversially been suggested to be the novel third cannabinoid receptor and has been identified as a potential novel target for the treatment of pain. Very few studies have investigated the effects of GPR55 receptor activation on nociceptive processing in vivo and only one at the level of the joint during acute inflammatory arthritis. The aim of this thesis was to investigate the role of GPR55 in the modulation of joint afferent mechanosensitivity in vivo, and whether this role is altered in an experimental model of OA during established pain.

Electrophysiological recordings of joint afferent nociceptors, taken from the saphenous nerve, which innervates the knee joint via the medial articular nerve,

were carried out in anaesthetised rats under non-pathological conditions (naïve rats) and in a model of OA following the development of pain behaviour, 14 days following knee joint injection of monosodium iodoacetate (MIA) and compared to saline control rats. Effects of peripheral administration of the putative endogenous GPR55 agonist L-α-lysophosphatidylinositol (LPI) on the mechanically-evoked responses of joint nociceptors were studied in naïve rats and in MIA and saline rats. An involvement of GPR55 in the effects of LPI was investigated using pre-administration of the GPR55 receptor antagonist cannabidiol. Further, the role of GPR55 in endogenously modulating joint afferent mechanosensitivity was investigated following the peripheral administration of cannabidiol alone. GPR55 receptor expression in knee innervating L3-L5 rat DRGs was studied by immunohistochemistry.

Joint nociceptors in MIA rats were mechanically sensitized compared to the saline rats at 14 days post-injection confirming the development of peripheral sensitization during established pain behaviour. LPI (150, 250μM) inhibited joint nociceptor mechanically-evoked responses in naïve and saline rats and inhibited peripheral sensitization in MIA rats. Cannabidiol blocked the LPI-induced inhibition of joint nociceptor mechanosensitivity in all groups of rats confirming an involvement of GPR55 in these effects. Cannabidiol alone had no effect on mechanically-evoked responses of joint nociceptors in naïve, saline and MIA rats indicating that any endogenous GPR55 tone does not modulate joint afferent mechanosensitivity. GPR55 receptor expression was detected in small, medium and large neurones (and possibly satellite glial cells) of L3-L5 DRG.

The findings of this thesis provide compelling evidence that activation of the GPR55 receptor in vivo modulates the mechanosensitivity of joint afferent nociceptors and this inhibitory effect is maintained during established peripheral sensitization and pain behaviour following OA development. GPR55 receptor-mediated control of joint afferent mechanosensitivity during established OA pain and expression of GPR55 in sensory neurones at the level innervating the joint highlights GPR55 as a potential new peripheral target for the modulation of joint pain including during OA. The findings of this thesis support further studies aimed at investigating the clinical utility of GPR55 agonists for the treatment of OA pain.

Publications

- Paton, K, Harris, J, Kelly, S. The GPR55 agonist L-α-lysophophatidylinositol attenuated knee afferent mechanosensitivity in the monosodium iodoacetate model of osteoarthritis pain. In preparation for submission to Osteoarthritis and Cartilage.

Abstracts and poster presentations

- Paton, K, Harris, J, Kelly, S. The GPR55 agonist L-α-lysophophatidylinositol attenuated knee afferent mechanosensitivity in the monosodium iodoacetate model of osteoarthritis pain. 8th Congress of the European Federation of IASP Chapters, Florence, Italy, 2013.

- Paton, K, Harris, J, Kelly, S. Cannabidiol blocks the inhibitory effect of the GPR55 agonist L-α-lysophosphatidylinositol on mechanosensitive knee joint afferents. British Society for Rheumatology, Glasgow, UK, 2012. Oral abstract: Volume 51, supplement 3, S4.

Acknowledgements

I would like to thank my supervisors Dr Sara Kelly and Dr John Harris for their support and guidance throughout my PhD they have always provided a motivation and balance without which this project would not have been possible. In particular, I would like to thank them for their patience and understanding.

I would like to acknowledge the BBSRC and the University of Nottingham for funding my studies, Dr Gareth Hathway for the use of his lab for GPR55 immunohistochemistry experiments and his PhD student Charlie Kwok for her advice and assistance in optimising this protocol.

I would also like to thank my parents for their understanding and encouragement for my decision to move away from Glasgow to further my career in particular I am grateful for the emotional and financial assistance throughout my studies.

Finally, I am forever indebted to my wife Jamie for her love, unconditional support and patience over the last few years and particularly during the preparation of this thesis.

Table of contents **Page No.**

Chapter 3

Chapter 6

List of Figures **Page No.**

List of Tables **Page No.**

List of Abbreviations

ABC avidin-biotin complex	**CGRP** calcitonin gene-related peptide
abn-CBD abnormal cannabidiol	**CNS** central nervous system
ACEA N-arachidonoyl-phosphatidylethanolamide	**CV** conduction velocity
ACLT anterior cruciate ligament transection	**DAG** diacylglycerol
2-AG 2-arachidonylglycerol	**DRG** dorsal root ganglia
AMPA alpha-3-hydroxy-5-methyl-4- isoxazolepropionic acid	**EDTA** ethylenediaminetetracetic acid
AP action potential	**ERK** extracellular regulated kinase
ASPA Animal Scientific Procedures Act	**EULAR** European League Against Rheumatism
ATF activating transcription factor	**FAAH** fatty acid amide hydrolase
ATP adenosine triphosphate	**FG** fluorogold
BK bradykinin	**GABA** γ-aminobutyric acid
BML bone marrow lesion	**GDNF** glial derived neurotrophic factor
cAMP cyclic adenosine monophosphate	**GPCR** G protein-coupled receptor
Ca_v voltage-gated calcium channel	**HRP** hydrogen peroxidase
$CB_{1/2}$ cannabinoid receptor type 1/2	**IASP** International Association for the Study of Pain
CCI chronic constriction injury	**IB4** isolectin B4
	IFN-γ interferon-γ
	IL interleukin
	KCl potassium chloride

LAN lateral articular nerve

LASA Laboratory Animal Science Association

LPI L-α-lysophophatidylinositol

LTM low threshold mechanoreceptors

MAN medial articular nerve

MAPK mitogen activated protein kinase

MFC medial femoral condyle

MGL monoacylglycerol lipase

mGluR metabotropic glutamate receptor

MIA monosodium iodoacetate

MNX meniscal transection

MRI magnetic resonance imaging

MTP medial tibial plateaux

NF200 neurofilament 200

NAPE N-arachidonoyl-Phosphatidylethanolamine

NGF nerve growth factor

NICE National Institute for Health and Clinical Excellence

NSAIDs non-steroidal anti-inflammatory drugs

KS Kolgomorov Smirnov

K_v voltage-gated potassium channel

Na_v voltage-gated sodium channel

NK-1 neurokinin -1

NMDA N-methyl-D-aspartate

NS nociceptor specific

O_2 oxygen

OA osteoarthritis

OCT optimum cutting temperature

OD outer diameter

PAG periaqueductal grey

PAN posterior articular nerve

PARs protease activated receptors

PFA paraformaldehyde

PGE_2 prostaglandin E2

PKA protein kinase A

PKC protein kinase C

PLC phospholipase C

PLD phospholipase D

RVM rostral ventral medulla

SP substance P

STT spinothalamic tract

TASK TWIK-related acid sensitive potassium channel

Δ^9-THC tetrahydrocannabinol

TRAAK TWIK-related arachidonic-acid stimulated potassium channel **TREK-1** TWIK related potassium channel -1 **TRG** trigeminal root ganglia **trkA** tyrosine receptor kinase type A **TRPA1** transient receptor potential cation channel subfamily A member 1 **TRPC** transient receptor potential canonical	**TNF-α** tumour necrosis factor-α **TRPM8** transient receptor potential cation channel subfamily M member 8 **TRPV1** transient receptor potential vanilloid 1 **TTX** tetrodotoxin **VIP** vasoactive intestinal peptide **WDR** wide dynamic range

Chapter One

General Introduction

1.1. Introduction

Deep somatic pain originating in synovial joints is a major therapeutic challenge, with joint pain being the most prominent and disabling symptom of musculoskeletal disorders, such as osteoarthritis (OA) (Felson, 2005). Musculoskeletal disorders are the most frequent cause of disability in the modern world with the World Health Organisation estimating that 1 in 3 adults are affected (Brundtland, 2003, McDougall, 2006). The analgesics that are currently used to treat joint pain (non-steroidal anti-inflammatory drugs (NSAIDs), weak opioids) are only partially effective and are associated with serious side effects that limit their long term use (Schaible et al., 2006). In order to develop improved analgesics for joint pain, a greater understanding of the mechanisms driving and modulating joint pain is required.

The identification of mechanisms that inhibit peripheral sensitization during joint disease has the potential to lead to the development of treatments that may reduce pain (McDougall, 2006). Furthermore, targeting pain at the peripheral source i.e. at the level of the joint with, for example, intra-articular (i.a.) therapies, may have the potential to maximise treatment efficacy, whilst reducing possible non-specific side effects associated with systemic drug treatment (McDougall, 2011). The orphan G protein-coupled receptor (GPCR) GPR55 has been controversially proposed as a novel third cannabinoid receptor (Ryberg et al., 2007). It is well established that cannabinoids are analgesic acting at supraspinal, spinal and peripheral sites within the pain pathway (Pertwee, 2001) with studies identifying a potential role in the modulation of

joint pain in OA (Richardson et al., 2008, Schuelert and McDougall, 2008, Schuelert et al., 2010, Schuelert et al., 2011). Evidence from transgenic mouse (Staton et al., 2008) and pharmacological (Schuelert and McDougall, 2011, Breen et al., 2012, Gangadharan et al., 2013) studies indicate that GPR55 has a role in the modulation of nociception. These findings together with the demonstrated expression of GPR55 in sensory neurones of the dorsal root ganglia (DRG) (Lauckner et al., 2008) suggests that the receptor could be a potential novel peripheral analgesic target. However, studies investigating the role of the GPR55 receptor in nociception are few in number and almost nothing is known about the role of GPR55 in joint pain mechanisms. Activation of cannabinoid receptors is known to modulate nociception in animal models of knee OA (Sagar et al., 2010, Schuelert et al., 2010, La Porta et al., 2013) and peripheral administration of the putative GPR55 agonist O-1602 inhibits nociception in a model of acute inflammatory arthritis (Schuelert and McDougall, 2011), suggesting that further studies examining the role of GPR55 in the modulation of joint pain are worthwhile. The overall aim of this thesis was to examine whether GPR55 has a role in modulating the peripheral mechanisms driving joint pain and to investigate the clinical relevance of this role in an experimental model of knee OA. These studies will increase understanding of whether targeting GPR55 may have therapeutic potential for the alleviation of joint pain in man.

1.2. Pain

In 1994, the International Association for the Study of Pain (IASP) defined pain as ‘an unpleasant sensory and emotional experience associated with actual or potential tissue damage or described in terms of such damage’. Pain occurs in response to tissue injury due to a noxious stimulus that may be mechanical, thermal or chemical in nature (Julius and Basbaum, 2001, Loeser and Treede, 2008, McDougall, 2011). The resultant pain can be acute (short-lasting) or chronic (more prolonged) (McDougall, 2011). Acute pain is usually beneficial by warning the organism of actual or impending tissue damage allowing rapid, evasive, reflex action to be carried out while chronic pain tends to be a maladaptive response due to underlying pathology (McDougall, 2011). Pain is defined as chronic if present unabated beyond approximately 3 months and if occurring after tissue healing or in the absence of tissue damage (McDougall, 2011). Symptoms of chronic pain can be defined as: hyperalgesia, allodynia and spontaneous pain (Kidd and Urban, 2001, Loeser and Treede, 2008). Hyperalgesia is defined as elevated pain response elicited by a noxious stimulus while allodynia is defined as pain produced by a previously innocuous stimulus (Kidd and Urban, 2001, Loeser and Treede, 2008). In addition, spontaneous pain is pain that occurs in the absence of any obvious precipitating external stimulus (Kidd and Urban, 2001).

1.3. Primary afferent neurones

Nociception is defined as ‘the neural processes encoding and processing noxious stimuli’ (Loeser and Treede, 2008). As such, pain is a subjective

experience, while nociception describes sensory physiology. Nociceptive transmission can be broadly separated into two phases: (1) noxious stimuli activating peripheral nociceptive primary afferent neurones and (2) afferent input generating pain sensation via the central nervous system (CNS) (Kidd and Urban, 2001, McDougall, 2011). Primary afferent neurones, which have cell bodies (soma) in the DRG, project to and innervate peripheral tissues, including skin, viscera, muscle and joints (Lawson, 2005). A single process, called the initial segment, leaves the soma of pseudo-unipolar primary afferent neurones. Following T junction branching, the initial segment projects peripherally and centrally (Lawson, 2005). Primary afferent neurones function to detect nociceptive or non-nociceptive stimuli that are mechanical, thermal or chemical in nature (Julius and Basbaum, 2001, Hucho and Levine, 2007, McGlone and Reilly, 2010, McDougall, 2011).

Primary afferent neurones are heterogeneous in that they have a range of conduction velocities (CVs), soma sizes, degrees of myelination, activation thresholds, adaptation rates and sensory receptive properties (see Table 1.1) (Lawson, 2005). Primary afferent neurones can be sub-classified according to their fibre CVs into Aαβ, Aδ and C fibres (Light, 1993, Djouhri and Lawson, 2004, Lawson, 2005). In studies using adult cats, the upper limit for Aδ and C fibre CVs are 30 m/s and 2.5m/s, respectively (Light, 1993). However, in adult rats, Aδ and C fibre CVs are 1-8m/s and <1m/s, respectively (Djouhri and Lawson, 2004). Aαβ fibres are classified as any fibre with a CV greater than the upper limit for Aδ fibres (i.e. 30m/s). Compound action potential recordings enable fibre CV boundaries to be defined (Light, 1993). It is

important to note that CV boundaries are influenced by age, species, temperature of the recording preparation, sensory nerve studied and the proximodistal position of the recording site as some fibres may conduct faster in the dorsal root compared to in the peripheral nerve (Light, 1993).

Primary afferent neurone CVs are related to cell size as well as degree of fibre myelination: large, fast conducting Aαβ fibres with cell soma sizes of 1142±366μm^2 are myelinated, Aδ fibres with medium sized cell somas of 702±488μm^2 are thinly myelinated and slowly conducting C fibres with small soma sizes of 449±148μm^2 are unmyelinated (Harper, 1985).

Several classes of primary afferent neurones have been defined:

(1) Low threshold mechanoreceptors (LTMs)

LTMs are the largest group of non-nociceptive afferents which innervate skin and skeletal muscle (Lawson, 2005).

(a) Cutaneous Aαβ fibre LTMs

Cutaneous Aαβ LTMs fibres can have slow or rapid adaptation rates and can have firing patterns that are either regular or irregular. The fibres detect stimuli of changing intensity and movement of mechanical stimuli (e.g. tap to the skin or rapid vibration) (Lawson, 2005).

(b) Cutaneous Aδ fibre LTMs

The majority of cutaneous Aδ LTMs project to hairy skin and are called 'D hair' units (Lawson, 2005). They are extremely sensitive to slow hair movement and additionally detect stretch and skin cooling (Light, 1993).

(c) Cutaneous C fibre LTMs

Cutaneous C fibre LTMs can be activated by extremely slow movements across the skin (Light, 1993), that are associated with pleasant sensations (Vallbo et al., 1993).

(2) Cutaneous thermoreceptors

In primates, cutaneous cooling and warming receptors have CVs in the C or Aδ fibre range (Light, 1993). A decrease in temperature below 30°C results in increased firing of cooling receptors (Davis and Pope, 2002) while warm receptors fire in the range 30 - 46°C (Light, 1993). The thermal threshold of C-fibre polymodal nociceptors is approximately 43°C and A-fibre mechanoheat unit threshold is greater than 53°C (Lawson, 2005).

(3) Nociceptors

(a) Cutaneous A-fibre nociceptors

Cutaneous A-fibre nociceptors are either activated by noxious mechanical stimuli or noxious mechanical and thermal stimuli (Lawson, 2005). This latter group of fibres are called mechanoheat sensitive units (Lawson, 2005). In primates, cutaneous A fibres respond differentially to noxious heat and are characterised as either type I or type II units (Treede et al., 1998). The type I units consist of two thirds Aδ fibres and one third Aβ fibres with a CV up to 60m/s while type II units consists of Aδ fibres only and have CVs less than 30m/s (Treede et al., 1998). Type I units have a higher heat threshold (53 vs 47°C) and a lower mechanical threshold compared to type II units (Treede et al., 1998). Further, type I units have a longer latency of response (5 vs 0.2 seconds) and later peak discharge (16 vs 0.2 seconds) compared to type II units (Treede et al., 1998).

Identification of A-fibre nociceptors with CVs greater than 30m/s has indicated some nociceptive fibres conduct in the Aβ range (Djouhri and Lawson, 2004). Studies have identified Aβ fibres detect noxious stimuli in a normal state and in a model of OA (Wu and Henry, 2010).

(b) Cutaneous C-fibre nociceptors

Cutaneous C fibre nociceptors are the most common sub-type of nociceptive primary afferent neurone (Lawson, 2005). Most of these fibres are activated by

noxious mechanical and thermal stimuli, and are named C-mechanoheat fibres (Light, 1993). C-fibres activated by noxious mechanical, thermal and chemical stimuli are named C-polymodal fibres (Light, 1993). However, a smaller proportion of fibres are selectively sensitive to noxious mechanical stimuli and are named C-fibre high-threshold mechanoreceptors (Lawson, 2005).

Polymodal C fibres nociceptors can be sub-classified as peptidergic or non-peptidergic based on peptide content and spinal cord dorsal horn termination patterns (Averill et al., 1995, Michaelis et al., 1996). Peptidergic nociceptors express calcitonin gene-related peptide (CGRP), substance P (SP) and tyrosine kinase receptor type-1 (trkA) while non-peptidergic nociceptors express isolectin B4 (IB4), the purinergic receptor $P2X_3$ and glial derived neurotrophic factor (GDNF) (Section 1.5.3).

(c) 'Silent' nociceptors

Inexcitable units, projecting to skin, joints (Schmidt, 1996) and visceral organs (Janig, 1996), have been identified and named silent nociceptors (Michaelis et al., 1996). These fibres only respond following repeated stimulation or by sub-threshold stimuli after acute tissue inflammation (Meyer et al., 1991, Michaelis et al., 1996). 'Silent' nociceptors could include very-high-threshold nociceptive fibres or units which inflammatory mediators released during tissue damage have excited or sensitised (Michaelis et al., 1996, Lawson, 2005).

Table 1.1. Properties of primary afferent fibres.

Fibre Type	Degree of Myelination	Cell size (µm)	CV (m/s)	Modalities
Aα	Myelinated	20	70-120	LTMs – proprioception, movement of mechanical stimuli (stroking, pressure)
Aβ	Myelinated	10	>15	LTMs - proprioception, movement of mechanical stimuli (stroking, pressure) Nociceptors
Aδ	Thinly myelinated	2.5	1-15	LTMs – slow hair movement and stretch Thermoreceptors – cooling (<30°C) and heat (>53°C) Nociceptors – polymodal, mechanoheat
C fibre	Unmyelinated	1	<1.0	LTMs – slow movement across skin, pleasant sensations Thermoreceptors - cooling (<30°C) and heat (>43°C) Nociceptors - polymodal, 'silent'

1.4. Joint Innervation

1.4.1. Innervation of joint structures and the relationship to pain

Detailed pain sensations in joints have been well characterised clinically for several decades, although understanding of articular innervation and the mechanisms of joint nociception are limited (Schaible and Grubb, 1993) as initial research focussed on cutaneous afferents (Schaible et al., 2009). Current understanding of the joint nociceptor system will be discussed separately below.

The main sensation that is evoked from the joint and other deep tissues is pain (Schaible and Grubb, 1993). The description of pain in the joint is in contrast to cutaneous pain in that it is often dull, aching and poorly localised (Lewis, 1938). Articular afferents are also important in the sense of movement and position (proprioception) (Skoglund, 1956, Proske et al., 1988, Schaible and Grubb, 1993).

Studies conducted in conscious human subjects that had not been injected with i.a. anaesthetic have defined the knee joint fibrous structures (ligaments, fibrous capsule) that evoke the sensation of pain when stimulated by noxious mechanical, thermal and chemical stimuli (see Figure 1.1) (Kellgren and Samuel, 1950, Schaible and Grubb, 1993, Dye et al., 1998). Mechanical stimulation of articular cartilage does not evoke the sensation of pain (Kellgren and Samuel, 1950, Dye et al., 1998). Therefore, the detection of knee joint pain

in response to noxious stimuli indicates that articular structures are innervated by nociceptors.

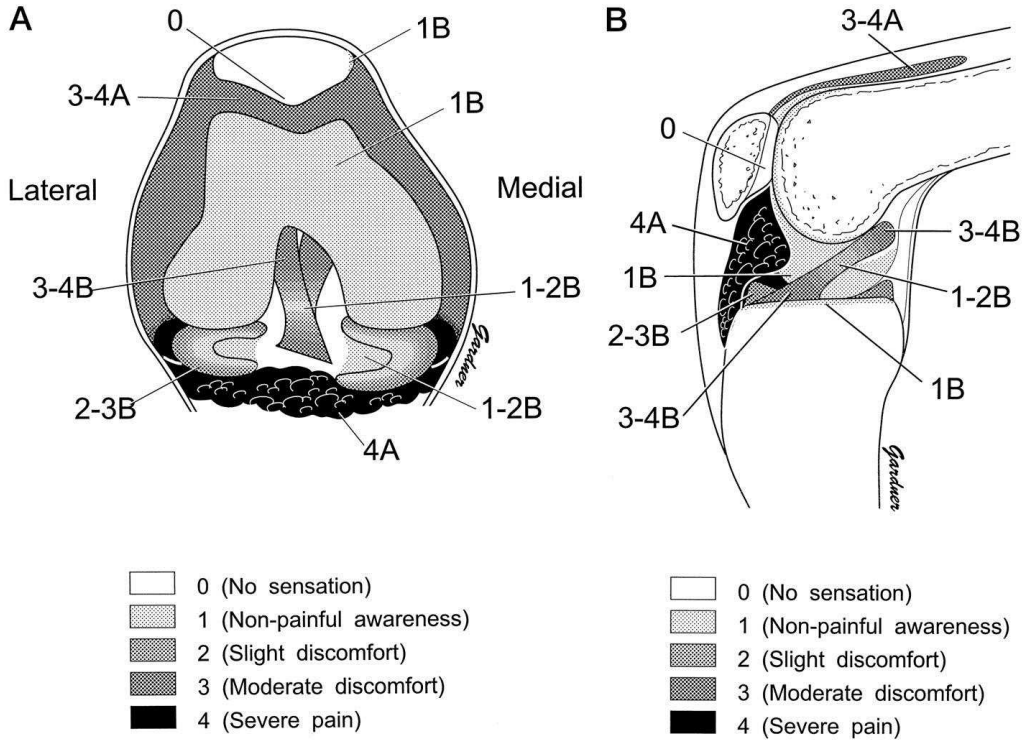

Figure 1.1. Conscious neurosensory findings of i.a. structures represented coronal (A) and sagittal (B). A: accurate spatial localisation, B: poorly localised sensation. Taken from (Dye et al., 1998).

1.4.2. Joint afferent anatomy

Joints are innervated by articular branches that descend from main nerve trunks or their muscular, cutaneous and periosteal branches (Schaible and Grubb, 1993). The primary articular nerves that innervate knee joint structures are the medial, lateral and posterior articular nerves (MAN, LAN, PAN). Knee joints in several species receive innervation from these articular nerves including, mice (Ebinger et al., 2001), rats (Hildebrand et al., 1991), dogs (O'Connor and Woodbury, 1982), cats (Freeman and Wyke, 1967), monkeys (Gardner and Lenn, 1977) and humans (Horner and Dellon, 1994). Only the MAN and PAN are identifiable in mouse (Ebinger et al., 2001) and rat (Hildebrand et al., 1991).

The PAN contains the highest number of nerve fibres (400 axons in the rat) and is the largest of the articular nerves (Hildebrand et al., 1991). In the rat (Hildebrand et al., 1991), mouse (Ebinger et al., 2001) and monkey (Gardner and Lenn, 1977) the PAN is predominantly composed of unmyelinated fibres (rat: ~80%, mouse: ~66%, monkey: ~80-85%). In the cat, there are thought to be a predominance of myelinated fibres (224 vs 162) however, this may be due to variations in technique between studies as electron microscopy enables easier detection of unmyelinated fibres (Gardner and Lenn, 1977). The PAN arises from the posterior tibial nerve and is embedded in the fascia that covers the deep surface of the gastrocnemius muscle (Freeman and Wyke, 1967). It innervates the lateral and medial aspects of the posterior capsule of the knee joint, posterior fat pads and posterior ligaments (Freeman and Wyke, 1967).

The MAN (articular nerve studied in this thesis) is a finer nerve than the PAN (Freeman and Wyke, 1967, Hildebrand et al., 1991) consisting predominantly of unmyelinated fibres and is present in both the mouse (Ebinger et al., 2001) and rat (Hildebrand et al., 1991). It arises in the antero-medial region of the thigh and branches from the saphenous nerve terminating in the upper border of the medial condyle of the femur (Freeman and Wyke, 1967, Hildebrand et al., 1991). The nerve divides into proximal and distal branches that give off fine filaments that form a plexus on the medial surface of the capsule of the knee joint (Freeman and Wyke, 1967, Hildebrand et al., 1991). Medial, antero-medial and posterior aspects of the knee joint fibrous capsule are supplied by the MAN (Freeman and Wyke, 1967, Hildebrand et al., 1991). Electrophysiological studies in the cat and rat have demonstrated that the knee joint is innervated by Aβ, Aδ and C fibre mechanoreceptors corroborating anatomical findings indicating the MAN and PAN consist of small, unmyelinated C fibres, small, thinly myelinated Aδ fibres and Aβ fibres (Schaible and Schmidt, 1983b, Schaible and Schmidt, 1983a, Craig et al., 1988, Schaible and Grubb, 1993, Kelly et al., 2012).

1.4.3. Classification of knee joint nociceptors: types and localisation of receptive endings

Characterisation of the cell body sizes of knee joint afferents identified by retrograde labelling of the joint has demonstrated that articular afferents consist of small, medium and large cell bodies with more small-medium soma sizes (Salo and Theriault, 1997). Data on cell size distribution alongside the

anatomical and electrophysiological findings described above (section 1.4.2) provide further evidence that articular structures are innervated by Aβ, Aδ and C fibres.

Articular afferents can also be classified based on their receptive endings. Aβ fibres terminate as Ruffini-, Golgi-, and Pacini-type corpuscular endings in joint structures including the fibrous capsule, articular ligaments, menisci and adjacent periosteum (Johannson, 1991, Schaible and Grubb, 1993, Schaible et al., 2009). Aδ and C fibre articular afferents innervate the fibrous capsule, adipose tissue, ligaments, menisci and periosteum where they terminate as non-corpuscular or free nerve endings (Johannson, 1991, Schaible and Grubb, 1993, Schaible et al., 2009). Cartilage is not innervated and as such is described as being aneural (Schaible and Schmidt, 1983b). Sympathetic efferents additionally innervate joint structures including synovium (Schaible and Grubb, 1993). Postganglionic sympathetic nerve fibres regulate blood flow as they terminate close to articular blood vessels and modulate vasomotor tone (McDougall, 2006).

1.4.4. Classification of knee joint nociceptors: mechanical sensitivity

Electrophysiological recordings from the MAN and PAN in rat and cat have enabled knee joint afferents to be characterised based on their response to innocuous and noxious mechanical stimuli (Schaible and Schmidt, 1983b, Schaible and Grubb, 1993). In this context, innocuous stimuli can be defined

by light to moderate pressure applied to the joint, which does not elicit pain, and non-painful movements within the working range. Noxious stimuli can be defined as strong pressure applied to the joint, which elicits pain, and movements outside the normal working range of the joint.

Articular afferents of the cat knee joint have been defined into five distinct fibre types (Schaible and Schmidt, 1983b): (1) low threshold Aδ fibres activated by knee joint inward rotation with strongest responses occurring after noxious movements (2) Aδ fibres responding weakly to innocuous joint movements and displaying an elevated response to noxious movements (3) Aδ fibres that selectively respond to noxious pressure while no response is elicited by innocuous and noxious movements (4) C fibres that are only activated by noxious movements (5) 'silent nociceptors' which become mechanosensitive during inflammation. In addition, the knee joint is also innervated by Aβ fibres which encode and transmit proprioceptive signals that informs the brain about joint position (McDougall, 2006). These signals are interpreted as either dynamic (movement sense) or static (position sense). In the cat, the majority of Aβ fibres are either strongly or weakly activated by innocuous movements while approximately 50% of Aδ fibres and 70% of C fibres are high threshold nociceptive units (Schaible and Schmidt, 1983b). Nociceptors have been identified in different joint regions including the capsule, ligaments, menisci, periosteum and subchondral bone (Marinozzi et al., 1991). In addition, studies have found that 80% of knee joint afferent nerve fibres in the rat (Hildebrand et

al., 1991) and cat (Langford and Schmidt, 1983) function to detect noxious stimuli.

1.5. Primary afferent neurone neurochemistry

1.5.1. Transduction of noxious stimuli

The expression of a distinct array of receptors and ion channels by sub-types of nociceptive peripheral endings enables detection of a range of noxious stimuli.

Psychophysical studies in humans have identified an ability to discriminate between the perception of innocuous warmth and noxious heat (Basbaum et al., 2009). The pain threshold for noxious heat detection in clinical studies rests at approximately 43°C, paralleled by C and Aδ fibre thresholds (Cesare and McNaughton, 1996b, Kirschstein et al., 1997, Basbaum et al., 2009, Julius, 2013). The transient receptor potential (TRP) vanilloid 1 (TRPV1) cation channel has been attributed with the detection of noxious heat (Cesare and McNaughton, 1996b, Caterina et al., 1997, Kirschstein et al., 1997, Caterina et al., 2000, Davis et al., 2000, Julius, 2013). TRPV1 mRNA (Caterina et al., 1997) and protein (Tominaga et al., 1998) is predominantly expressed on caspsaicin-sensitive peptidergic and non-peptidergic small diameter C fibres that are activated in response to noxious heat. Genetic deletion of TRPV1 in the mouse reduces the number of heat-responsive C fibres which is in agreement with deficits in thermally-evoked pain behaviour including cutaneous inflammatory thermal hyperalgesia induced by complete Freund's

adjuvant (CFA) (Caterina et al., 2000) and carrageenan (Davis et al., 2000). Further members of the TRP family enable primary afferent nociceptors to detect changes in thermosensation over a wide physiological range as TRPV2 , TRPV3 and TRPV4 have thermal activation thresholds of >55°C, >33°C and 27-42°C respectively (Guler et al., 2002, Smith et al., 2002, Xu et al., 2002, Leffler et al., 2007) .

Distinct molecular mechanisms for the detection of noxious cold have been identified with the temperature threshold approximately 4°C (Reid and Flonta, 2001, McKemy et al., 2002). Several lines of evidence indicate the TRP melastatin 8 (M8) cation channel functions as a noxious cold sensor with an activation threshold of 25-28°C (McKemy et al., 2002, Bautista et al., 2007, Colburn et al., 2007). TRPM8 is expressed predominantly on C fibres although lower levels of expression have been observed on Aδ fibres while the channel is activated by noxious cold (McKemy et al., 2002, Kobayashi et al., 2005). Pain behaviour in response to innocuous and noxious cold stimuli was reduced in TRPM8 knockout mice corroborating electrophysiological data that identified a reduction in the number of C fibres responsive to noxious cold compared to wild types (Bautista et al., 2007, Dhaka et al., 2007, Knowlton et al., 2010, Yudin and Rohacs, 2012). A number of vinylcycloalkyl-substituted benzimidazole TRPM8 antagonists alleviated cold allodynia in the chronic constriction injury (CCI) model of neuropathic pain indicating a role in the hypersensitivity to cold induced by nerve injury (Calvo et al., 2012). It is thought that distinct subpopulations of nociceptors detect heat and cold

sensitivities evident by an absence of co-expression with TRPV1 on DRG neurones (Kobayashi et al., 2005). Further cold sensing targets include TRP cation channel subfamily A member 1 (A1) (Bandell et al., 2004b) and the two-pore domain K^+ channel TWIK-related arachidonic-acid stimulated potassium channel (TRAAK) and TWIK related potassium channel -1 (TREK-1) (Noel et al., 2009).

Knowledge of the molecular mechanisms that detect mechanical stimuli is limited although recent studies have indicated potential novel mechanotransducers (Kwan et al., 2006, Dunham et al., 2008, Alessandri-Haber et al., 2009, Kim et al., 2012, Quick et al., 2012, Wood and Eijkelkamp, 2012, Eijkelkamp et al., 2013). As well as detecting noxious thermal and cold stimuli, members of the TRP family are also candidate mechanotransducers. A recent study indicated that TRPA1 is expressed by mechanosensitive Aδ and C fibre nociceptors (Dunham et al., 2008). Further, genetic deletion of TRPA1 (Kwan et al., 2006, Wood and Eijkelkamp, 2012) and TRPV4 (Tabuchi et al., 2005) abolishes mechanical hypersensitivity while a mutation in the TRPA1 gene results in familial episodic pain syndrome characterised by an increase in secondary mechanical hyperalgesia (Kremeyer et al., 2010). The stretch activated ion channels TRP canonical 1 (C1), TRPC3 and TRPC6 have been identified as possible detectors of noxious mechanical stimuli, including following inflammation (Alessandri-Haber et al., 2009, Quick et al., 2012). In addition, recent evidence has demonstrated a role for Piezo proteins in mechanosensory nociception (Kim et al., 2012, Eijkelkamp et al., 2013).

Genetic deletion of Dmpiezo (gene for the Piezo family of transmembrane proteins) in Drosphilia melanogaster reduces behavioural responses to noxious mechanical stimuli without impact on responses to innocuous mechanical stimuli (Kim et al., 2012). Down regulation of DRG expression of piezo2 in mice using antisense oligonucleotides reduces mechanical allodynia induced by the cyclic adenosine monophosphate (cAMP) analogue 8-pCPT (Eijkelkamp et al., 2013). Further, piezo2 down regulation abolishes mechanical allodynia in CCI and L5 nerve transection models of neuropathic pain (Eijkelkamp et al., 2013).

As well as transducing thermal and mechanical stimuli the TRP family can also function to detect chemical stimuli including capsaicin (TRPV1) (Caterina et al., 1997), menthol (TRPM1) (McKemy et al., 2002), mustard oil and formalin (TRPA1) (Bandell et al., 2004b). TRPA1 in particular detects a wide range of plant compounds, environmental irritants, volatile irritants and chemotherapeutic by-products (Bandell et al., 2004a). Chemoreceptive targets expressed on nociceptors also include adenosine triphosphate (ATP) receptors, P2X receptors, acid sensing ion channels (ASICs) and 5-hydroxytryptamine (5-HT) receptors (Lawson, 2005).

1.5.2. Nociceptive transmission

The activation of transduction molecules as previously described (see Section 1.5.1) results in generator potentials that activate voltage-gated ion channels

expressed on nociceptors and generates action potentials in the cell body. The resultant action potentials are transmitted along the primary afferent axon centrally to the spinal cord dorsal horn culminating in neurotransmitter release at the central terminals of primary afferent neurones. Voltage-gated Na^+, Ca^{2+} and K^+ channels are important for the generation and propagation of action potentials (Wall, 2006).

Voltage-gated Na^+ (Na_v) channels can be classified as tetrodotoxin (TTX)-sensitive ($Na_v1.3$, $Na_v1.8$ and $Na_v1.9$) or TTX-resistant ($Na_v1.7$) on the basis of their sensitivity to block by the neurotoxin TTX (Liu and Wood, 2011). The different biophysical properties of Na_vs are important for setting peripheral pain thresholds and thresholds of excitability in nociceptors (Liu and Wood, 2011). The $Na_v1.3$ channel has a slow closed-state inactivation that results in a substantial ramp current in response to slow, small depolarisations (Cummins et al., 2001). Antisense oligonucleotides targeting $Na_v1.3$ in rats reduced the hyperexcitability of dorsal horn neurones while also preventing mechanical allodynia and thermal hyperalgesia after spinal cord injury (Hains et al., 2003). $Na_v1.7$ is characterised by a slow closed-state inactivation that produces a substantial inward current due to transient channel activation in response to small, depolarisations of cell membranes (Dib-Hajj et al., 2013). As a result, the probability of nociceptors reaching activation thresholds are increased which contributes to the triggering and upstroke of action potentials (Dib-Hajj et al., 2013). Humans that lack $Na_v1.7$ display congenital pain insensitivity (Cox et al., 2006) while gain of function mutations in genes encoding $Na_v1.7$

results in the increased pain during erythermalgia (Han et al., 2006) and paroxysmal extreme pain disorder (Fertleman et al., 2006). Pre-clinical evidence identified pharmacological $Na_v1.7$ channel blockade reduced pain behaviour in a CCI model of neuropathic pain and following oxaliplatin treatment (Ghelardini et al., 2010). $Na_v1.8$ channels have a depolarised voltage dependence of activation and are the major contributor to the inflow of Na^+ during the upstroke of the action potential (Patrick Harty and Waxman, 2007). $Na_v1.8$ channels are slow to inactivate during a maintained depolarising stimulus and would be expected to contribute to the longer duration action potential characteristic of nociceptors (Djouhri et al., 2003). The importance of the $Na_v1.8$-mediated increase in action potential duration to nociception is evident in a study that used $Na_v1.8$ channel knockout mice and found that inflammatory hyperalgesia developed more slowly compared to wild-type mice (Akopian et al., 1999). Antisense oligonucleotides for $Na_v1.8$ reversed pain behaviour after spinal nerve injury in rats indicating a role in neuropathic pain (Lai et al., 2002). $Na_v1.9$ channels are open at negative (-80mV) membrane potentials and remain active at more depolarised potentials (Cummins et al., 1999, Dib-Hajj et al., 2010). As such, $Na_v1.9$ channels generate a small, persistent current when the neurone is at rest (Cummins et al., 1999, Dib-Hajj et al., 2010). Genetic deletion of $Na_v1.9$ reduced the development of thermal hypersensitivity in a CFA model of cutaneous inflammation (Amaya et al., 2006b).

The opening of voltage-gated Ca^{2+} channels that are expressed on nociceptors in response to depolarization of the cell membrane results in neurotransmitter release. N- and P-type channels are expressed on C fibres where they contribute to excitatory neurotransmission (Meir et al., 1999).

The excitability of nociceptors is regulated by opening of voltage-gated K^+ channels that result in a reduction in resting membrane potential and firing frequency (Hodgkin and Huxley, 1952). Voltage-gated K^+ channels also mediate action potential after-hyperpolarization (Hodgkin and Huxley, 1952). Small nociceptive neurones express several K^+ channel family members including delayed rectifier channels, inwardly rectifier channels (e.g. Kir2.1), background channels (e.g, TASK and TREK-1) and fast transient current channels (e.g. $K_v1.4$) (Lawson, 2005).

1.5.3. Neurotransmitters and receptors expressed by primary afferent neurones

Neurotransmitters and neuropeptides are released from primary afferent neurones at their peripheral and central terminals (Lawson, 2005). The release of neurotransmitters and neuropeptides at peripheral terminals can result in peripheral sensitization of nociceptors and neurogenic inflammation (McDougall, 2006). Central release leads to the activation of post-synaptic receptors expressed on spinal cord dorsal horn neurones and enables nociceptive transmission to the CNS (Lawson, 2005). Several

neurotransmitters, neuropeptides, receptors and ion channels have been identified in nociceptors (see Tables 1.2 and 1.3).

Glutamate is released from the central terminals of Aδ and C fibres and activates ionotropic N-methyl-D-aspartate (NMDA), alpha-3-hydroxy-5-methyl-isoxazolepropionic (AMPA) and metabotropic glutamate receptors, present on post-synpatic spinal cord neurones which results in hyperexcitability (Schaible et al., 2009). Glutamate immunoreactivity has been observed in approximately 70% of Aδ and C fibres (De Biasi and Rustioni, 1988). Further, glutamate co-localisation with SP has been identified in the central terminals of primary afferent C fibres in the dorsal horn (De Biasi and Rustioni, 1988). Glutamate receptors are expressed on DRG neurones: Aαβ, Aδ and C fibre primary afferents express NMDA receptor subunit 1 and AMPA receptors, while GluR1, GluR2/3 and GluR5 are present on C fibres (Sato et al., 1993). Aα/β fibres express GluR2/3 (Sato et al., 1993).

Peptidergic C fibres express SP, CGRP and trkA while non-peptigeric fibres express the plant lectin IB4, $P2X_3$ and GDNF (Lawson, 2005). Expression of SP and CGRP has been observed predominantly in C fibre nociceptors, however both peptides are present in Aδ fibres and CGRP in Aα/β fibres (Lawson, 2005). Noxious stimuli induces release of SP and CGRP from peripheral and central terminals of primary afferents (Richardson and Vasko, 2002). Centrally SP and CGRP depolarise dorsal horn neurones via activation

of neurokinin-1 (NK-1) receptors and CGRP receptors, respectively (Snijdelaar et al., 2000). Injection of SP into rat skin produces mechanical hyperalgesia and allodynia (Carlton, 2001), while inflammation up regulates NK-1 receptor (Carlton and Coggeshall, 2002) and CGRP receptor component expression (Ma et al., 2003). The peripheral release of the neuropeptides SP and CGRP leads to neurogenic inflammation, characterised by vasodilation and wound healing (Holzer, 1998) while SP additionally produces plasma extravasation from blood vessels (Holzer, 1998).

The hormone somatostatin is antinociceptive and anti-inflammatory (Malcangio et al., 2002). It is released both peripherally and centrally from C fibre nociceptors and attenuates neuronal firing at the level of the dorsal horn and DRG (Malcangio et al., 2002). The GPCR somatostatin receptor 2a is present on both C and Aδ fibres and in post-synaptic dorsal horn neurones (Bar et al., 2004). The neuropeptide galanin is typically not present in high levels in nociceptors (Liu, 2002) although peptide and mRNA is upregulated following inflammation and nerve injury (Liu, 2002). Peripheral administration of galanin modulated the mechanically-evoked responses of hind paw afferents in an in vivo electrophysiology study using a partial saphenous nerve ligation injury (PSNI) model; low concentrations facilitated and high concentrations inhibited activity (Hulse et al., 2011). Overexpression of galanin reversed the mechanical allodynia observed in the PSNI model (Hulse et al., 2011). Galanin receptors (GAL) are GPCRs expressed on primary afferents; GAL1 is present on Aα/β fibres and GAL2 on peptidergic C fibres (Liu, 2002). Inflammation

reduces GAL1 mRNA levels and transiently elevates GAL2 mRNA (Liu, 2002). A study investigated the expression of the neuropeptide vasoactive intestinal peptide (VIP) in fibres innervating ankle joints and in L2-L6 DRG with expression identified mainly on small diameter C knee joint fibres (Ahmed et al., 1995) although presence on Aδ has also been observed (Dickinson and Fleetwood-Walker, 1999). VIP sensitized knee joint nociceptor Aδ- and C-fibres to innocuous and noxious mechanical stimuli under non-pathological conditions while inducing a desensitizing effect in a model of knee OA (McDougall et al., 2006).

Investigation of joint nociceptor neurochemistry and receptor/ion channel expression has demonstrated the expression of many of the neurotransmitters, neuropeptides and receptors expressed in cutaneous afferents detailed above (see Table 1.2) including substance P (Donaldson et al., 1995), CGRP (Donaldson et al., 1995), glutamate (Sluka and Westlund, 1993), TRPV1 (Fernihough et al., 2005), Na_vs (Strickland et al., 2008), cannabinoid receptors (Schuelert et al., 2010) and protease activated receptors (Russell et al., 2012). Characterisation of joint neurochemistry has demonstrated that nociceptors innervating articular structures are exclusively peptidergic (Salo et al., 1997, Ivanavicius et al., 2004, Fernihough et al., 2005, Ferreira-Gomes et al., 2010, Orita et al., 2011). A study using retrograde tracing found a complete absence of IB4 expressing knee joint afferents (Ivanavicius et al., 2004).

Table 1.2. Neurotransmitters and peptides expressed by nociceptors.

Neurotransmitter/peptide	Fibre type	Inhibitory	Excitatory	Joint nociceptor expression	Citation
Nociceptin	C	x	√	√	(Pettersson et al., 2002, Haversath et al., 2013)
VIP	C, Aδ	x	√	√	(Mulderry and Lindsay, 1990, Donaldson et al., 1995)
Substance P	C, Aδ	x	√	√	(Barakat-Walter et al., 1991, Donaldson et al., 1995)
Glutamate	C, Aδ, Aβ	x	√	√	(Sluka and Westlund, 1993, Stoyanova et al., 1998)
Bradykinin	C, Aδ,	x	√	√	(Seabrook et al., 1997, Russell et al., 2012)
ATP	C	x	√	√	(Kobayashi et al., 2013)
Neuropeptide Y	C	√	x	Not studied	(Bleakman et al., 1991)
Somatastatin	C	√	x	√	(Donaldson et al., 1995, Heppelmann and Pawlak, 1997a)

Galanin	C, Aδ	√	x	√	(Kashiba et al., 1992, Heppelmann et al., 2000)
Dynorphin	C	√	x	Not studied	(Romero et al., 2012)
CGRP	C, Aδ, Aβ	x	√	√	(Noguchi et al., 1990, Donaldson et al., 1995)

Table 1.3. Receptors and ion channels expressed by nociceptors.

Receptor/ion channel	Cell type	Cellular effect	Target	Expressed by joint nociceptors	Citation
TRPV1	C, Aδ	Excitation	Ligand-gated ion channel	√	(Greffrath et al., 2003, Kelly et al., 2013a)
ATP (P2X)	C	Excitation	Ligand-gated ion channel	√	(Kobayashi et al., 2013)
NMDA, AMPA	C	Excitation	Ligand-gated ion channel	√	(Lee et al., 2004)
Glycine	C, Aδ	Inhibition	Ligand-gated ion channel	Not studied	(Furuyama et al., 1992)
Bradykinin B_2	C	Excitation	GPCRs	√	(Segond von Banchet et al., 1996)
PGE2 receptor (EP2)	C, Aδ	Excitation	GPCRs	√	(Southall and Vasko, 2001, Kras et al., 2013)

NK1	C, Aδ	Excitation	GPCRs	√	(Andoh et al., 1996, McDougall et al., 2001)
Galanin receptors	C, Aδ	Inhibition	GPCRs	√	(Liu, 2002)
Somatostatin	C, Aδ	Inhibition	GPCRs	√	(Bar et al., 2004)
$CB_{1/2}$	C, Aδ	Inhibition	GPCRs	√	(Anand et al., 2008)
Ca^{2+} L and N type	C, Aδ	Excitation	Ion channels	√	(McCallum et al., 2011)
$Na_v1.9$	C	Excitation	Ion channels	√	(Fang et al., 2002)
$Na_v1.7$, $Na_v1.8$	C, Aδ	Excitation	Ion channels	√	(Djouhri et al., 2003, Tamura et al., 2014)

1.6. Nociceptive transmission to the dorsal horn

Since this thesis is focused on the peripheral mechanisms of joint pain and its modulation only an overview of central mechanisms will be provided.

The spinal cord dorsal horn in the pain pathway functions to transmit nociceptive information from primary afferent nociceptors to brain regions that are involved in the conscious perception of pain (Todd, 2010). Neuronal sub-types present in the dorsal horn include: (1) primary afferent neurones which synapse at distinct dorsal horn laminae (described below) (2) intrinsic neurones that terminate within the spinal cord (3) neurones that project rostrally to reach supraspinal brain regions involved in nociceptive processing (4) descending neurones which project caudally from brain regions and modulate nociceptive transmission at the level of the dorsal horn (Schaible et al., 2009, Todd, 2010). The dorsal horn can be divided into ten distinct laminae, laminae I–X, depending on neuronal size and packing density (Rexed, 1952). Nociceptive primary afferent neurones terminate predominantly in laminae I and II, the superficial dorsal horn (Wall, 2006). However, nociceptive primary afferent neurones additionally synapse in deeper laminae, laminate III-VI (Wall, 2006).

Primary afferent neurone sub-types terminate in distinct dorsal horn laminae. The substantia gelatinosa (lamina II) receives input from Aδ- and C-fibre nociceptors, including joint nociceptors (Wall, 2006). Myelinated LTMs terminate between inner lamina II and lamina V, including Aδ fibres that innervate hair follicles and synapse extensively into inner lamina II (Light et al., 1979). Nociceptive myelinated Aδ fibres synapse with laminae I, outer II,

IV and V neurones (Light and Perl, 1979). Non-peptidergic unmyelinated C-fibres terminate in lamina II (Averill et al., 1995). Anatomical studies investigating articular afferent dorsal horn termination have produced conflicting findings. Joint afferents have been demonstrated to terminate within laminae I, IV, V and VI (Schaible et al., 1987) as well as terminating exclusively in laminae II and III.

Glutamate is a key excitatory neurotransmitter released from presynaptic terminals at the spinal endings of primary afferent neurones (Schaible et al., 2002). Glutamate is released from Aβ LTMs in response to innocuous mechanical stimuli to the joint, activating AMPA receptors (Schaible et al., 2002). However, noxious mechanical stimulation of the joint evokes an increased release of glutamate from Aβ, Aδ and C fibres, activating AMPA and NMDA receptors resulting in a strong depolarization (Schaible et al., 2002). Systemic administration of NMDA and AMPA receptor antagonists abolished the change in responsiveness of spinal cord dorsal horn neurones observed using an acute model of knee joint inflammation in the rat (Neugebauer et al., 1993b). The same effect was observed in a chronic model of knee joint arthritis, antagonism of NMDA and AMPA receptors abolished the responses of nociceptive wide dynamic range neurones to innocuous and noxious mechanical stimuli applied to the knee joint (Neugebauer et al., 1994).

SP and its receptor NK-1 have been shown to have an important role in spinal nociception (Hunt and Mantyh, 2001). Spinal SP release only occurs following exposure to noxious thermal and chemical stimuli (Lawson et al., 1997). SP containing primary afferent neurones innervate NK-1-expressing projection neurones in lamina I (Yu et al., 1999) and laminae III-IV (Todd, 2002). The NK-1 receptor is predominantly expressed in lamina I (Todd, 2002). Selective ablation of dorsal horn NK-1 expressing neurones following intrathecal administration of SP conjugated to the cytotoxin saporin attenuates inflammatory and neuropathic hyperalgesia in rats (Mantyh et al., 1997). However, no reduction in inflammatory hyperalgesia was observed in mice genetically deleted for the NK-1 receptor (De Felipe, 1988) and the preprotachykinin gene (Cao et al., 1998), which transcribes the receptor. Further, NK-1 antagonists were observed to have limited efficacy as analgesics in human clinical trials (Hill, 2000). Therefore, although NK-1 expressing neurones are vital for the development of hyperalgesia, spinal nociception is not mediated by SP activation of NK-1 receptors (Hill, 2000). It has been proposed that SP-containing C fibre nociceptors release glutamate at their synapses with NK-1 expressing projection neurones and that this induces hyperalgesia (Hill, 2000).

1.7. Ascending pain pathways

The spinothalamic tract (STT) projects directly to the thalamus (Dostrovsky, 2006). STT neurones originate in laminae I, IV-V and VII-VIII of the spinal cord dorsal horn (Dostrovsky, 2006) and terminate in the thalamus and brain

stem regions, including the periaqueductal grey (PAG) (Dostrovsky, 2006). Sensations of itch, pain and temperature are linked with STT activation (Dostrovsky, 2006). The spinobulbar and medullary tracts project directly to medulla and brainstem homeostatic control regions (Craig, 2003). Neurones in this ascending pathway originate in laminae I, V and VII (Wiberg et al., 1987) and the integration of nociceptive homeostasis and behaviour has been associated with this pathway (Sato and Schmidt, 1973). The spinohypothalamic tract (SHT) projects directly to the hypothalamus and ventral forebrain (Wall, 2006). Neurones of the SHT originate in laminae I, V, VII and X of the dorsal horn (Wall, 2006). Activation of the SHT is vital for the autonomic, neuroendocrine and emotional aspects of pain (Dado et al., 1994).

1.8. Supraspinal sites of nociception

Nociceptive signals are transmitted to the brain by the neurones of ascending tract pathways described above (see Section 1.7). The pain experience consists of different aspects, including discriminative and affective components, said to be mediated by different brain regions (Bushnell, 2006). The discriminative aspect (e.g. location, duration and intensity) of pain is mediated by somatosensory cortices SI and SII of the cortex, which receive projections from the lateral thalamocortical system (Schaible et al., 2006). The medial thalamocortical system sends projections to the anterior cingulated cortex, insula and prefrontal cortex (Schaible et al., 2006). These brain sites are vital for the affective (unpleasantness and aversive reactions) component of pain (Schaible et al., 2006). During chronic pain conditions, increased activity in the

prefrontal cortex occurs in response to noxious stimuli (Lassen et al., 1978) while thalamic-related activity in response to a stimulus attenuates pain (Di Piero et al., 1991). These alterations in cortical nociceptive processing could contribute to hyperalgesia and sensory deficits, respectively. Brain regions which may be involved in pain processing include the basal ganglia, cerebellum, amygdala, hippocampus and the parietal and temporal cortices (Tracey and Mantyh, 2007).

1.9. Descending modulatory pathways

Spinal dorsal horn nociceptive neurones are inhibited by brainstem regions, including the PAG and rostral ventromedial medulla (RVM) (Wall, 1967). Serotonergic and noradrenergic PAG neurones project to and activate cells in the RVM, including the nucleus raphe magnus, which project inhibitory neurones to the spinal cord dorsal horn via the dorsolateral funiculus (Millan, 2002). RVM neurones project directly to and synapse with dorsal horn projection neurones and interneurones (Millan, 2002). In addition, descending RVM neurons modulate nociceptive primary afferent neurones (Millan, 2002). RVM neurones, consisting of approximately 20% 5-HT-containing neurones, release 5-HT, which excites inhibitory interneurones (Millan, 2002). These interneurones synapse with projection neurones and central terminals of primary afferent neurones, releasing neurotransmitters (e.g. glycine, enkephalin) which inhibit nociceptive transmission (Millan, 2002). Cannabinoid and opioid-based drugs induce analgesia by targeting neurones in the PAG and RVM (Fields, 2006).

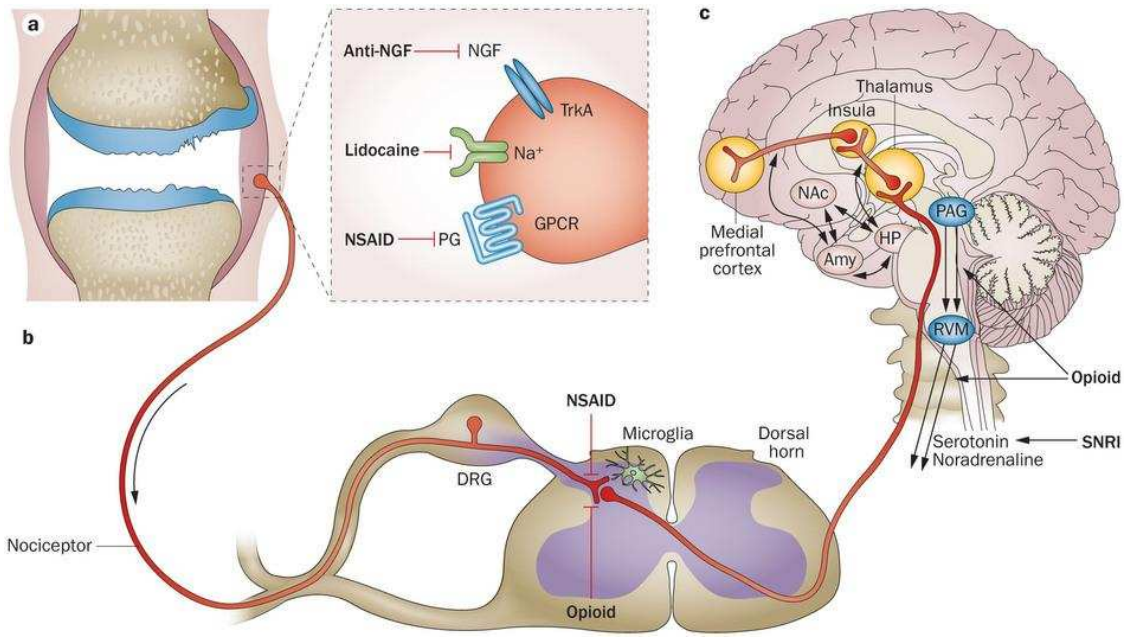

Figure 1.2. Neuroanatomy of joint pain pathway and analgesic targets. Transmission of nociceptive information from knee joint afferents (a) to the spinal cord (b) then to brain regions important in the conscious perception of pain (c). Taken from (Malfait and Schnitzer, 2013).

1.10. Peripheral sensitization

The clinical symptoms of joint pain (e.g. during OA) include spontaneous pain, hyperalgesia and allodynia which are driven by changes in the excitability of the peripheral and CNS (Schaible et al., 2002). The importance of changes in the sensitivity of articular sensory nerves during chronic pain in OA is evident by the abolishment of pain following joint replacement surgery and i.a. local anaesthetic in man (Creamer et al., 1996, Kosek and Ordeberg, 2000a) and following a desensitization or ablation of nociceptors within the OA joint in

rats (Kalff et al., 2010, Kosuwon et al., 2010). These findings indicate that joint nociceptors inputs are required for the development and maintenance of chronic joint pain (Schaible et al., 2002, Schaible et al., 2009).

Sensitization of knee joint nociceptors results in excessive central neurotransmitter and neuropeptide release which increases dorsal horn spinal neuronal activity (Neugebauer et al., 1993a, Neugebauer et al., 1996, Schaible et al., 2009). This process results in central sensitization and pain chronicity (Schaible et al., 2009). Therefore, identification of mechanisms that sensitize joint nociceptors and those that could potentially modulate (i.e. inhibit) sensitization during conditions such as OA is likely to be fundamental to the development of more effective analgesics.

Nociceptor plasticity manifested as an increase in sensitivity to peripheral stimuli, occurs during inflammation or injury, and is referred to as 'peripheral sensitization' (Coggeshall et al., 1983, Schaible and Schmidt, 1985, Grigg et al., 1986, Schaible and Schmidt, 1988b, McDougall, 2006, Schaible et al., 2009). Peripheral sensitization is characterised by a reduction in mechanical activation thresholds, elevated response to suprathreshold mechanical stimuli and increased nociceptor spontaneous activity (Coggeshall et al., 1983, Schaible and Schmidt, 1985, Grigg et al., 1986, Schaible and Schmidt, 1988b, McDougall, 2006, Schaible et al., 2009). Peripheral sensitization has been

demonstrated to make a significant contribution to the severity of pain during OA (Arendt-Nielsen et al., 2010).

Nociceptors are sensitized during inflammation by the release of inflammatory mediators from damaged tissue or cells, tumour cells or inflammatory cells (such as mast cells, neutrophils and monocytes) as well as from sensory and sympathetic nerve fibres, that bind to receptors expressed on their peripheral endings (Schaible et al., 2006, Cheng and Ji, 2008, Schaible et al., 2009, Gangadharan and Kuner, 2013a). These inflammatory mediators include prostaglandin E_2 (PGE_2), bradykinin (BK), ATP, protons, nerve growth factor (NGF), histamine, 5-HT, tumour necrosis factor-alpha (TNF-α), interleukin 1-beta (IL-1β), and CGRP (Julius and Basbaum, 2001, Gangadharan and Kuner, 2013b). Nociceptors can be directly activated (e.g. protons, ATP) and/or sensitized (e.g. BK, CGRP, NGF, PGE_2) to mechanical, chemical or thermal stimuli (Julius and Basbaum, 2001, Gangadharan and Kuner, 2013b). Inflammatory mediators that do not directly activate nociceptors increase excitability and sensitivity by activating receptors that are coupled to intracellular signalling pathways involving adenylate cyclase, cAMP, protein kinase A (PKA), C (PKC) and Ca^{2+} (Julius and Basbaum, 2001, Gangadharan and Kuner, 2013b). Activation of protein kinases via these signalling pathways sensitizes nociceptors through phosphorylation of ion channels such as TRPV1 and $Na_v1.8$ (Taiwo et al., 1989, Taiwo and Levine, 1991, Kress et al., 1996, Gold et al., 1998, Linhart et al., 2003). Phosphorylation of TRPV1 and $Na_v1.8$ results in a reduction in the threshold for nociceptor activation and further

release of pro-inflammatory substances from C fibre nociceptors via increasing currents, lowering the voltage threshold for activation and producing a depolarizing shift in inactivation (Kessler et al., 1999, Oshita et al., 2005, Wu et al., 2012, Li et al., 2014).

The identification of mechanisms that have the potential to inhibit sensitization of joint afferents during joint disease could provide novel analgesic targets. This thesis has focused on the role of the putative third cannabinoid receptor GPR55 in the modulation of joint afferent mechanosensitivity under normal and pathological (OA) conditions. As such, it is relevant firstly to review current knowledge of the peripheral cannabinoid receptor system in the modulation of pain before moving on to what is currently known with regard to GPR55.

1.11. Cannabinoids

The plant Cannabis sativa has been used for recreational and medicinal purposes for thousands of years due to its psychoactive properties. The discovery of Δ^9-tetrahydrocannabinol (Δ^9-THC) as the principal psychoactive component of Cannabis sativa initiated serious interest in the therapeutic potential of the cannabinoid system (Mechoulam et al., 1967). Cannabinoids are sub-classified as phytocannabinoids (e.g. constituents of the Cannabis Sativa), endocannabinoids (e.g. anandamide) or synthetic cannabinoids (e.g. WIN 55,212-2) (Howlett et al., 2002).

Cannabinoids mediate their effects via two characterised CB_1 and CB_2 receptors (Howlett et al., 2002, Howlett et al., 2004). Cannabinoid receptors are distinguished by variations in amino acid sequences, intracellular signalling and tissue distribution (Howlett et al., 2002, Howlett et al., 2004). The CB_1 receptor was cloned from rat in 1990, its mRNA was identified in brain regions known to contain cannabinoid receptors including: dentate gyrus, hippocampal formation and cerebral cortex (Matsuda et al., 1990). Following this in 1993, the CB_2 receptor mRNA was found in spleen marginal zone macrophages but was absent from the brain (Munro et al., 1993). At the protein level, CB_1 and CB_2 receptors share 44% identity which increases to 68% in the transmembrane region (Munro et al., 1993). Cannabinoid receptors are GPCRs which couple to $G_{i/o}$ proteins and subsequently attenuate adenylate cyclase activity (Howlett et al., 2004). Activation of CB_1 receptors inhibits Ca^{2+} and elevates K^+ channel conductance, which is thought to suppress neuronal excitability and neurotransmitter release (Howlett et al., 2004). In addition, CB_1-mediated inhibition of 5-HT_3 ion channels (Barann et al., 2002), nitric oxide production (Pertwee, 2001) and Na^+ channel conductance (Nicholson et al., 2003) has been demonstrated. The Na^+/H^+ exchanger is activated by CB_1 receptors (Bouaboula et al., 1999). CB_1 and CB_2 receptors activate mitogen activated protein kinase (MAPK) and increase Krox-24 expression (Bouaboula et al., 1995).

Beneficial effects of cannabinoids mediated in the CNS have been identified which include analgesia (Howlett et al., 2002). However, effects mediated by

CNS expressed cannabinoid receptors, including sedation, dysphoria/euphoria and alterations in cognition and memory, have restricted their clinical use (Howlett et al., 2002). In order to overcome these unwanted effects, amongst other strategies the therapeutic potential of cannabinoid receptors expressed in peripheral tissues has been investigated (Guindon and Hohmann, 2009, Engeli, 2012, Basu et al., 2014).

1.11.1. Phytocannabinoids and synthetic cannabinoids

Phytocannabinoids include Δ^9-THC and cannabidiol. Δ^9-THC has similar affinities for CB_1 and CB_2 receptors (Howlett et al., 2002). At CB_1 receptors, Δ^9-THC functions as a partial agonist with studies demonstrating Δ^9-THC as having lower efficacy than some synthetic cannabinoids (Howlett et al., 2002). Δ^9-THC has lower efficacy at the CB_2 receptor compared to the CB_1 receptor (Howlett et al., 2002). In a N18TG-2 neuroblastoma cell line expressing CB_1 receptors, the CB_1 and CB_2 receptor agonist CP 55,940 produced an increased attenuation of cAMP levels compared to Δ^9-THC (Matsuda et al., 1990). The development of synthetic cannabinoid ligands has enabled further research into the functional role of the cannabinoid system include ligands derived from Δ^9-THC (HU210 and CP55940) and aminoalkylindoles (R-(+)-WIN55212 and JWH-015) (Pertwee, 2001).

1.11.2. Endocannabinoids

Endocannabinoids are cannabimimetic substances which are synthesised, released and degraded naturally in the body (Guindon and Hohmann, 2009). The initial endocannabinoids to be discovered were arachidonylethanolamine (anandamide) (Devane et al., 1992) and 2-arachidonylglycerol (2-AG) (Sigiura et al., 1995). Subsequently, further less well characterised endocannabinoids have been proposed, including: noladin ether (Hanus et al., 2001), virodhamine (Porter et al., 2002) and N-archidonyldopamine (Ross et al., 2009). Endocannabinoids are synthesised 'on demand' from phospholipid precursors present in the cell membrane (Guindon and Hohmann, 2009). The cleavage of membrane phospholipids and resultant endocannabinoid synthesis is initiated by membrane depolarisation, elevated intracellular Ca^{2+} levels and receptor stimulation (Guindon and Hohmann, 2009).

Preceding anandamide synthesis, the phospholipid precursor N-arachidonoyl-phosphatidylethanolamine (NAPE) is formed following enzymatic transfer of arachidonic acid, present in the sn-1 position of a phosphatidylcholine, to a phosphatidylethanolamine amide group (Jin et al., 2009). This process requires the Ca^{2+}-independent enzyme N-acyl-transferase. Following this, NAPE is hydrolysed to anandamide by a specific phospholipase D (NAPE-PLD). However, studies using mice with a deleted NAPE-PLD gene have implicated several enzymatic pathways involved in anandamide synthesis (Leung et al., 2006). 2-AG is also synthesised via a two-step process. The enzyme phospholipase C (PLC) cleaves membrane phospholipid precursors to form

diacylglycerol (DAG), which in turn is hydrolysed to 2-AG by DAG lipase (Di Marzo et al., 1999, Jin et al., 2009). Once released, the endocannabinoids exert their effects via cannabinoid receptor activation. Anandamide preferentially binds to CB_1 receptors (Piomelli, 2001) and has low affinity to TRPV1 channels (Smart et al., 2000), while 2-AG is efficacious at CB_1 and CB_2 receptors (Sigiura et al., 1995). Endocannabinoids can function to modulate synaptic transmission (Guindon and Hohmann, 2009). Following release from depolarised postsynaptic neurones endocannabinoids act via a retrograde signalling mechanism and activate CB_1 receptors on presynaptic terminals (Guindon and Hohmann, 2009). Consequently, the release of neurotransmitters (e.g. GABA and glutamate) is attenuated. Therefore, endocannabinoids can control excitatory and inhibitory synaptic transmission, suggesting a regulatory role in neuronal excitability and homeostasis.

The mechanisms of endocannabinoid re-uptake have not been clarified, although several have been proposed (Hillard and Jarrahian, 2003). This includes a yet to be cloned transporter and facilitated diffusion via a saturable, temperature-dependent, ATP-independent process driven by a transmembrane concentration gradient (Hillard and Jarrahian, 2003). Endocannabinoids are hydrolysed by specific intracellular enzymes. Fatty-acid amide hydrolase (FAAH) hydrolyses anandamide to form arachidonic acid and ethanolamine (Giang, 1997). FAAH is found in regions of the pain pathway, including: the termination zone of the spinothalamic tract in the ventral posterior lateral nucleus of the thalamus, the superficial dorsal horn and DRG neurones. The

serine hydrolase monoacylglycerol lipase (MGL) hydrolyses 2-AG into arachidonic acid and glycerol (Dinh et al., 2002). However, endocannabinoids have been shown to be degraded via alternative processes to hydrolysis. Anandamide and 2-AG have been shown to be metabolised by cyclooxygenase (COX), lipoxygenase and cytochrome P450 enzymes (Alexander and Kendall, 2007).

1.11.3. Cannabinoid receptor expression

CB_1 receptor expression was initially thought to be localised to CNS neurones with CB_2 receptor expression restricted to immune tissues (Herkenham, 1995). Brain regions expressing the CB_1 receptor include: the cerebral cortex, amygdala, basal ganglia, substantia nigra pars reticulata, internal and external segment of the globus pallidus, cerebellum and hippocampus (Pertwee, 1997). CB_2 receptor expression is present in tissues responsible for immune cell production and regulation including the spleen, tonsils and thymus (Howlett et al., 2004). CB_2 expressing immune cells are mast cells, macrophages, natural killer cells, B cells, T4 and T8 cells, microglial cells, monocytes and polymorphonuclear neutrophils (Howlett et al., 2004). CB_1 receptor is expressed in peripheral tissues (Galiegue et al., 1995, Kaplan, 2013) and the CB_2 receptor in non-immune tissue (Herkenham, 1995). Peripheral tissues expressing the CB_1 receptor include the adrenal gland, adipose tissue, heart, liver, lung, prostrate, uterus, ovary, testis, bone marrow, thymus, tonsils and presynaptic nerve terminals (Galiegue et al., 1995). Studies have also identified

the receptor in the brain, lumbar spinal cord, microglia and DRG (Jhaveri et al., 2007).

1.11.4. Cannabinoid receptor expression on primary afferent neurones

Several studies have confirmed CB_1 receptor expression in primary afferent neurones using in situ hybridisation and immunolabelling (Hohmann and Herkenham, 1999, Ahluwalia et al., 2000, Ahluwalia et al., 2002b, Bridges et al., 2003, Binzen et al., 2006). CB_1 receptor protein was expressed in approximately 36% (Binzen et al., 2006), 47% (Ahluwalia et al., 2002a) and 57% (Ahluwalia et al., 2002a) of rat DRG neurones. Pharmacological and immunohistochemical characterisation identified co-expression of CB_1 on neurofilament 200 (NF200) (Bridges et al., 2003), IB_4, CGRP (Ahluwalia et al., 2002b), (Ahluwalia et al., 2000, Binzen et al., 2006) and $K_v1.4$ channel (Binzen et al., 2006) expressing afferents. Further evidence identified CB_1 expression on small-, medium- and large-sized DRG neurones (Bridges et al., 2003). This indicates the CB_1 receptor is present on all major subpopulations of DRG neurones with predominant localisation on peptidergic and non-peptidergic small diameter C fibre nociceptors. CB_2 receptor expression is present on small/medium and large sized DRG neurones with expression up-regulated following nerve injury in small- and medium-sized DRG (Ross et al., 2001, Anand et al., 2008).

1.11.5. Role of the peripheral cannabinoid receptor system in the modulation of nociception

Evidence from behavioural and in vivo electrophysiological studies in animal models have identified an anti-nociceptive effect in response of peripheral cannabinoid receptor activation (Calignano et al., 1998, Richardson et al., 1998, Nackley et al., 2003, Quartilho et al., 2003, Johanek and Simone, 2004, Elmes et al., 2005, Sagar et al., 2005, Amaya et al., 2006a, Agarwal et al., 2007, Gutierrez et al., 2007, Kelly and Donaldson, 2008, Potenzieri et al., 2008, Schuelert et al., 2010, Schuelert and McDougall, 2011). Activation of peripheral CB_1 receptors reduced pain behaviour in response to a mild heat injury (Johanek and Simone, 2004), formalin (Calignano et al., 1998, Agarwal et al., 2007) and capsaicin (Agarwal et al., 2007). Recordings from dorsal horn neurones (Kelly et al., 2003) and the saphenous nerve (Kelly and Donaldson, 2008, Schuelert and McDougall, 2008) observed an inhibition in mechanically-evoked responses after administration of CB_1 and CB_2 receptor agonists in naïve rats.

Peripheral cannabinoid receptors also modulate nociception in models of inflammatory pain. The CB_1 receptor agonist arachidonyl-2-chloroethylamide (ACEA) reduced thermal hyperalgesia in the CFA model following peripheral administration (Amaya et al., 2006). An anti-nociceptive role for peripheral cannabinoid receptors is further highlighted in the carrageenan model with peripheral administration of anandamide (Richardson et al., 1998), ACEA (Gutierrez et al., 2007) and the CB_2 receptor agonist AM1241 (Quartilho et al.,

2003) all having an analgesic effect. Peripheral administration of AM1241 reduced carrageenan-induced thermal and mechanical hyperalgesia and allodynia while inhibiting the expression of spinal c-Fos expression, a marker for neuronal activation suggesting that activation of peripheral CB_2 receptors inhibits nociceptive transmission to the spinal cord (Nackley et al., 2003). ACEA and methACEA reduced mechanical allodynia and hyperalgesia in CFA injected rats via peripheral CB_1 receptor activation and inhibited mechanically-evoked responses of cutaneous Aδ nociceptors, in an AM251-sensitive manner (Potenzieri et al., 2008). These findings suggest that activation of CB_1 receptors on Aδ-fibre nociceptors contributes to the anti-nociceptive effects of ACEA and methACEA observed behaviourally. The importance of CB_1 receptors expressed by nociceptors in mediating inhibition of inflammatory hyperalgesia is highlighted by the exacerbation of CFA-induced mechanical hyperalgesia and allodynia in transgenic mice in which CB_1 receptors have been selectively deleted from $Na_v1.8$ expressing nociceptors (Agarwal et al., 2007) indicating a tonic inhibition of inflammatory nociception by peripheral CB_1 receptors. Collectively these studies suggest that targeting of the peripheral cannabinoid receptor system could be a useful strategy in the treatment of chronic inflammatory pain.

1.11.6. Novel cannabinoid receptors

Until relatively recently, the physiological effects of cannabinoids were thought to be exclusively mediated via CB_1 and CB_2 receptors. However, in studies using CB_1 and CB_2 receptor knockout mice, cannabinoids have been

shown to act independently of the classical cannabinoid receptors (Brown, 2007). These additional sites have been termed non-CB_1/CB_2 receptors and are thought to be present in the vasculature, CNS and immune cells (Brown, 2007). In resistance arteries of the mesenteric vasculature, anandamide-mediated vasodilation is blocked by cannabidiol and O-1918, antagonists with no efficacy or affinity at CB_1 or CB_2 receptors (Offertaler et al., 2003). The presence of non-CB_1/CB_2 receptor sites in the CNS was detected using brain slices and membrane preparations from CB_1 receptor knockout mice (Breivogel et al., 2001). WIN55212 was found to stimulate [^{35}S]-GTPγS binding, identifying GPCR activation. The immune expression of non-CB_1/CB_2 receptor sites has been found in resting and activated T cells from mice genetically deleted for the classical cannabinoid receptors (Rao and Kaminski, 2006). In resting T cells from wild type and CB_1/CB_2 receptor knockout mice, Δ^9-THC, cannabidiol and HU210-induced increases in intracellular Ca^{2+} (Rao and Kaminski, 2006). Despite these pieces of evidence for the existence of non-CB_1/CB_2 receptors, studies aimed at identifying these receptors have not conclusively identified a novel cannabinoid receptor. However, several candidates have been proposed including the GPR55 receptor (described below).

1.12. GPR55 receptor

The GPR55 receptor is an orphan GPCR initially identified in silico from the expressed sequence tags database (Sawzdargo et al., 1999). It consists of 319 amino acids containing glycosylation consensus sequences and protein kinase

A/C phosphorylation sites (see Figure 1.3) (Sawzdargo et al., 1999). Despite being implicated as a novel cannabinoid receptor, the GPR55 receptor displays low sequence identity (10-15%) to CB_1 and CB_2 receptors (Sawzdargo et al., 1999). The receptors with highest amino acid similarity are the $P2Y_5$ purinoceptor, CCR4 chemokine receptor and the orphan GPR23 and GPR35 (Sawzdargo et al., 1999).

The GPR55 receptor has been identified in the genome of rat, mouse, dog, cow, chimpanzee and human (Sawzdargo et al., 1999). In humans, GPR55 mRNA expression is present in the spleen and brain, specifically the caudate nucleus and putamen (Sawzdargo et al., 1999). In the rat and mouse, GPR55 mRNA is found in spleen, intestine, adrenals, and CNS (Ryberg et al., 2007). In the mouse brain, GPR55 receptor mRNA is broadly distributed although its levels are significantly lower compared to CB_1 receptor expression. GPR55 mRNA has also been found in primary mouse microglia and the BV-2 mouse microglia cell line (Pietr et al., 2009) and in both human and mouse osteoclasts and osteoblasts (Whyte et al., 2009).

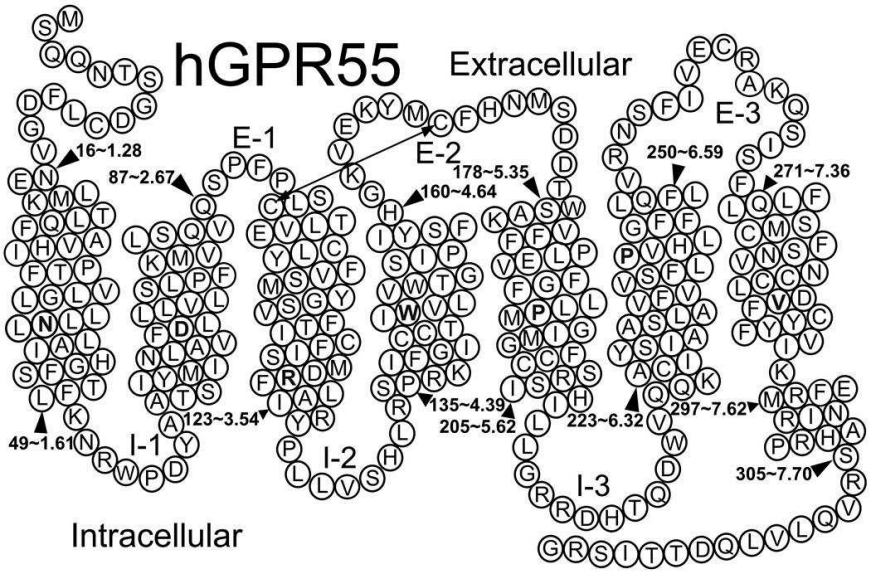

Figure 1.3. Structure of GPR55. Figure from (Sharir and Abood, 2010).

1.12.1. GPR55 receptor pharmacology

The GPR55 receptor was initially proposed as a novel third cannabinoid receptor on the basis of AstraZeneca and GlaxoSmithKline (GSK) patents identifying cannabinoid ligands (CP55940, SR141716A and AM251) as GPR55 agonists. Subsequent studies revealed a complex pharmacological profile for cannabinoid ligands at GPR55 with agonist or antagonist activity observed for an individual ligand that seemed to be dependent on the cell- and assay-type studied (Ross, 2009, Sharir and Abood, 2010). These studies are summarised in Table 1.4 below. Cell systems used to investigate GPR55 pharmacology and downstream signalling include: HEK293 (Johns, 2007, Oka et al., 2007, Ryberg et al., 2007, Lauckner et al., 2008, Kapur et al., 2009, Yin, 2009, Anavi-Goffer et al., 2012), human umbilical vein endothelial cell (HUVEC) (Waldeck-Weiermair et al., 2008), DRG (Lauckner et al., 2008), U2OS (Kapur et al., 2009) and osteoclasts (Whyte et al., 2009). Assay systems

used to determine the efficacy and potency of ligands at GPR55 include: extracellular regulated kinase (ERK) 1/2 phosphorylation (Oka et al., 2007, Lauckner et al., 2008, Waldeck-Weiermair et al., 2008, Kapur et al., 2009, Whyte et al., 2009, Anavi-Goffer et al., 2012), Rho (Ryberg et al., 2007, Lauckner et al., 2008, Whyte et al., 2009), nuclear factor of activated T cells (NFAT) activation (Waldeck-Weiermair et al., 2008), mobilisation of intracellular Ca^{2+} (Oka et al., 2007, Lauckner et al., 2008, Waldeck-Weiermair et al., 2008), GTPγS (Johns, 2007, Oka et al., 2007, Ryberg et al., 2007) and βarrestin binding (Kapur et al., 2009, Yin, 2009). Despite the controversy, it seems conclusive that the endogenous lysophospholipid LPI functions as a GPR55 agonist (Oka et al., 2007, Lauckner et al., 2008, Kapur et al., 2009, Whyte et al., 2009, Yin, 2009).

Table 1.4. A comparison of the pharmacological profile of ligands for GPR55. Adapted from (Sharir and Abood, 2010)

Ligand	Cell type	Read Out								Citation
		GTPγS Assay	ERK 1/2	$[Ca^{2+}]^i$ mobilisation	B-arrestin	Internalization	RhoA activation	NFAT	PKCβ	
LPI	hGPR55-HEK293	Agonist	Agonist	Agonist	Agonist	Agonist	Agonist	Agonist	Not tested	(Oka et al., 2007, Lauckner et al., 2008, Henstridge et al., 2009, Yin, 2009)
	hGPR55E-HEK293	Not tested	Not tested	Not tested	Not tested	Agonist	Not tested	Not tested	Not tested	(Kapur et al., 2009)
	hGPR55-PKCβII-GFP-HEK293	Not tested	Not tested	Not tested	Not tested	Not tested	Not tested	Not tested	Agonist	(Kapur et al., 2009)
	hGPR55E-U2OS	Not tested	Agonist	Not tested	Agonist	Agonist	Not tested	Not tested	Not tested	(Kapur et al., 2009)
	Mouse DRG	Not tested	Not tested	Agonist	Not tested	Not tested	Not tested	Not tested	Not tested	(Lauckner et al., 2008)

Table 1.4. (cont)

	EA.hy926	Not tested	Not tested	Agonist	Not tested	Not tested	Not tested	Not tested	Not tested	(Waldeck-Weiermair et al., 2008)
	Human osteoclasts	Not tested	Agonist	Not tested	Not tested	Not tested	Not tested	Not tested	Not tested	(Whyte et al., 2009)
	Mouse osteoclasts	Not tested	Not tested	Not tested	Not tested	Not tested	Agonist	Not tested	Not tested	(Whyte et al., 2009)
	BV-2	Not tested	Agonist	Agonist	Not tested	Not tested	Agonist	Not tested	Not tested	(Pietr et al., 2009)
AEA	hGPR55-HEK293	Agonist	Agonist	No effect	Agonist	Not tested	Not tested	Not tested	Not tested	(Oka et al., 2007, Ryberg et al., 2007, Lauckner et al., 2008, Henstridge et al., 2009, Yin, 2009)
	hGPR55E-HEK293	Not tested	No effect	Not tested	Not tested	No effect	Agonist	Not tested	Not tested	(Kapur et al., 2009)
	hGPR55E-U2OS	Not tested	No effect	Not tested	No effect	Not tested	Agonist	Not tested	Not tested	(Kapur et al., 2009)

Table 1.4. (cont)

	BV-2	Not tested	Not tested	No effect	Not tested	Not tested	Not tested	Not tested	Not tested	
2-AG	hGPR55-HEK293	Agonist	No effect	No effect	No effect	Not tested	Not tested	Agonist	Not tested	(Oka et al., 2007, Ryberg et al., 2007, Lauckner et al., 2008, Henstridge et al., 2009, Yin, 2009)
	hGPR55E-HEK293	Not tested	No effect	Not tested	Not tested	No effect	Not tested	Not tested	Not tested	(Kapur et al., 2009)
	hGPR55E-U2OS	Not tested	No effect	Not tested	No effect	Not tested	Not tested	Not tested	Not tested	(Kapur et al., 2009)
	BV-2	Not tested	Not tested	No effect	Not tested	Not tested	Not tested	Not tested	Not tested	
Δ^9-THC	hGPR55-HEK293	Agonist	No effect	Agonist	Agonist	Not tested	Not tested	Not tested	Not tested	(Oka et al., 2007, Ryberg et al., 2007, Lauckner et al., 2008, Yin, 2009)
	mGPR55-HEK293	Not tested	Not tested	Agonist	Not tested	Not tested	Not tested	Not tested	Not tested	(Lauckner et al., 2008)

Table 1.4. (cont)

	hGPR55E-HEK293	Not tested	Not tested	Not tested	Not tested	No effect	Agonist	Not tested	Not tested	(Kapur et al., 2009)
	hGPR55E-U2OS	Not tested	Not tested	Not tested	No effect	Not tested	Not tested	Not tested	Not tested	(Kapur et al., 2009)
	Mouse DRG	Not tested	Not tested	Agonist	Not tested	Not tested	Not tested	Not tested	Not tested	(Lauckner et al., 2008)
	BV-2	Not tested	Not tested	Agonist	Not tested	Not tested	Not tested	Not tested	Not tested	
CBD	hGPR55-HEK293	Agonist	No effect	No effect	No effect	Not tested	Not tested	Not tested	Not tested	(Ryberg et al., 2007, Lauckner et al., 2008, Yin, 2009)
	hGPR55E-U2OS	Not tested	Not tested	Not tested	No effect	Not tested	Not tested	Not tested	Not tested	(Lauckner et al., 2008)
	BV-2	Not tested	Not tested	Agonist	Not tested	Not tested	Agonist	Not tested	Not tested	
	Human osteoclasts	Not tested	Antagonist	Not tested	Not tested	Not tested	Not tested	Not tested	Not tested	(Whyte et al., 2009)
abnCBD	hGPR55-HEK293	Agonist	No effect	No effect	No effect	Not tested	Not tested	Not tested	Not tested	(Ryberg et al., 2007, Lauckner et al., 2008, Yin, 2009, (Johns, 2007)

Table 1.4. (cont)

	hGPR55E-U2OS	Not tested	Not tested	Not tested	No effect	No tested	Agonist	Not tested	Not tested	(Kapur et al., 2009)
O-1602	hGPR55-HEK293	Agonist	Not tested	No effect	No effect	Not tested	Not tested	Not tested	Not tested	(Ryberg et al., 2007, Yin, 2009, (Johns, 2007, Oka et al., 2007)
	hGPR55E-U2OS	Not tested	Not tested	Not tested	No effect	Not tested	Not tested	Not tested	Not tested	(Kapur et al., 2009)
	EA.hy926	Not tested	Not tested	Agonist	Not tested	Not tested	Not tested	Not tested	Not tested	(Waldeck-Weiermair et al., 2008)
	human osteoclasts	Not tested	Agonist	Not tested	Not tested	Not tested	Agonist	Not tested	Not tested	(Whyte et al., 2009)
	Mouse osteoclasts	Not tested	Not tested	Not tested	Not tested	Not tested	Agonist	Not tested	Not tested	(Whyte et al., 2009)
CP55940	hGPR55-HEK293	Agonist	No effect	No effect + Antagonist	No effect	Not tested	Not tested	Not tested	Not tested	(Oka et al., 2007, Ryberg et al., 2007, Henstridge et al., 2009, Yin, 2009)
	hGPR55E-HEK293	Not tested	Not tested	Not tested	Not tested	No effect	Not tested	Not tested	Not tested	(Kapur et al., 2009)

Table 1.4. (cont)

	hGPR55-PKCβII-GFP-HEK293	Not tested	Not tested	Not tested	Not tested	Not tested	Not tested	Not tested	Agonist	(Kapur et al., 2009)
	hGPR55E-U2OS	Not tested	Antagonist	No effect	Not tested	Not tested	Not tested	Not tested	Not tested	(Kapur et al., 2009)
	BV-2	Not tested	Not tested	No effect	Not tested	Not tested	Not tested	Not tested	Not tested	
JWH-015	hGPR55-HEK293	Not tested	No effect	Agonist	Not tested	Not tested	Agonist	Not tested	Not tested	(Lauckner et al., 2008)
	mGPR55-HEK293	Not tested	Not tested	Agonist	Not tested	Not tested	Not tested	Not tested	Not tested	(Lauckner et al., 2008)
	Mouse DRG	Not tested	Not tested	Agonist	Not tested	Not tested	Not tested	Not tested	Not tested	(Lauckner et al., 2008)
	hGPR55E-U2OS	Not tested	Not tested	Not tested	Not tested	No effect	Not tested	Not tested	Not tested	(Kapur et al., 2009)
SR141716A	hGPR55-HEK293	Not tested	Agonist	Agonist + Antagonist	Agonist	Agonist	Not tested	Agonist	Not tested	(Oka et al., 2007, Lauckner et al., 2008, Henstridge et al., 2009, Yin, 2009)

Table 1.4. (cont)

	hGPR55E-HEK293	Not tested	No effect	Not tested	Not tested	Agonist	Not tested	Not tested	Not tested	(Kapur et al., 2009)
	hGPR55E-U2OS	Not tested	No effect	Not tested	Agonist	Agonist	Not tested	Not tested	Agonist	(Kapur et al., 2009)
	hGPR55-PKCβII-GFP-HEK293	Not tested	Not tested	Not tested	Not tested	Not tested	Not tested	Not tested	Not tested	(Kapur et al., 2009)
	EA.hy926	Not tested	Not tested	Antagonist	Not tested	Not tested	Not tested	Not tested	Not tested	(Waldeck-Weiermair et al., 2008)
	Mouse DRG	Not tested	Not tested	Antagonist	Not tested	Not tested	Not tested	Not tested	Not tested	(Lauckner et al., 2008)
	BV-2	Not tested	Not tested	No effect	Not tested	Not tested	Not tested	Not tested	Not tested	
AM251	hGPR55-HEK293	Agonist	Not tested	Agonist	Agonist	Agonist	Not tested	Agonist	Not tested	(Ryberg et al., 2007, Henstridge et al., 2009, Yin, 2009)
	hGPR55E-HEK293	Not tested	No effect	Not tested	Not tested	Agonist	Not tested	Not tested	Not tested	(Kapur et al., 2009)

Table 1.4. (cont)

	hGPR55E-U2OS	Not tested	Not tested	Not tested	Not tested	Not tested	Not tested	Not tested	Agonist	(Kapur et al., 2009)
	hGPR55-PKCβII-GFP-HEK293	Not tested	No effect	Not tested	Agonist	Agonist	Not tested	Not tested	Not tested	(Kapur et al., 2009)
AM281	hGPR55-HEK293	Agonist	Not tested	Agonist	Not tested	Agonist	Not tested	Agonist	Not tested	(Kapur et al., 2009)
	hGPR55E-U2OS	Not tested	Not tested	Not tested	No effect	Not tested	Not tested	Not tested	Not tested	(Ryberg et al., 2007, Henstridge et al., 2009)

Several studies have investigated the effect of the aforementioned ligands using various pharmacological end-points that have furthered understanding of GPR55 downstream signalling (see Figure 1.4).

Figure 1.4. Downstream signalling events initiated by GPR55.

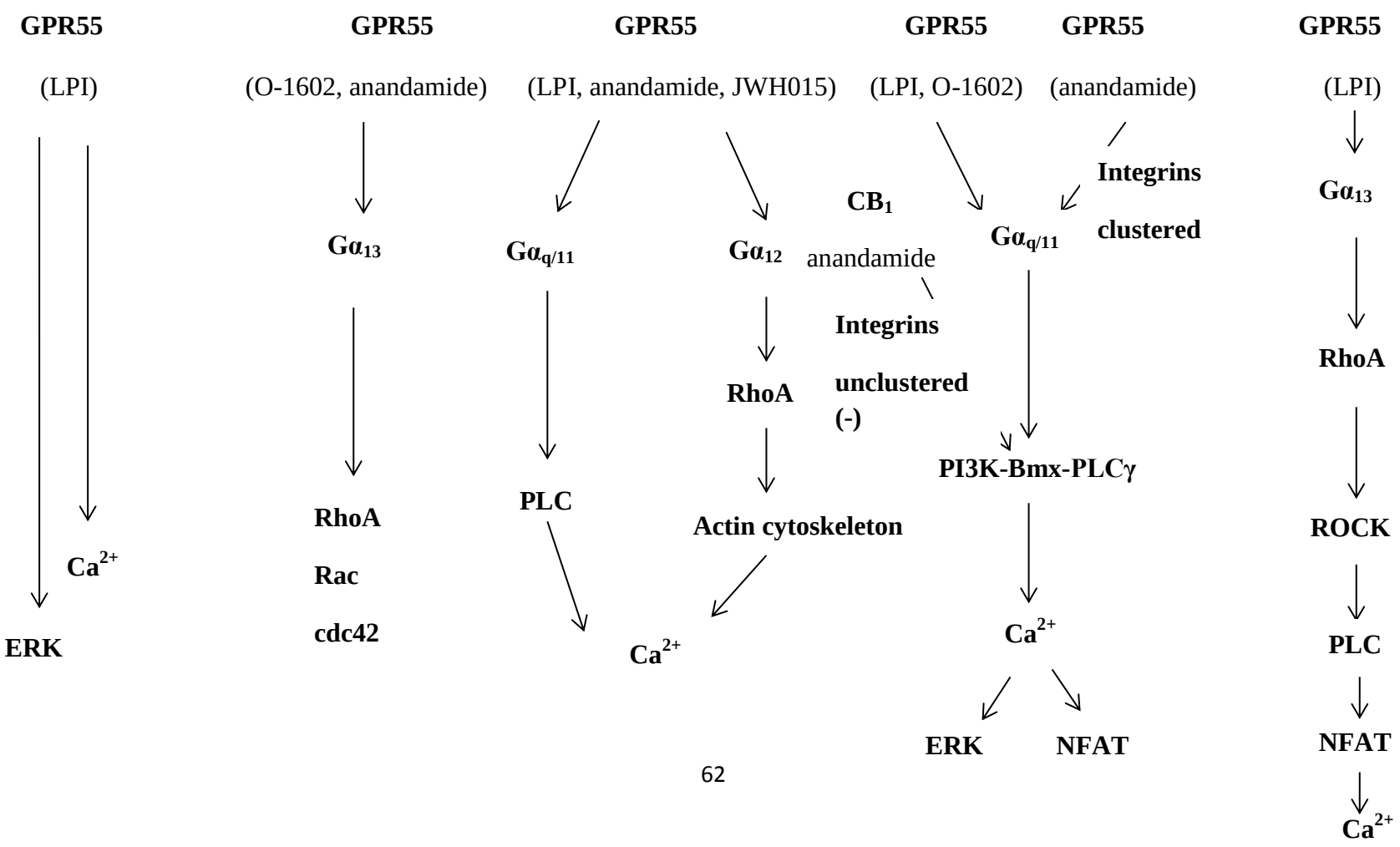

1.12.2. GPR55 receptor and nociception

A role for the GPR55 receptor in the modulation of nociception has been proposed (Lauckner et al., 2008, Staton et al., 2008, Schuelert and McDougall, 2011, Breen et al., 2012, Gangadharan et al., 2013). A study from GSK suggested GPR55 as a novel target for inflammatory and neuropathic pain (Staton et al., 2008). Cutaneous mechanical hyperalgesia failed to develop in GPR55 knockout mice subjected to CFA induced inflammation and partial sciatic nerve ligation induced nerve injury (Staton et al., 2008). Hind paw levels of anti-inflammatory cytokines (IL-4 and IL-10) were increased in GPR55 knock out compared to wild-type mice. Evidence suggests pro-inflammatory cytokines involved in pain and inflammation are modulated by a cascade of anti-inflammatory cytokines (Kanaan et al., 1998, George et al., 2004, Kleinschnitz et al., 2004) suggesting GPR55 potentially contributes to inflammatory pain by inhibiting anti-inflammatory cytokine activity. Further evidence suggesting a role for GPR55 in nociception was provided by a study demonstrating that intra-peritoneal (i.p) administration of the putative GPR55 agonist O-1602 in an ethanol vehicle prevented the anti-allodynic effects observed following administration of the vehicle alone in the CCI model of nerve injury and exacerbated the CCI-induced reduction in paw withdrawal thresholds (Breen et al., 2012).

Recent evidence has implicated a peripheral site of action of the GPR55 receptor in the modulation of nociception (Lauckner et al., 2008, Gangadharan et al., 2013). Behavioural and electrophysiological studies in naïve mice

demonstrated that intra-plantar administration of the GPR55 agonist LPI induced hind paw mechanical allodynia and mechanical hyperalgesia while cutaneous A fibre mechansensitivity assessed in an ex vivo skin nerve preparation was increased by LPI (Gangadharan et al., 2013). Although the use of GPR55 knock out mice confirmed a contribution of GPR55, a contribution of a non-GPR55 mechanism(s) was proposed to mediate effects of LPI at higher concentrations and during acute mechanical hyperalgesia. A peripheral site of action is corroborated by the demonstration of GPR55 expression in mouse DRG neurones predominantly in large diameter (>35µm) neurones but also at low levels in small-medium diameter neurones (Lauckner et al., 2008). Almost all NF200-positive DRG neurones were strongly GPR55-immunoreactive, whereas very few/no IB4- and CGRP-positive neurones were found to be strongly GPR55-immunoreactive. Medium and large DRG neurones expressing GPR55 were weakly and strongly TRPV-1 positive respectively (Lauckner et al., 2008). The expression of GPR55 in DRG neurones is corroborated by the demonstration that LPI increased intracellular Ca^{2+}concentration in large diameter DRG neurones (Lauckner et al., 2008), an effect that would be expected to increase neuronal excitability and could be the mechanistic basis of the pro-nociceptive role of GPR55 demonstrated in the aforementioned behavioural studies.

Studies have also investigated the intracellular signalling pathways involved in mediating GPR55 effects on nociception. Genetic deletion of G_{13} and $G_{q/11}$ abolished LPI-induced mechanosensitization of cutaneous A-fibre nociceptors

to low intensity mechanical stimulation although at higher intensities mechanical hypersensitivity to LPI remained (Gangadharan et al., 2013). This finding indicates that the hyperalgesic effect of LPI occurs via a G_{13}- and $G_{q/11}$-independent manner. LPI-induced behavioural allodynia was found to be dependent on ERK-1/2 activation in DRG nociceptors which was predominantly mediated by the G_{13} pathway although $G_{q/11}$ was partially involved (Gangadharan et al., 2013).

Despite the existence of evidence suggesting a pro-nociceptive role, the GPR55 receptor has been demonstrated to have an anti-nociceptive role in a model of acute inflammatory joint pain (Schuelert and McDougall, 2011). Peripheral administration of the synthetic GPR55 agonist O-1602 attenuated the mechanosensitivity of nociceptive knee joint afferent C-fibres which was abolished by the GPR55 antagonist O-1918, contrasting with the sensitizing effects on cutaneous A-fibres described above (Gangadharan et al., 2013). This data provides further evidence of a peripheral site of action for the GPR55 receptor and collectively with data described above suggests that the role of the GPR55 receptor in the modulation of nociception is complex and tissue-specific roles i.e. cutaneous vs joint nociception may be apparent. As such, further studies are required to increase understanding of GPR55 and its role in modulating nociception and the potential of targeting GPR55 in joint pain. This thesis has investigated the role of GPR55 in the modulation of joint afferent nociceptor mechanosensitivity under non-pathological conditions and has

translated these investigations into a model of arthritic pain (i.e. OA), to assess the potential of targeting GPR55 for the relief of chronic joint pain.

1.13. Introduction to OA

OA is the most common form of arthritis with 8.75 million people in the UK alone seeking clinical help for treatment each year (Pereira et al., 2011, Conaghan et al., 2014). The number of patients suffering from OA is expected to double in the next 20 years due to an ageing population and an obesity epidemic (Conaghan et al., 2014). The impact of OA on patients and their families is comparable to cardiac, neurological and pulmonary diseases while loss of working hours due to OA costs the UK economy up to £18 billion per year (Loza et al., 2008, Cooper et al., 2011, Nuesch et al., 2011). Therefore, long term conditions such as OA are a current NHS priority with an aim to improve health-related quality of life (Conaghan et al., 2014).

OA was defined by the OA Research Society International (OARSI) in 2011 as ‘a progressive disease affecting synovial joints that can result in degeneration of cartilage and subchondral bone with swelling of the joint’ (see Figure 1.5) (Lane et al., 2011). OA is most common in load bearing joints of the knee, hip but also in joints of the hand and feet with the disease localised to a single joint, a few joints or generalized (Lane et al., 2011). The aetiology of OA is complex although risk factors have been identified, including increasing age (Arden and Nevitt, 2006, Scott, 2006), obesity (Grotle et al., 2008, Lohmander

et al., 2009) and gender with women 1.7 times more at risk (Felson et al., 1995). Several studies have suggested that OA is a result of abnormal i.a. stress and an inability to repair joint damage arising from biomechanical (Sharma et al., 2001, Sharma et al., 2006) or biochemical and genetic factors (Garnero et al., 2008, Cheung et al., 2010, Valdes and Spector, 2010, Valdes et al., 2011).

The symptoms of OA include functional disability and stiffness of the joint but pain is the dominant symptom. Pain is the most common complaint in OA patients seeking help from a physician (Gwilym et al., 2008) and as such OA pain is a major clinical problem that can lead to a poor quality of life and significant levels of morbidity (Conaghan et al., 2014). The analgesics that are currently available to treat OA pain (e.g. NSAIDs and weak opioids) have limitations such as variable pain relief, potential for abuse and use limiting side effects associated with chronic usage (Breivik et al., 2006, McDougall and Linton, 2012). Due to the limited effectiveness of current analgesics, many patients with chronic OA pain eventually undergo joint replacement surgery (Dixon et al., 2004) although around 20% of patients still experience pain following arthroplasty (Saxler et al., 2007, Gwilym et al., 2008, Wylde et al., 2011).

In order to develop improved analgesics for OA pain, a greater understanding of the pathophysiological mechanisms that occur during OA pain development is required. It has been proposed that targeting pain at the level of the joint, the

source of the injury, may alleviate pain more effectively and reduce the prevalence of side-effects (McDougall, 2011). Identification of the importance of a peripheral drive to OA pain has already been established with the alleviation of pain in 60-80% of patients (depending on the affected site) following joint replacement surgery (Kosek and Ordeberg, 2000b) and i.a. injection of local anaesthetic (Creamer et al., 1996, Crawford et al., 1998). These findings suggest that pain is driven by factors within the local joint environment in most patients.

In this thesis, knee joint OA was studied as it is the most common joint to be affected (Scott, 2006). Methods for assessing pain behaviour and electrophysiological characteristics of joint nociceptors that can be applied to animal models of knee OA are available (Schaible and Schmidt, 1983a, Schaible and Schmidt, 1983b, Kelly et al., 2012). Changes to joint histology, pain behaviour and nociceptor mechanosensitivity that mimic the human disease have also been established (Vincent et al., 2012).

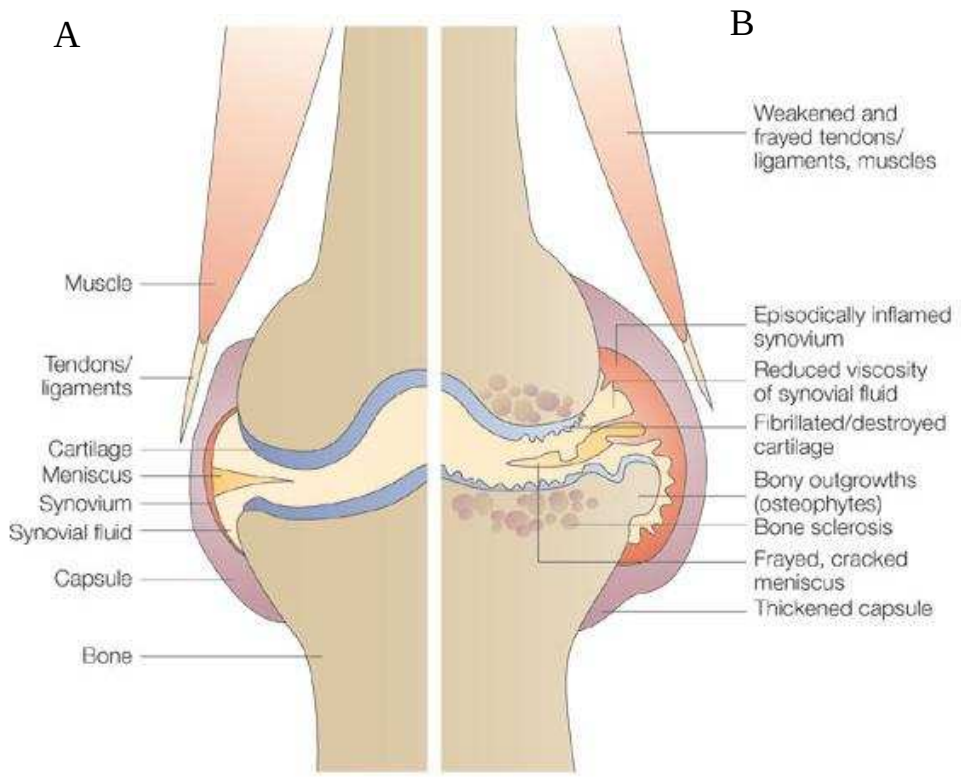

Figure 1.5. Comparison of a normal (A) and OA (B) joint. Taken from (Wieland et al., 2005).

1.13.1. Pain in OA

Pain in OA is debilitating and disabling affecting normal daily activities and reducing the quality of life of sufferers (Creamer et al., 1998). The pain can be use-related as well as spontaneous. Understanding of the mechanisms of OA pain has been limited as previous research has focused on the mechanisms driving joint degeneration (Neogi et al., 2009) which may not be same as those causing pain. Since the development of preclinical models of OA pain (Bendele, 2001) the situation is improving.

Studies examining radiological and magnetic resonance imaging (MRI) findings have found that a direct correlation between joint pathology and pain severity does not occur for most patients; some patients report severe pain with extensive joint pathology while others have extensive joint pathology and are asymptomatic with respect to pain (Hannan et al., 2000, Scott, 2006). These clinical findings are in line with the monosodium iodoacetete (MIA) rat model of OA (Kelly et al., 2012) and spontaneous model of OA in the Dunkin Hartley guinea pig in which a correlation between pain behaviour and joint pathology did not exist (McDougall et al., 2009). Therefore, it is possible that the mechanisms driving OA pain are not identifiable by radiographic and histological means.

1.13.2. Contribution of joint structure degeneration to OA pain

The exact anatomical source(s) of pain in OA is not known. The subchondral bone, periosteum, joint capsule, synovium, ligaments and meniscus are all highly innervated structures and may represent potential sources of pain during OA (McDougall and Linton, 2012). The absence of articular cartilage innervation indicates that it is unlikely to contribute to pain directly (McDougall and Linton, 2012). However, a study identified that in OA, angiogenesis occurs within the subchondral bone and extends past the calcified/non-calcified joint tidemark into the normally aneural cartilage (Suri et al., 2007). Cartilage vascularisation is followed by peri-vascular free nerve endings that may enable the previously aneural cartilage to mediate nociception and contribute to OA pain (Suri et al., 2007).

The presence of bone marrow lesions (BMLs) in knees identified by knee MRI has been associated with symptomatic OA (Felson et al., 2001). BMLs could be a consequence of an increase of water, blood or fluid inside the bone, reflecting oedema or contusions to the joint which may contribute to pain in OA patients by increasing intraosseous pressure and activating sensory nerves (Felson et al., 2001).

The association of synovial inflammation and synovial thickening with pain in OA indicates that nociceptor innervation of the synovium may contribute to pain (Hill et al., 2001, Ashraf et al., 2011a). Inflammation of the synovium in OA is characterised by synovial hyperplasia, tissue fibrosis, thickening of the synovial capsule and B and T cell infiltration (Hunter et al., 2008). The proinflammatory and pronociceptive mediators (BK, PGs, neuropeptides and cytokines) released during the inflammatory response may cause pain by directly exciting and/or sensitizing knee joint nociceptors (Heppelmann and Pawlak, 1997b, Wang et al., 2006b, Hunter et al., 2008, Richter et al., 2012).

The recent development of animal models of OA that not only model its histological features but also the associated pain symptoms has broadened our understanding of the underlying mechanisms contributing to pain in OA and of novel analgesic targets. In this thesis the MIA model was chosen to investigate the effects of GPR55 receptor activation on joint nociceptive mechanisms.

1.13.3. Pain behaviour and joint degeneration in the MIA model of OA

Studies aimed at identifying novel analgesic strategies for human OA have been hampered due of the lack of rapid, reproducible models that closely mimic both the pain and structural changes associated with the disease. The MIA model of OA has been recently characterised in the rat (Bove et al., 2003, Guzman et al., 2003, Combe et al., 2004, Fernihough et al., 2004, Kelly et al., 2012, Mapp et al., 2013) and mouse (Harvey and Dickenson, 2009, Ogbonna et al., 2013) with studies describing pathological progression, pain symptoms and peripheral nerve sensitisation that parallel human OA.

MIA is a chemical that when injected into the rodent knee joint (under general anaesthesia) inhibits the activity of glyceraldehyde-3-phosphate dehydrogenase in chondrocytes which prevents glycolysis and induces cell death leading to pathological articular changes that resemble human OA (Guzman et al., 2003). Degradation of chondrocytes and an inflammatory response (persisting up to 49 days) have been observed from day one post-injection (Guzman et al., 2003, Fernihough et al., 2004, Mapp et al., 2013). At day 7 post-injection, proteoglycan levels in cartilage are reduced and osteoclast numbers are increased at the junction between cartilage and subchondral bone, signalling the beginning of changes to the subchondral bone and bone resorption. Extensive loss of cartilage proteoglycan occurs by 14 days post-injection with additional signs of sheer stress in the cartilage. Further, bone resorption continues and osteophytes appear by 14 days (Mapp et al., 2013). At 21-28 days, the cartilage is extensively thinned and the subchondral bone thickened

with continued development of osteophytes (Fernihough et al., 2004). By day 56, joint degeneration is vast with extensive remodelling of the bone, subchondral sclerosis and fragmented and necrotic areas of cartilage (Guzman et al., 2003).

In addition to joint pathology, intra-articular injection of MIA results in pain behaviour that mimics pain symptoms associated with human OA including significant weight bearing asymmetry, pain in response to movement of the joint (flexion and extension of the knee), hind paw mechanical hyperalgesia, and secondary tactile allodynia (Bove et al., 2003, Combe et al., 2004, Fernihough et al., 2004, Ferreira-Gomes et al., 2010, Kelly et al., 2012). The extent of pain behaviour is related to the concentration of MIA (ranging from 1-3mg) injected (Bove et al., 2003, Guzman et al., 2003, Schuelert and McDougall, 2009, Sagar et al., 2010). Weight bearing asymmetry is evident from day 1 and peaks at day 3 - 7 with increasing concentrations of MIA prolonging the effect, persisting for up to at least 35 days following a 1mg (Ashraf et al., 2013) and until at least 63 days following 2mg injection (Combe et al., 2004). Ipsilateral hind paw hypersensitivity is evident from days 3 - 7 post-MIA injection following a 1mg (Fernihough et al., 2004, Ashraf et al., 2013) or 3mg (Sagar et al., 2010) injection and is maintained at 35 days. In this thesis, a 1mg dose was chosen, and studies have been conducted primarily at 14 days post-injection during established joint pathology and pain behaviour.

Pain behaviour in the MIA model is attenuated following administration of analgesics or anti-inflammatory (e.g. diclofenac and morphine) agents that are

affective in man (Combe et al., 2004, Pomonis et al., 2005a, Schuelert and McDougall, 2009). This responsiveness to analgesics in clinical use justifies the inclusion of the MIA model in studies aimed at understanding mechanisms of pain in OA and in the potential screening of therapeutic agents or identification of novel analgesic targets. MIA-induced hyperalgesia is attenuated by diclofenac and paracetamol (NSAIDs) at 3-14 days post-injection although NSAIDs have reduced efficacy at later stages of the model (Fernihough et al., 2004, Ivanavicius et al., 2007), suggesting an early inflammatory phase followed at later stages by a reduced inflammatory component. Evidence suggests that a neuropathic component may also contribute to pain in the MIA model. Gabapentin and amitriptyline (used to treat neuropathic pain) alleviate pain throughout the progression of the MIA model, while ATF-3, a neuronal marker of nerve injury, is upregulated in the cell bodies of afferents which innervate the joint (Ivanavicius et al., 2007).

Studies have also investigated OA using spontaneously developing (Bendele and Hulman, 1988, Mason et al., 2001, McDougall et al., 2009) and surgically-induced models (Fernihough et al., 2004, Ashraf et al., 2013, Mapp et al., 2013). Spontaneously developing OA has been identified in some strains of mice (e.g. STR/ort), guinea pigs (e.g. Dunkin Hartley), Syrian hamsters and non-human primates (Bendele, 2001). Histological characteristics of OA develop including, cartilage degeneration, osteophyte formation, damage to subchondral bone and thickening of synovial membrane (Bendele and Hulman, 1988, Bendele, 2001). Increased numbers of spontaneously activate knee joint

nociceptors were recorded in a guinea pig model of spontaneous OA (McDougall et al., 2009). Limitations of spontaneous models include a slowly developing OA (e.g. guinea pigs; 18 months, mice; 9 - 12 months) resulting in increased study time and planning, difficulties with regard to selecting an adequate control for aged animals and pain testing in animals with bilateral disease, as well as variability and uncertainty of the time of onset between different animals within an experimental group (Bendele, 2001). Further, a limited number of studies have characterised pain behaviour in spontaneously developing models of OA (Bendele, 2001).

Surgical models of OA have been studied in dogs and rodents including, anterior cruciate ligament transection (ACLT) and partial medial meniscectomy (MNX) (Bendele, 2001). These models closely resemble the human condition and develop more rapidly than spontaneous OA models (Bendele, 2001). Pain behaviour has been characterised in the MNX model with weight bearing asymmetry and mechanical allodynia developing at 5 days post-surgery (Fernihough et al., 2004). However, mechanical hyperalgesia does not develop (Fernihough et al., 2004). An absence of weight bearing deficits and mechanical allodynia in the ACLT model prevents use in the study of pain behaviour (Ferland et al., 2011). The variations in pain behaviour limit the use of surgically-induced models of OA.

In this thesis, the MIA model was chosen as an experimental model of OA pain in which to investigate the in vivo effects of GPR55 receptor activation on joint nociception during joint disease as it is a reliable and reproducible model that mimics clinically observed joint pathology and pain symptoms. The MIA model is associated with both peripheral (Kelly et al., 2012, Kelly et al., 2013a, Bullock et al., 2014) and central sensitization (Sagar et al., 2010, Kelly et al., 2013b), features of human OA pain and is sensitive to analgesics used to treat OA pain in man.

1.14. Peripheral mechanisms of OA pain

As discussed previously (Section 1.6.4), understanding of the relationship between joint structural change and OA pain are limited. The innervation pattern of joint structures indicates that pain may rise from a number (or a combination) of articular structures. The innervation of the articular cartilage (aneural under non-pathological conditions) during OA disease onset may contribute to pain (Suri et al., 2007). Exposure of the OA cartilage to aberrant mechanical and chemical stimuli may sensitize innervating nociceptors (Schaible and Grubb, 1993, Suri et al., 2007). Subchondral bone may also contribute to OA pain as it receives sensory and nociceptive input from trkA expressing nociceptors (Aso et al., 2014, Mantyh, 2014). During the OA disease process, the subchondral bone plates become denuded and exposed to chemical and mechanical stimuli that they would not normally be exposed to (Felson et al., 2001, Kidd, 2006). Subchondral bone turnover, dependent on the activity of osteoclasts and osteoblasts, precedes changes in cartilage in OA and

inhibition of osteoclast activity prior to MIA-induced OA can attenuate the development of weight bearing deficits suggesting osteoclast activity may contribute to the development of pain in OA (Sagar et al., 2013).

Evidence suggests that the sensitization of knee joint nociceptors is an important feature associated with the severity of OA pain in humans and animal models (Arendt-Nielsen et al., 2010). The pain behaviour that follows MIA injection into rat knee joints (including weight bearing asymmetry) is associated with a mechanical sensitization of joint nociceptors (Fernihough et al., 2004, Schuelert and McDougall, 2009, Kelly et al., 2012, Kelly et al., 2013a, Bullock et al., 2014). This sensitization is manifest as an increased firing frequency of knee joint nociceptors in response to the application of von Frey (vF) monofilaments to their joint associated receptive fields and to noxious rotation of the joint as well as reduced mechanical thresholds for firing (Schuelert and McDougall, 2006b, Schuelert and McDougall, 2009, Schuelert et al., 2010, Kelly et al., 2012, Kelly et al., 2013a, Bullock et al., 2014). This increased sensitivity to mechanical stimuli as well as increased rates of spontaneous activity of joint nociceptors may underlie the pain OA patients experience during joint loading associated with normal daily activities (e.g. walking, climbing stairs) and pain at rest, respectively. Identifying the substrates and mechanisms that drive the sensitization of knee joint nociceptors during OA and thus the underlying pain as well as those that modulate this sensitization are likely to be important to the development of improved

analgesic strategies. Local targeting of these mechanisms within the diseased joint has the potential to reduce side-effects.

1.15. Putative peripheral chemical mediators of OA pain

1.15.1. BK

BK has been measured in the synovial fluid (SF) of OA joints and the likely source of this could be sensory nerves or damaged tissue (Bellucci et al., 2013). BK levels correlate with cartilage degradation and markers of inflammation (e.g. IL-6) (Bellucci et al., 2013). Evidence suggests that the bradykinin receptors (B1 and B2) contribute to OA pain (Kaufman et al., 2011). i.a. injection of B1 receptor antagonists in the ACLT surgical model of OA alleviates pain behaviour (weight bearing asymmetery) and joint pathology (e.g. chondropathy) (Kaufman et al., 2011). B2 receptor polymorphisms in humans are associated with increased risk of knee OA and augmented radiographic severity (Chen et al., 2012). Further, an i.a. B2 receptor antagonist alleviated pain in the MIA model (Cialdai et al., 2009) suggesting that BK has local sensitizing effects within the diseased joint. This is supported by the fact that BK increases the sensitivity of joint nociceptors to mechanical stimulation (Cesare and McNaughton, 1996a, Calixto et al., 2000, Wang et al., 2006a). The sensitizing effect of BK (via BK1 and BK2 receptors) is proposed to be mediated by an influx of Ca^{2+} ions and a phosphorylation and facilitation of TRPV1 function (Linhart et al., 2003) providing a putative mechanism by which bradykinin may contribute to pain in OA.

1.15.2. Prostanoids

The important role of PGs in OA pain is evident from the use of NSAIDs as a first line analgesic treatment for OA in the clinic (Hunter et al., 2008). PGE_2 levels have been measured in the SF of knee joints from OA patients (Li et al., 2009). Prostanoids such as PGI_2 and PGE_2 induce spontaneous activity and mechanical sensitization of knee joint afferents and also sensitize neurones to other inflammatory agents e.g. BK (Schaible and Schmidt, 1986, Schaible and Schmidt, 1988a, Neugebauer et al., 1989, Grubb et al., 1991, McQueen et al., 1991, Schepelmann et al., 1992, Schaible et al., 2006). Surgical induction of OA (cranial cruciate ligament transection) in dogs results in increases in the levels of PGE_2 in the SF that correlate with pain (lameness and weight bearing) (Trumble et al., 2004). In the MIA model of OA, oral administration of a PGI_2 antagonist reduced pain behaviour (weight bearing), similar to that of the NSAID diclofenac indicating that PGI_2 may contribute to the peripheral mechanisms of OA pain (Pulichino et al., 2006). However, as the antagonist was administered orally it could be acting centrally so this is not unequivocal evidence for a peripheral role.

1.15.3. TRPV1

Evidence from clinical studies has confirmed the relevance of TRPV1 in peripheral OA pain mechanisms in man (Remadevi and Szallisi, 2008). Knee OA pain is associated with increased TRPV1 expression in human synovia (Kelly et al., 2013a) and a single nucleotide polymorphism in the gene encoding TRPV1 is associated with the risk of developing symptomatic knee

OA (Valdes et al., 2011). Desensitization of TRPV1 expressing nociceptors with topical capsaicin patches is effective at alleviating pain in OA patients (Kosuwon et al., 2010) and ablation of capsaicin sensitive fibres prevents the development of pain behaviour in the MIA model. Systemic administration of TRPV1 antagonists in the MIA model abolished increased mechanosensitivity (Chu et al., 2011) and thermal hypersensitivity (Okun et al., 2012).

Evidence suggests that the analgesic effect of systemically administered TRPV1 antagonists is mediated at the level of the joint. A study using Fast Blue backlabelled L4 DRG joint afferents identified increased expression of TRPV1 in the MIA model compared to control rats (Fernihough et al., 2005). Further, i.a injection of the TRPV1 antagonist JNJ-17203212 reversed MIA-induced weight bearing asymmetry (Kelly et al., 2013a). Electrophysiological recordings in the same study identified that JNJ-17203212 inhibited mechanically-evoked responses and increased mechanical thresholds in MIA rats effectively reversing MIA-induced sensitization. Collectively these studies highlight the importance of TRPV1 and TRPV1 expressing afferents in the pathogenesis of OA pain.

1.15.4. CGRP

It has been proposed in clinical and pre-clinical studies that the sensory neuropeptide CGRP has an important role in the modulation of peripheral sensitization during OA pain (Fernihough et al., 2005, Saxler et al., 2007,

Ashraf et al., 2011b, Bullock et al., 2014). CGRP immunoreactive fibres innervate the joint capsule, synovial membrane, joint ligaments, subchondral bone, meniscus, fat pad and tendons (Fernihough et al., 2005). The number of CGRP-expressing sensory neurones innervating the outer menisci increased in knee OA patients with high chondropathy scores (Ashraf et al., 2011c). A role in the modulation of OA pain was indicated by an increase in the number of nerve fibres containing GGRP in the hip of painful OA patients while the sensory neuropeptide was not found in asymptomatic patients (Saxler et al., 2007).

CGRP-expressing joint nociceptors are also increased in the MIA model (Fernihough et al., 2005). Peripheral administration of exogenous CGRP sensitizes joint nociceptors to mechanical stimuli in MIA and saline rats with a greater proportion sensitized after the development of knee OA (Bullock et al., 2014).. The mechanically sensitized responses of joint nociceptors were inhibited by a CGRP receptor antagonist in both MIA and MNX rats whereas CGRP receptor antagonism had no effect in both saline and sham control rats (Bullock et al., 2014). These data suggest that CGRP has an important role in the mechanisms driving peripheral sensitization during OA.

1.15.5. NGF

A role for neurotrophin NGF in the mechanisms of OA pain has been suggested from studies in humans (Aloe et al., 1992, Iannone et al., 2002, Lane

et al., 2010, Balanescu et al., 2013) and animal models (Orita et al., 2011, Ashraf et al., 2013). NGF expression increases in the SF of OA patients (Aloe et al., 1992) and human OA chondrocytes (Iannone et al., 2002). Recent clinical trials have demonstrated that anti-NGF antibodies effectively reduce pain and improve joint function in OA patients (Lane et al., 2010, Balanescu et al., 2013, Spierings et al., 2013). However, clinical trials were halted because a minority of patients developed worsening OA symptoms (rapidly progressing OA with osteonecrosis) which eventually required joint replacement highlighting a need for a better understanding of the role of NGF in OA. In agreement with human studies, the MIA model of OA is associated with an up-regulation of NGF in joint tissues (whole joint homogenates) (Orita et al., 2011) and MIA-induced pain is augmented following i.a. NGF, which may be related to increased expression of the NGF receptor trkA in joint nociceptors and facilitated NGF signalling in this model (Ashraf et al., 2013). A broader understanding of the consequences of NGF inhibition on the joint is required before the full clinical utility of NGF antagonists can be realised.

1.16. The peripheral cannabinoid receptor system as a novel target for the treatment of pain in OA

Both clinical and pre-clinical studies have identified that the peripheral cannabinoid receptor system is a potential novel analgesic target for the treatment of OA pain (Richardson et al., 1998, Schuelert and McDougall, 2008, Schuelert et al., 2010). The expression of protein and RNA for CB_1 and CB_2 has been identified in the synovium of OA patients undergoing knee

arthoplasty (Richardson et al., 2008). The endocannabinoids anandamide and 2-AG have been measured in the SF of OA patients. Activation of peripheral CB_1 and CB_2 receptors modulates knee joint nociceptor mechanosensitization in the MIA model of knee OA (Schuelert and McDougall, 2008, Schuelert et al., 2010). The peripheral administration of ACEA (CB_1 agonist) inhibited the mechanically-evoked firing rate of joint nociceptors (Schuelert and McDougall, 2008) while in a separate study GW405833 (CB_2 agonist) had a paradoxical mechanosensitizing effect (Schuelert et al., 2010). The identification of peripheral cannabinoid receptors as modulators of nociception in knee OA and the inhibitory effects of GPR55 receptor activation by a synthetic agonist in a model of acute joint inflammation (Schuelert and McDougall, 2011) provide the rationale for assessing the potential of GPR55 activation in modulating joint nociception during OA.

1.17. Overall aim of this thesis

GPR55 has recently been identified as a potential novel peripheral target in the treatment of pain. However, investigations of the role of GPR55 in nociception are at an extremely early stage and evidence for both a pro- and anti-nociceptive role has been provided that seems to be dependent on the tissue-type and perhaps pathological condition studied. Given this paucity of data and lack of clarity, further studies are required to increase understanding of the role of GPR55 in nociception. The mechanical sensitization of joint nociceptors is thought to be important in driving joint pain mechanisms in man as well in animal models. No studies to date have directly investigated the role of

peripheral GPR55 in the modulation of joint nociceptor mechanosensitivity under normal conditions, or its modulation of peripheral sensitization in OA pain models. Therefore, the overall aim of this thesis was to define the potential of GPR55 receptor activation in modulating joint nociceptor mechanical sensitivity under non-pathological conditions (naive) and in the MIA model of OA pain in the rat.

Chapter Two

Materials and methods

2.1. Animals

All in-vivo experiments were carried out in accordance with the Animals Scientific Procedures Act (ASPA) 1986 and European Directive 2010/63/EU. Licensed procedures were carried out under project and personal license numbers 40/3246 and 44/9956, respectively. All experiments were approved by the University of Nottingham Animal Welfare and Ethical Review Body (AWERB) and were carried out in accordance with the 3R's (reduction, refinement and replacement) and ARRIVE guidelines.

Male Sprague Dawley rats (Charles River, Margate, Kent, UK) were used in all experiments. Animals were housed 3 per cage in temperature and humidity controlled rooms on a 12:12hr light: dark cycle (lights on at 8:00am). Food (standard rat chow) and water were freely available.

2.2. Induction of knee OA with MIA

The MIA model of knee OA was established as described previously (Bove et al., 2003, Sagar et al., 2010, Liu et al., 2011, Kelly et al., 2012, Kelly et al., 2013a, Kelly et al., 2013b, Mapp et al., 2013). Aseptic techniques were used throughout, in accordance with Laboratory Animal Science Association (LASA) guidelines along with Home Office and Named Veterinary Surgeon (NVS) advice. Rats had an average weight of 208 ± 4.96g (range: 152 - 301g) at the time of OA induction and 209 ± 4.71g (range: 146 - 266g) at the time of saline injection. Animals undergoing recovery procedures were placed into a

transparent induction box and anaesthetised with isoflurane (3% in oxygen (O_2); 2 litres/min) until the righting reflex was lost. The rat was then removed from the induction box and anaesthesia was maintained via a facemask, allowing the isoflurane concentration to be reduced (2.0 - 2.5% in O_2; 1.5 litres/min) and more precisely controlled. Once an adequate depth of anaesthesia was achieved, determined by a lack of withdrawal reflex to a strong pinch to the hind paw and monitoring of the rate and depth of breathing, the left knee joint was shaved and cleaned with surgical spirit (Vetasept, Animalcare, York). With the left knee joint flexed at a 90º angle, 1mg of MIA in 50µl sterile saline was injected into the joint space, through the patella tendon, using a 0.5ml insulin syringe with a 0.5 inch, 28-gauge needle (Bunzl Healthcare, London, UK). Rats in the control group underwent the identical procedure but received a 50µl injection of sterile saline. Following knee joint injection, rats were recovered and monitored closely until consciousness was fully regained before they were returned to fresh home cages and monitored daily until completion of the study.

2.3. Assessment of pain behaviour

Pain-like behaviour was assessed immediately prior to knee joint injection (baseline; day 0) and then 7, 14 (immediately prior to electrophysiology), and in some cases 21 and 28 days post-MIA/saline injection. Behaviour was initially assessed up to day 28 post-injection to enable identification of a time-point where the MIA-induced pain behaviour was maximal. At least one day prior baseline testing, each rat was habituated to the testing equipment

(incapacitance tester and vF hair testing chamber) and behavioural testing room to minimise the effects of stress induced analgesia (Butler and Finn, 2009). On the day of testing, before commencement all rats were allowed to briefly (10 minutes) acclimatise to the testing room. For consistency, behavioural testing occurred at a similar time each day (generally 8 - 10am) whenever possible in order to minimise the influence of circadian rhythms on pain behaviour (Christina et al., 2004).

2.3.1. Weight bearing analysis

Pain arising from the knee joint (and to some extent the hind paw of the affected limb in rats) can be measured indirectly by assessing the weight borne by each leg (in a clinical setting for OA patients) or hind limbs (in pre-clinical tests with animals) (Neugebauer et al., 2007). A shifting of the weight borne by the arthritic limb to the non-arthritic limb is used as a translatable measure of joint pain (Bove et al., 2003, Combe et al., 2004, Fernihough et al., 2004, Pomonis et al., 2005b, Ivanavicius et al., 2007, Schuelert et al., 2010, Kelly et al., 2012). An incapacitance tester (Linton Instruments, Norfolk, UK) was used to measure alterations in weight distribution between the ipsilateral (injected) and contralateral (non-injected) hind limb of each rat. Each rat was placed into an angled plexiglass chamber that allowed each hind paw to rest on a separate force transducer pad which records the weight borne by each hind limb separately (see Figure 2.1). Once the rat was settled, the weight borne in grams by each hind limb was taken over a three second period and averaged by the incapacitance tester. Recordings were taken in triplicate and averaged for

analysis. Results are presented as the weight borne by the contralateral or ipsilateral hind limb, expressed as a percentage of the total weight borne by both hind limbs, such that a value of 50% represents normal weight bearing and anything under 50% represents a deficit in weight bearing (Kelly et al., 2012).

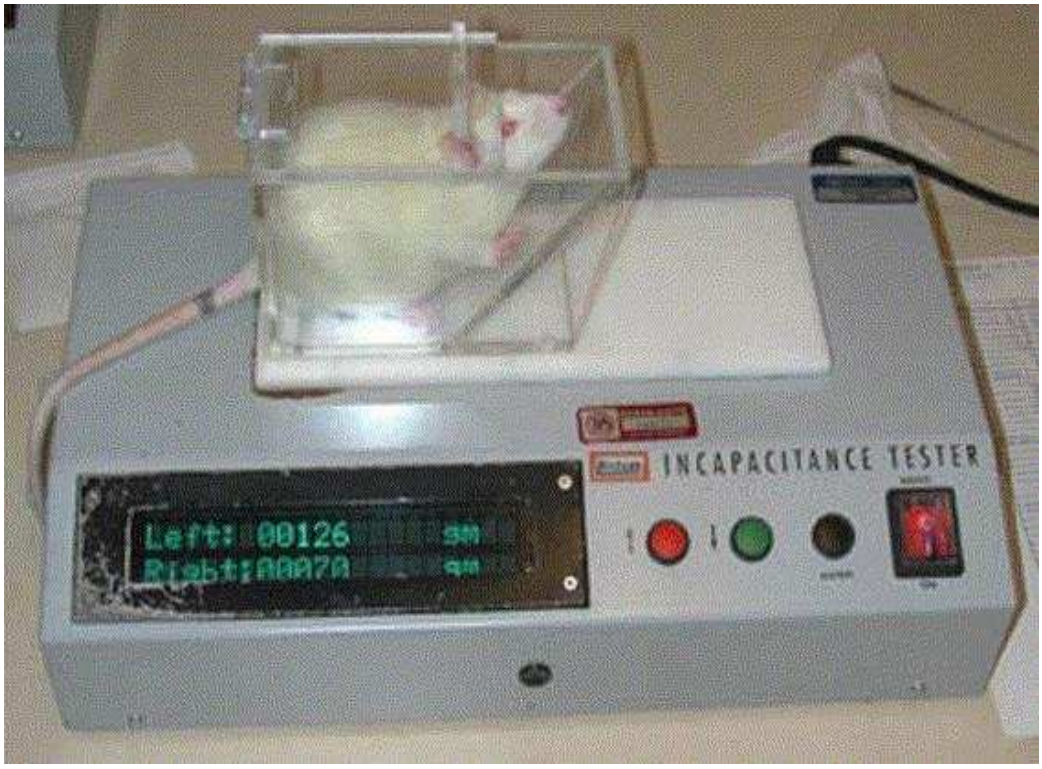

Figure 2.1. Weight bearing measurements (Figure modified from (Bove et al., 2003)).

2.3.2. Assessment of hind paw vF hair withdrawal thresholds

The development of secondary mechanical allodynia can be used as a measure of referred pain and provides evidence of changes in central pain pathways (Neugebauer et al., 2007). The presence of hind paw mechanical allodynia can be assessed using vF monofilaments applied to the plantar surface of the hind paw, an approach frequently used in the pain field (Combe et al., 2004, Fernihough et al., 2004, Ferreira-Gomes et al., 2010, Sagar et al., 2010). To monitor the development of mechanical allodynia in the MIA model of OA pain, rats were placed into a Perspex chamber on a metal grid floor that allowed access to the plantar surface of each hind paw. Hind paw withdrawal thresholds were assessed by applying vF monofilaments (Ugo Basile, Varese, Italy, 1-26g), in an ascending order of force, to the mid-plantar region of the hind paw for up to 5 seconds. Testing began with the application of a 6g vF monofilament to the plantar surface followed by ascending weights of vF monofilaments (filaments used were 1g, 1.6g, 2g, 4g, 6g, 8g, 10g, 15g and 26g) until a rapid withdrawal response of the hind paw to the mechanical stimulation was observed. Following a withdrawal response the paw was re-tested with the next lower vF monofilament weight. Again, if no response occurred, ascending weights of vF monofilament would be applied until a withdrawal response was observed. If no response was elicited by the initial 6g vF monofilament, the next lowest weight would be applied (4g) followed by descending weights until a withdrawal response was observed. A total of 6 withdrawal responses were recorded with the lowest consistent force required to evoke a withdrawal being recorded as the paw withdrawal threshold. To avoid sensitising the hind paw

and preventing lifting of the paw during testing by the vF monofilament, the 26g vF was used as the maximum force to assess paw withdrawal thresholds.

2.4. Electrophysiology

Surgical procedures and extracellular recordings from fine filaments of the saphenous nerve were carried out largely in accordance with previously published work (Kelly et al., 2012, Kelly et al., 2013b, Bullock et al., 2014). Rats had an average weight of 322 ± 3.6g (range: 272 - 412g) at the time of electrophysiology. In early experiments carried out in naïve rats (see Chapter 3) anaesthesia was induced using sodium pentobarbital (Sigma Aldrich, UK) (intraperitoneal (i.p); 40 - 60mg/kg). However, following advice from the NVS a more easily controllable induction method with isoflurane was adopted for subsequent experiments. However, throughout all studies anaesthesia was maintained with sodium pentobarbital so electrophysiological recordings were always carried out under the same anaesthetic.

2.4.1. Surgical preparation for electrophysiological recordings

Anaesthesia was induced with either sodium pentobarbital (50mg/kg, i.p; dissolved in ethanol (10%), propylene glycol (20%) and saline (70%)) or isoflurane (induction: 3% in O_2; 2 litres/min, maintenance: 2 - 2.5% in O_2; 0.6 litres/min). Rats were placed supine onto a homeothermic heating blanket (Harvard Apparatus, Kent, UK) which maintained core body temperature (37.5ºC) via a rectal probe connected to a feedback control unit which adjusted

the blanket temperature automatically. Areflexia and depth of anaesthesia were determined by pinch to the contralateral hind paw (and occasionally the fore paw) and by monitoring the depth and rate of breathing, and anaesthetic levels were adjusted accordingly. Once areflexic, a longitudinal midline incision was made in the neck and using blunt dissection (to minimise tissue trauma and blood loss) the right external jugular vein and trachea were exposed and cannulated to provide anaesthetic maintenance and airway clearance, respectively. The jugular vein was cannulated with a 0.5mm outer diameter (OD), green luer tipped nylon cannula (SLS, Nottingham, UK) and the trachea was cannulated with a 1.5mm internal diameter and 2.1mm OD nylon cannula (SLS, UK). In rats anaesthetised with isoflurane, a further cannula was inserted into the left carotid artery to allow recording and monitoring of blood pressure. The carotid artery was cannulated with a 1.0mm OD, pink luer tipped nylon cannula (SLS, UK) connected to a blood pressure transducer (NL108A, Digitimer, Hertfordshire, UK). Blood pressure was recorded for offline analysis and monitored regularly via a PC interface running Spike2 (v4) software (Cambridge Electronic Design (CED), UK). All cannulae were secured using non-sterile braided silk suture (size 5 - 0; Harvard Apparatus, Kent, UK) and skin incisions were closed with the same suture. Anaesthesia was maintained in all rats using sodium pentobarbital administered via the external jugular vein (15 - 40 mg/kg/hr, i.v). In rats that had anaesthesia induced with isoflurane, sodium pentobarbital anaesthesia was commenced following completion of trachea, carotid artery and jugular vein cannulations (at least one hour prior to electrophysiological recordings). During the anaesthetic switch over, isoflurane levels were slowly reduced with careful

monitoring of blood pressure and the hind paw withdrawal reflex to a strong pinch. Once blood pressure began to rise and a small withdrawal reflex became apparent, sodium pentobarbital bolus injections (0.05ml sodium pentobarbital washed in with 0.5ml saline) began and isoflurane was gradually reduced until anaesthesia was maintained entirely by sodium pentobarbital.

Next, an incision was made along the medial aspect of the right (contralateral) hind limb from the abdominal midline extending towards the ankle. The femoral artery was then exposed during blunt and fine dissection and a 0.5mm OD, green luer tipped nylon cannula (SLS, Nottingham, UK) was inserted into and advanced along the artery up to the point of bifurcation of the descending aorta (see Figure 2.2). This distance was estimated prior to cannula insertion by measuring approximately the distance from where the cannula would enter into the femoral artery to the midline of the rat. This distance was marked on the cannula to be inserted and the cannula was advanced along the artery until this mark was observed. To confirm the cannula remained inside the artery, and that it had not ruptured through the vessel wall, blood was gently drawn up the cannula prior to securing with suture. This cannula enabled drugs and vehicles to be delivered to the ipsilateral hind limb, providing a semi-local, close intra-arterial administration (Dunham et al., 2008, Kelly et al., 2013a).

The left (ipsilateral) hind limb was then attached to a raised Perspex platform using modelling clay. An incision was made along the medial aspect of the

limb from the inguinal fossa to a midpoint distal to the knee joint and proximal to the ankle. The skin overlying the hind limb was then separated from the underlying subcutaneous tissue by blunt dissection and attached via thick non-sterile braided silk suture (size 1; Harvard Apparatus, Kent, UK) to a metal 'O' shaped ring. The resulting pool was filled with warmed mineral oil (37ºC; Sigma-Aldrich, Dorset, UK) to prevent dehydration of tissues. The fat pad within the inguinal fossa, which obscures access to the saphenous nerve in the groin, was dissected and removed following occlusion and sectioning of a branch of the femoral vein. To prevent the recording of activity originating from distal parts of the hind limb (ankle and paw) the saphenous nerve was transected at a point just distal to the knee. The saphenous nerve was then dissected free from connective tissue in the inguinal fossa and sectioned centrally in the inguinal region to prevent the recording of antidromic activity originating centrally. The medial aspect of the knee joint is innervated by the MAN, which arises as a branch of the saphenous nerve (Hildebrand et al., 1991) (see Section). Recordings from the saphenous nerve, proximal to its MAN branch point ensured that knee joint-associated afferents were studied.

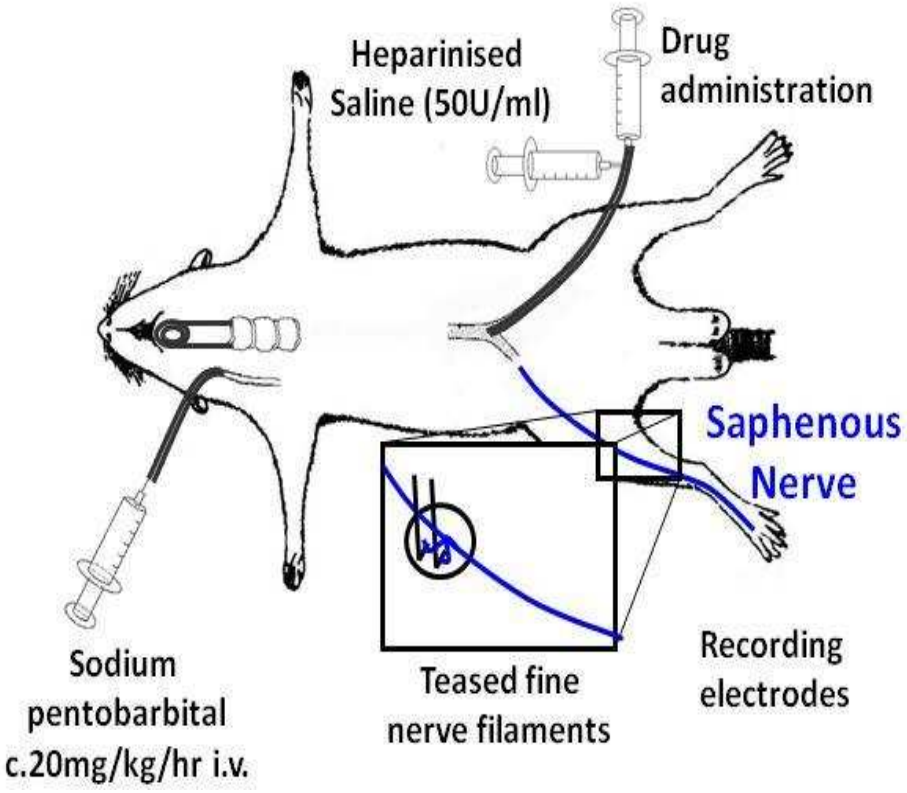

Figure 2.2. Surgical preparation for electrophysiological recordings.

2.4.2. Extracellular recordings

The central cut end of the saphenous nerve was placed onto a miniature dissecting platform. Using fine watch maker forceps the perineurium was removed and the nerve was teased into fine filaments which were placed over a pair of platinum (0.125mm diameter, Advent Research Materials, Oxford, UK) recording electrodes to enable the recording of neuronal activity (see Figure 2.3). Mechanosensitive knee afferents were identified by probing the subcutaneous structures over and around the knee joint with a 15g vF monofilament. Recorded units had receptive fields in structures accessible to

local mechanical stimulation over the medial aspect of the joint capsule, the medial collateral ligament and surrounding tissues.

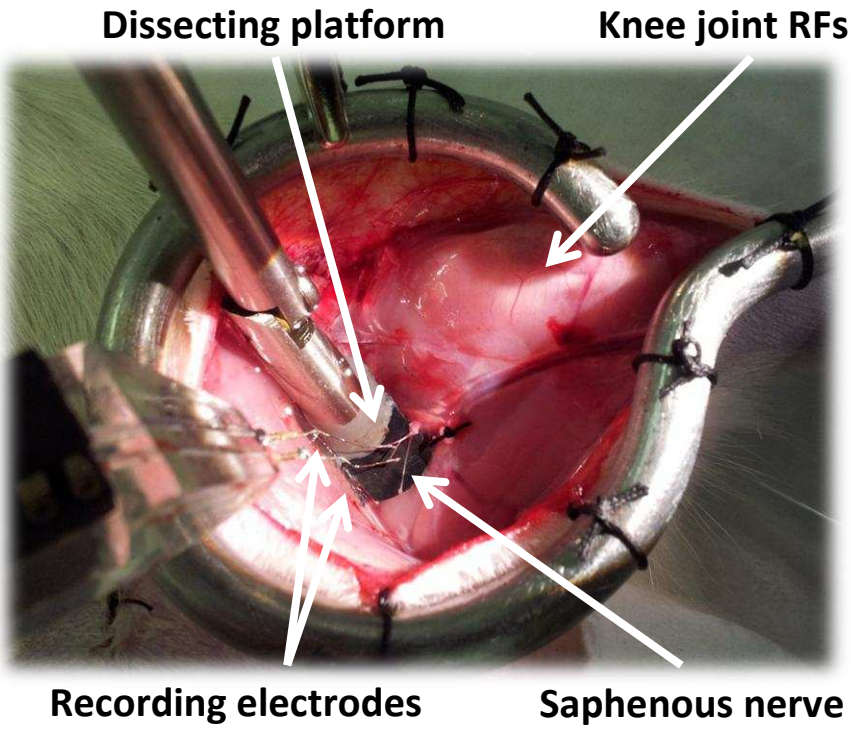

Figure 2.3. View of the recording chamber. Fine filaments of the saphenous nerve were placed over a pair of bipolar platinum recording electrodes. Neuronal activity is recorded in response to vF stimulation of the knee joint RFs.

Nerve filaments were teased until 1 - 3 single units could be identified and sorted offline using Spike 2 software (CED, Cambridge, UK). Electrical activity detected by the recording electrodes underwent first-stage

amplification (x10) and then pre-amplification by an AC pre-amplifier (x200 - 2000, NL2014, Digitimer, UK; see Figure 2.4). The analogue signal then underwent a further stage of amplification (x4.8, NL106, Digitimer, UK) then was digitally filtered (NL125, Digitimer, UK) before finally being digitally converted (Micro 1401, CED, UK). The low pass frequency cut-off was set at 5Hz with the notch filter set to reject line frequency interference at 50Hz. The high pass frequency cut-off was set at 50Hz with the notch filter set at 10Hz. From the filters the signal was sent to an audio amplifier (NL120, Digitimer, UK) and speaker as well as digital oscilloscope (OS300 Gould 20MHz Oscilloscope) and captured using a micro 1401 and computer interface running Spike2 software (CED, UK).

Figure 2.4. Flow of recording set-up and signal acquisition.

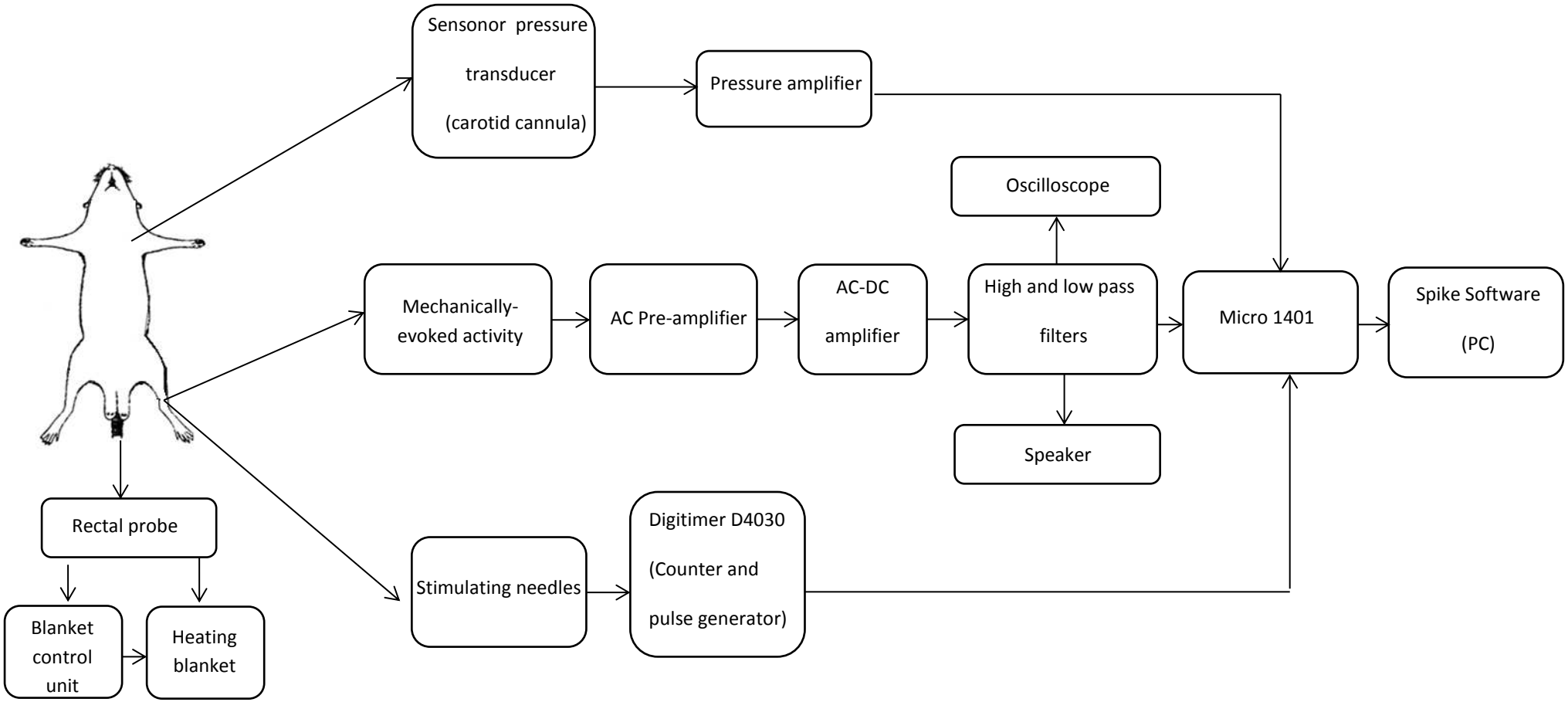

Single unit recordings were acquired by stimulating within discrete receptive fields, only activating a single unit or 1 - 3 units that could be sorted offline, and by adjusting discriminator settings within the Spike software. Using the Spike software it was possible to adjust window discriminator thresholds to ensure neuronal activity within a discrete range was recorded. This allowed for the selection of recording parameters specific for a single unit or several different units that could be sorted offline. Once a single unit with a knee joint receptive field was identified, responses of the unit to ascending trains of vF monofilament weights (0.16g, 0.4g, 0.6g, 1g, 2g, 4g, 6g, 8g, 10g, 15g) were recorded. Each individual vF monofilament was applied to the centre of the receptive field for five seconds. To avoid sensitization, a five minute interval was used between trains of vF monofilaments i.e. 5 minutes between the 15g vF of one train and 0.16g vF of the next train. Trains of stimulation were repeated until stable and reproducible responses were obtained (typically 3 - 6 trains). These responses were used as control responses in subsequent analyses. Following stable control responses, drugs were administered (see Section 2.4.4).

At the end of each experiment (to avoid unit loss) the CV of a recorded unit was estimated following electrical stimulation (up to 10V, 400ms; DS2A MkII, Digitimer, UK) of the centre of the receptive field via bipolar needle (25G) stimulating electrodes. Electrical stimulations were controlled by a digital counter and a pulse generator (D4030, Digitimer, UK) which delivered trains of 10 individual pulses at 0.3Hz. CVs were estimated using the latency

between the onset of an action potential and the stimulus artefact and the distance between the recording and stimulating electrodes (see Figure 2.5). Based on compound action potential recordings in rats of the same gender, similar recording conditions and similar weight range (Dunham et al., 2008, Kelly et al., 2012), C-fibres had CVs <1.3m/s and Aδ-fibres had CVs of 1.3 - 15m/s with Aβ fibres CVs above 15m/s. At the end of each experiment 100µl potassium chloride (KCl) (250mM) was administered through the contralateral femoral artery cannula to confirm that administered drugs reached the peripheral terminals of the recorded afferent. Any unit not activated by KCl was omitted from further analysis. At the end of each experiment rats were euthanized by anaesthetic overdose and death was confirmed by cervical dislocation.

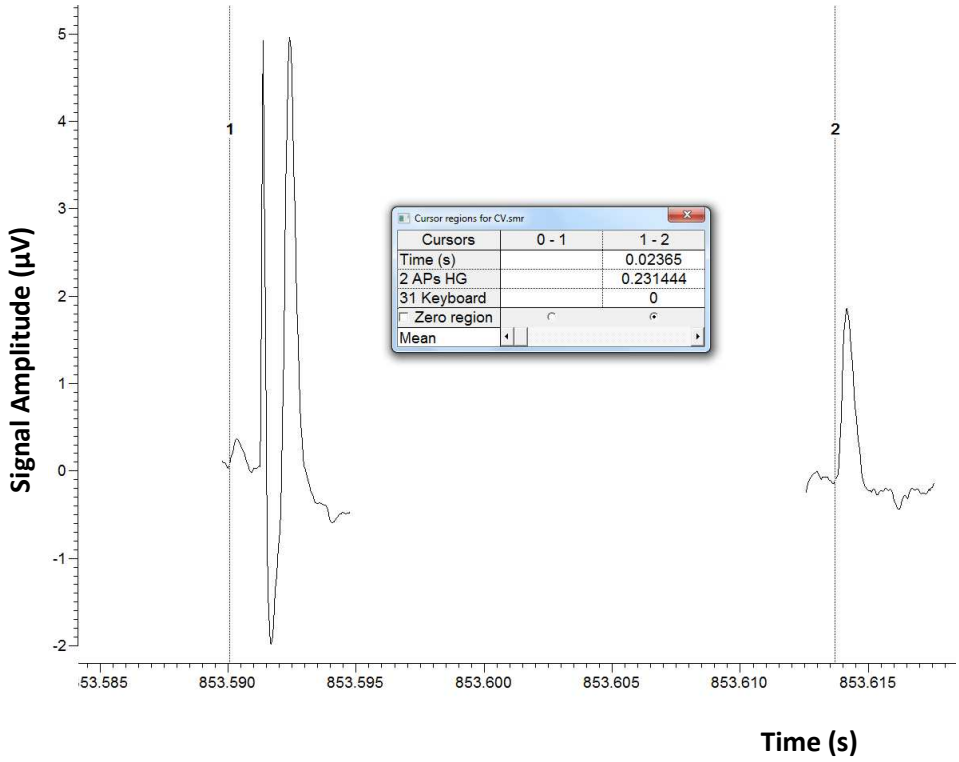

Figure 2.5. Calculating CVs. Estimation of CVs was made by calculating the latency between the stimulus artefact (left hand spike, Cursor 1) and action potential onset (right hand spike Cursor 2). For the example in this figure the latency = 0.02 m/s (given in the box at the centre of the figure) and the distance between electrodes was 24.5mm. The CV for this unit is 1.22 m/s (C-fibre, from a naïve rat).

2.4.3. Data analysis

Neuronal activity was recorded and captured for offline analysis using Spike 2 software (CED, UK) version 4 (v4). Units were first sorted on the basis of the shape of the action potential and filtered using the Edit Wavemark function of Spike2 software such that only the unit of interest was analysed. This was necessary when more than one unit was present during electrophysiological recordings. Spike software is able to scan the neuronal activity recorded and assign wavemark templates based upon action potential shape and amplitude to individual action potentials. The unit of interest can then be selected and filtered from other units recorded.

Firing rates of the most reliable unit recorded were determined. To determine the firing rate, the recording channel was duplicated and a rate histogram of the recorded action potential responses was plotted (1s bins) (see Figure 2.6). The mean rate of firing over the five second stimulating period for each vF monofilament was measured by placing horizontal cursors 5 seconds apart. Neuronal activity is expressed throughout as the number of action potentials per second (APs/s).

The mechanical thresholds of a unit was calculated as the minimum vF monofilament weight required to evoked $\geq$ 2 action potentials over the 5 second stimulating period.

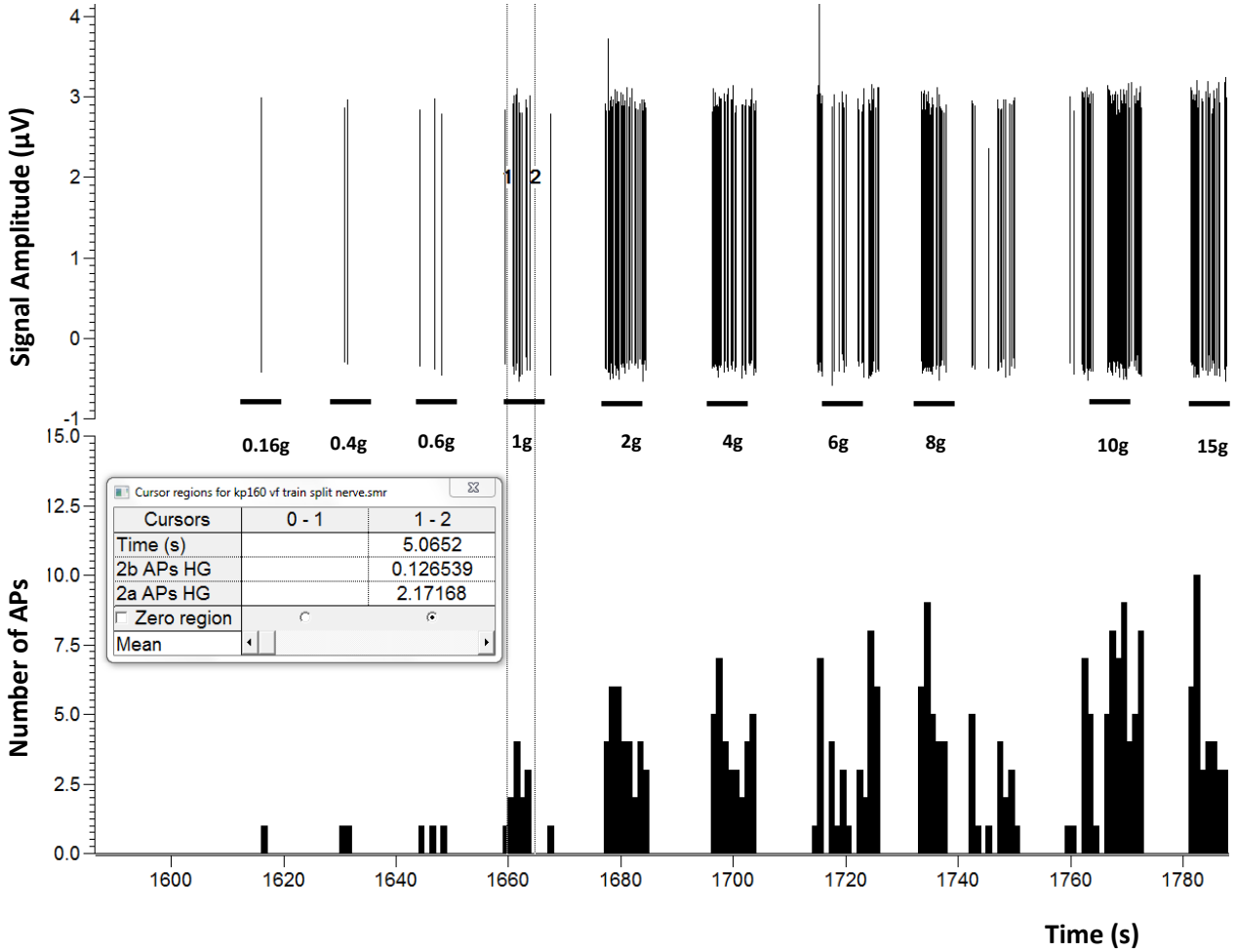
Signal Amplitude (µV)
4
3
2
1
0
-1
1
2
0.16g
0.4g
0.6g
1g
2g
4g
6g
8g
10g
15g
Cursor regions for kp160 vf train split nerve.smr
Cursors
0 - 1
1 - 2
Time (s)
5.0652
2b APs HG
0.126539
2a APs HG
2.17168
Zero region
Mean
Number of APs
15.0
12.5
10.0
7.5
5.0
2.5
0.0
1600
1620
1640
1660
1680
1700
1720
1740
1760
1780
Time (s)

Figure 2.6. Example recordings of mechanically-evoked responses of a single knee joint nociceptor and analysis of firing rates. (A) The captured spike trace. (B) The rate histogram corresponding to the evoked responses in (A). Two cursors (1 and 2) are placed 5 seconds apart (timing of the stimulus; see cursor regions dialogue box). The dialogue box shows the mean rate of firing between the two cursors. In this case the rate of firing of knee joint afferents to stimulation with a 1g vF monofilament is 2.17 APs/s. A bold line indicates the onset of stimulation with the corresponding vF monofilament weight shown beneath. The above example is taken from a naïve rat, CV for fibre = 1.11m/s (C fibre).

2.4.4. Drug administration

Following the acquisition of stable and reproducible control mechanically-evoked firing rates, drugs were administered via the contralateral femoral artery. Details of specific drugs can be found in relevant experimental chapters. In all instances 100µl bolus injections of drugs were administered and washed through the femoral artery cannula with 300µl heparinised (10IU/ml; Wockhart, Wrexham, UK) rat Ringer (0.9% NaCl, 0.24% $CaCl_2$, 0.042% KCl, 0.02% $NaHCO_3$). Effects of drugs on mechanically-evoked responses of individual units were recorded at 5 minute intervals for up to approximately 60 minutes (i.e. 12 trains of vF monofilament stimulation). In vehicle experiments, two 100µl injections of Ringers were administered via the contralateral femoral artery. This ensured that drug and vehicle experiments were conducted over an identical time course so that any increase in neuronal activity could not be attributed to mechanical stimulation due to the experimental protocol, and any inhibition could not be attributed to general run down of neuronal responses. Only one fibre was recorded per rat in drug studies.

Figure 2.7. Electrophysiology recording protocol.

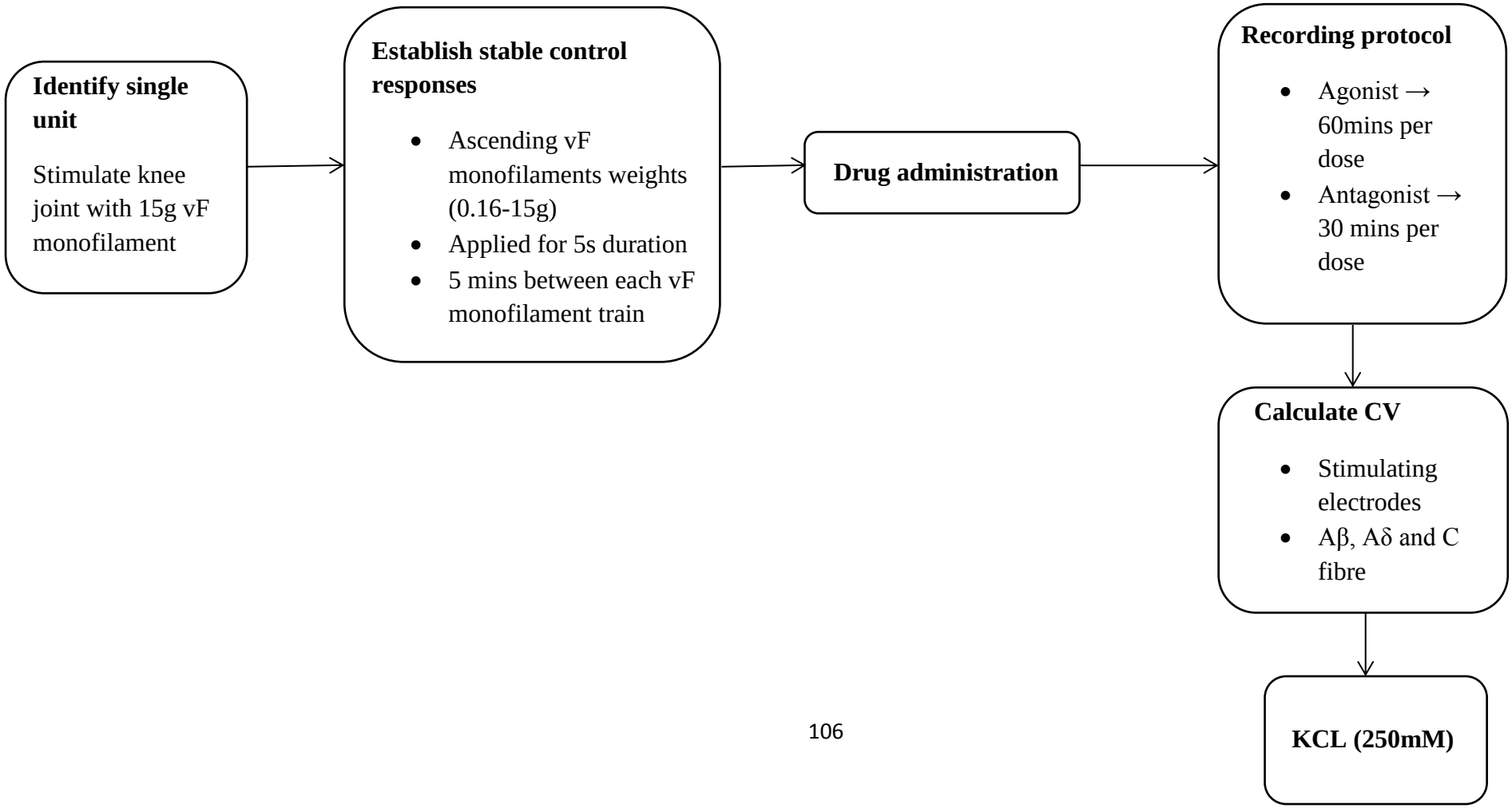

Chapter Three

Characterisation of pain behaviour and electrophysiological properties of knee joint nociceptors in the MIA model of OA pain

3.1. Introduction

The aims of this thesis were firstly to investigate the role of GPR55 in the modulation of acute joint nociception and secondly to translate these findings to a clinically relevant model associated with chronic joint pain, OA. Investigations aimed at identifying novel analgesic targets for OA pain have been furthered by the development and use of animal models that replicate the articular joint destruction and pain symptoms of the human condition (see Chapter 1, Section 1.13.2. and 1.13.3.). After an initial focus on structural pathology more recent studies have investigated mechanisms of pain and the effectiveness of novel and existing analgesic therapies (Bove et al., 2003, Combe et al., 2004, Fernihough et al., 2004, Kelly et al., 2012, Kelly et al., 2013a, Bullock et al., 2014). The work described in this chapter has characterised the development of pain behaviour in the MIA model and has used teased saphenous nerve fibre electrophysiological recordings in vivo to characterise the mechanical sensitivity of knee joint nociceptors in MIA rats during established pain behaviour and compared these responses to those recorded in saline controls. The MIA model of OA pain in the rat was selected for investigations of the role of GPR55 in the modulation of peripheral sensitization during established OA pain behaviour (see Chapter 5).

3.1.1. Pain behaviour in the MIA model

Characterisation of the MIA model has confirmed the development of pain behaviour that closely resembles the pain symptoms associated with human OA. The weight bearing asymmetry that manifests in this model reflects the

activity-dependent pain during joint loading (e.g. walking, climbing stairs) seen in human OA (Christiansen and Stevens-Lapsley, 2010). i.a. injection of MIA into the rat knee joint results in a concentration- (0.3 - 3mg) and time-dependent decrease in weight bearing on the ipsilateral hind limb (Bove et al., 2003, Fernihough et al., 2004, Kelly et al., 2012). The associated weight bearing asymmetry is evident from day 1 post-injection, peaking at day 3 - 7 and persists for up to at least 35 days following a 1mg (Ashraf et al., 2013) and until at least 63 days following 2mg injection (Combe et al., 2004).

Tactile allodynia in the ipsilateral hind paw is also a feature of the MIA model consistent with the referred hypersensitivity seen in OA pain patients (Hendiani et al., 2003, Neugebauer et al., 2007). i.a. injection of MIA into the rat knee joint results in a concentration- (0.3 - 3mg) and time-dependent decrease in ipsilateral hind paw mechanical withdrawal thresholds (Fernihough et al., 2004, Sagar et al., 2010, Ashraf et al., 2013). The MIA-associated development of ipsilateral hind paw hypersensitivity is evident from days 3 - 7 following a 1mg (Fernihough et al., 2004, Ashraf et al., 2013) or 3mg (Sagar et al., 2010) injection and is maintained at 35 days. Injection of 0.3mg MIA does not significantly reduce withdrawal thresholds until 28 days post-injection indicating a more slowly developing profile (Sagar et al., 2010).

The development of pain behaviour in the MIA model mimicking pain symptoms in human OA validates the use of this model for the study of OA pain mechanisms. The pain relieving effects of joint replacement (Dixon et al.,

2004) and i.a. local anaesthetic (Creamer et al., 1996) highlights the critical role of peripheral mechanisms in the drive to OA pain.

3.1.2. Electrophysiological studies of joint afferent responses in OA animals

The effect of experimental OA (spontaneous, chemically and surgically induced) on the in vivo electrophysiological properties of knee joint afferents have been partially investigated (Schuelert and McDougall, 2006a, Gomis et al., 2007, McDougall et al., 2009, Schuelert and McDougall, 2009, McDougall et al., 2010, Schuelert et al., 2010, Kelly et al., 2012). These studies of knee joint nociceptor recordings have indicated increases in excitability following the induction of experimental OA. Changes in joint nociceptor sensitivity to mechanical stimulation (Schuelert and McDougall, 2009, Kelly et al., 2012, Kelly et al., 2013a, Bullock et al., 2014) of the joint as well as the development of spontaneous firing (Kelly et al., 2012) have been reported.

The contribution of knee afferent nociceptor sensitization to pain behaviour in these models of OA is poorly understood as many of these studies did not assess pain in these animals preventing a direct correlative analysis between electrophysiological properties of knee joint nociceptors and pain behaviour within individual rats.

In the MIA model, the development of knee joint nociceptor mechanical sensitization (reduced mechanical thresholds and increased firing rates) present by day 3 and which is maintained at day 14 post-injection, demonstrates a similar temporal profile to the development of weight bearing asymmetry (Kelly et al., 2012). The mechanical sensitization of knee joint nociceptors is graded in response to increasing concentrations of MIA, as is the degree of pain behaviour (Schuelert and McDougall, 2009). These findings suggest that knee joint nociceptors contribute to pain behaviour in this model. If present in humans, the increased mechanical sensitivity of Aδ-fibres and spontaneous activity in C-fibres may underlie the clinical features of human OA including use-dependent pain and spontaneous pain, respectively (Kelly et al., 2012).

Peripheral sensitization appears to be a robust and consistent observation in pre-clinical models of OA given that mechanical sensitization of knee joint nociceptors has been reported in other experimental models of OA including spontaneous OA in the guinea pig (McDougall et al., 2009, McDougall et al., 2010) and surgically induced OA in the guinea pig (Gomis et al., 2007) and rat (Bullock et al., 2014). As such, peripheral sensitization is likely to make an important contribution to the associated pain behaviour in these models. In support of this, pharmacological agents that reverse the established sensitization of knee joint nociceptors reduce OA pain behaviour (McDougall et al., 2006, Schuelert and McDougall, 2006b, Schuelert et al., 2011, Kelly et al., 2013a). This association provides justification for studies investigating

OA-induced excitability changes in joint nociceptors and the modulation of this response in OA pain models.

3.2. Aims and Objectives

The aims of the work presented in this chapter were to establish the MIA model in male Sprague Dawley rats and to characterise the development of pain behaviour and mechanically-evoked responses of knee joint afferents. Whether in my hands alterations in pain behaviour and changes in mechanical hypersensitivity are observed following the induction of OA and how these responses are related were examined. The development of pain behaviour 0 - 28 days following the induction of the MIA model was characterised and joint nociceptor responses were recorded at day 14.

3.3. Methods

Refer to Chapter 2 for detailed methods regarding OA induction (see Section 2.2), assessment of pain behaviour (see Section 2.3) and electrophysiology (see Section 2.4).

3.3.1. Animals

Male Sprague Dawley rats (n = 75) with an average weight of 317.5 ± 5.24g at the time of electrophysiology were obtained from Charles River (Kent, UK). Rats were naïve (n = 39), MIA injected (n = 19) and saline injected (n = 17). Control (baseline) data are included in later chapters (see chapters 4 and 5).

3.3.2. Knee joint histology

Following anaesthetic overdose and cervical dislocation at the end of electrophysiological recording, ipsilateral and contralateral knee joints were removed from 3 MIA and 3 saline rats and trimmed of excess surrounding muscle. Joints were placed in 25ml universal tubes (Sarstedt, Leicester, UK) and post-fixed for 48 hours in 10% formal saline (v/v), at room temperature on a rocker before being decalcified in 10% ethylenediaminetetraacetic acid (EDTA) (w/v) for at least 5 weeks under the same conditions. Using a razor blade, joints were then split along the coronal plane, using the medial collateral ligament as an anatomical marker. The anterior and posterior joint halves were then placed into separate plastic cassettes (VWR, Lutterworth, UK) and sent for wax embedding at Kings Mill Hospital using a TEC5 EME2 Tissue Tek

embedding centre (Sakura Finetek Europe, The Netherlands) (performed by Mr Roger Hill). A single 5µm coronal section was collected onto a polysine coated glass slide (Thermo Scientific, UK) using a Thermo Scientific rotary Microm microtome HM 355. Sections were collected from the mid-point of the ipsilateral joint for saline (n = 3) and MIA (n = 3) rats and left to dry overnight at room temperature. For proteoglycan determination, slides were incubated in the following solutions:

1) De-waxed in Histo-clear (Fisher Scientific, UK) x 2 – 5 mins each
2) 100% ethanol x 2 – 5 mins each
3) 70% ethanol x 2 – 5 mins each
4) Water – 5 mins
5) 1% toluidine blue (prepared in 70% ethanol) – 6 mins
6) Washed in flowing water – 5 mins
7) 70% ethanol x 2 – 5 mins each
8) 100% ethanol x 2 – 5 mins each
9) De-waxed in Histo-clear (Fisher Scientific, UK) x 2 – 5 mins each
10) Mounted and coversliped using DPX Mounting Medium (Sigma, UK)

Images of the medial tibial plateau were captured on a Leica DM400B microscope using a 5x or 20x objective lens. Images were acquired using SimplePCI software (Hamamatsu) and qualitatively analysed offline comparing toluidine blue staining intensity and cartilage integrity (loss of cartilage and fibrillation of the cartilage surface).

3.3.3. Data analysis

Pain behaviour scores are expressed as detailed in the general methods (see Chapter 2, Section 2.3). Neuronal activity is expressed as described previously (see Chapter 2, Section 2.4.4).

3.3.4. Statistical analysis

Data analysis was performed using Prism software (v5 or 6; GraphPad Software). Data were tested for normality using the Kolmogorov Smirnov test and where normally distributed parametric stats (e.g. two-way ANOVA) were used. When data were not normally distributed, non-parametric stats (e.g. Mann-Whitney u-test and Friedman's ANOVA) were used.

3.4. Results

3.4.1. Histological changes in joint sections from MIA and saline rats

Qualitative histological analysis of toluidine blue stained joint sections was performed in order to confirm the presence of OA-like changes in joint structure in the MIA model of OA pain. Toluidine blue stains proteoglycan content, a marker of cartilage integrity (Sandell and Aigner, 2001, Gerwin et al., 2010). Loss of proteoglycan content indicates cartilage dysfunction and the early signs of OA development (Milner et al., 2010).

Saline injection (n = 3) had no effect on cartilage, which displayed a smooth surface with intense proteoglycan staining (Figure 3.1A and C). A higher intensity magnification view of the cartilage from saline rats revealed intense proteoglycan staining with an organised arrangement of lacuna and chondrocytes (Figure 3.1C). 14 days following i.a. MIA (1mg) injection, a loss of cartilage proteoglycan content, spanning the length of the tibial plateau, with evident damage to the cartilage surface including cartilage loss and fibrillation was observed through the full thickness of the cartilage up to the tidemark (black arrow, see Figure 3.1B). MIA rats had reduced chondrocyte numbers, indicating chondrocyte cell death (Figure 3.1D) and areas of chondrocyte proliferation and early osteophyte formation was evident (Figure 3.1E).

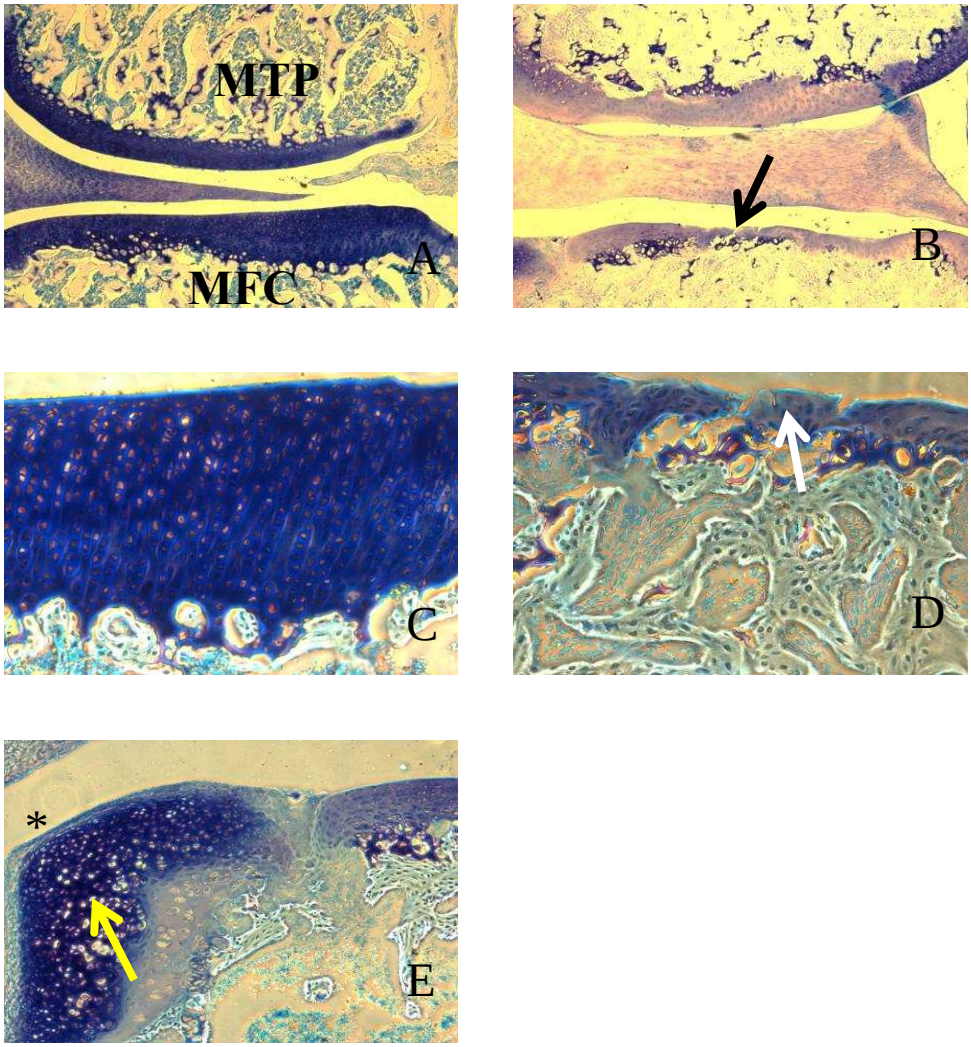

Figure 3.1. Effect of MIA (1mg/50µl) injection on joint histology at day 14. Representative ipsilateral knee joint sections from saline (A&C) and MIA (B, D & E) rats. Saline rats displayed intense toluidine staining blue staining and smooth cartilage surfaces. MIA injection resulted in loss of toluidine blue stain, fibrillation of the cartilage (black arrow), reduced chondrocyte numbers (white arrow) and disruption to the cartilage surface. Chondrocyte proliferation (yellow arrow) and small osteophytes (asterisk) were also evident in MIA rats. Images were taken at x5 (A and B) and x10 (C, D & E) magnifications. MFC = medial femoral condyle, MTP = medial tibial plateaux.

3.4.2. Characterisation of pain behaviour in the MIA model of OA

An initial study was performed in order to assess the impact of MIA injection on pain behaviour over time in my hands and to enable the subsequent selection of an appropriate time point at which to conduct my electrophysiological experiments. Hind limb weight bearing and hind paw withdrawal thresholds were assessed in 12 rats in total (n = 6 each MIA and saline) over a 28 day period. i.a. MIA or saline injection did not affect weight gain over the course of the 28 day study with rats gaining weight within the normal range expected for Sprague Dawley rats (Figure 3.2).

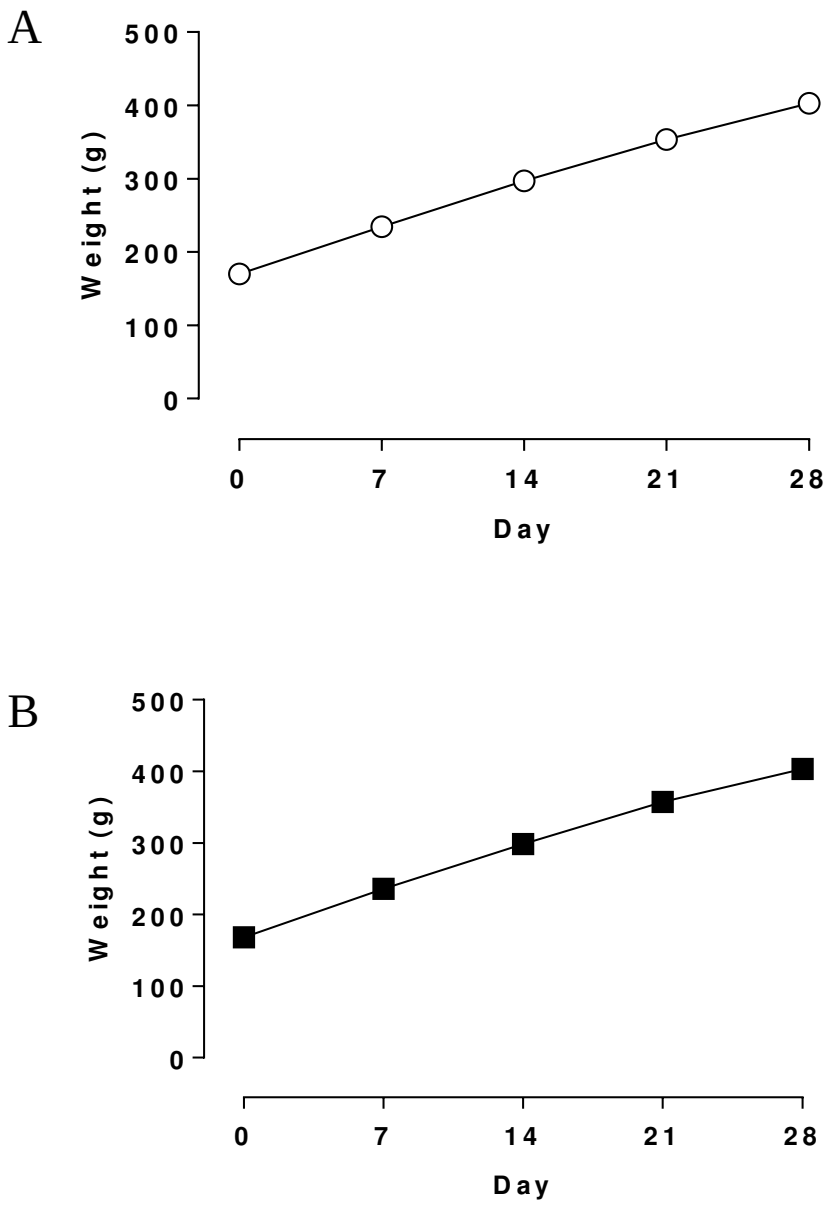

Figure 3.2. Effect of MIA injection on weight gain. Weight gain in rats injected with MIA (1mg/50µl) (n=6) (A) and saline (n=6) (B). Both groups of rats continued to gain weight throughout the course of the study.

At day 0 (immediately before MIA/saline injection) as expected the percentage weight borne by the ipsilateral hind limbs was equal in both groups (% ipsilateral weight bearing: saline = 49.52 ± 0.69%, MIA = 49.93 ± 1.01%). Treatment with saline (n = 6) had no effect on ipsilateral hind limb weight bearing compared to baseline throughout the study (two-way ANOVA with Bonferroni multiple comparisons test, Figure 3.3). i.a. injection of MIA (n=6) however, was associated with a significant reduction in ipsilateral hind limb weight bearing at all-time points compared to baseline (day 0) ($p<0.0001$ at days 7 and 14, $p<0.05$ at day 21 and $p<0.01$ at day 28, two-way ANOVA with Bonferroni multiple comparisons test, Figure 3.3) and saline rats ($p<0.0001$ at days 7, 14, $p<0.05$ at day 21 and $p<0.01$ at day 28, two-way ANOVA with Bonferroni multiple comparison, Figure 3.3).

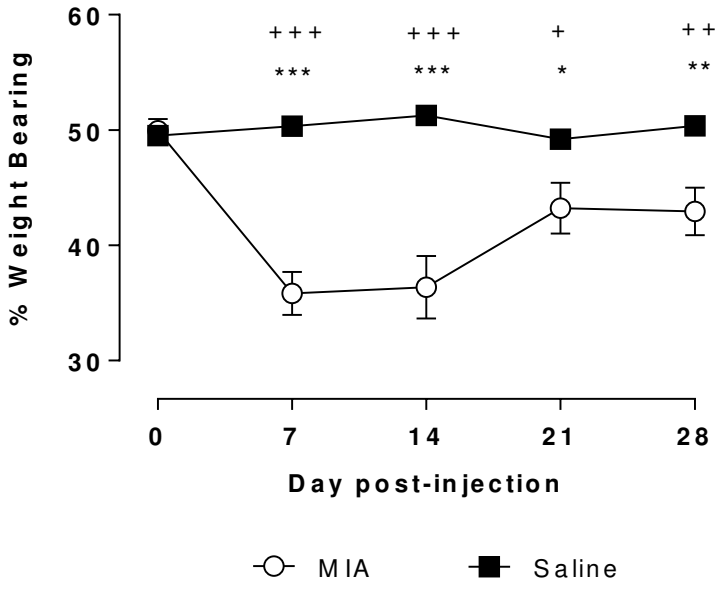

Figure 3.3. Effect of MIA injection on ipsilateral hind limb weight bearing over a 28 day period. Weight bearing in MIA (n=6) rats was significantly reduced compared to baseline (day 0) and saline rats at all time points tested. Data presented as mean ipsilateral weight borne as a percentage of the total hind limb weight bearing ± SEM. $^{+++}p<0.0001$, $^{++}p<0.01$ and $^{+}p<0.05$ compared to MIA day 0, $^{***}p<0.0001$, $^{**}p<0.01$ and $^{*}p<0.05$, MIA compared to saline, two-way ANOVA plus Bonferroni multiple comparisons test.

Further assessment of the impact of MIA injection on pain behaviour was carried out by determining hind paw withdrawal thresholds in MIA (n = 6) and saline (n = 6) rats over the same 28 day period (Figure 3.4). Ipsilateral hind paw withdrawal threshold in MIA and saline rats were not significantly altered compared to baseline at any time point (two-way ANOVA, Figure 3.4A). However, ipsilateral mechanical withdrawal thresholds in MIA rats were significantly reduced compared to saline at day 7 ($p>0.05$, two-way ANOVA with Bonferroni multiple comparisons test, Figure 3.4A).

There was no significant difference in contralateral hind paw withdrawal thresholds in either MIA or saline rats compared to their respective baseline thresholds (two-way ANOVA with Bonferroni multiple comparisons test, Figure 3.4B) or when comparing MIA and saline rats (two-way ANOVA with Bonferroni multiple comparisons test, Figure 3.4B).

A

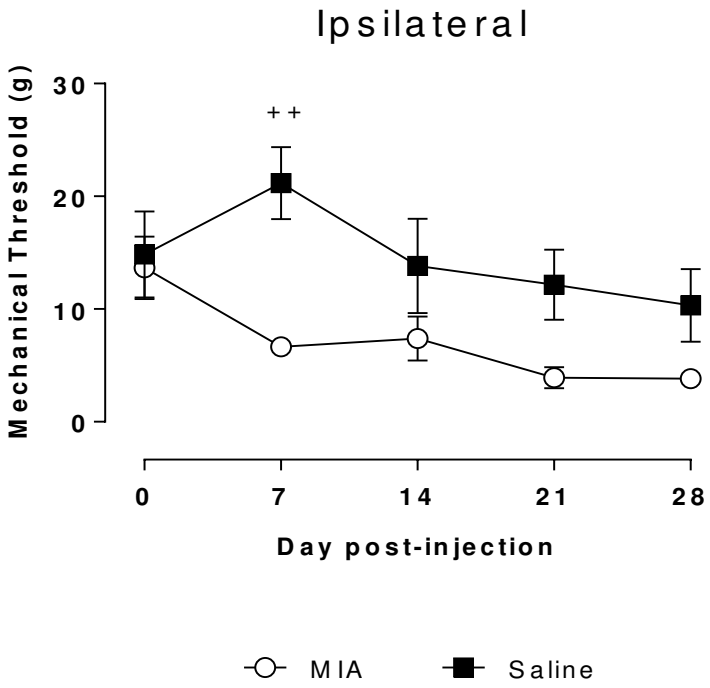

B

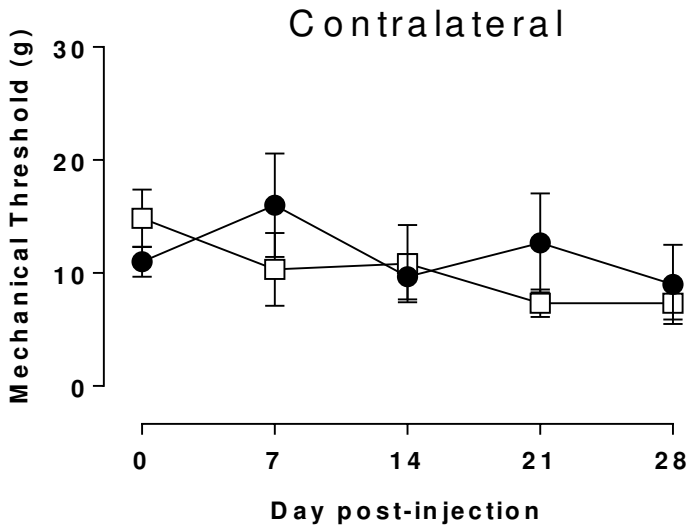

Figure 3.4. Effect of MIA injection on ipsilateral (A) and contralateral (B) hind paw withdrawal thresholds. MIA (n = 6) rats had significantly lower ispilateral paw withdrawal thresholds than saline rats (n = 6) at day 7 post-injection. Data presented as mean paw withdrawal thresholds ± SEM.

$^{++}p<0.01$, compared to saline, two-way ANOVA plus Bonferroni multiple comparisons test.

This initial 28 day time course study demonstrated that in my hands maximal changes in weight bearing are evident 14 days following MIA injection. Therefore subsequent electrophysiological studies characterising the effects of MIA on knee afferent mechanically-evoked responses were performed at this time point (a time point associated with OA-like changes in joint histology, see Figure 3.1). In these animals pain behaviour was assessed at day 7 and immediately prior to electrophysiological recordings on day 14

In these rats, overall, in agreement with the initial 28 day time course study ipsilateral hind limb weight bearing was significantly reduced in MIA compared to saline rats ($p<0.0001$, two-way ANOVA, Figure 3.5). At day 14, MIA rats exhibited a mean % ipsilateral hind limb weight bearing of 38.14 ± 1.4%, compared to 50.12 ± 0.38% in saline rats ($p<0.001$, two-way ANOVA with Bonferroni's multiple comparisons test, Figure 3.5).

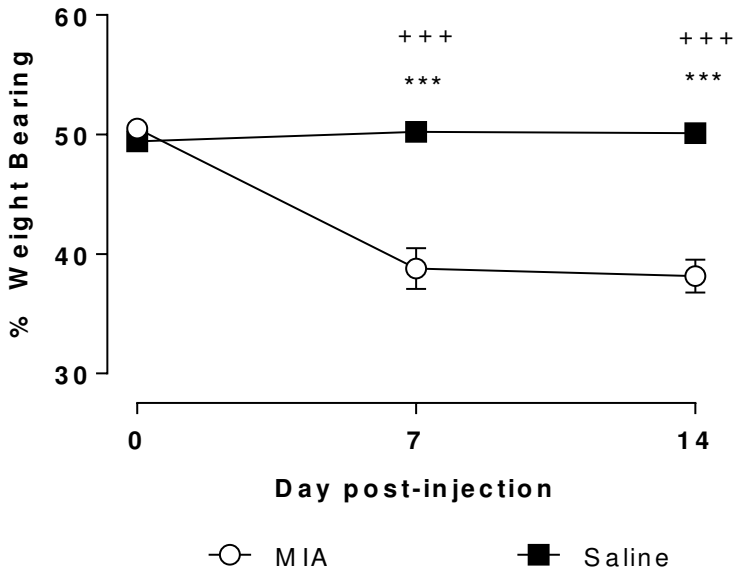

Figure 3.5. Effect of MIA injection on ipsilateral hind limb weight bearing in rats subsequently used for electrophysiological study. MIA injection (n = 19) resulted in a significant reduction in weight bearing compared to saline (n = 17) control rats at all-time points investigated. Data presented as mean ipsilateral weight borne as a percentage of the total hind limb weight bearing ± SEM. $^{+++}p<0.0001$, compared to MIA day 0, $^{***}p<0.0001$, MIA compared to saline, two-way ANOVA plus Bonferroni's multiple comparisons test.

Also, in agreement with the 28 day time course study ipsilateral hind paw mechanical thresholds were significantly reduced in MIA (n = 19) compared to saline (n = 17) rats ($p<0.001$, two-way ANOVA, Figure 3.6A). At the time of electrophysiology (day 14), saline median withdrawal thresholds were 11g (range = 1 - 26g) whilst median MIA withdrawal thresholds were 5g (range = 0.6 - 26g) ($p<0.001$, two-way ANOVA with Bonferroni's multiple comparisons test, Figure 3.6A).

Again, there were no differences in contralateral hind paw withdrawal thresholds in MIA and saline rats when compared to their respective baseline control thresholds (two-way ANOVA with Bonferroni's multiple comparisons test, Figure 3.6B).

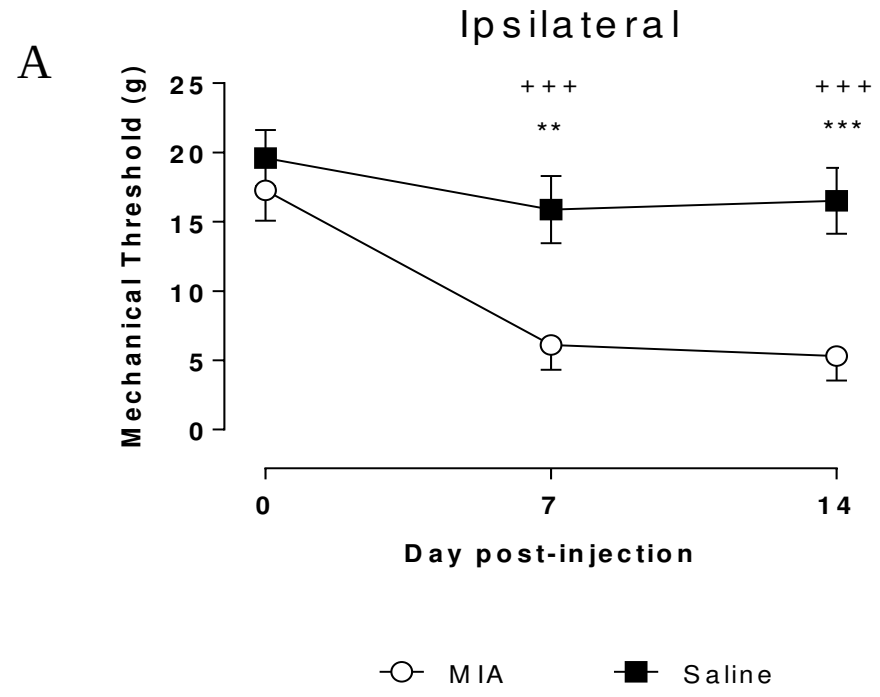

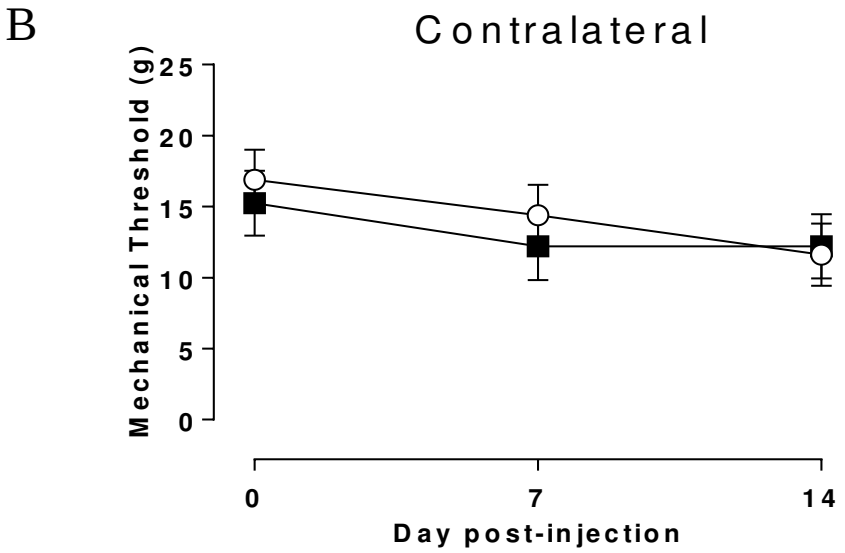

Figure 3.6. Effect of MIA injection on ipsilateral hind limb mechanical thresholds in rats subsequently used for electrophysiological study. MIA (n = 19) rats had significantly lower ipsilateral paw withdrawal thresholds than saline (n = 17) controls. Data presented as mean paw withdrawal thresholds ± SEM. $^{+++}p<0.0001$, compared to MIA day 0, $^{**}p<0.01$ and $^{***}p<0.001$, MIA

compared to saline, two-way ANOVA plus Bonferroni's multiple comparisons test.

3.4.3. Electrophysiological characterisation of knee joint nociceptors in naïve rats

During the first pharmacological study of this thesis (see Chapter 4) the response properties of knee joint afferents to mechanical stimulation of the knee joint under normal (naïve) conditions were characterised. Mechanically sensitive receptive fields were located over the medial aspect of the knee joint, including the joint capsule, medial collateral ligament and surrounding tissue and were typically discrete, covering no more than 1 - 3mm in diameter. CVs were estimated following electrical stimulation of their receptive fields (see Chapter 2, section 2.4.2) in order to classify them as either A- or C-fibres. Figure 3.7 shows the distribution of CVs for the recorded knee joint nociceptors (n = 30). CVs ranged from 0.15 - 37 m/sec. Compound action potentials recorded in rats of the same sex and similar weight range have demonstrated that C-fibres conduct at <1.3m/s, Aδ-fibres at 1.3 - 15m/s and Aβ-fibres at >15m/s. Therefore, the majority of knee joint nociceptors recorded were C- and Aδ-fibres in agreement with previous studies of knee joint nociceptors in the rat (Schaible and Schmidt, 1983b, Schaible and Schmidt, 1983a, Kelly et al., 2012). A- and C-fibres are discussed collectively throughout this thesis.

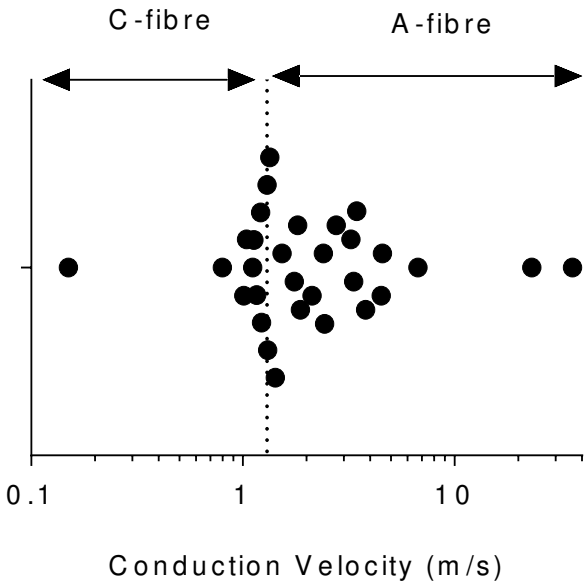

Figure 3.7. Distribution of CVs of knee joint nociceptors recorded in naïve rats (n = 30) (range = 0.15 - 37 m/s). Fibres in both the A- and C-fibre CV ranges were recorded.

A typical example single unit recording in response to mechanical stimulation (15g vF) is shown in Figure 3.8. The C-fibre unit adapted slowly in response to the maintained (5 second) mechanical stimulus.

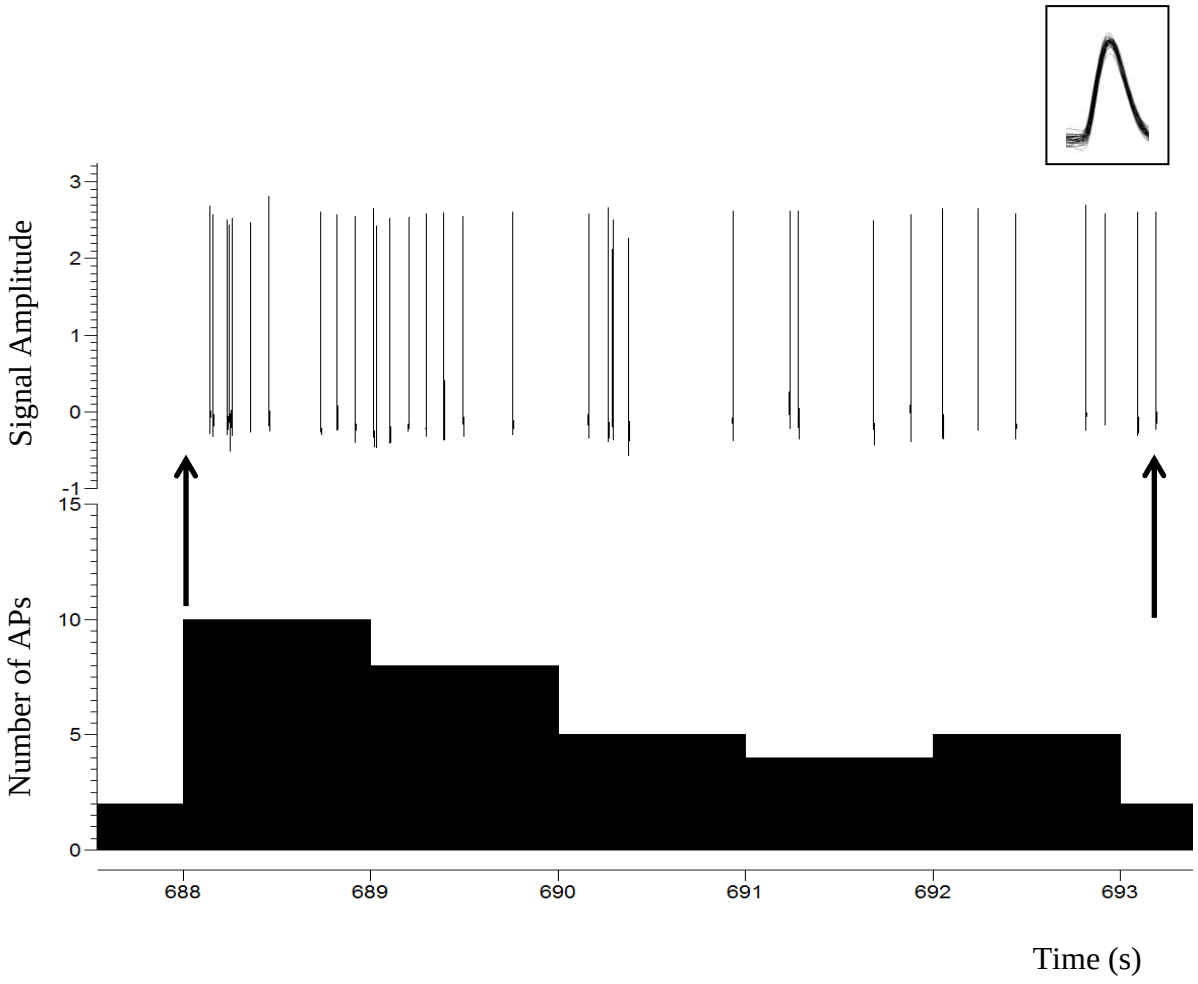

Figure 3.8. Example recording of a knee joint nociceptor response to application of a 15g vF monofilament to the knee joint-associated receptive field in a naïve rat. A) Raw data trace and B) rate histogram illustrating a slowly adapting response that was maintained throughout the 5 second stimulation. Insert = AP overlay demonstrating single unit recording. The CV of the studied unit was 1.13m/s indicating a C-fibre.

Responses to a range of increasing weights of vF monofilaments (0.16 - 15g) were recorded to characterise the mechanical sensitivity of the recorded knee afferents. An example recording representing the response of a single unit, from a naive rat, to increasing weights of vF stimulation is shown in Figure 3.9. This particular knee joint afferent exhibited a graded response to increasing intensity of mechanical stimulation that is characteristic of nociceptors and was typical of the afferents studied in this thesis.

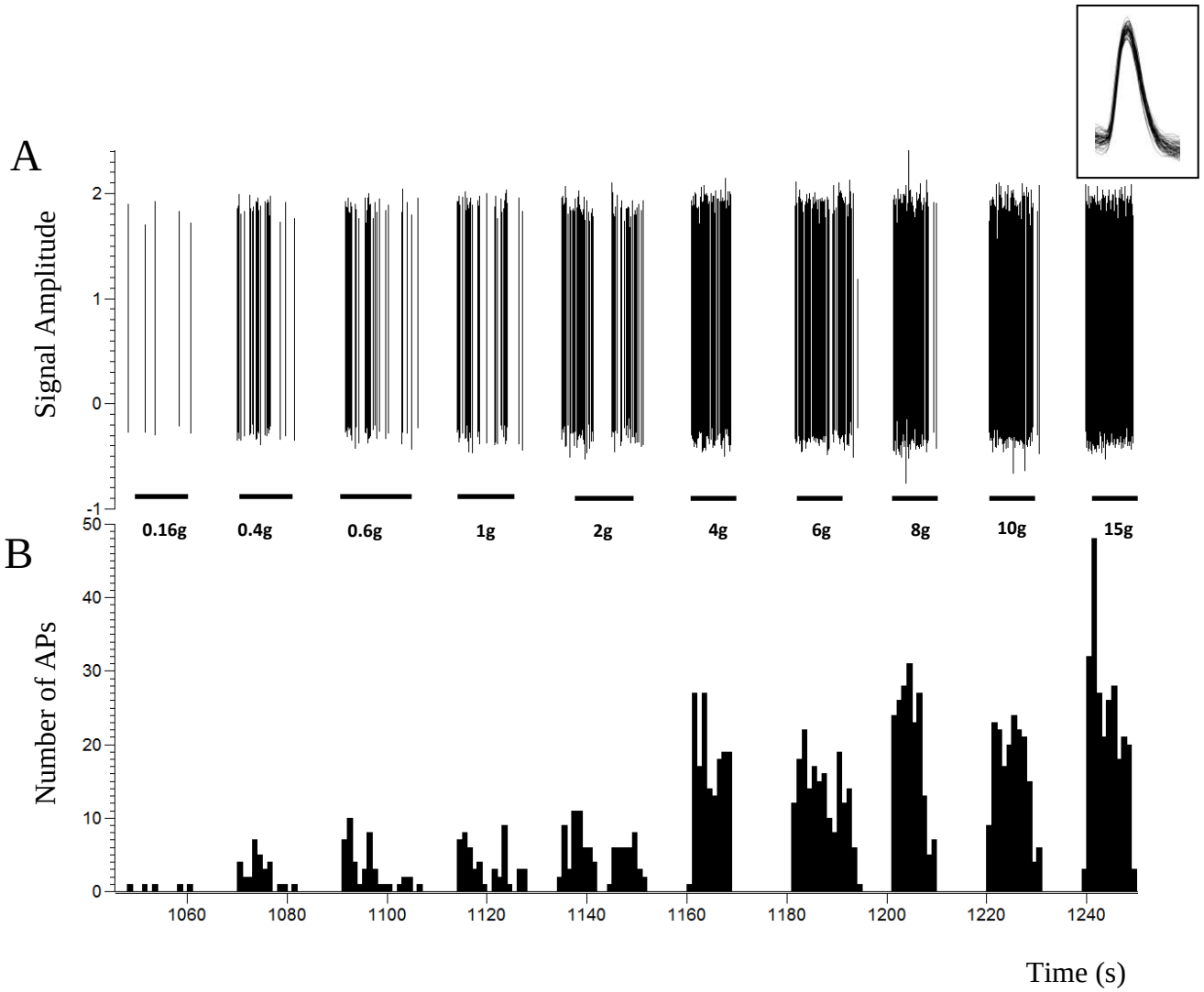
A
Signal Amplitude
2
1
0
-1
0.16g
0.4g
0.6g
1g
2g
4g
6g
8g
10g
15g
B
Number of APs
50
40
30
20
10
0
1060
1080
1100
1120
1140
1160
1180
1200
1220
1240
Time (s)

Figure 3.9. A representative example Spike2 data trace of mechanically-evoked firing of a knee joint nociceptor in a naïve rat. (A) Afferent firing evoked by 0.16 - 15g vF stimulation (B) corresponding rate histogram of evoked responses (1s bins). Increasing the weight of vF stimulation resulted in a graded increase in the rate of mechanically-evoked responses. The unit had a CV of 1.87 m/s and was an Aδ-fibre. Insert = AP overlay demonstrating single unit recording. Horizontal lines represent the timing of mechanical stimulation.

The mean vF stimulus response data for all fibres recorded in naïve rats demonstrated that the fibres recorded from the MAN, with knee joint receptive fields (n = 39), were typically nociceptive, with firing rates exhibiting a graded increase to increasing intensity of stimulation, thus encoding stimulus intensity (Figure 3.10).

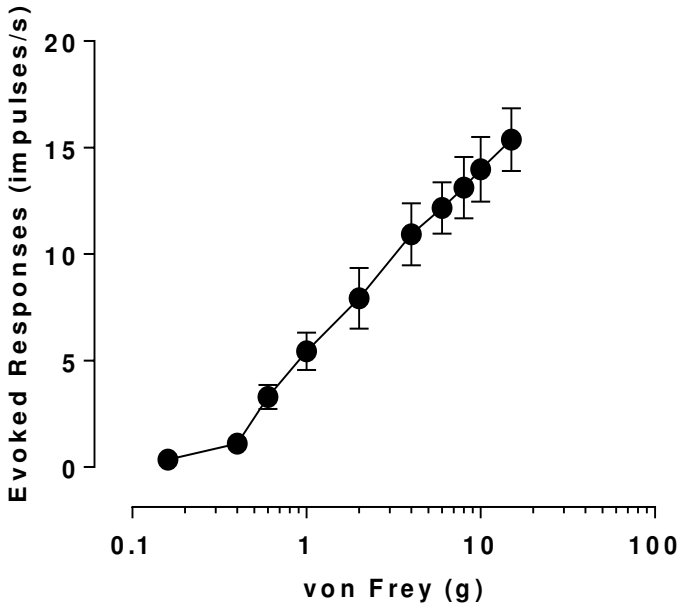

Figure 3.10. Mechanically-evoked responses of knee joint nociceptors recorded in naïve rats. These fibres exhibited a graded response to increasing intensity of mechanical stimulation (0.16-15g vF monofilament) of the knee joint (n = 39). Data presented as mean ± SEM.

The median mechanical threshold of these fibres (the lowest weight vF monofilament required to evoke ≥ 2 APs) was 0.6g (Figure 3.11) and ranged from 0.16 - 6g indicating that knee joint nociceptors can have low- or high-threshold mechanical thresholds.

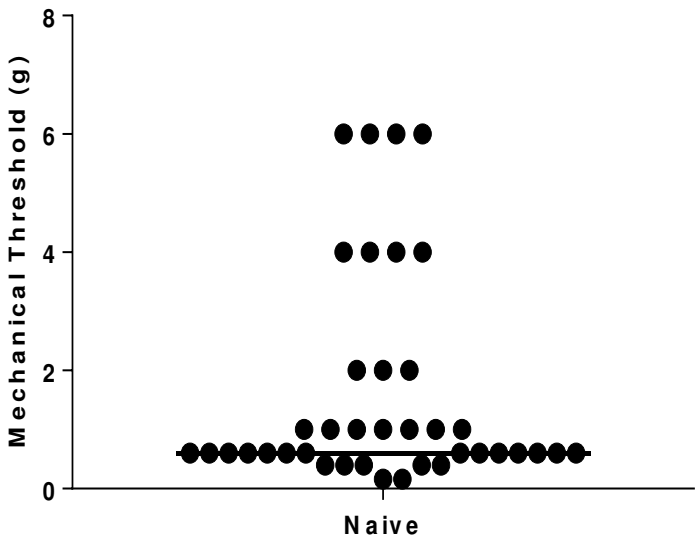

Figure 3.11. Mechanical thresholds of knee joint nociceptors recorded in naïve rats (n = 39). Horizontal line represents the median mechanical threshold = 0.6g, median range = 0.16 - 6g.

3.4.4. Electrophysiological characterisation of knee joint nociceptor responses to mechanical stimulation in MIA rats

The data presented here was collected during the control (pre-drug) period of the pharmacological experiments included in chapter 5. Data from these different studies has been pooled and enables the assessment of the impact of MIA-induced OA on mechanically-evoked responses of knee joint afferents 14 days post-induction. Since these data were collected from rats used in pharmacological experiments in all cases one fibre was recorded per rat.

Both Aδ- and C-type fibres were recorded in MIA and saline rats and have been included in the analysis, with CVs ranging from 0.23 - 12.1m/s (median = 1.79m/s) in MIA rats and 0.18 - 8.1m/s (median = 1.5m/s) in saline rats. There was a similar distribution of CVs when comparing between the two groups and there were no significant differences in the CVs of these fibres (Mann Whitney t-test, Figure 3.12). In a small number of cases (n = 5) CV measurement was not possible following drug treatment as the fibre response had been fully inhibited.

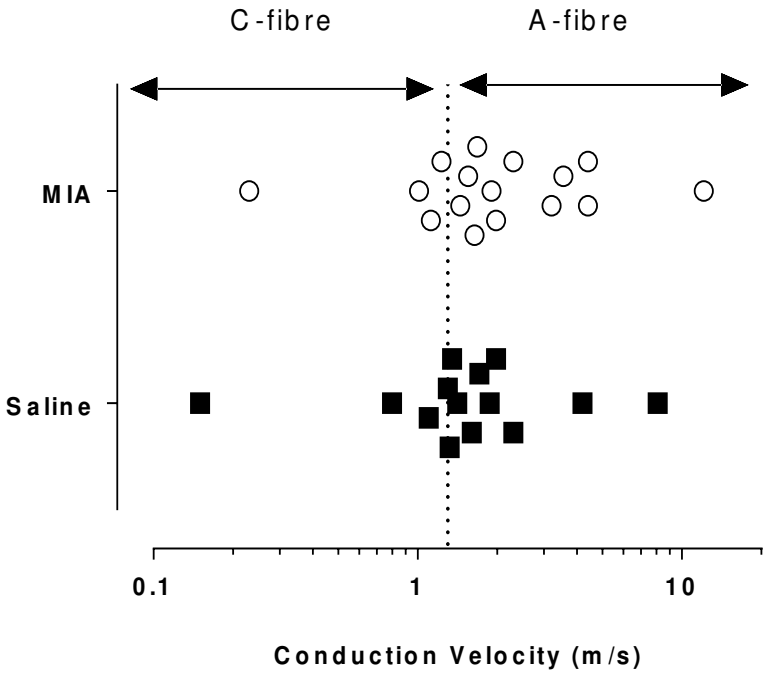

Figure 3.12. Distribution of CVs of knee joint nociceptors recorded in MIA (n = 16) and saline (n = 14) rats. Fibres in both Aδ- and C-fibre CVs were recorded.

Similar to the firing properties of knee joint afferents in naïve rats, nociceptors from MIA and saline rats exhibited a graded increase in response to stimulation by vF monofilaments of increasing weight. Consistent with the recordings in naïve rats and with previously published reports of knee joint nociceptor receptive fields (Kelly et al., 2012), mechanically-evoked neuronal activity could be recorded in response to vF monofilament stimulation of the medial aspect of the knee joint including the joint capsule, medial collateral ligament and surrounding tissue (see Chapter 2 Figure 2.3). Receptive fields were again discrete, covering no more than 1-3mm in diameter.

To enable direct comparison, Figure 3.13 below contains raw data traces and corresponding rate histograms that are typical examples of mechanically-evoked responses recorded from Aδ-fibres in a saline and MIA rat. The fibre recorded in the MIA rat exhibited increased mechanically-evoked firing rates and a lowered mechanical threshold.

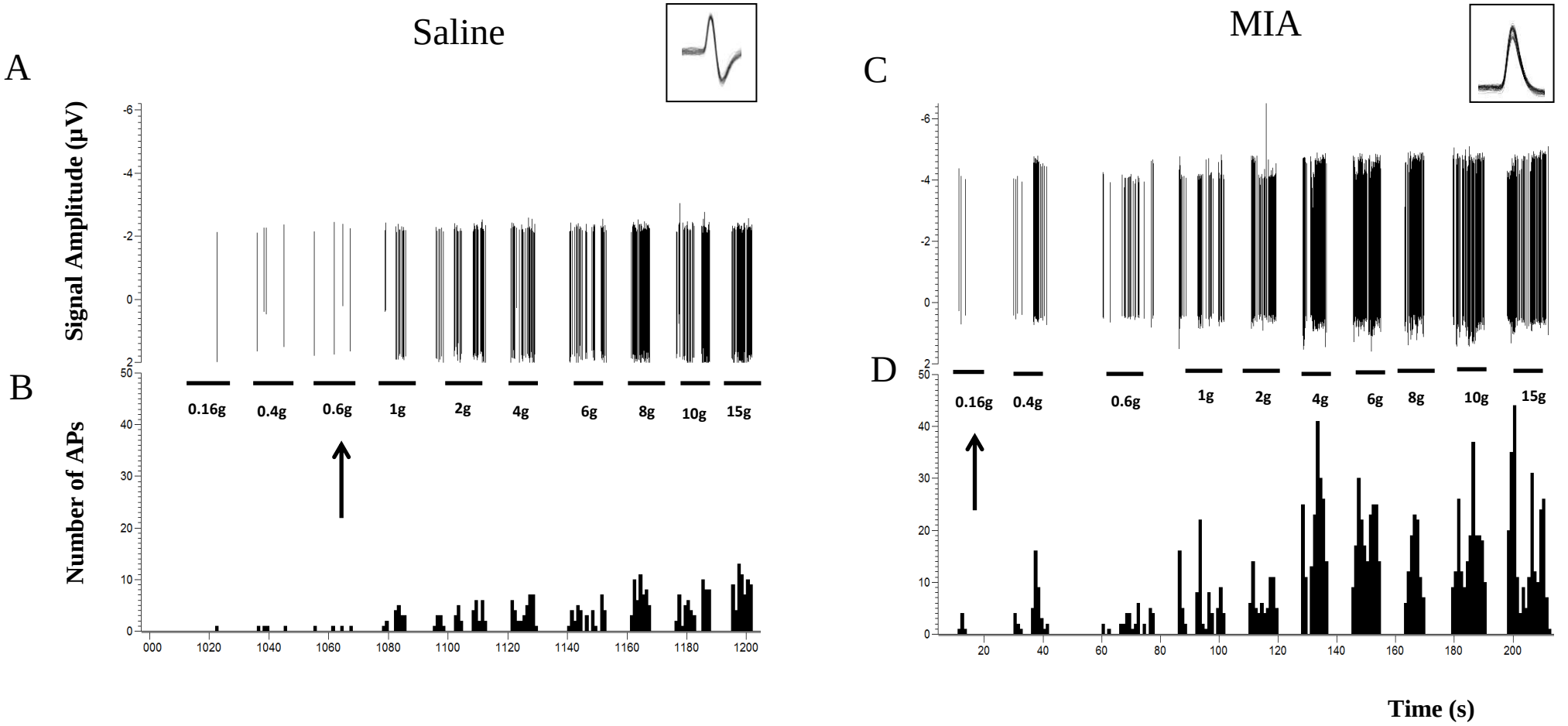
A
Saline
Signal Amplitude (µV)
B
Number of APs
0.16g
0.4g
0.6g
1g
2g
4g
6g
8g
10g
15g
C
MIA
D
Time (s)

Figure 3.13. Typical example raw data traces of mechanically-evoked responses of knee joint nociceptors recorded in a saline (A) and MIA rat (B). An overlay of the action potentials recorded during each trace is shown as an inset in the respective figures, demonstrating single unit recording. Corresponding rate histograms for the saline and MIA rats are shown below each figure demonstrating and enhanced firing rate in the MIA example. Arrows in A and C indicate mechanical thresholds. CV for the fibre in A/B is 1.71m/s and in C/D are 1.55m/s indicating that these fibres are Aδ-fibres.

When mean mechanically-evoked response data from all fibres recorded in saline and MIA rats were compared, the vF stimulus response curve for knee joint afferents recorded in MIA rats was shifted upwards compared to responses in saline rats (Figure 3.14), demonstrating increased knee joint nociceptor firing to vF monofilament stimulation (i.e. peripheral sensitization). Mechanically-evoked responses were significantly increased in MIA rats compared to responses in saline rats ($p<0.0001$, two-way ANOVA with Bonferroni multiple comparison; Figure 3.14). The maximum firing rate of nociceptors in MIA rats (evoked by 15g vF monofilament) was 11.95 ± 2.09APs/s compared to 8.63 ± 1.61AP/s in saline rats. These firing rates are consistent with those published from joint nociceptors in similar studies.

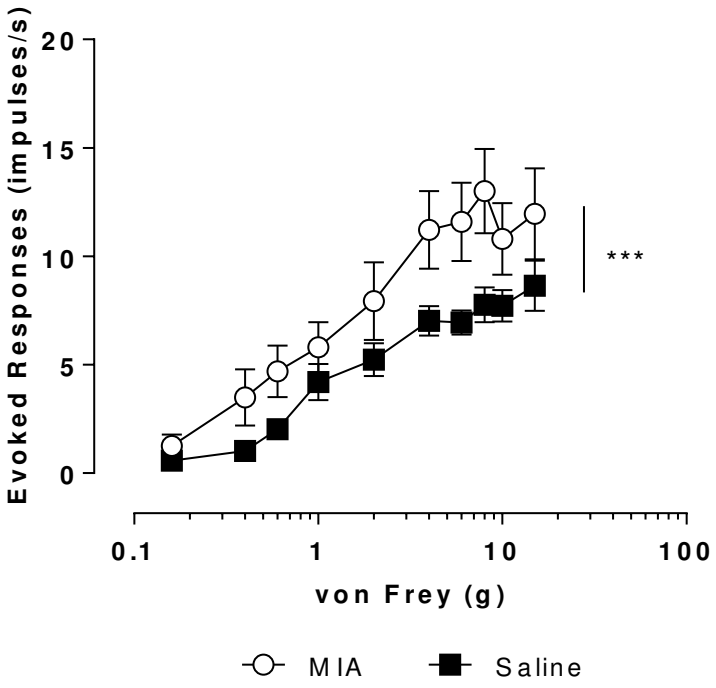

Figure 3.14. Effect of MIA treatment on mechanically-evoked responses of knee joint nociceptors. The stimulus response curve in MIA rats (n = 9) is shifted upwards compared to saline rats (n = 8) demonstrating significantly increased responses to both low and high intensity stimuli. Data represented as mean rate of firing ± SEM. $^{***}p<0.001$, two-way ANOVA with Bonferroni multiple comparison.

Despite previous reports of lowered mechanical thresholds of joint nociceptors in the MIA model, in my hands mechanical thresholds were not significantly different in MIA compared to saline rats (median thresholds; MIA = 1g, range 0.16 - 4g, saline = 0.6g, range, 0.16g - 4g; $p>0.05$, Mann Whitney u test; Figure 3.15).

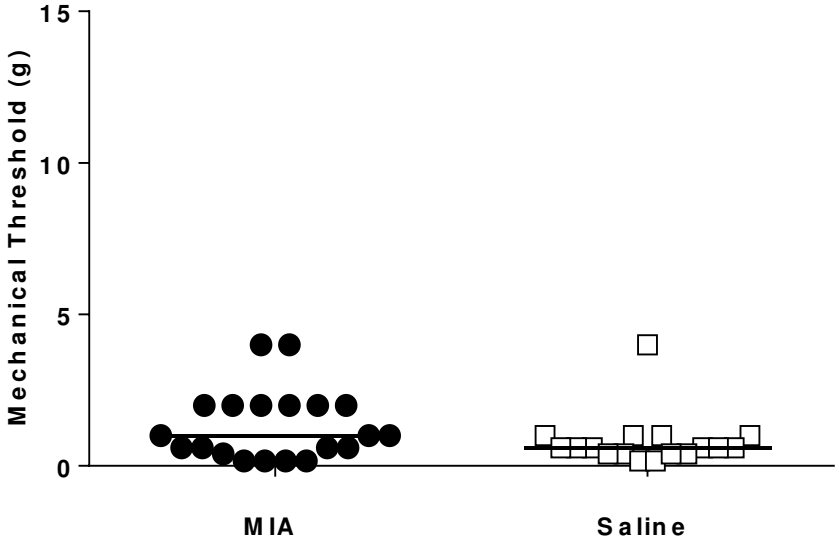

Figure 3.15. Effect of MIA treatment on knee joint nociceptor mechanical thresholds 14 days post-injection. MIA injection had no significant effect on the mechanical thresholds of knee joint afferents compared to saline controls. Line represents median vF monofilament weight. $p<0.05$, Mann Whitney u test.

3.4.5. Correlation analysis of pain behaviour and electrophysiological responses of knee joint nociceptors in the MIA model

In MIA rats there was no correlation between the ipsilateral day 14 weight bearing deficits and paw withdrawal thresholds suggesting that the mechanisms underlying these different types of pain behaviour may be distinct ($p = 0.98$, $r = -0.1394$, Spearman Correlation; Figure 3.16).

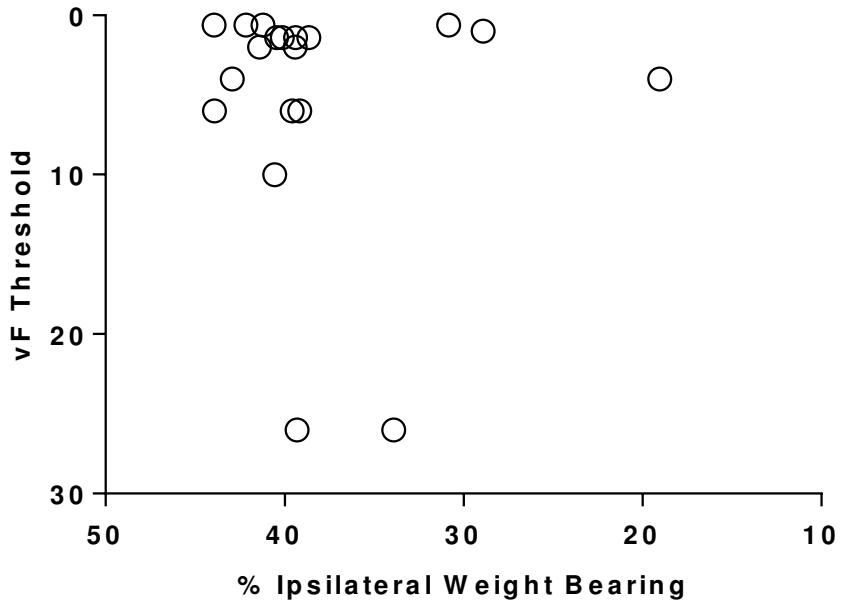

Figure 3.16. Ipsilateral hind limb weight bearing and paw withdrawal thresholds in MIA rats (n = 19) do not correlate.

Since pain behaviour measures were obtained along with matched recordings of joint afferent mechanically-evoked responses in individual rats, the relationship between pain behaviour and mechanical sensitivity of knee joint nociceptors in the MIA model was investigated. Correlation analysis of the rate of knee afferent firing and pain behaviour measures (weight bearing and hind paw withdrawal thresholds at days 7 and 14) was performed. No significant correlations were found were found between pain behaviour at days 7 and 14 and joint nociceptor firing at day 14.

	Weight Bearing		Paw Withdrawal Threshold	
	Post-injection Day		Post-injection Day	
vF monofilament weight (g)	**7**	**14**	**7**	**14**
0.16	-0.34	-0.02	0.04	-0.05
0.4	-0.44	0.008	-0.04	-0.12
0.6	-0.45	-0.32	0.23	0.28
1	-0.37	-0.11	-0.009	0.01
2	-0.61	0.1	-0.2	-0.23
4	-0.43	0.11	-0.09	-0.2
6	-0.43	0.1	0.03	-0.09
8	-0.52	0.11	-0.06	-0.19
10	-0.49	0.19	-0.14	-0.19
15	0	0.17	0.06	-0.16

Table 3.1. Summary of spearman correlation ‘R values’ for knee joint nociceptor firing rates and pain behaviour data (weight bearing and hind paw withdrawal thresholds).

3.5 Discussion

The work outlined in this chapter describes the characterisation of pain behaviour and electrophysiological properties of knee joint nociceptors in the MIA model of OA. This work was essential to confirm that the MIA model had been successfully established and developed as expected in my hands. Data was collected in 'normal' and OA animals under the same laboratory conditions in which subsequent pharmacological studies were performed and compared (chapters 4 and 5). i.a. injection of 1mg MIA induced the expected changes in pain behaviour including a reduction in hind limb weight bearing and mechanical allodynia (Bove et al., 2003, Kelly et al., 2012, Ashraf et al., 2013, Kelly et al., 2013a, Kelly et al., 2013b, Mapp et al., 2013). Only a very limited number of studies have characterised joint nociceptor responses to a range of mechanical stimuli following MIA injection (Kelly and Donaldson, 2008, Kelly et al., 2012, Kelly et al., 2013a, Bullock et al., 2014); most have used only a single innocuous and noxious mechanical stimulus (i.e. joint rotation) (Schuelert and McDougall, 2006b, Schuelert and McDougall, 2008, Schuelert and McDougall, 2009, Schuelert et al., 2010, Schuelert and McDougall, 2011, Schuelert and McDougall, 2012). Electrophysiological recordings of knee joint nociceptors reported here confirmed the development of peripheral sensitization in the MIA model manifested by an increase in mechanically-evoked firing rates of joint-associated nociceptors compared to control rats and validated the further study of pharmacological modulation of peripheral sensitization in chapter 5. These findings in the MIA model are consistent and build upon published findings from our group (Kelly et al., 2012, Kelly et al., 2013a, Bullock et al., 2014) and suggest that peripheral

sensitization is a robust feature of the MIA model of OA during established pain and that the study of its modulation is likely to have relevance to the treatment of OA pain.

3.5.1. Pain behaviour

Joint pain is the most debilitating and disabling symptom of OA and the primary reason for patients seeking clinical help. A requirement of animal models of OA is to mirror key aspects of human OA pain which validates the study of the model to increase the mechanistic understanding of human OA pain mechanisms and aid the development of improved analgesics for OA treatment. Studies using preclinical models of OA measure weight bearing to indirectly measure the development of joint pain (Bove et al., 2003, Sagar et al., 2010, Kelly et al., 2012, Mapp et al., 2013). The measurement of weight bearing has clinical relevance to human OA as patients report pain in joint use e.g. climbing the stairs/walking the dog, running (Messier, 1994, Kul-Panza and Berker, 2006). The behavioural data in this chapter demonstrate that MIA reduces ipsilateral hind limb weight bearing and hind paw mechanical thresholds compared to the saline control group which is in line with studies using the same concentration of MIA (1mg) (Bove et al., 2003, Combe et al., 2004, Fernihough et al., 2004, Kelly et al., 2012, Kelly et al., 2013a, Mapp et al., 2013, Bullock et al., 2014). The magnitude and time course of the reduction in ipsilateral weight bearing I observed is consistent with that reported in other groups (Fernihough et al., 2004, Kelly et al., 2012, Kelly et al., 2013b). However, an absence in weight bearing asymmetry (Mapp et al., 2013) and

almost a complete reversal to baseline at days 7 and 14 has been observed (Bove et al., 2003, Pomonis et al., 2005b).

Pain behaviour in animal models of OA can be assessed by methods other than weight bearing which enables the measurement of different aspects of human OA pain symptoms. Human OA is accompanied by hypersensitivity of distal regions and is suggestive of referred pain, indicating central sensitization. In rodent models of OA mechanical allodynia reflective of referred pain can be assessed by determining the hind paw withdrawal threshold to vF monofilament stimulation (Neugebauer et al., 2007, Mogil, 2009). Evidence from clinical studies have demonstrated the translatability of this pain measure to human OA as reduced pain pressure thresholds have been detected in OA patients at sites distal to the knee joint (Suokas et al., 2012). The magnitude and time course reported here is similar to published reports with over 50% reduction in mechanical thresholds at days 7-28 post-injection (Combe et al., 2004, Fernihough et al., 2004, Mapp et al., 2013).

3.5.2. Peripheral sensitization as a contributor to OA-induced joint pain

Electrophysiological characteristics of knee joint nociceptors, including mechanically-evoked firing rates, mechanical thresholds, CVs and receptive fields are reported in this chapter. The magnitude of evoked responses and mechanical thresholds of knee joint nociceptors in naïve, saline and MIA rats were consistent with previous studies (Schaible and Schmidt, 1983b, Schaible and Schmidt, 1983a, Kelly et al., 2012) including those conducted in our lab

(Kelly et al., 2012, Kelly et al., 2013a, Bullock et al., 2014). Early studies of this type that recorded from the MAN in the cat classified the majority of knee joint afferents as nociceptors with CVs in the C-type and Aδ fibre ranges (Schaible and Schmidt, 1983a, Schaible and Schmidt, 1983b). The finding in this chapter that knee joint nociceptors are predominantly Aδ and C-type fibres is consistent with this published data. The distribution of receptive fields of the studied afferents in this chapter is also similar to published studies recording from the cat and rat MAN/saphenous (Schaible and Schmidt, 1983a, Schaible and Schmidt, 1985, Kelly et al., 2012, Kelly et al., 2013a, Bullock et al., 2014). Discrete receptive fields were located on the medial aspect of the joint with activity evoked by probing structures overlying the joint capsule, the heads of the femur and tibia, the medial collateral ligament and the surrounding tissue and muscle (Schaible and Schmidt, 1983b, Schaible and Schmidt, 1983a, Kelly et al., 2012, Kelly et al., 2013a)

The sensitization of knee joint afferents during OA has been indirectly suggested in clinical studies and demonstrated here and by others pre-clinically. In human knee OA, this sensitization has been suggested to be an important contributor to the severity of pain experienced (Arendt-Nielsen et al., 2010) and may promote the transition from acute to chronic pain (Hunter et al., 2009). Recent published studies have demonstrated peripheral sensitization in animal models of OA including following MIA-treatment (Schuelert and McDougall, 2009, Kelly et al., 2012, Schuelert and McDougall, 2012), spontaneous OA (McDougall et al., 2009) and following surgically induced OA in the guinea pig (Gomis et al., 2007). The demonstration in this chapter of

an increase in mechanical responsiveness after MIA (1mg) treatment is consistent with this and adds to these reports and the degree of sensitization was in good agreement with recent studies from our group (Kelly et al., 2012, Kelly et al., 2013a, Bullock et al., 2014). A limited number of these previous studies have investigated the relationship between the impact of OA on joint nociceptor sensitivity and its relationship to pain behaviour. No significant correlation between pain behaviour at days 7 and 14 and joint nociceptor firing recorded at day 14 was observed in this study. Despite this, the coincident presence of peripheral sensitization and pain behaviour suggests a strong association between the two. Peripheral sensitization following OA development would be expected to increase nociceptive input from the joint to the spinal cord and is likely to make an important contribution to driving maladaptive central processes that result in central sensitization and chronic pain (Sagar et al., 2010, Sagar et al., 2011, Woolf, 2011, Kelly et al., 2013b). The findings in this chapter therefore add further understanding to this area.

The peripheral substrates that drive peripheral sensitization in the MIA model and in human OA are currently unknown and this remains an important unanswered question. Recent evidence suggests that joint inflammation plays a role in OA joint pain (Pelletier et al., 2001, Tindell et al., 2012). An inflammatory component has been implicated to contribute to pain in the MIA model. Several characteristics of inflammatory pain have been demonstrated including an increase in knee joint diameter, expansion of the synovial membrane and infiltration of the synovium by inflammatory cells such as macrophages (Bove et al., 2003, Fernihough et al., 2004, Mapp et al., 2013).

Electrophysiological changes in the Kaolin/Carrageenan model of inflammatory arthritis including Aδ and C-type fibres developing increased mechanosensitivity and spontaneous activity (Schaible and Schmidt, 1985) are similar to the OA-induced peripheral sensitization reported here.

Inflammation in the MIA model could drive peripheral sensitization following the release of pro-inflammatory mediators (IL-1, IL-6, TNF-α, PGE_2) known to modulate nociceptor sensitivity (Orita et al., 2011, Bowles et al., 2014). A recent study in our laboratory identified an important role for the sensory neuropeptide CGRP in the sensitization of joint nociceptors in the MIA model (Bullock et al., 2014). Exogenous CGRP increased the mechanosensitivity of knee joint nociceptors in MIA and saline rats and blockade of local CGRP receptors reversed MIA- and MNX-induced joint nociceptor sensitization. The importance of inflammation to peripheral sensitization and pain behaviour in the MIA model is evident from the inhibition of increased knee joint nociceptor mechanosensitivity (Schuelert and McDougall, 2009) and weight bearing deficits following treatment with anti-inflammatory drugs including diclofenac (Bove et al., 2003, Ivanavicius et al., 2007).

3.5.3. Choice of the MIA dose used in this thesis

A 1mg dose of MIA was chosen to induce this model of OA since 1mg was sufficient to produce robust and reproducible pain behaviour (weight bearing deficits and reduced paw withdrawal thresholds) and OA-like changes in joint structure as reported previously (Bove et al., 2003, Kelly et al., 2012, Mapp et

al., 2013), without causing the joint destruction elicited by higher doses (e.g. 3mg) (Bove et al., 2003, Pomonis et al., 2005a). High doses of MIA causes the development of large scale chondrocyte cell death and gross joint pathology (Pritzker, 1994). In addition, studies have identified that doses of MIA lower than 1mg (e.g. 0.3mg) produce minimal changes in pain behaviour compared to control rats (Bove et al., 2003, Pomonis et al., 2005a, Sagar et al., 2010) rendering those doses ineffective for studies investigating OA-induced pain. Thus, a 1mg dose of MIA enables a balance between ensuring the model is clinically relevant by mirroring key aspects of human OA, whilst minimising the impact on the animal.

3.5.4. Conclusions

The work in this chapter characterised the MIA model, with respect to pain behaviour and electrophysiological responses of joint nociceptors. Electrophysiological and behavioural analysis confirmed that peripheral sensitization developed as expected and was coincident with established pain behaviour. These findings further highlight the important role that peripheral sensitization is likely to play in the development and progression of pain in pre-clinical models of OA. The presence of peripheral sensitization in the MIA model provides an ideal opportunity for the identification and study of novel analgesic targets that might serve to reduce this sensitization, having possible relevance to the treatment of OA pain.

Chapter Four

Effect of the GPR55 receptor agonist LPI on knee joint nociceptor mechanosensitivity in naïve rats

4.1. Introduction

Consistent with their role as nociceptive neurones, findings from the previous chapter have demonstrated that joint afferent nociceptors encode mechanical stimulus intensity to punctate stimulation of their receptive fields (Kelly and Donaldson, 2008, Kelly et al., 2012, Kelly et al., 2013a, Bullock et al., 2014). The mechanical sensitivity of joint afferent neurones can be subject to plasticity as demonstrated in chapter 3 and the identification of mechanisms leading to a decrease in mechanical responsiveness may be future targets for the treatment of joint pain. Targeting the pain pathway at the level of the joint could potentially maximise analgesia without causing systemically mediated side effects. The GPCR GPR55 is known to be present in sensory neurones (Lauckner et al., 2008) of the DRG and is thought to have a role in the modulation of pain processing (see Chapter 1, Section 1.12.2) (Staton et al., 2008, Schuelert and McDougall, 2011, Breen et al., 2012, Gangadharan et al., 2013). However, very few studies have investigated effects of GPR55 receptor activation in vivo and almost nothing is known about the role of the GPR55 receptor in the modulation of joint nociception.

4.1.1. GPR55 receptor and nociception

Compelling evidence indicates a role for the GPR55 receptor in the modulation of nociception. Behavioural studies have identified a pro-nociceptive role in acute mechanical nociception (Gangadharan et al., 2013) and in models of inflammatory and neuropathic pain (Staton et al., 2008, Breen et al., 2012). The periphery appears to be an important site of GPR55 receptor mediated

pronociception since expression has been detected in sensory neurones of the DRG (Lauckner et al., 2008), intraplantar administration of LPI causes mechanical hypersensitivity and electrophysiological recordings from a mouse skin-nerve preparation in vitro demonstrated mechanical sensitization of cutaneous afferents by LPI (Gangadharan et al., 2013). Although these published studies indicate a pro-nociceptive role for GPR55, a recent study provided evidence that under some conditions GPR55 receptor activation in vivo may be anti-nociceptive. In the 2% kaolin and 2% carrageenan model of acute inflammatory joint pain, the synthetic GPR55 agonist O-1602 attenuated the mechanosensitivity of nociceptive knee joint afferent C fibres (Schuelert and McDougall, 2011). The anti-nociceptive effect of O-1602 was abolished by the GPR55 receptor antagonist O-1918. Overall then, the available evidence indicates that the GPR55 receptor may have an important role in the modulation of nociception, with studies indicating a pro-nociceptive role in cutaneous afferent nociceptors under non-pathological, inflammatory and neuropathic conditions and an anti-nociceptive role in articular afferents.

4.2. Aims and objectives

Given the controversy described above, the work presented in this chapter sought to further interrogate the role of GPR55 in the modulation of joint nociception. LPI was chosen as an experimental tool to examine the effects of GPR55 receptor activation in vivo under non-pathological conditions. LPI was chosen rather than for example the synthetic agonist O-1918 as it has been proposed as the endogenous agonist of GPR55. The effects of LPI on

mechanically-evoked responses of knee joint afferent nociceptors were studied and the involvement of GPR55 in these effects was determined using the GPR55 antagonist cannabidiol.

4.3. Methods

4.3.1. Animals

Male Sprague Dawley rats (n = 39) (Charles River, Margate, Kent, UK) weighing between 336 ± 4.4gms were used in these experiments. Animals were housed 3 per cage in temperature and humidity controlled rooms on a 12:12hr light: dark cycle (lights on at 8:00am). Food (standard rat chow) and water were freely available to animals.

4.3.2. Electrophysiology

For detailed methods outlining rat surgical preparation for electrophysiology and extracellular recordings of knee joint afferent nociceptor responses see Chapter 2 (see Section 2.4).

4.3.3. Drug administration

All drugs and vehicles were administered once stable control responses had been established (see Chapter 2, Section 2.4.4). LPI (150 and 250µM; Sigma, UK), saline and the putative GPR55 antagonist cannabidiol (50µg/100µl; Tocris, UK) were administered peripherally via the contralateral femoral artery at a volume of 100µl and washed in with 300µl heparinised saline. The CB_1 antagonist AM281 (1mg/kg; Tocris, UK) was administered via an i.p injection. Unless otherwise stated drug effects on mechanically-evoked (vFs 0.6-15g) responses were studied at 5 minute intervals for 60mins per dose (see chapter

2, section 2.4.2). At the end of the recording period, KCl (250mM) was administered via the contralateral femoral artery to confirm that drugs accessed the peripheral terminals of joint afferent nociceptors (see chapter 2, Section 2.4.2). Finally, the CV of the studied afferent was calculated to determine the afferent fibre type (see Chapter 2, Section 2.4.2).

A number of separate experimental studies were performed as outlined below:

Study 1: Effects of cumulative administration of 150µM and 250µM LPI on knee afferent nociceptor mechanically-evoked responses were determined (n = 10).

Study 2: Effects of administration of two consecutive volumes of saline (vehicle) (n = 16) on knee afferent mechanically-evoked responses were studied over an identical time frame as LPI experiments serving as vehicle controls.

Study 3: Effects of cannabidiol (diluted in saline to a concentration of 50µg/100µl) alone on knee afferent mechanically-evoked responses were studied for 30 minutes (n = 12) at which point LPI (250µM) was administered. Effects of LPI on knee afferent nociceptor mechanically-evoked responses

following cannabidiol pre-administration were then studied for a further 60 minutes (n = 9).

Study 4: Effects of the CB_1 antagonist AM281 (diluted in DMSO, cremaphor and distilled H_2O to a concentration of 1mg/kg i.p) on knee afferent mechanically-evoked responses were studied for 30 minutes (n = 9) at which point LPI (250µM) was administered. Effects of LPI post-AM281 administration were then studied for a further 60 minutes (n = 9).

4.3.4. Statistical analysis

Data analysis was performed using Prism software (versions 5 or 6; GraphPad Software). Data were tested for normality using the Kolmogorov Smirnov (KS) test. Where data were normally distributed, a parametric test was used (e.g. two-way ANOVA) and where data was not normally distributed a non-parametric test was used (e.g. Mann Whitney unpaired u-test or Freidman's ANOVA).

4.4. Results

4.4.1. Conduction velocities and fibre type

Aβ- (n = 1), Aδ- (n = 20) and C-type (n = 9) fibres have been included in the analysis for this chapter (median = 1.78m/s, range = 0.15 - 37m/s). CVs could not be confirmed in 8 fibres due to complete inhibition of excitability. A- and C-fibres are discussed collectively.

4.4.2. Effect of the GPR55 receptor agonist LPI on mechanically-evoked responses of knee joint primary afferent nociceptors in naïve rats

The effect of peripherally administered LPI (150 and 250µM, i.ar) on mechanically-evoked responses of knee joint primary afferent nociceptors were studied in naïve rats (n = 10) (see Figure 4.3). Generally, an increase in the weight of vF stimulation resulted in a graded increase in evoked responses. The representative digitised traces included below show typical examples of the effects of LPI (250µM) (Figure 4.1) and vehicle saline (see Figure 4.2) on the rate of mechanically-evoked firing of two Aδ knee afferent nociceptors. LPI almost completely abolished the rate of firing 45 minutes post-administration (Figure 4.1 B and D) compared to the control responses (Figure 4.1 A and C). Saline had no effect on mechanically-evoked responses 45 minutes post-administration (Figure 4.2 B and D) compared to control (Figure 4.2 A and C).

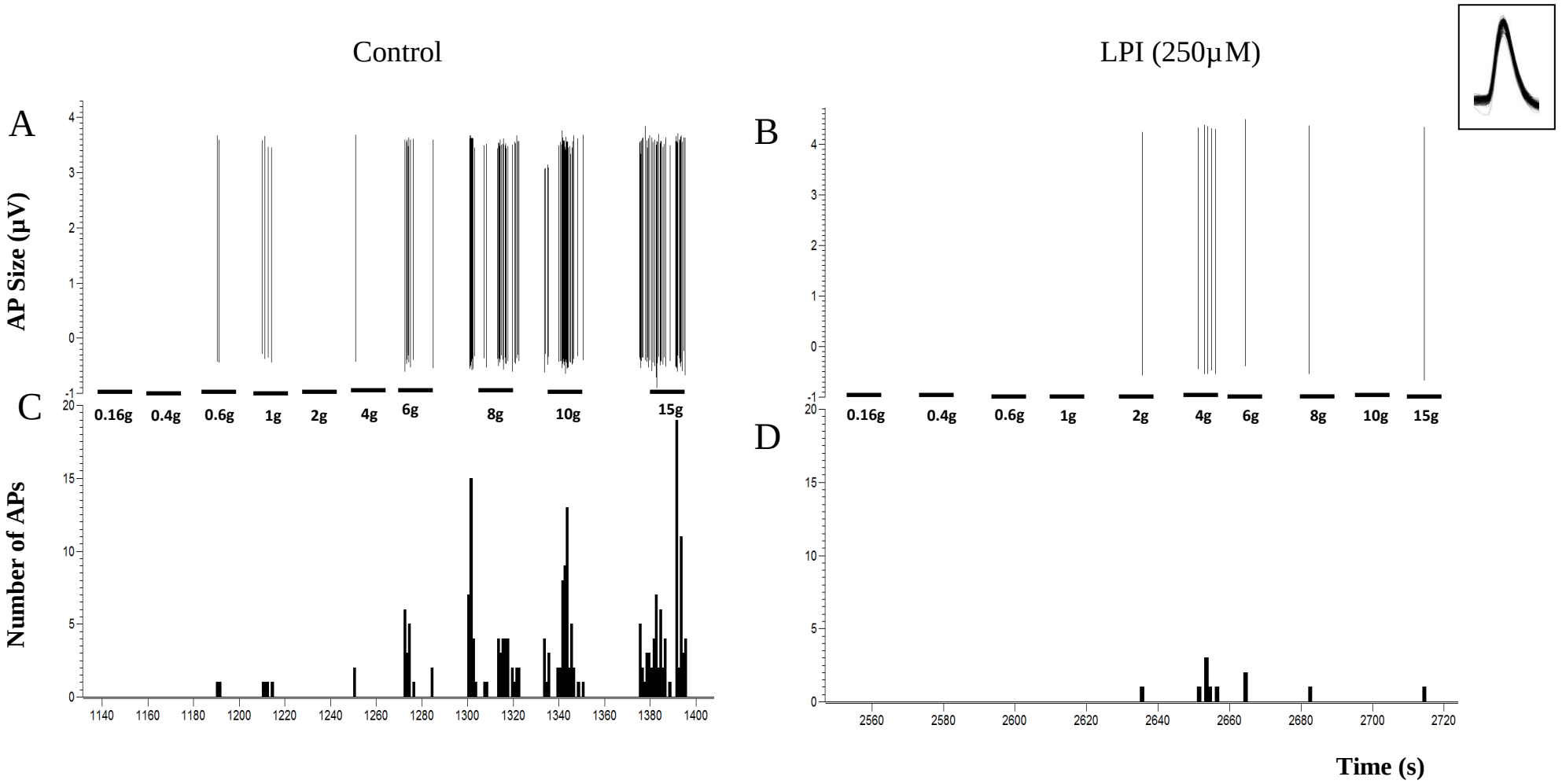
Control
LPI (250µM)
A
B
C
D
AP Size (µV)
Number of APs
0.16g
0.4g
0.6g
1g
2g
4g
6g
8g
10g
15g
Time (s)

Figure 4.1. Typical example raw data traces of control mechanically-evoked responses of knee joint nociceptors (A) and 45 minutes post-administration of 250µM LPI (B) in a naïve rat. An overlay of the action potential recorded in the figures, demonstrating single unit activity. Corresponding rate histograms for the control (C) and post-administration of 250µM LPI (D) are shown below each figure showing an inhibition in the mechanically-evoked firing rate of knee joint nociceptors after administration of LPI. CV of fibre = 3.45m/s.

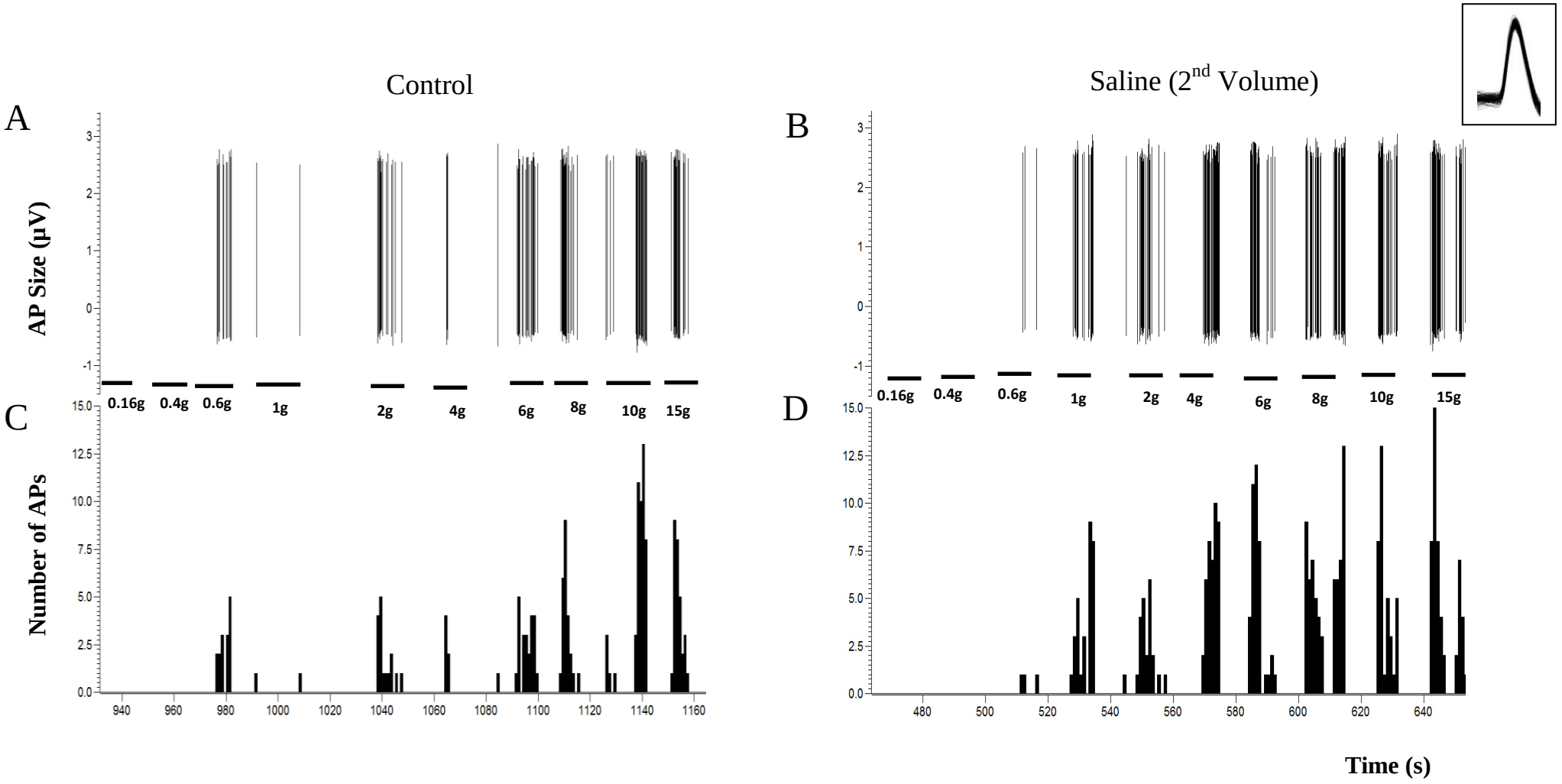
Control
Saline (2nd Volume)
A
B
C
D
AP Size (µV)
Number of APs
0.16g
0.4g
0.6g
1g
2g
4g
6g
8g
10g
15g
Time (s)

Figure 4.2. Typical example raw data traces of control mechanically-evoked responses of knee joint nociceptors (A) and 45 minutes post-administration of 2nd volume of saline (B) in a naïve rat. An overlay of the action potential recorded in the figures, demonstrating single unit activity. Corresponding rate histograms for the control (C) and post-administration of 2nd volume of saline (D) are shown below each figure showing no effect on the mechanically-evoked firing rate of knee joint nociceptors after administration of saline. CV of fibre = 3.3m/s.

When mean responses were analysed, it was found that the administration of 150µM and 250µM LPI significantly inhibited joint nociceptor mechanically-evoked responses compared to control (pre-drug) responses ($p<0.0001$, two-way ANOVA; Figure 4.3). The inhibition following 250µM LPI was significantly greater than at 150µM demonstrating a concentration-dependent effect ($p< 0.0001$, two-way ANOVA).

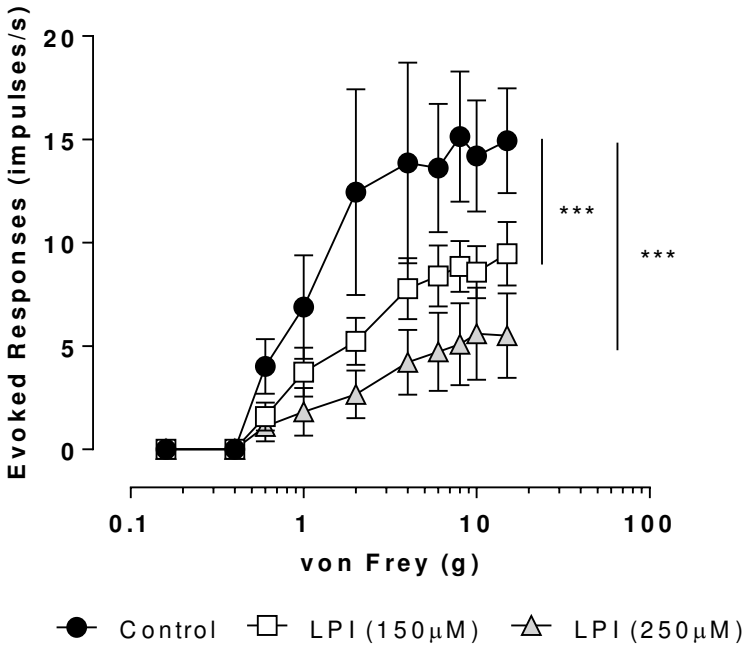

Figure 4.3. Effect of LPI (150µM and 250µM) on knee joint nociceptor mechanically-evoked responses in naïve rats (n = 10). LPI (150µM and 250µM) had significant inhibitory effects compared to control. *** $p < 0.0001$, two-way ANOVA. Data are presented as mean ± SEM.

The effect of peripherally administered LPI (150 and 250µM) on the mechanical thresholds of knee joint primary afferent nociceptors was also determined (n = 10; Figure 4.4). LPI significantly increased knee afferent mechanical thresholds (i.e. inhibited mechanosensitivity) at a concentration of 250µM (median = 0.6g, range = 0.6 - 2g) when compared to control thresholds (median = 4g, range = 0.6 - 15g) ($p<0.05$, Friedman's ANOVA with Dunn's Multiple Comparisons Test). 150µM LPI had no significant effect (median = 1g, range = 0.6 - 4g) (Friedman's ANOVA with Dunn's Multiple Comparisons Test).

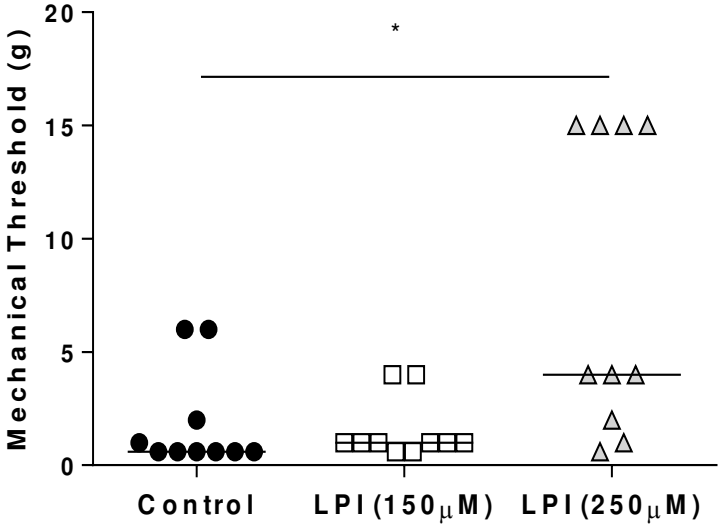

Figure 4.4. Effect of LPI (150µM and 250µM) on knee afferent nociceptor mechanical thresholds in naïve rats (n = 10). LPI (250µM) significantly increased knee afferent mechanical thresholds. Horizontal lines represent median values. * $p < 0.05$, Friedman's ANOVA with Dunn's Multiple Comparisons Test.

To confirm that these inhibitory effects on joint nociceptor mechanosensitivity were mediated by LPI, vehicle control experiments were conducted in a separate group of naïve rats.

The effect of vehicle saline on mechanically-evoked responses was studied in 8 naïve rats (Figure 4.5). Neither administration of saline (i.e. 1^{st} or 2^{nd} 100µl bolus) had any effect on knee afferent mechanically-evoked responses when compared to control (two-way ANOVA; Figure 4.5) confirming effects observed in the LPI experiment were LPI-mediated.

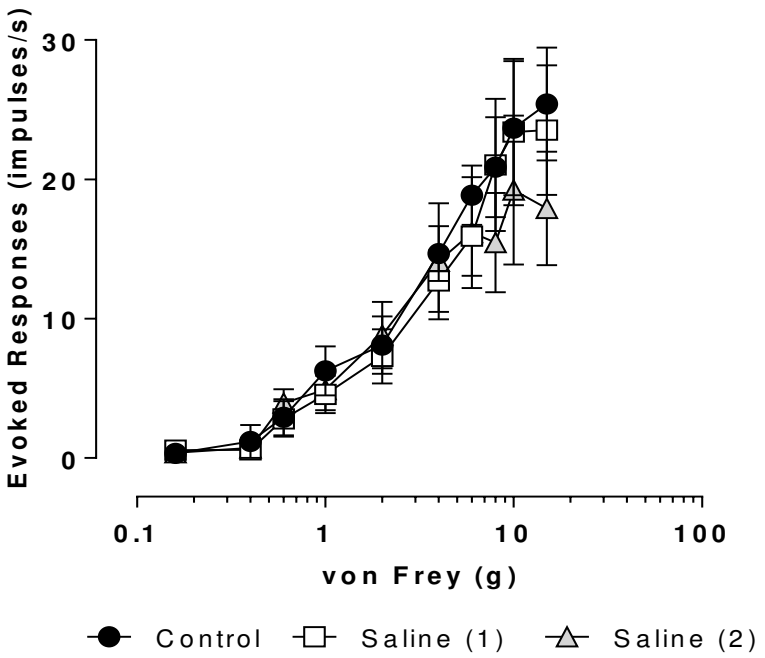

Figure 4.5. Effect of saline on knee joint afferent mechanically-evoked responses in naïve rats (n = 8). Neither administration of saline had any effect compared to control (two-way ANOVA). Data are expressed as mean ± SEM.

The effect of saline on knee afferent nociceptor mechanical thresholds was also studied (n = 8) (Figure 4.6). Neither volume of saline had any effect on knee afferent nociceptor mechanical thresholds (1st volume: median = 0.8g, range = 0.6 - 4g; 2nd volume: median = 0.6g, range = 0.6 - 2g) when compared to control thesholds (median = 0.8g, range = 0.6 - 4g) (Friedman's ANOVA with Dunn's Multiple Comparisons Test, Figure 4.6). These data confirm that the increase in mechanical thresholds observed following LPI was LPI-mediated.

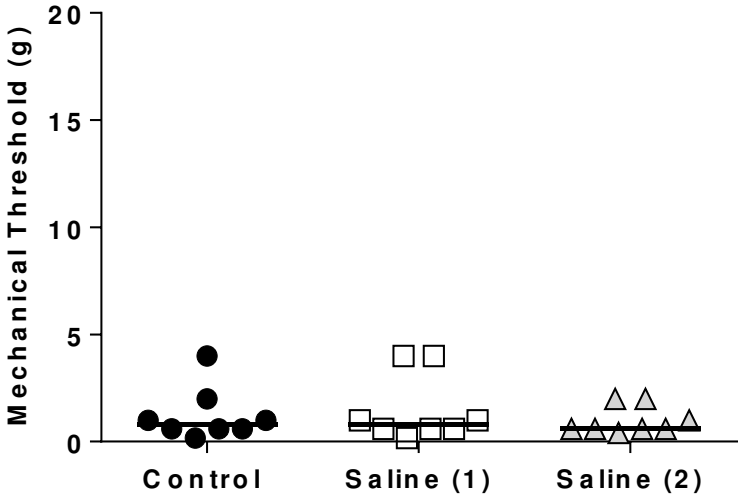

Figure 4.6. Effect of saline on knee afferent mechanical thresholds in naïve rats (n = 8). Neither dose of saline had any effect compared to control (Friedman's ANOVA with Dunn's Multiple Comparisons Test). Horizontal lines represent median values.

4.4.3. Effect of the GPR55 receptor antagonist cannabidiol on knee afferent nociceptor mechanically-evoked responses and on LPI-mediated inhibition

The effect of blocking any endogenous GPR55 tone on joint nociceptor mechanically-evoked responses was determined by peripheral administration of cannabidiol (50µg/100µl) in naïve rats (n = 12) (Figure 4.7). Cannabidiol alone (over a period of 30mins) had no effect on joint nociceptor mechanically-evoked firing rates compared to control (pre-drug) responses (two-way ANOVA; Figure 4.7). This finding indicates that any endogenous activation of the GPR55 receptor does not modulate knee afferent nociceptor mechanosensitivity under normal conditions.

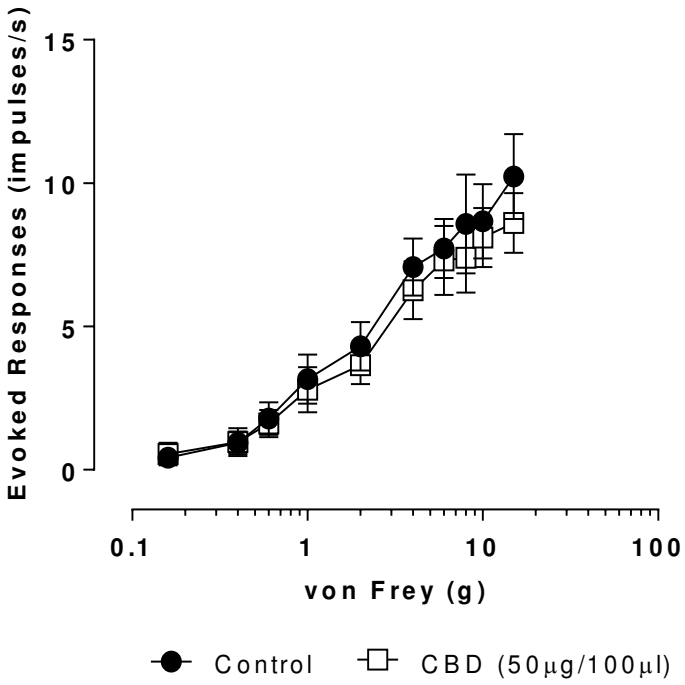

Figure 4.7. Effect of cannabidiol on knee afferent mechanically-evoked responses (n = 12). Cannabidiol had no effect on knee afferent mechanosensitivity (two-way ANOVA). Data are expressed as mean ± SEM.

The effect of cannabidiol (50µg/100µl) on LPI-mediated inhibition was also studied in naïve rats (n = 8) (Figure 4.8). Following the pre-administration of cannabidiol, LPI (250µM) had no significant effect on knee afferent mechanically-evoked responses (two-way ANOVA, Figure 4.8), indicating that pre-administered cannabidiol completely blocked the inhibitory effects of LPI observed in previous experiments (see above).

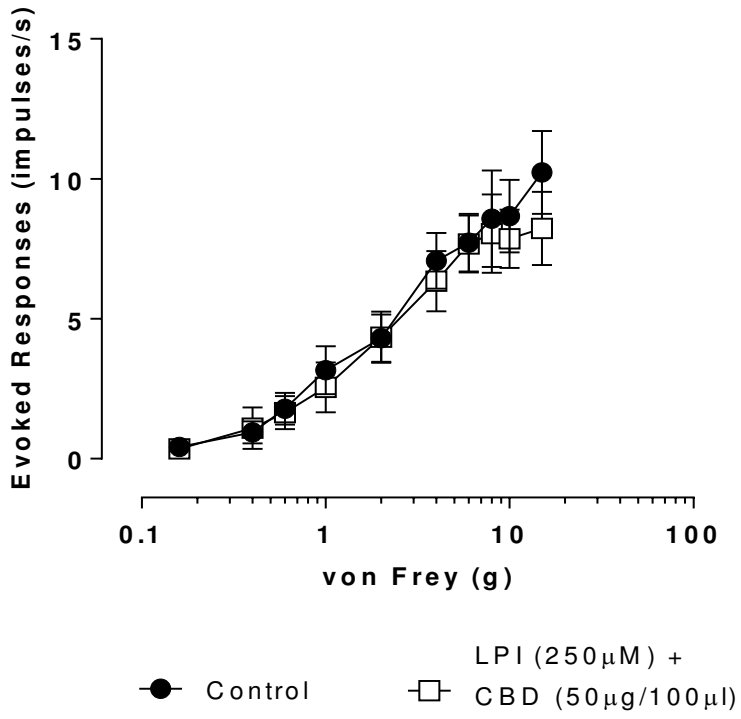

Figure 4.8. Effect of cannabidiol on LPI-mediated inhibition of knee joint nociceptor mechanically-evoked responses (n = 8). LPI had no effect when administered 30 minutes post-cannabidiol (two-way ANOVA). Data are expressed as mean ± SEM.

Since the effect of LPI alone (250µM) and following pre-administration of cannabidiol (50µg/100µl) were studied in separate groups of rats the data from these two separate studies were normalised and expressed as a percentage (%) of control (Figure 4.9) to enable a direct comparison of LPI effects in the absence/presence of cannabidiol. Overall, the pre-administration of cannabidiol significantly blocked the inhibitory effects of LPI on mechanically-evoked responses of joint nociceptors (Fig 4.9; $p<0.001$, Kruskal-Wallis). When post-LPI % of control responses at individual weights were compared in the presence and absence of cannabidiol, 8g responses were significantly greater following pre-administration of cannabidiol compared to LPI alone ($p<0.05$, Kruskal-Wallis with Dunn's multiple comparison). This cannabidiol mediated block of LPI-induced inhibition suggests an involvement of GPR55.

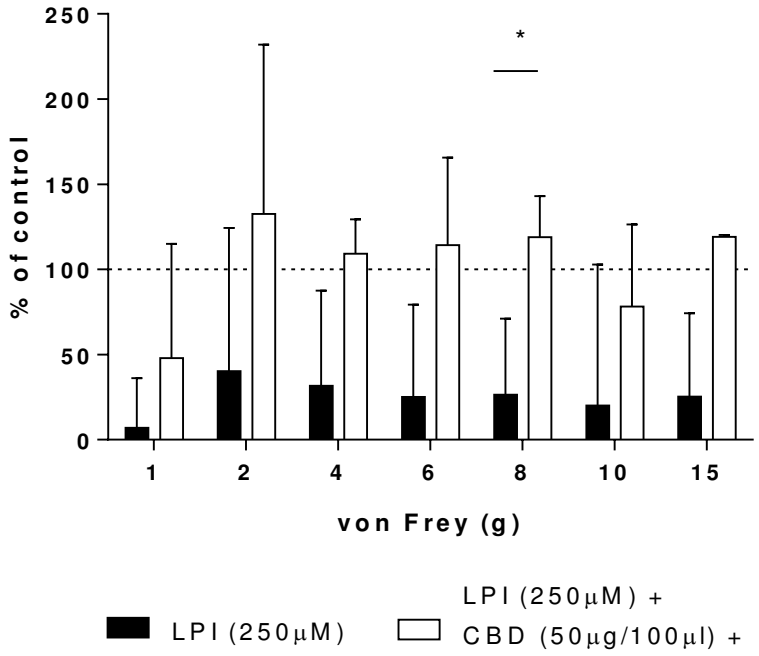

Figure 4.9. Direct comparisons of the effect of LPI (250µM) alone and following the pre-administration of cannabidiol (50µg/100µl) as expressed as % of control (represented as a dotted line at 100%). The inhibitory effect of LPI on knee afferent nociceptor mechanically-evoked responses was reduced after pre-administration of cannabidiol, an effect significant at 8g. * $p<0.05$, Kruskal-Wallis with Dunn's Multiple Comparisons Test. Data are expressed as median with interquartiles range.

4.4.4. Effect of the CB_1 receptor antagonist AM281 on knee afferent nociceptor mechanically-evoked responses and LPI-mediated inhibition

AM281 (1mg/kg, i.p) was administered 30 minutes prior to the administration of LPI (250µM) to investigate if CB_1 receptors are involved in the LPI-mediated inhibition of joint nociceptor mechanically-evoked responses in naïve rats (n = 9) (Figure 4.10). The administration of AM281 alone had no effect on knee afferent responses compared to control (two-way ANOVA; Figure 4.10). This finding indicates that the CB_1 receptor does not endogenously modulate knee afferent mechanosensitivity under normal conditions.

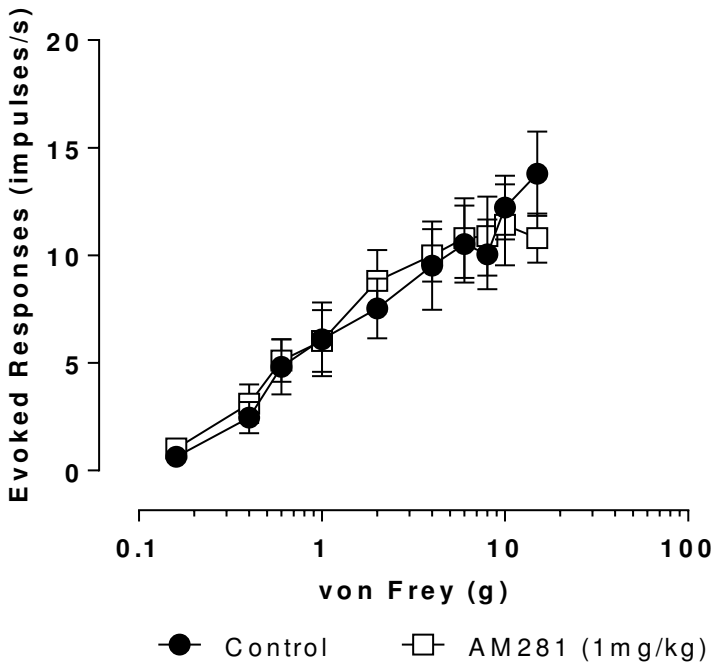

Figure 4.10. Effect of AM281 (1mg/kg) on knee afferent mechanically-evoked responses (n = 9). AM281 had no effect on knee afferent mechanosensitivity (two-way ANOVA). Data are expressed as mean ± SEM.

In the presence of AM281, LPI (250µM) caused a significant inhibition of the mechanically-evoked responses of knee afferent nociceptors (two-way ANOVA; Figure 4.11).

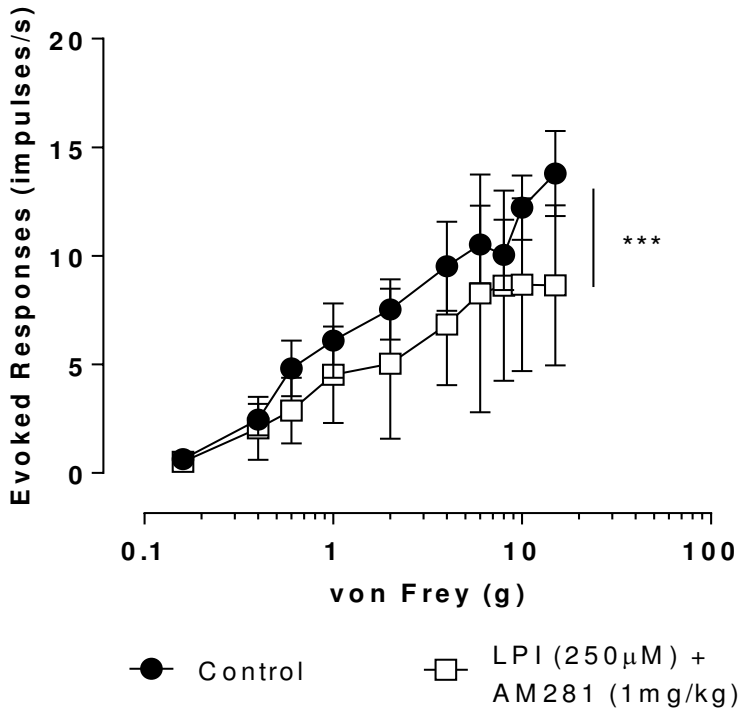

Figure 4.11. Effect of AM281 (1mg/kg) on the LPI-mediated inhibition of knee joint nociceptor mechanically-evoked responses (n = 9). LPI (250µM) significantly inhibited responses following administration of AM281. *** $p < 0.0001$, two-way ANOVA. Data are expressed as mean ± SEM.

Since the effects of LPI alone and following pre-administration of AM281 were studied in separate groups of rats the data was normalised and expressed as a percentage (%) of control (Figure 4.12) to enable a direct comparison of effects of LPI in the presence/absence of AM281. Overall, the pre-administration of AM281 significantly reduced the inhibitory effects of LPI on joint nociceptor mechanically-evoked responses ($p>0.01$, Kruskal-Wallis; Figure 4.12). However, when post-LPI % of control responses at individual weights were compared in the presence and absence of AM281, responses did not differ significantly at any weight (Kruskal-Wallis with Dunn's multiple comparison). These data indicate that LPI-mediated inhibition of knee afferent mechanically-evoked responses was partially reduced by the CB_1 receptor antagonist.

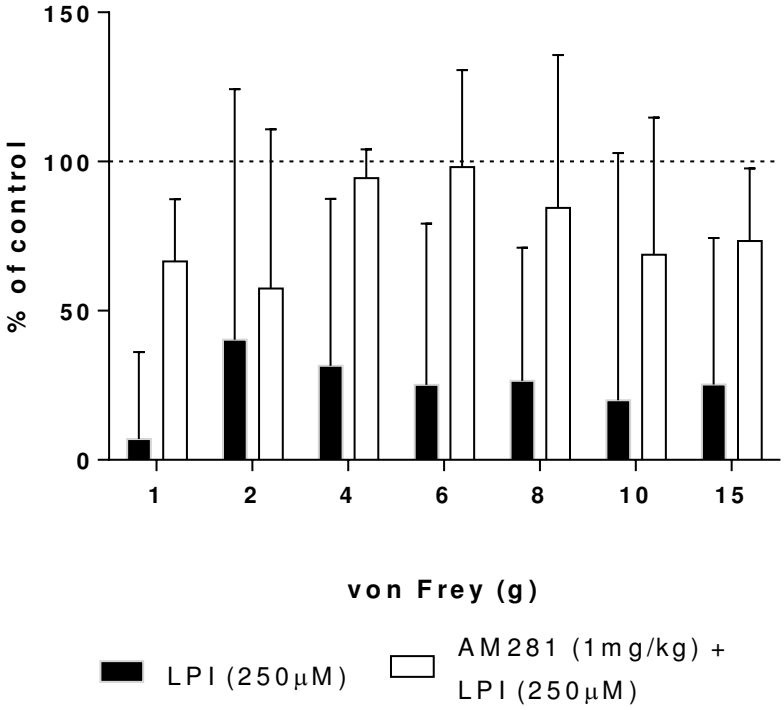

Figure 4.12. Direct comparisons of the effect of LPI (250µM) alone and following the pre-administration of AM281 (1mg/kg) as expressed as % of control (represented as a dotted line at 100%). Overall there was a significant difference in the inhibitory effect of LPI alone compared to after pre-administration of AM281 although this did not reach significance for individual weights ($p>0.01$, Kruskal-Wallis with Dunn's multiple comparisons). Data are expressed as median with interquartile range.

4.5. Discussion

The work described in this chapter aimed to determine the effects of GPR55 receptor activation on joint nociception in vivo under non-pathological conditions. Effects of the endogenous GPR55 agonist LPI on the mechanosensitivity of joint nociceptors was examined using electrophysiological recordings of mechanically-evoked neuronal responses taken from the saphenous nerve in naïve Sprague Dawley rats. Peripheral administration of LPI profoundly inhibited the mechanical sensitivity of joint nociceptors reducing mechanically-evoked firing rates and increasing mechanical thresholds in a concentration-dependent manner. Saline vehicle had no effect on joint nociceptor firing rates or mechanical thresholds confirming that the reduction in mechanical sensitivity is attributable to LPI.

An involvement of GPR55 in mediating the inhibitory effects of LPI was examined using the putative GPR55 receptor antagonist cannabidiol (Ryberg et al., 2007, Whyte et al., 2009, Li et al., 2013). Cannabidiol has been shown to antagonise the GPR55 receptor (Ryberg et al., 2007, Whyte et al., 2009, Li et al., 2013) and attenuates LPI-evoked increases in ERK phosphorylation in human osteoclasts (Whyte et al., 2009). Pre-administration of cannabidiol completely prevented the inhibitory effects of LPI confirming that LPI effects on joint nociceptor mechanosensitivity were mediated via GPR55 receptor activation. Since GPR55 has controversially been proposed to be a 'third novel cannabinoid receptor' and given that activation of the cannabinoid CB_1 receptor is known to inhibit responses of nociceptive neurones in vivo (Kelly

and Donaldson, 2008, Schuelert and McDougall, 2008) the potential contribution of the CB_1 receptor was also examined. The CB_1 receptor antagonist AM281 did not block the inhibitory effects of LPI on mechanically-evoked responses of joint nociceptors, however these inhibitory effects did appear to be partially attenuated. These data may suggest an unexpected contribution of CB_1 to LPI mediated effects in vivo, although there is no supporting published literature demonstrating affinity of LPI at CB_1 receptors. Studies examining ligand activity of cannabinoids in hGPR55 transfected HEK293 cells have demonstrated that AM281 exhibits agonist activity (Henstridge et al., 2010, Anavi-Goffer et al., 2012). Moreover, AM281 inhibits LPI-mediated ERK1/2 phosphorylation in these cells suggesting that AM281 can behave as both an agonist of GPR55 and an inhibitor of GPR55-mediated LPI effects. It has been suggested that AM281 may represent a bitopic ligand at GPR55 and could modulate LPI activity at the orthosteric (agonist) and allosteric site (Anavi-Goffer et al., 2012). These properties of AM281 may account for the apparent partial reduction in LPI-mediated inhibition reported here.

Both cannabidiol and AM281 alone had no effect on mechanically-evoked firing rates (at least within the 30 minute period studied) indicating that GPR55 and CB_1 receptors do not tonically modulate knee afferent mechanosensitivity under normal conditions. These findings of a lack of GPR55 and CB_1 endogenous tone are in agreement with the published literature as deletion of GPR55 in mice does not profoundly alter normal nociceptive thresholds (Staton et al., 2008) and a number of studies have demonstrated a lack of effect

of CB_1 receptor antagonists on nociceptive responses (Kelly and Donaldson, 2008, Schuelert and McDougall, 2008), although there are studies that contradict this.

The published literature confirms LPI as a GPR55 receptor agonist (Oka et al., 2007, Henstridge et al., 2009, Jin et al., 2009, Oka, 2009, Whyte et al., 2009, Bondarenko et al., 2010, Ford et al., 2010, Henstridge et al., 2010, Oka et al., 2010, Obara et al., 2011, Anavi-Goffer et al., 2012, Sharir et al., 2012, Yu et al., 2013). However, LPI has been shown to cause opening of the two-pore domain mechano-gated K^+ channels TREK-1 and TRAAK in COS-7 cells in culture (Maingret et al., 2000). TREK-1 and TRAAK mRNA is expressed on DRG neurones (Talley et al., 2001) with specific expression of TREK-1 mRNA evident on small diameter peptidergic and non-peptidergic fibres (Alloui et al., 2006). Further, TREK-1 genetic deletion in mice increased mechanical hypersensitivity indicating an important role in modulation of nociception (Alloui et al., 2006). K^+ channel activation would hyperpolarise the cell membrane and decrease neuronal excitability which would be expected to have an anti-nociceptive effect. Whether opening of TREK-1 or TRAAK channels makes a contribution to the inhibitory effects of LPI reported here was not investigated. However, the complete block of LPI's inhibitory effects by cannabidiol argue against a contribution of these channels. The data presented in this chapter demonstrates a novel anti-nociceptive effect of LPI on knee afferent mechanosensitivity mediated by GPR55 receptor activation in vivo.

Previous studies have investigated the role of GPR55 in the modulation of nociception (Staton et al., 2008, Breen et al., 2012, Gangadharan et al., 2013). A pro-nociceptive role has been suggested in the CFA-induced model of cutaneous inflammation (Staton et al., 2008), chronic constriction (Breen et al., 2012) and partial nerve injury models (Staton et al., 2008) of neuropathic pain and cutaneous nociception in naïve mice (Gangadharan et al., 2013). Although, most published studies on the role of GPR55 in nociceptive processing to date have suggested a pro-nociceptive role, a recent study of joint afferent nociceptors observed an anti-nociceptive effect of the GPR55 receptor synthetic agonist O-1602 in a model of acute joint inflammation (Schuelert and McDougall, 2011). The data included in this chapter are in agreement with this previous joint afferent recording study and perhaps identifies a novel anti-nociceptive role for the GPR55 receptor in the modulation of nociceptive inputs from the joint under normal conditions. The McDougall study demonstrated an inhibition of mechanosensitive C-fibres only, by O-1602 which was abolished by the GPR55 receptor antagonist O-1918 (Schuelert and McDougall, 2011). The categorisation of recorded fibres studied in this chapter demonstrated that LPI inhibits the mechanosensitivity of both Aδ- and C-fibres in naive rats, while O-1602 had no effect on the firing rate of Aδ-fibres (Schuelert and McDougall, 2011). This might be explained by methodological differences between this study and the McDougall study, for example the GPR55 agonist used (LPI in this study, O-1602 in the McDougall study) and in the McDougall study 8 fibres were unclassified, some of these fibres may have been Aδ-fibres which could explain the discrepancy. Only one study has investigated the expression of the GPR55 receptor in DRG neurones (Lauckner

et al., 2008). Large diameter (>35µm) NF200 positive DRG neurones, dissociated from BALB/c mice, expressed high levels of GPR55 with low levels detected in small and medium sized neurones (Lauckner et al., 2008) suggesting a high abundance in Aβ- and Aδ-fibres and low amounts in small diameter neurones receiving C-fibres. Electrophysiological effects of LPI on A- and C-fibres reported here corroborate these findings. Despite this expression in DRG neurones it is not possible to identify with certainty the exact site of LPI action in the present study i.e. neuronal or non-neuronal as the effects of locally administered LPI were examined in vivo. However, expression in mouse DRG neurones points towards a direct action on the peripheral terminals of joint innervating nociceptors. No published studies have directly investigated GPR55 expression in rat DRG neurones or specifically in knee joint afferents and thus further investigation is required.

The McDougall study, taken together with the current study and recently published data in cutaneous afferents nociceptors (Gangadharan et al., 2013) suggests that the GPR55 receptor may mediate a tissue specific anti-nociceptive effect at the level of the joint. This theory is supported by studies that have observed a tissue-specific effect of GPR55 on cancer cell proliferation (Hamtiaux et al., 2011, Huang et al., 2011, Pineiro et al., 2011, Perez-Gomez et al., 2013), increasing proliferation in a mouse model of skin cancer (Perez-Gomez et al., 2013) and in prostrate and ovarian cancer cell lines (Pineiro et al., 2011) whilst reducing proliferation of cholangiocarcinoma (Huang et al., 2011) and murine N1E-155 neuroblastoma cells (Hamtiaux et al., 2011). Tissue/cell-specific effects might be explained by the complexity of

GPR55 receptor-mediated intracellular downstream signalling that is ligand- and cell-type dependent (see Figure 1.4) (Johns, 2007, Oka et al., 2007, Ryberg et al., 2007, Lauckner et al., 2008, Kapur et al., 2009, Ross, 2009, Yin, 2009, Anavi-Goffer et al., 2012). In prostrate and ovarian cancer cell lines, GPR55 receptor-mediated proliferation is dependent on ERK (Pineiro et al., 2011), while in cholangiocarcinoma cells, the anti-proliferative effect of the GPR55 receptor was mediated by c-Jun N-terminal kinase and the fas death receptor complex (Huang et al., 2011).

Studies investigating the intracellular signalling mechanisms of GPR55 receptor-mediated modulation of nociception are limited. In large diameter DRG neurones, activation of the GPR55 receptor by certain cannabinoid ligands inhibited M-type K^+ currents and elevated intracellular Ca^{2+} levels which would be expected to potentiate neuronal excitability (Lauckner et al., 2008). A recent study investigated the intracellular signalling pathways in DRG neurones activated by LPI and is the only current published literature that identifies intracellular signalling effectors involved in LPI- and GPR55-mediated nociception in vivo (Gangadharan et al., 2013). This study demonstrated a reduction in LPI-induced mechanical hypersensitivity in mice lacking G_{13} and $G_{q/11}$ and following the administration of ERK1/2 and Rho A kinase inhibitors. Due to the small number of studies investigating the role of GPR55 in models of nociception, the intracellular signalling pathways that mediate LPI and GPR55 receptor-mediated anti-nociception are not known and therefore knowledge of the mechanisms underlying GPR55 mediated anti-nociception are incomplete and warrant further investigation.

In conclusion, the data presented in this chapter identifies a novel anti-nociceptive role of the endogenous lysophospholipid and GPR55 agonist LPI in the modulation of knee afferent mechanosensitivity. These findings and those already published (Schuelert and McDougall, 2011) indicate an anti-nociceptive role for GPR55 that may be specific for joint afferent nociceptors.

Chapter Five

Modulation of joint nociceptor mechanosensitivity by the GPR55 receptor agonist LPI in the MIA model of osteoarthritis

5.1. Introduction

The work in chapter 4 examined the effects of peripheral administration of the endogenous lysophospholipid and GPR55 agonist LPI on joint nociceptor mechanosensitivity in naive rats. LPI decreased Aδ- and C-fibre mechanical responsiveness in a GPR55 receptor-dependent manner. These findings provide further evidence that the GPR55 receptor has a role in the modulation of nociception and suggests that GPR55 may be a novel analgesic target in the treatment of joint pain. This is consistent with an anti-nociceptive effect of the synthetic GPR55 agonist O-1602 on joint nociceptor responses in an acute model of joint inflammation (Schuelert and McDougall, 2011). However, the impact of GPR55 receptor activation on joint nociceptor mechanosensitivity in a model of chronic arthritis, in particular chronic knee OA has yet to be investigated.

5.1.1. Modulation of joint nociceptor mechanically-evoked responses by peripheral administration of pharmacological agents in the MIA model

An increase in the mechanical sensitivity of joint nociceptors has been demonstrated in rat MIA and MNX models and spontaneously and surgically induced OA in the guinea pig (Schuelert and McDougall, 2006a, Gomis et al., 2007, McDougall et al., 2009, Schuelert and McDougall, 2009, McDougall et al., 2010, Kelly et al., 2012, Schuelert and McDougall, 2012, Kelly et al., 2013a, Bullock et al., 2014). Thus, this mechanical sensitization is a key feature of preclinical models of OA pain and is likely to contribute to the associated pain behaviour. Studies of the effects of peripheral administration of

pharmacological agents on knee joint nociceptor mechanosensitivity in the MIA model have identified potential novel targets for the treatment of this pain, including TRPV1 channels (Kelly et al., 2013a), CGRP (Bullock et al., 2014), VIP (Schuelert and McDougall, 2006b), CB_1 (Schuelert and McDougall, 2008) and CB_2 receptors (Schuelert et al., 2010) as well as $Na_v1.8$ Na^+ channels (Schuelert and McDougall, 2012).

Studies demonstrating inhibitory effects of cannabinoid agonists on joint nociceptor responses in the MIA model have indicated the potential importance of the peripheral cannabinoid receptor system (Schuelert and McDougall, 2008, Schuelert et al., 2011). Activation of CB_1 receptors attenuated non-noxious and noxious joint rotation evoked responses in both MIA and saline rats (Schuelert and McDougall, 2008). Interestingly, inhibition is enhanced following the development of OA pain. Further, following the development of OA pain the mechanosensitivity of joint nociceptors is under the endogenous inhibitory control of endocannabinoids acting via CB_1 (Schuelert and McDougall, 2008, Schuelert et al., 2011).

The CB_2 receptor agonist GW405833 sensitizes knee joint nociceptors in the MIA model paradoxical to inhibitory effects in saline rats (Schuelert et al., 2010). The sensitizing effect in MIA joints could be a result of TRPV1 activation (Kelly et al., 2013a) as GW405833 also functions as a weak partial agonist at TRPV1 and the TRPV1 antagonist SB366791 blocks this sensitization (Schuelert et al., 2010). TRPV1 activation in vivo would result in

the secondary release of the sensitizing neuropeptide CGRP (Bullock et al., 2014) and may account for these paradoxical sensitizing effects of GW405833.

5.1.2. A role for the GPR55 receptor in the modulation of OA pain?

As described above, the cannabinoid receptor system modulates joint nociception during OA (Schuelert and McDougall, 2008, Schuelert et al., 2010). Since GPR55 has been proposed as a novel third cannabinoid receptor (Johns, 2007, Ryberg et al., 2007, Waldeck-Weiermair et al., 2008, Kapur et al., 2009, Yin, 2009) and GPR55 receptor activation modulates joint nociceptor responses in naïve rats (see Chapter 4) it may also be a novel target with relevance for OA pain treatment. In fact, it is possible that GPR55 mediates the paradoxical effects of the CB_2 receptor agonist GW405833 on joint nociceptor mechanosensitivity described above (Schuelert et al., 2010). GW405833 functions as a partial agonist at hGPR55 in transfected HEK293 cells (Anavi-Goffer et al., 2012) and the CB_2 receptor antagonist AM630 does not completely abolish the modulatory effects of GW405833 in control or MIA rats (Schuelert et al., 2010). Thus, it is possible that the non-CB_2 receptor mediated effects of GW405833 on joint nociceptors may be mediated by GPR55. Whether following the development of OA a change in the functional role of GPR55 in joint nociception from an inhibitory (see chapter 4) to a facilitatory role could be responsible for mediating the pro-nociceptive effects of GW405833 in MIA rats is unknown. Compelling evidence exists for a pro-nociceptive role for GPR55 in cutaneous Aδ mechanoreceptors (Gangadharan et al., 2013) and in the CFA model of cutaneous inflammation (Staton et al.,

2008) as well as models of neuropathic pain (Staton et al., 2008, Breen et al., 2012). Furthermore, plasticity is known to occur in the peripheral cannabinoid receptor system following OA development (see above).

5.2. Aims and objectives

Despite previous study of the role of GPR55 in several pathological pain states, a role in the modulation of peripheral nociception during knee OA has not been investigated. The aim of the work presented in this chapter was to examine the effects of LPI on the mechanical sensitivity of knee afferent nociceptors in the MIA model during established pain. These studies will elucidate whether the role of GPR55 in modulating knee nociceptor mechanically-evoked responses is altered following the development of knee OA. A further aim of this work was to determine the effects of cannabidiol on knee afferent nociceptor mechanosensitivity in the MIA model to determine whether endogenous tone at GPR55 modulates joint nociceptor sensitivity during OA. A time point associated with joint nociceptor sensitization (day 14) and established pain (see chapter 3) was chosen for these studies.

5.3. Methods

5.3.1. MIA model

For detailed methods regarding OA induction and assessment of pain behaviour refer to Chapter 2 (Sections 2.2 and 2.3).

5.3.2. Electrophysiology

Detailed methods outlining rat surgical preparation and extracellular recording of joint afferent nociceptor mechanical responses are described in chapter 2 (Section 2.4).

5.3.3. Drug administration

All drugs were administered once stable control responses had been established (see Chapter 2, Section 2.4.2). LPI (150 and 250µM; Sigma, UK) and cannabidiol (50µg/100µl; Tocris, UK) were administered peripherally via a contralateral femoral artery cannula in a 100µl bolus injections washed in with 300µl heparinised saline. Unless otherwise stated, drug effects on mechanically-evoked responses (vF monofilaments 0.16-15g) were studied at 5 minute intervals for 60 minutes per dose (see Chapter 2, Section 2.4.2). At the end of the recording period, KCl (250mM) was administered to confirm that drugs accessed the peripheral terminals of joint afferent nociceptors (see Chapter 2, Section 2.4.2). Afferents not activated by KCl were excluded from

the analysis. At the end of the experiment, the CV of the studied afferent was estimated to determine the afferent fibre type (see Chapter 2, Section 2.4.2).

A number of separate experiments were performed as outlined below:

Study 1: Effects of consecutive administration of 150µM and 250µM LPI on knee afferent nociceptor mechanically-evoked responses were determined in MIA (n = 9) and saline (n = 8) rats.

Study 2: Effects of cannabidiol (50µg/100µl) alone on knee afferent nociceptor mechanically-evoked responses were studied in MIA (n = 9) and saline (n = 9) rats at 5 minute intervals for 30 minutes at which point 250µM LPI was administered and effects were followed for a further 60 minutes (n = 6 MIA; n = 8 saline).

5.3.4. Statistical analysis

Data analysis was performed using Prism software (versions 5 or 6; GraphPad Software). Data were tested for normality using the KS test. Where data were normally distributed, a parametric test was used (e.g. two-way ANOVA) and where data was not normally distributed a non-parametric test was used (e.g. Mann Whitney unpaired u-test or Freidman's ANOVA).

5.4. Results

5.4.1. MIA injection evoked pain behaviour

Analysis of weight bearing and hind paw mechanical withdrawal thresholds confirmed OA pain development. As previously described (see Chapter 3 Section 3.4.2), there was a significant reduction in weight bearing and mechanical thresholds on the ipsilateral hind limb in MIA compared to saline rats immediately prior to electrophysiology (day 14) ($p<0.0001$, two-way ANOVA with Bonferroni's multiple comparisons test). Ipsilateral weight bearing in MIA-treated rats was 38.14 ± 1.4% compared to 50.12 ± 0.38% in saline-treated rats ($p<0.001$, two-way ANOVA with Bonferroni's multiple comparisons test) with ipsilateral mechanical thresholds of 5 ± 1.77g in MIA rats compared to 11 ± 2.39g in saline rats ($p<0.001$, two-way ANOVA with Bonferroni's multiple comparisons test). These data confirm the presence of pain behaviour in MIA rats subsequently used in electrophysiology experiments described below.

5.4.2. Conduction velocities and fibre types

Both Aδ- and C-type fibres have been included in the analysis for this chapter. CVs were over a similar range for both MIA (n = 15 fibres) and saline rats (n = 15 fibres). CVs ranged from 0.2 - 12.1m/s in MIA rats (median = 1.5m/s) and 0.12 - 9.8m/s in saline rats (median = 1.79m/s). Aδ- and C-fibres are discussed collectively. In some cases (n = 5 fibres) CV measurement was not possible following drug treatment as the fibre response was completely inhibited.

5.4.3. Effect of MIA on knee joint nociceptor mechanically-evoked responses

Figure 5.1 contains raw data traces and corresponding rate histograms that are typical examples of mechanically-evoked responses recorded from an Aδ-fibre in a saline rat compared to an Aδ fibre recorded in an MIA rat. The fibre recorded in the MIA rat (Figure 5.1B and D) exhibited an increased firing rate to mechanical stimulation and a lowered mechanical threshold compared to the fibre recorded in the saline rat (Figure 5.1A and C).

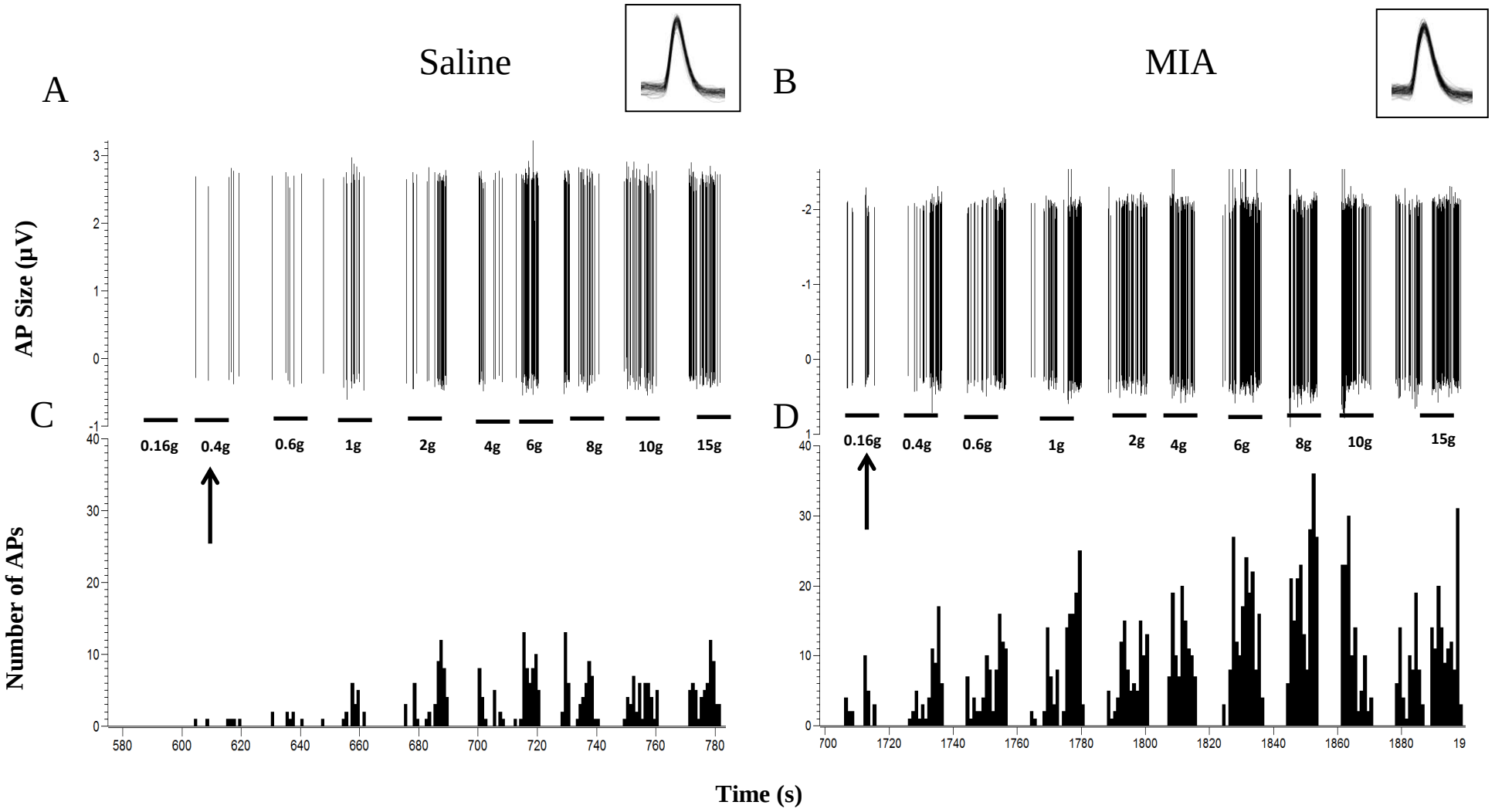
A
Saline
B
MIA
AP Size (µV)
C
D
0.16g
0.4g
0.6g
1g
2g
4g
6g
8g
10g
15g
Number of APs
Time (s)

Figure 5.1. Typical example raw data traces of mechanically-evoked responses of knee joint nociceptors recorded in a saline- (A) and MIA (B) rat. An overlay of the action potentials recorded in the respective figures, demonstrates single unit activity. Corresponding rate histograms for the saline (C) and MIA rat (D) are shown below each figure demonstrating an enhanced firing rate in the MIA example. Arrows in A and B indicate mechanical thresholds (0.4g in the saline rat and 0.16g in the MIA rat). CV of fibre in saline rat = 1.41m/s and in MIA rat = 1.64m/s.

Mean control (pre-LPI administration) joint nociceptor mechanically-evoked responses in MIA and saline rats were compared (Figure 5.2). Overall, control responses were significantly increased in MIA rats compared to saline rats ($p<0.001$, two-way ANOVA, Figure 5.2) indicating the presence of peripheral sensitization 14 days following treatment.

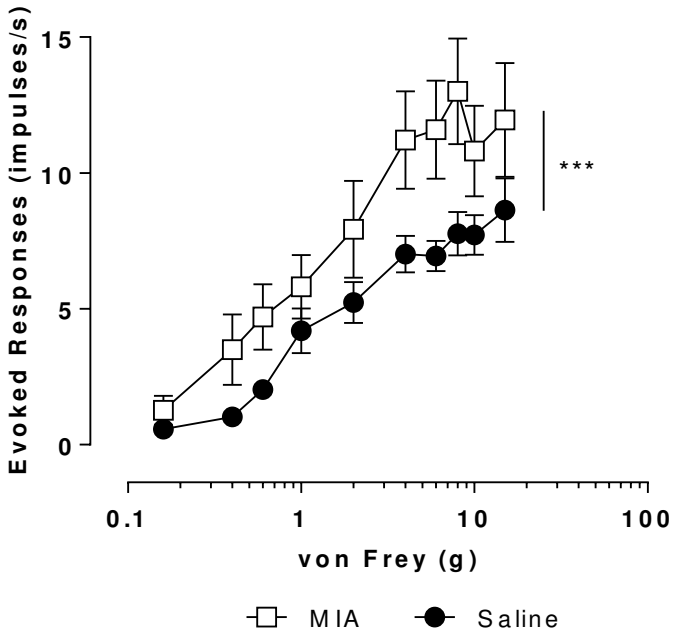

Figure 5.2. Effect of MIA (n = 9) and saline treatment (n = 8) on mechanically-evoked responses of knee joint nociceptors 14 days following injection. Data represented as mean rate of firing ± SEM. $^{***}p<0.0001$, two-way ANOVA.

5.4.4. Effect of LPI on knee joint nociceptor mechanically-evoked responses in the MIA model of OA pain

Figure 5.3 and 5.4 below include example mechanically-evoked firing rate histograms for knee joint afferent nociceptors in a saline and MIA rat, pre- and post LPI and illustrates the effects of semi-local LPI administration on responses. In these typical examples, LPI causes a marked inhibition in both the MIA and saline rats.

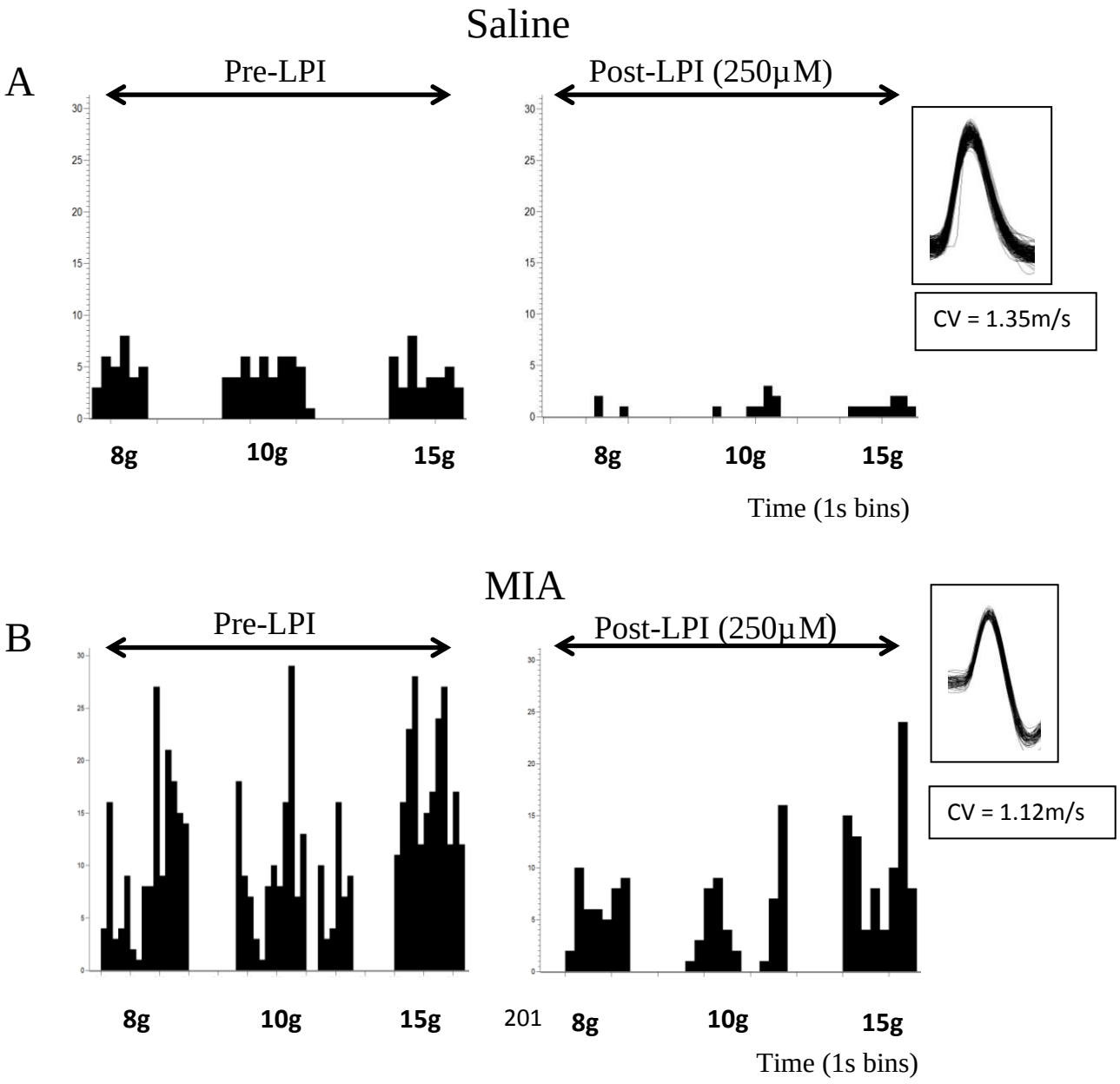
Saline
A
Pre-LPI
Post-LPI (250µM)
CV = 1.35m/s
8g
10g
15g
8g
10g
15g
Time (1s bins)
MIA
B
Pre-LPI
Post-LPI (250µM)
CV = 1.12m/s
8g
10g
15g
8g
10g
15g
Time (1s bins)

Figure 5.3. Representative examples of knee afferent mechanically-evoked (8 - 15g vF monofilaments) response data recorded pre- and post-administration of 250µM LPI in a saline- (A) and MIA- (B) treated rat. Data are rate histograms (1s bins) of action potential firing of joint nociceptor (single unit) in response to vF monofilament stimulation. Small inset figures show an overlay of each example fibre recording with the corresponding CV, demonstrating single fibre recordings. Both fibres are Aδ-fibres.

When mean responses were analysed for all fibres studied it was found that in MIA rats the administration of 150µM and 250µM LPI significantly attenuated knee afferent mechanically-evoked responses compared to control ($p<0.0001$, two-way ANOVA, Figure 5.4A). The inhibition following 250µM LPI was significantly greater than at 150µM demonstrating a concentration-dependent effect ($p<0.05$, two-way ANOVA, Figure 5.4A). In saline rats, the administration of 150µM and 250µM LPI also significantly attenuated knee afferent mechanically evoked responses compared to control ($p<0.0001$, two-way ANOVA, Figure 5.4B) in a concentration-dependent manner ($p<0.0001$, two-way ANOVA, Figure 5.4B).

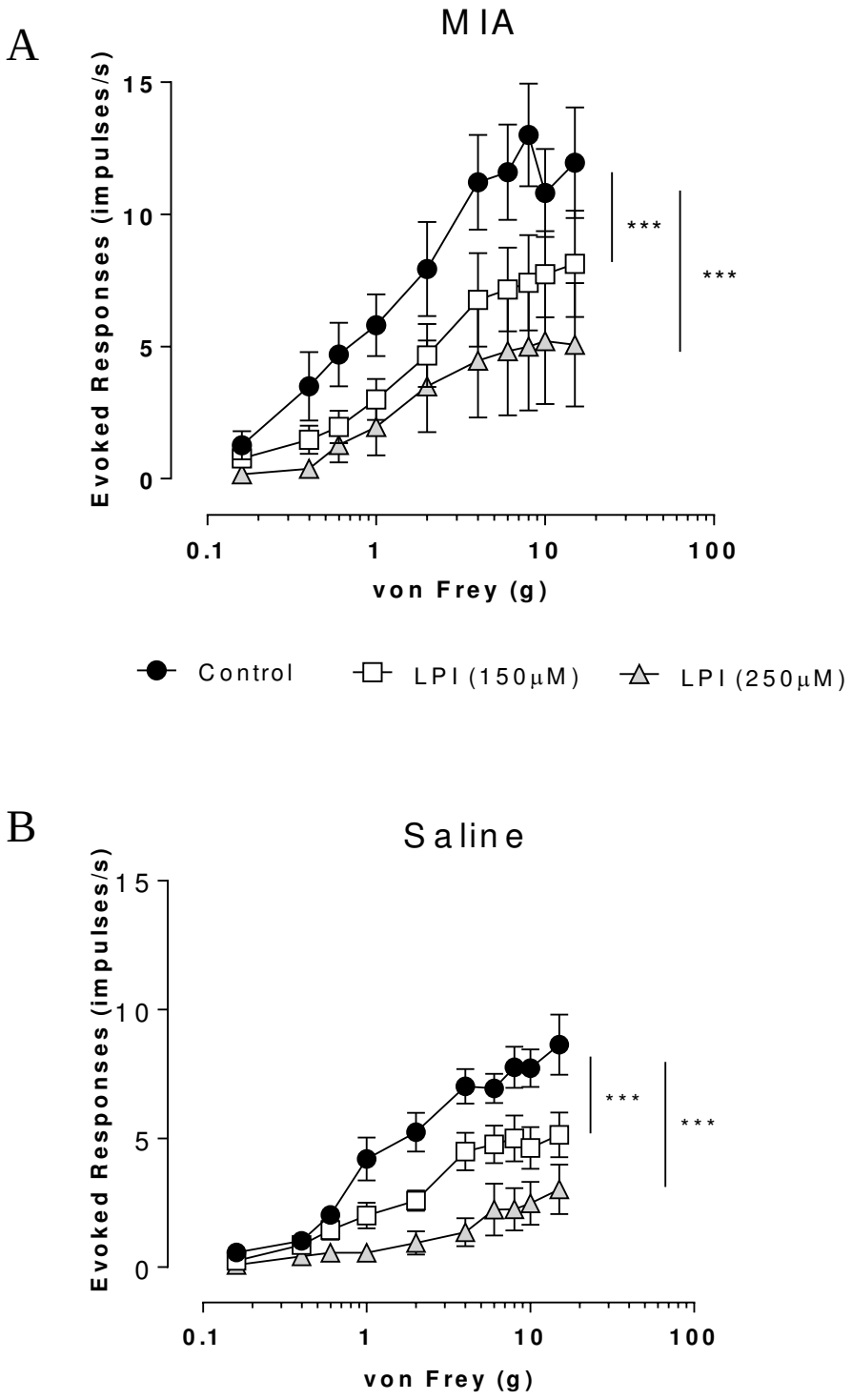

Figure 5.4. Effect of LPI on mechanically-evoked responses of knee afferent nociceptors in MIA (n=9) and saline (n=8) rats. There was a significant inhibition of knee joint nociceptor mechanically-evoked responses in (A) MIA

and B) saline rats. Data are mean evoked responses ± SEM. $^{***}p<0.001$, two-way ANOVA.

Figure 5.5 illustrates the inhibitory effect of LPI (150 µM and 250µM) on 2g and 15g mechanically-evoked responses of knee joint afferent nociceptors over time in MIA rats. Evoked responses were typically reduced by 15-20 minutes and remained inhibited for the duration of the experiment.

Figure 5.6 illustrates the timecourse of the inhibitory effects of LPI (150 µM and 250µM) on 2g and 15g mechanically-evoked responses of knee joint afferent nociceptors in saline rats. In response to a 2g vF monofilament, evoked responses were typically reduced by 0-5 minutes while in response to a 15g vF monofilament, evoked responses were inhibited for the duration of the experiment.

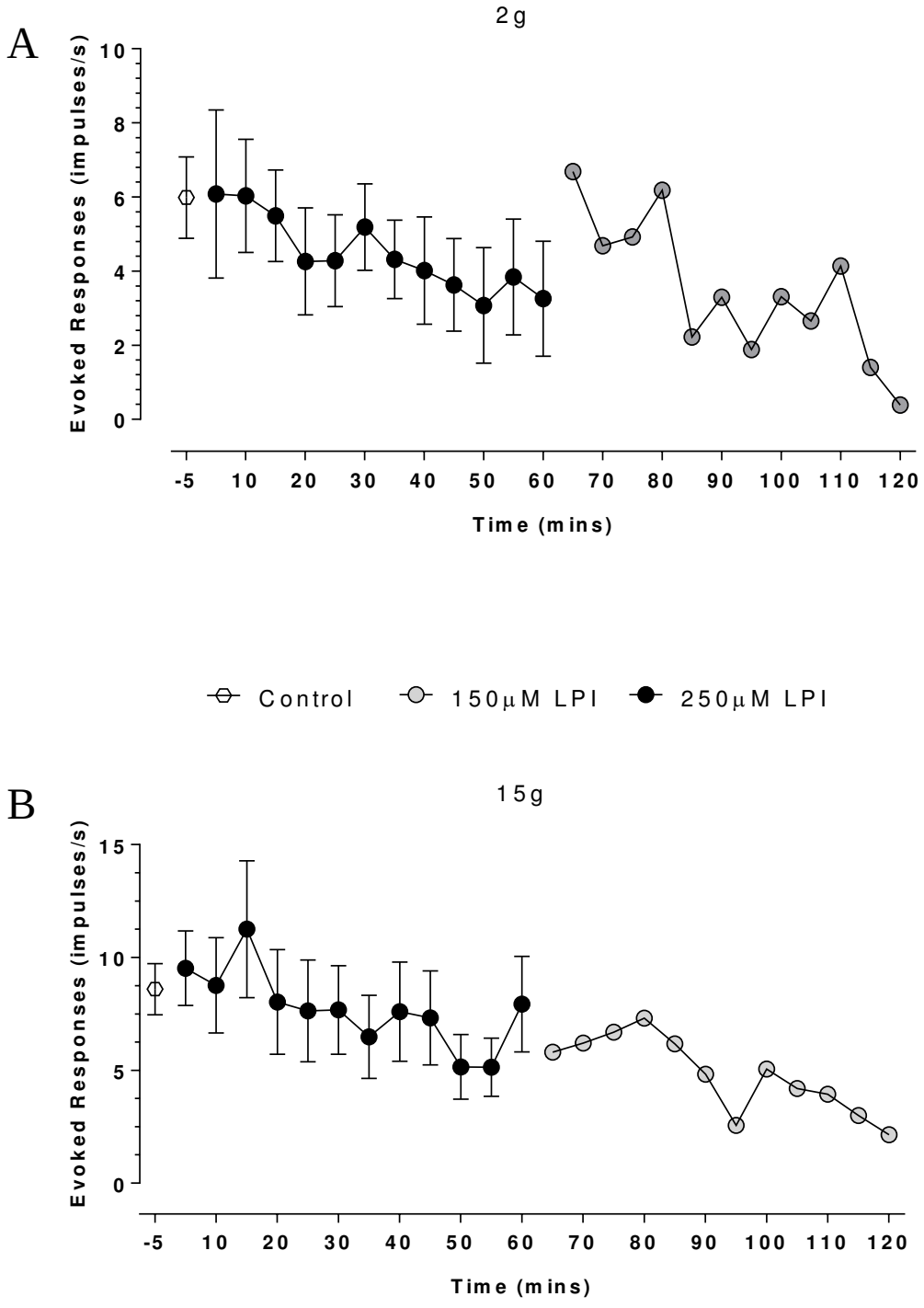

Figure 5.5. Time course of the inhibitory effect of LPI on mechanically-evoked responses of joint nociceptors in MIA rats. Inhibitory effects of LPI in MIA rats over an hour recording period for each dose of LPI, at a low (2g) (A)

and high (15g) (B) vF monofilament. Data presented as the average rate of firing for each vF monofilament train ± SEM.

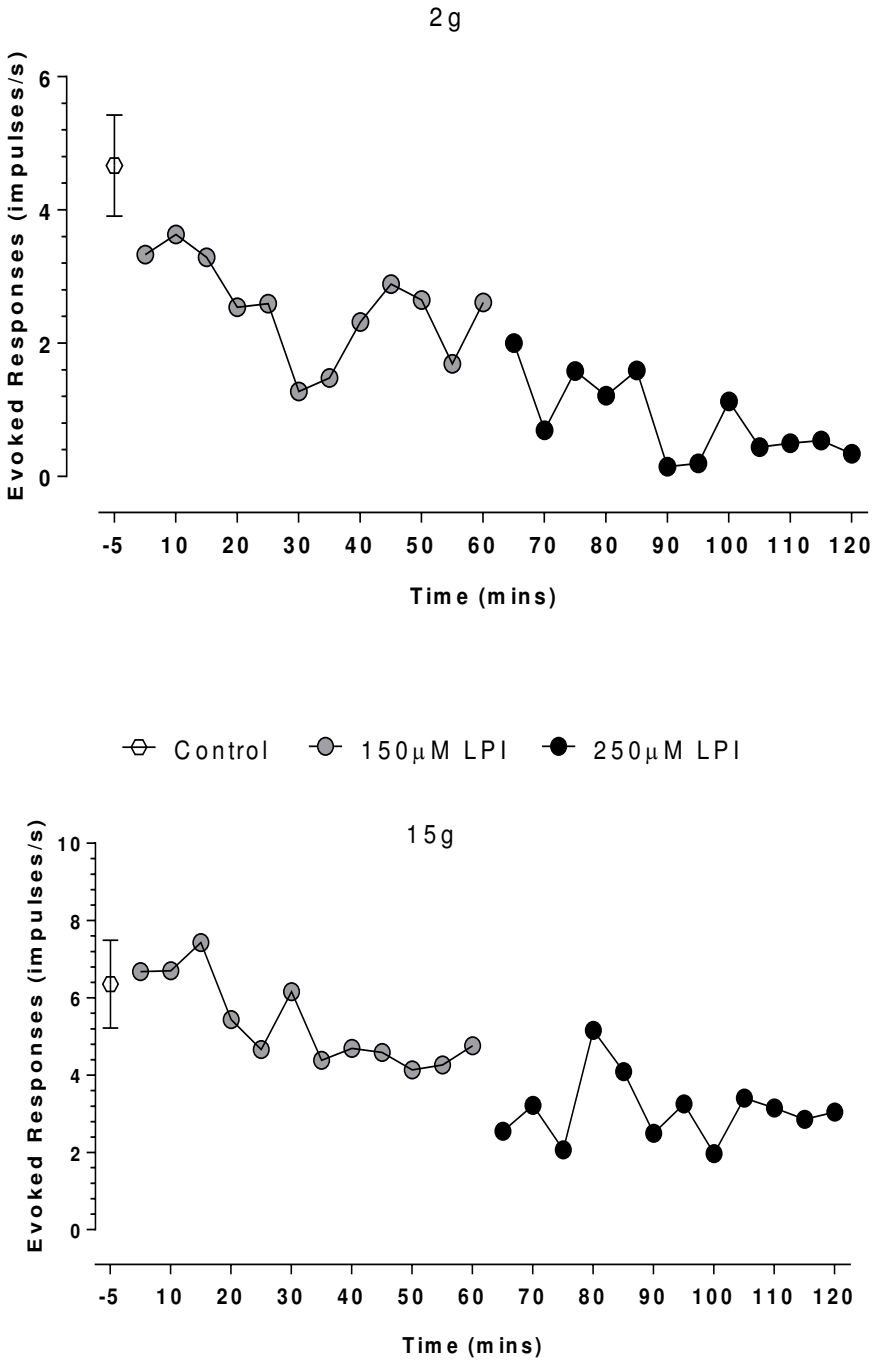

Figure 5.6. Time course of the inhibitory effect of LPI on mechanically-evoked responses of knee joint nociceptors in saline rats. The inhibitory effects of LPI on knee joint nociceptor responses in saline rats over an hour recording

period for each dose of LPI, at a low (2g) and high (15g) vF monofilament. Data presented as the average rate of firing for each vF monofilament train ± SEM.

5.4.5. Comparison of the inhibitory effects of LPI on knee joint nociceptor mechanically-evoked responses in MIA and saline rats

To enable a direct comparison of the magnitude of the inhibitory effects of LPI in MIA and saline data were normalised and expressed as % of control (Figure 5.7). The inhibition of joint nociceptor mechanosensitivity after administration of both concentrations of LPI was not different in MIA-compared to saline rats (two-way ANOVA with Bonferroni's Multiple Comparisons Test, Figure 5.7).

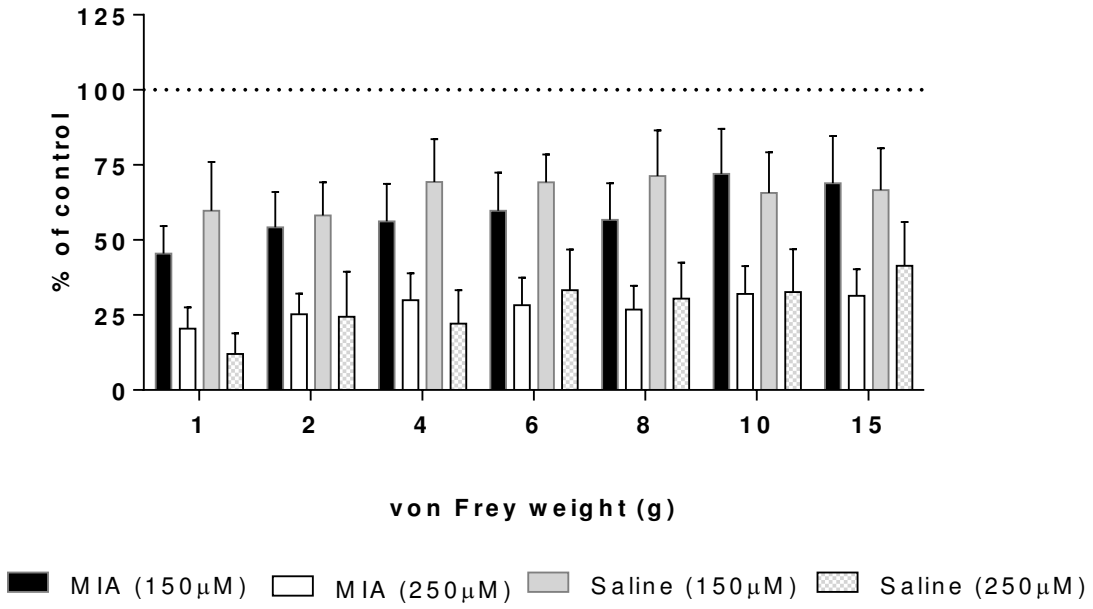

Figure 5.7. Direct comparison of the effect of LPI (150µM, 250µM) on joint nociceptor mechanically-evoked responses in MIA (n = 9) and saline (n = 8) rats as expressed as % of control (represented as a dotted line at 100%). The inhibitory effects of LPI in MIA and saline rats were not different (two-way ANOVA with Bonferroni's Multiple Comparisons Test). Data are expressed as mean ± SEM.

5.4.6. Effect of LPI on knee afferent mechanical thresholds in the MIA model of OA pain

The effect of LPI on knee afferent mechanical thresholds in MIA (n = 9) and saline (n = 8) rats were also determined (Figure 5.8). Control (pre-drug) mechanical thresholds showed a tendency to be lowered in MIA rats (median = 0.6g, range = 0.16 - 4g) compared to saline (median = 1g, range = 0.4 - 4g) although overall thresholds were not significantly different (Mann Whitney u-test, Figure 5.8). In MIA rats, 150µM LPI had no effect on mechanical thresholds (n = 0.6g, range = 0.6 - 15g), whereas 250µM LPI significantly increased thresholds (median = 6g, range = 0.6 - 15g) ($p<0.05$, Friedman's ANOVA with Dunn's Multiple Comparisons Test, Figure 5.8).

In saline rats, LPI (150 and 250µM) increased mechanical thresholds (significantly at 250µM, $p<0.01$, Friedman's ANOVA with Dunn's Multiple Comparisons Test, Figure 5.8). The effects of LPI (150 and 250µM) on mechanical thresholds were not different when comparing MIA and saline rats (Mann Whitney u-test, Figure 5.8).

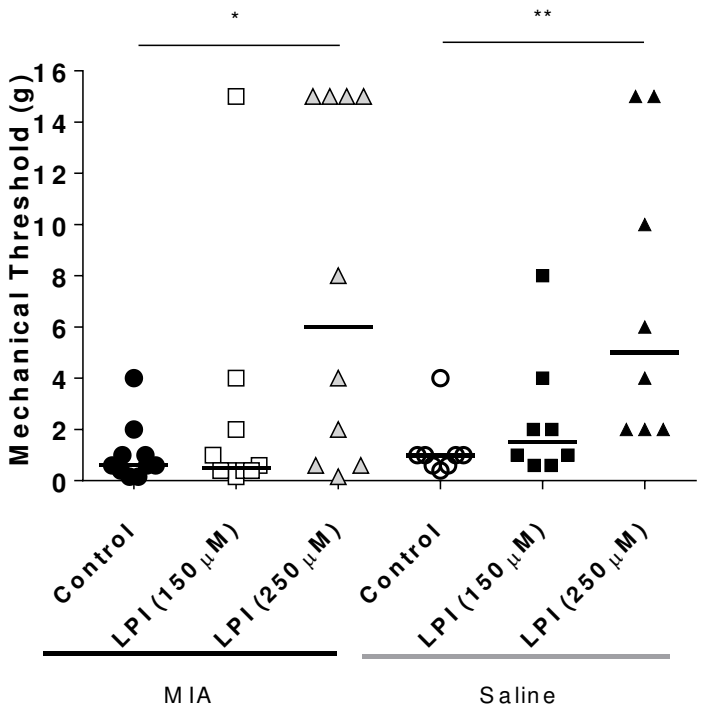

Figure 5.8. Effect of LPI on joint nociceptor mechanical thresholds in MIA (n=10) and saline (n=8) rats. LPI (150 and 250µM) increased the mechanical thresholds of fibres in saline and MIA rats. A significant increase was observed in response to 250µM LPI in both groups. Horizontal lines are medians. * $p < 0.05$ and ** $p < 0.01$, Friedman's ANOVA with Dunn's Multiple Comparisons Test comparing to control mechanical thresholds.

5.4.7. Effects of the GPR55 receptor antagonist cannabidiol on LPI-mediated inhibition of joint nociceptor mechanically evoked responses in the MIA model of OA pain

In order to investigate the involvement of GPR55 in the effects of LPI on joint nociceptor mechanosensitivity LPI effects of pre-administration of cannabidiol on LPI (250µM)-mediated inhibition of joint nociceptor mechanical evoked responses was studied in MIA (n = 6) and saline (n = 8) rats (Figure 5.9A & B). Pre-administration of cannabidiol (50µg/100µl) completely blocked the inhibitory effects of LPI (250µM) on joint nociceptor mechanically-evoked responses in both MIA and saline rats; post-LPI responses were not significantly different when compared to control (pre-LPI) responses (recorded 60 minutes post-cannabidiol) in both groups (two-way ANOVA, Figure 5.9A & B).

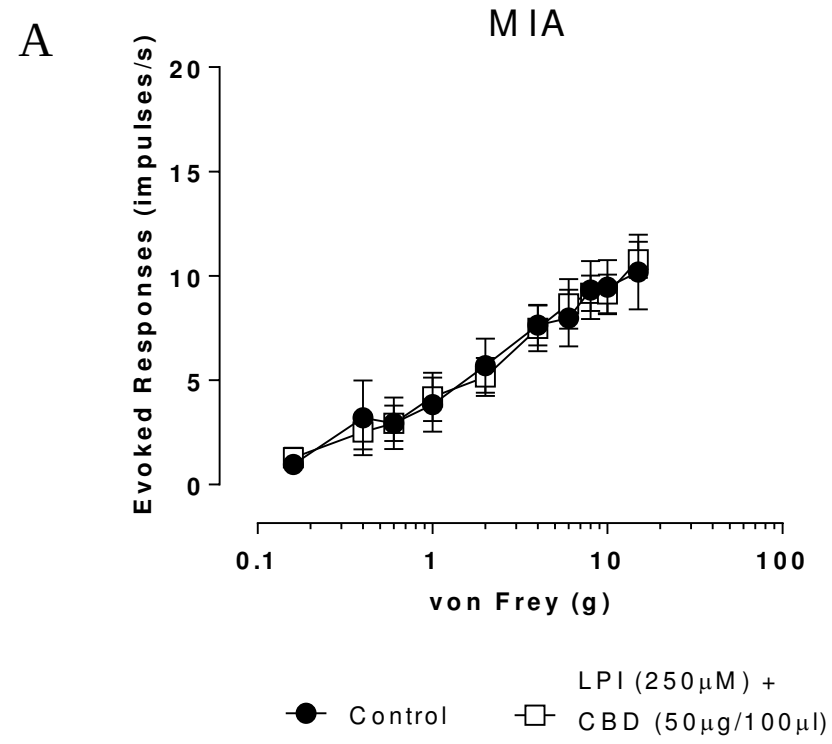

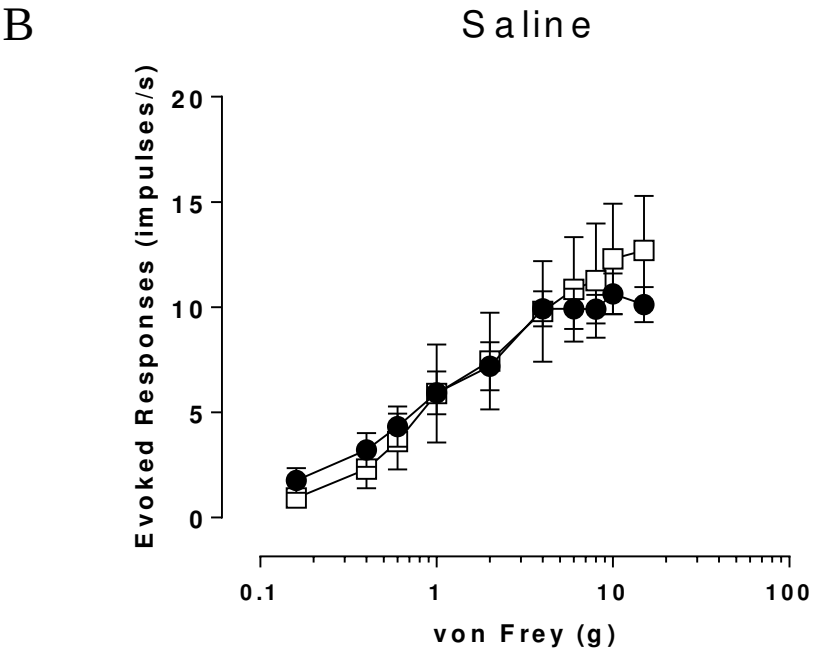

Figure 5.9. Effect of cannabidiol (50µg/100µl) on LPI (250µM)-mediated inhibition of joint nociceptor mechanically-evoked responses in MIA (n = 6) and saline-(n = 8) rats. LPI had no significant effect on mechanically-evoked

responses in MIA (A) and saline (B) rats compared to control responses (recorded 60 minutes post-cannabidiol). Data are expressed as mean evoked responses ± SEM. $p>0.05$, two-way ANOVA.

5.4.8. Effect of cannabidiol on joint nociceptor mechanically-evoked responses in the MIA model of OA pain

In order the examine whether GPR55 endogenous tone modulates joint nociceptor mechanosensitivity following the development of MIA-induced OA pain the effects of peripheral administration of cannabidiol (50µg/100µl) on joint nociceptor mechanically-evoked responses was investigated in MIA (n = 9) and saline (n = 9) rats (Figure 5.10).. Cannabidiol alone had no effect on responses compared to control (pre-cannabidiol) in both MIA or saline rats (two-way ANOVA, Figure 5.1A & B).

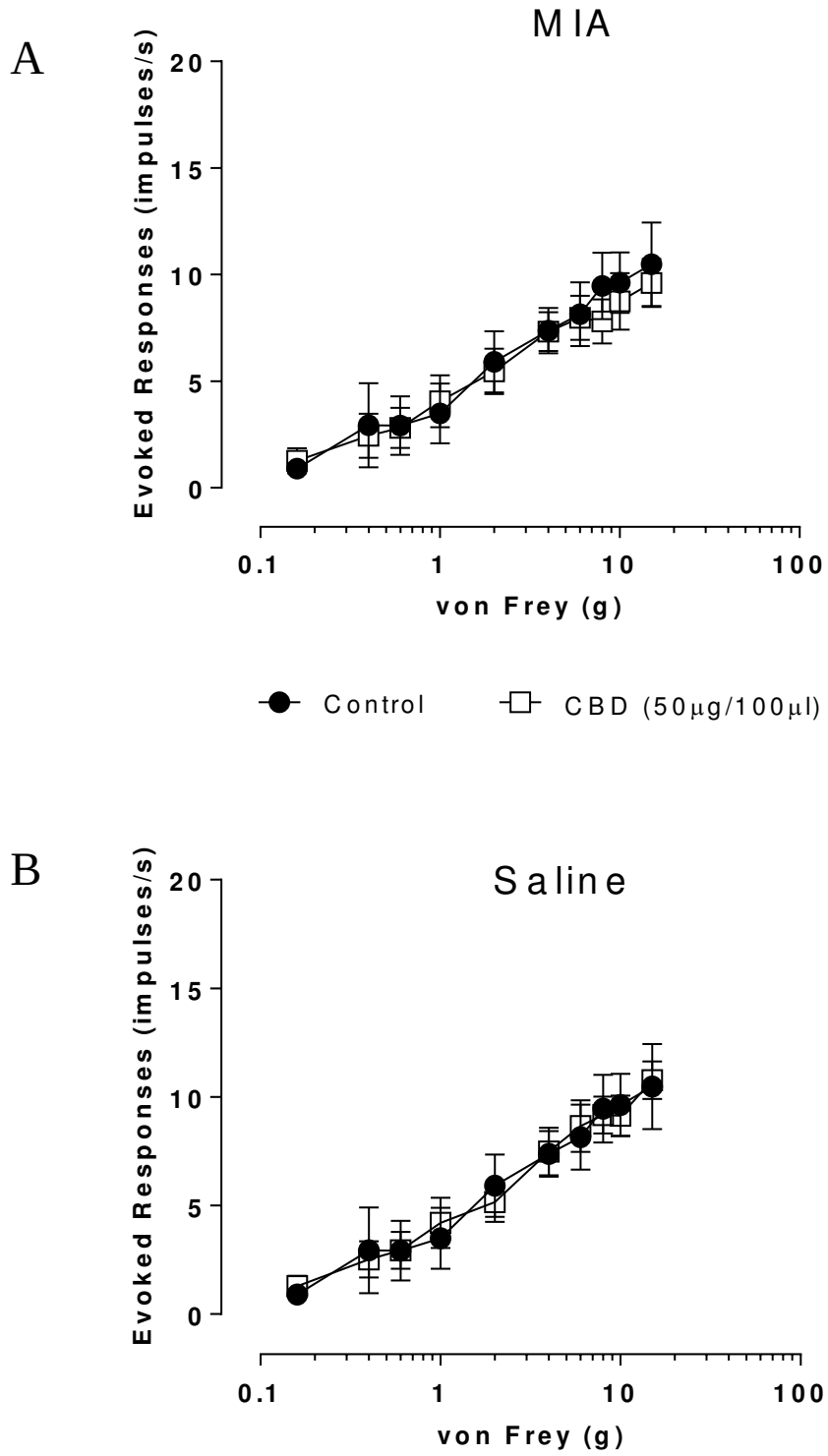

Figure 5.10. Effects of cannabidiol (50µg/100µl) on joint nociceptor mechanically-evoked responses in MIA (n = 9) and saline (n = 9) rats. There was no significant effect of cannabidiol on responses in MIA (A) and saline

(B) rats. Data are expressed as mean evoked responses ± SEM. Two-way ANOVA.

5.4.10. Effects of LPI on mean arterial blood pressure

Mean arterial blood pressure (MAP) was measured throughout the recording protocol (including during LPI administration) via a cannula inserted into the carotid artery to ascertain whether any effects of LPI on knee afferent nociceptor function are related to effects on blood pressure. LPI had no effect on MAP in both MIA and saline rats which remained stable throughout the period of vF monofilament stimulation. Example raw MAP recordings pre- and post-LPI are included in Figure 5.11.

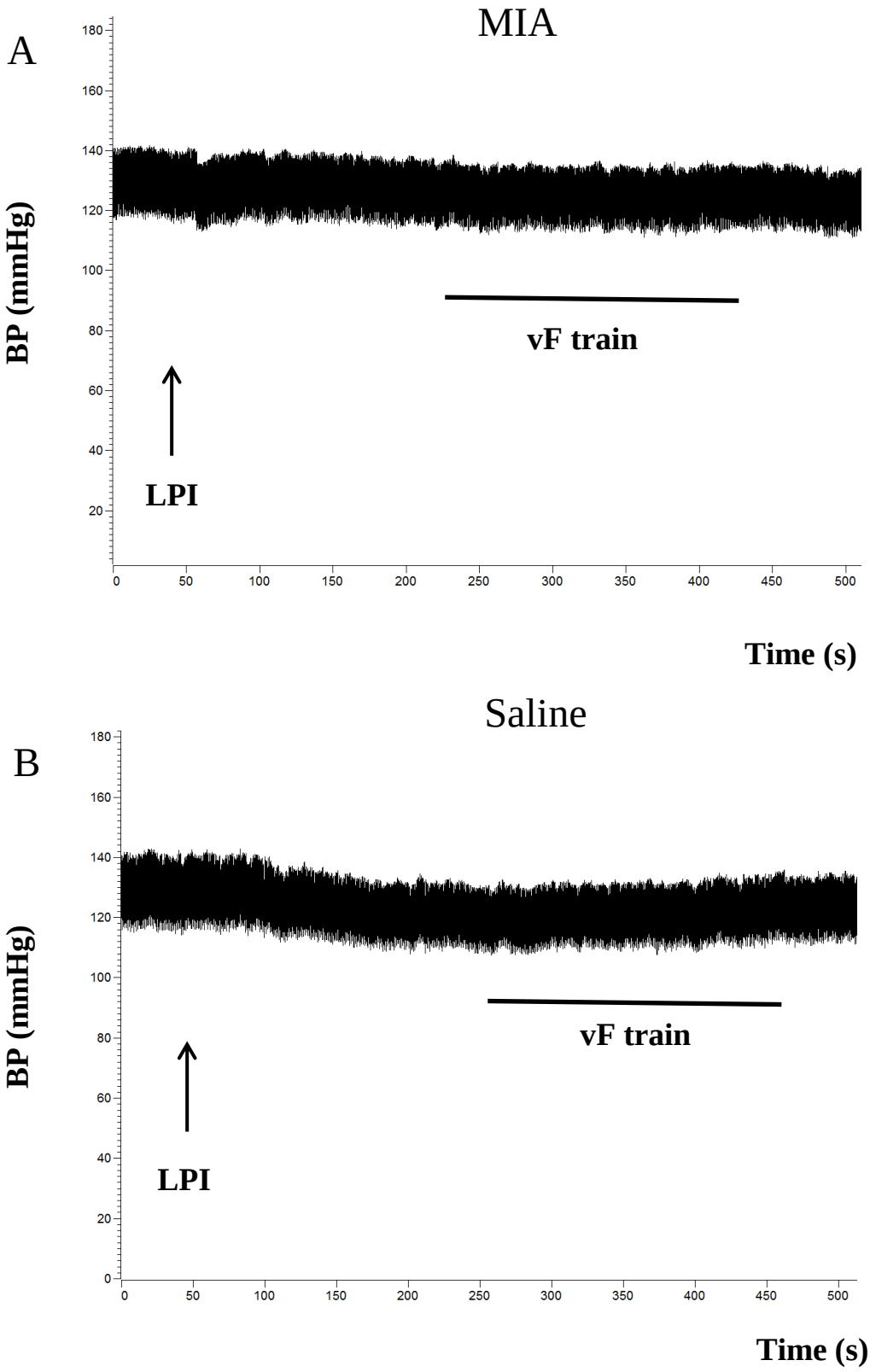

Figure 5.11. Effect of LPI on blood pressure recordings in MIA (A) and saline (B) rats. Representative raw blood pressure traces demonstrating the lack of effect of LPI in an MIA and a saline rat.

5.5. Discussion

The work presented in this chapter investigated whether the GPR55 receptor has a role in the modulation of joint nociceptor mechanosensitivity during established pain in the MIA model of knee OA. Effects of the endogenous GPR55 receptor agonist LPI on the mechanosensitivity s of joint nociceptors in MIA and saline rats were examined using electrophysiological recordings of mechanically-evoked neuronal responses taken from the saphenous nerve in vivo. Peripheral administration of LPI inhibited the mechanosensitivity of joint nociceptors in both groups of rats reducing the magnitude of mechanically-evoked firing rates and increasing mechanical thresholds. These data indicate that the inhibitory effects of peripherally administered LPI are maintained during established OA pain. The involvement of the GPR55 receptor in mediating the inhibitory effects of peripheral administration of LPI was confirmed using the GPR55 receptor antagonist cannabidiol (Whyte et al., 2009). Pre-administration of cannabidiol entirely prevented the inhibitory effects of LPI in both MIA and saline rats. These data indicate that LPI has a novel anti-nociceptive effect on joint nociceptor mechanosensitivity in the MIA model of knee OA and that the inhibitory effects of GPR55 receptor activation in vivo are maintained during established OA pain.

The findings of an anti-nociceptive role for the GPR55 receptor on knee afferent nociceptors in the MIA model are in agreement with the data presented in chapter 4 from naïve rats as well as the McDougall study that demonstrated an anti-nociceptive effect of the synthetic GPR55 receptor agonist O-1602 on C-fibre knee afferent nociceptors in a model of acute joint inflammation

(Schuelert and McDougall, 2011). The effects of GPR55 receptor activation following the development of chronic OA pain have not previously been reported. Consistent with data presented in chapter 4 from naïve rats, the categorisation of recorded fibres studied in this chapter demonstrated that LPI inhibits the mechanosensitivity of both Aδ- and C-fibres in both MIA- and saline treated rats , while O-1602 had no effect on the firing rate of Aδ-fibres (Schuelert and McDougall, 2011). Possible reasons accounting for this discrepancy were discussed in chapter 4.

An inflammatory component has been implicated to contribute to pain in the MIA model (Bove et al., 2003, Fernihough et al., 2004, Ivanavicius et al., 2007, Schuelert and McDougall, 2009, Mapp et al., 2013, Bullock et al., 2014). Several characteristics of inflammatory pain have been demonstrated including an increase in knee joint diameter, expansion of the synovial membrane and infiltration of the synovium by inflammatory cells such as macrophages (Bove et al., 2003, Fernihough et al., 2004, Mapp et al., 2013). Electrophysiological changes in the Kaolin/Carrageenan model of inflammatory arthritis including Aδ and C-type fibres developing increased mechanosensitivity and spontaneous activity (Schaible and Schmidt, 1985) are similar to the OA-induced peripheral sensitization reported here.

Up-regulation of inflammatory mediators (e.g. IL-1, IL1β, IL-6, IL-10, NGF) known to modulate nociceptor sensitivity occurs in the MIA model (Orita et al., 2011, Bowles et al., 2014). Blockade of the CGRP receptor reversed the

increased joint nociceptor sensitization in the MIA model (Bullock et al., 2014). Clinically used anti-inflammatory drugs including diclofenac (Schuelert and McDougall, 2009), naproxen, rofecoxib and acetaminophen (Bove et al., 2003, Ivanavicius et al., 2007) have an analgesic effect on pain behaviour and knee afferent mechanosensitivity in the MIA model. Studies have indicated a modulatory role for GPR55 in inflammatory pain as genetic deletion in mice abolished mechanical hyperalgesia (Staton et al., 2008) and receptor activation attenuated C fibre mechanosensitivity in an acute model of joint inflammation (Schuelert and McDougall, 2011).

The MIA model is also thought to have a neuropathic component (Ivanavicius et al., 2007, Ferreira-Gomes et al., 2010, Orita et al., 2011, Thakur et al., 2012). Up-regulation of markers of nerve injury are known to occur in the DRG following MIA, including the ATF-3 (Ivanavicius et al., 2007, Ferreira-Gomes et al., 2010, Orita et al., 2011, Thakur et al., 2012), neuropeptide Y (Ferreira-Gomes et al., 2010) and growth associated peptide-43 (Ferreira-Gomes et al., 2010, Orita et al., 2011). Further evidence of the contribution of nerve injury to pain in the MIA model can be observed by the analgesic effect of gabapentin (Ivanavicius et al., 2007, Vonsy et al., 2009) and amitriptyline (Ivanavicius et al., 2007) which are used clinically to treat neuropathic pain. A role for the GPR55 receptor in neuropathic pain is evidenced by the absence of hind paw mechanical hyperalgesia following sciatic nerve ligation in GPR55 receptor knockout mice (Staton et al., 2008). Although this pro-nociceptive role is in contrast to the inhibition of knee joint nociceptor mechanosensitivity

demonstrated here, an anti-nociceptive role in modulating the response to nerve injury in the MIA model, could be explained by a tissue-specific role of GPR55 in articular (Schuelert and McDougall, 2011) versus cutaneous (Gangadharan et al., 2013) nociceptors.

Cannabidiol alone had no effect on knee afferent mechanically-evoked responses in rats injected with MIA or saline indicating that the GPR55 receptor does not have a basal modulatory role on knee joint nociception under non-pathological conditions (chapter 4) and this remains true following the development of OA. The absence of a tonic modulatory role in saline-injected (normal) rats is in agreement with data presented in chapter 4 and with published literature (Staton et al., 2008). However, the genetic deletion of GPR55 prevented the development of mechanical hyperalgesia in an CFA model of cutaneous inflammation and a partial nerve ligation model of neuropathic pain indicating that the GPR55 receptor develops a tonic role under certain pathological pain conditions, the present data here indicates that the same cannot be said for MIA-induced OA, at least at the level of the joint and under the conditions of this study.

In summary, the data presented in this chapter identifies a novel peripheral anti-nociceptive role for the endogenous lysophospholipid LPI in the MIA model of OA pain. These findings support and extend data presented in chapter

4 and those already published (Schuelert and McDougall, 2011) that indicate an anti-nociceptive role that appears to be specific for joint afferent nociceptors. These data demonstrating an inhibition of OA-induced peripheral sensitization suggest that local administration of GPR55 receptor agonists may have potential to treat the pain of established OA and this warrants further investigation.

Chapter Six

Immunohistochemical investigations of GPR55 expression in L3-L5 dorsal root ganglia in the rat

6.1. Introduction

In vivo electrophysiological data presented in chapters 4 and 5 (see Sections 4.4.2 and 5.4.4) demonstrated that peripheral administration of the GPR55 agonist LPI to the ipsilateral limb attenuates mechanically-evoked responses of knee joint nociceptors in naïve, MIA and saline rats. Experiments with the putative GPR55 receptor antagonist cannabidiol (see Chapter 4, Section 4.4.3 and Chapter 5, Section 5.4.7) indicate that these inhibitory effects are mediated by activation of peripherally expressed GPR55 receptors. Since the electrophysiological effects of peripherally administered LPI were studied in vivo, it is not known on what tissues of the joint (neuronal or non-neuronal) the effects of LPI were mediated. Previous published findings in the mouse suggest that GPR55 receptors are expressed on large, medium and small sensory neurones of the DRG (Lauckner et al., 2008). The work presented in this chapter sought to investigate whether the in vivo electrophysiological effects of LPI reported in this thesis could be mediated via a direct action on the peripheral terminals of joint innervating afferent nociceptors.

6.1.1. Evidence supporting sensory neuronal GPR55 receptor expression

A small number of published studies have demonstrated a role for the GPR55 receptor in the modulation of nociception with reports of both pro- (Staton et al., 2008, Breen et al., 2012, Gangadharan et al., 2013) and anti-nociceptive roles (Schuelert and McDougall, 2011). Behaviourally, activation of peripheral GPR55 induces an increase in sensitivity to non-noxious and noxious mechanical stimuli which is indicative of allodynia and hyperalgesia,

respectively (Gangadharan et al., 2013). Electrophysiological studies in the rat (in vivo teased nerve) (Schuelert and McDougall, 2011) and mouse (skin nerve preparation) (Gangadharan et al., 2013) have demonstrated effects of GPR55 activation on sensory neurone responses. Local GPR55 receptor activation in vivo has previously been shown to have an inhibitory influence on knee joint afferent nociceptor mechanosensitivity in a rat model of acute joint inflammation (Schuelert and McDougall, 2011) findings corroborated and extended by data presented in chapters 4 and 5. Sensitizing effects of LPI on A-fibre cutaneous afferents of the mouse in a skin-nerve preparation were found to be partially mediated via GPR55 (Gangadharan et al., 2013). These behavioural and electrophysiological effects of GPR55 activation on sensory afferents in both in vivo and ex vivo preparations are in line with responses to GPR55 receptor activation on sensory neurones in vitro (Lauckner et al., 2008, Gangadharan et al., 2013). In cultured DRG neurones, LPI increases the phosphorylation of ERK1/2, an effect absent in cultured DRG neurones from GPR55 knockout mice (Gangadharan et al., 2013). LPI-evoked an increase in intracellular Ca^{2+} levels in large diameter DRG neurones in vitro (Lauckner et al., 2008). Collectively, these findings suggest that GPR55 receptors are expressed by sensory neurones of the DRG and that the effects of LPI reported in this thesis could be mediated by GPR55 expressed by knee joint afferent nociceptors in addition to possible expression by other tissues of the joint.

Direct immunohistochemical evidence of GPR55 expression on DRG neurones is limited. In DRG neurones dissociated from naïve BALB/c mice, high levels

of GPR55 receptor expression were found on large diameter cells (>35µm) with low levels of expression in small cells (Lauckner et al., 2008). To date there has been no published studies that have investigated GPR55 expression in rat DRG neurones and whether DRGs at levels that innervate the knee joint (L3-L5) (Salo and Theriault, 1997) express GPR55 is currently unknown.

6.2. Aims and objectives

The overall aim of the work presented in this chapter was to establish an immunohistochemistry protocol to enable the investigation of GPR55 protein expression in rat DRG neurones at the levels that innervate the knee. The primary objective of this work was to increase our understanding of the mechanisms of action of LPI and of GPR55 activation on knee afferent mechanosensitivity. To this end, immunohistochemistry protocols using an avidin-biotin complex (ABC) and hydrogen peroxidase (HRP) approach were developed.

6.3. Methods

6.3.1. DRG isolation

Rats were deeply anaesthetised with sodium pentobarbital (120mg/kg, i.p, Sigma, UK) and transcardially perfused with at least 150ml each of ice cold PBS followed by 4% paraformaldehyde (PFA) and left and right L3-L5 DRGs were removed. Lumbar DRGs were identified based on previous dissections of the sciatic nerve and originating DRGs (L4-6) (Decosterd and Woolf, 2000). Based on this, L5 was consistently found to be at the level of the pelvic horn allowing caudal and rostral DRGs to be identified. The spinal cord of 10 day old (p10) male Sprague Dawley rats was a gift from Dr Gareth Hathway (University of Nottingham) and was utilized as a positive control as GPR55 expression had been demonstrated previously in this tissue (Dr Gareth Hathway, personal communication).

6.3.2. DRG and p10 spinal cord processing and sectioning

Dissected L3-L5 DRGs and p10 spinal cord were post-fixed overnight in 4% PFA and then cryoprotected overnight in 30% sucrose (at 4°C). Following this, DRGs and p10 spinal cord were rapidly frozen in optimum cutting temperature (OCT) compound (VWR, UK) filled plastic moulds (Dispomould, 24 x 37 x 5mm) using liquid nitrogen chilled isopentane (Fischer Scientific, UK). Moulds were filled with OCT compound and 3 adjacent DRGs or 2 sections of p10 spinal cord taken from the lumbar enlargement were placed into each mould using a paint brush, separated such that they could be cut out of the block individually. Moulds were labelled so that each individual DRG or p10 spinal cord could be identified. Following equilibrium of the DRGs and p10 spinal cord in the OCT (2-5 minutes), moulds were carefully lowered into isopentane that had been chilled over liquid nitrogen. Freezing of the moulds was rapid (<1 minute) and once the OCT had frozen completely, blocks were wrapped in parafilm and tin foil, labelled and stored at -80°C until sectioning. DRGs and p10 spinal cord were sectioned sequentially at 10µm onto SuperFrost Plus slides (6 sections per slide) (Fischer Scientific, UK) using a Bright OFT5000 cryostat (Bright Instruments, Cambridge, UK) with a chamber temperature of -30°C and a specimen temperature of -26°C. Pairs of slides that contained sectioned DRG or p10 spinal cord were wrapped in parafilm and aluminium foil and stored at -20°C until use.

6.3.3. Primary and secondary antibodies

Antibodies were aliquoted into single use volumes upon arrival and stored at -20°C prior to use. Details of antibodies used can be found in Table 6.1 below.

Table 6.1. Details of primary and secondary antibodies used.

Target	**Species Specificity**	**Host**	**Dilution**	**Incubation Time**	**Supplier**	**Cat. Number**
TRPV1 Channel	Human, rat	Guinea pig	1:1500	48 hours	Neuromics, USA	GP14100
GPR55 Receptor	Rat	Rabbit	1:1000-1:10000	24-96 hours	Professor Ken Mackie, University of Indiana, USA	N/A (Gift)
NeuN	Human, rat and mouse	Rabbit	1:300	1 hour	Millipore, UK	ABN78
Anti-TRPV1 Secondary	Guinea pig	Goat	1:300	2 hours	Molecular Probes, UK	A-11073
Anti-GPR55 Secondary	Rabbit	Goat	1:400	2 hours	Vector Laboratories, UK	AK-500
Anti-GPR55 Secondary (HRP)	Rabbit	Goat	1:100	1 hour	Molecular Probes, UK	T-20922

6.3.4. TRPV1 immunohistochemistry

Immunohistochemistry training was carried out by Dr Rebecca Chapman initially using a TRPV1 antibody used in house (Kelly et al., 2013a) for which an optimised protocol for use in DRGs had already been developed. L3-L5 DRG sections were blocked with 1% blocking solution (1ml 0.1M PBS, 3µl triton X-100, 30µl donkey serum) for 1 hour and then incubated with a guinea pig polyclonal anti-TRPV1 antibody (1:1500**;** Neuromics, USA) for 48 hours at 4°C. Following 3 x 10 minute washes with PBS, sections were incubated for 2 hours with a donkey anti-guinea pig secondary antibody (1:300; Molecular Probes, UK). Slides were washed with PBS for 5 x 10 minutes then mounted and coverslipped with Fluoromount (Sigma, UK). A no primary antibody negative control (incubation with TTBS) slide was included. Apart from the primary antibody incubation, all other incubations took place at room temperature and the antibody was prepared in TTBS.

6.3.5. GPR55 immunohistochemistry: ABC method

A schematic is included below to illustrate the principles of the ABC method used (Figure 6.1). Slides containing L3-L5 DRG and p10 spinal cord sections were incubated with 1% blocking solution (see Section 6.3.4 above) overnight at 4°C. Sections were incubated with a rabbit polyclonal anti-GPR55 antibody (1:10000) (generous gift from Dr Ken Mackie, Indiana University, USA, supplied by Dr Gareth Hathway) for 72 hours at 4°C. The primary antibody binds to the target antigen via immunoaffinity (Figure 6.1). Following primary antibody incubation, slides were washed with 0.1M PBS for 3 x 10 minutes.

Sections were incubated with a biotinylated goat anti-rabbit secondary antibody (1:400; Vector Laboratories, UK) for 90 minutes at room temperature. The biotinylated secondary antibody detects the target antigen by binding to the primary antibody (Figure 6.1). Sections were incubated with reagents A (Avidin DH) and B (biotinylated alkaline phosphatase H) (4µl of each in 1ml TTBS; Vector Laboratories, UK) for 30 minutes at room temperature. The preformed ABC covalently binds to the biotinylated secondary antibody (Figure 6.1). Following 3 x 10 minute washes with PBS, sections were incubated with tyramide solution (1:75; Perkin Elmer, UK) for 7 minutes at room temperature. The alkaline phosphatase in the ABC activates multiple copies of the Alexa Fluor 488-labeled tyramide derivative and the resultant highly reactive, short-lived tyramide radicals covalently couple to nucleophilic residues in the vicinity of the alkaline phosphatase-target interaction site (Figure 6.1). As a result, there is a minimal diffusion-related loss of signal localization. Sections were washed with PBS for 2 x 15 minutes. Sections were incubated with FITC avidin (1:600; Invitrogen, UK) and then washed with PBS for 5 x 10 minutes. FITC avidin binds to the biotinylated antibody and is a further staining step to increase the sensitivity of antigen detection (Figure 6.1). Slides were mounted and coverslipped with Fluoromount (Sigma, UK). A no primary antibody negative control (incubation with TTBS) slide was included.

Figure 6.1. Schematic illustration of the ABC method.

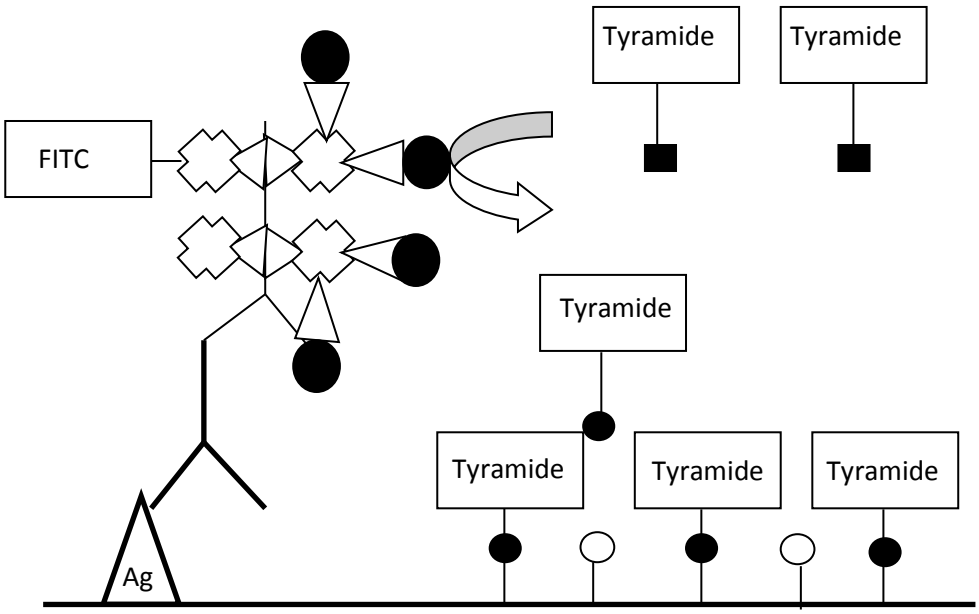

Key:

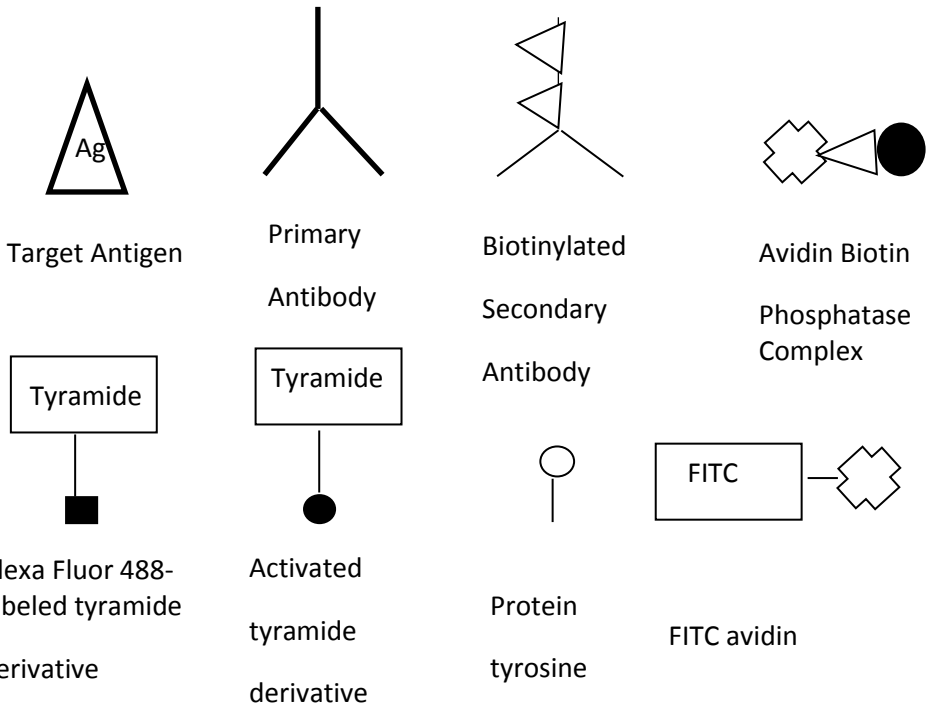

A number of subsequent studies were conducted with the aim of optimising the detected immunoreactivity by varying either a) the primary antibody incubation period or b) the primary antibody dilution factor. Tissue sections were incubated with different concentrations of the anti-GPR55 antibody (1:5000, 1:2500 and 1:1500) for 48 hours andin a separate study, sections were incubated with the rabbit polyclonal anti-GPR55 antibody (1:1000) for 24, 48 or 72 hours at room temperature.

In these latter experiments autofluorescence was detected and further studies were conducted with the aim of determining its cause (see Section 6.4.5). Sections were either a) incubated with TTBS after incubation with the rabbit polyclonal anti-GPR55 antibody (1:2500) for 48 hours at room temperature or b) incubated with TTBS instead of the primary antibody for 48 hours at room temperature then underwent the secondary antibody steps described above.

6.3.6. GPR55 immunohistochemistry: HRP method

In order to overcome problems associated with tissue autofluorescence when using the ABC method, HRP was utilised to detect antigen-antibody binding. A schematic is included below to illustrate the principles of the HRP method used (Figure 6.2). L3-L5 DRG and p10 spinal cord sections were incubated with a 10mg/ml blocking solution for 1 hour at room temperature or 4°C. Tissue sections were incubated with the rabbit polyclonal anti-GPR55 antibody (1:1000) (see above) for 72 hours at room temperature. The primary antibody

binds to the target antigen via immunoaffinity (Figure 6.2). Slides were then washed with PBS for 3 x 10 minutes then incubated with a HRP-conjugated goat anti-rabbit secondary antibody (1:100; Molecular Probes, UK) for 60 minutes at room temperature. The HRP-conjugated secondary antibody detects the target antigen by bindings to the primary antibody (Figure 6.2). Following washing of sections with PBS for 3 x 10 minutes, they were incubated with tyramide working solution (1:100; Molecular Probes, UK) for 10 minutes at room temperature. Slides were washed with PBS for 3 x 10 minutes then mounted and coverslipped with Fluoromount (Sigma). A no primary antibody negative control (incubation with TTBS) slide was included.

Figure 6.2. Schematic illustration of HRP method.

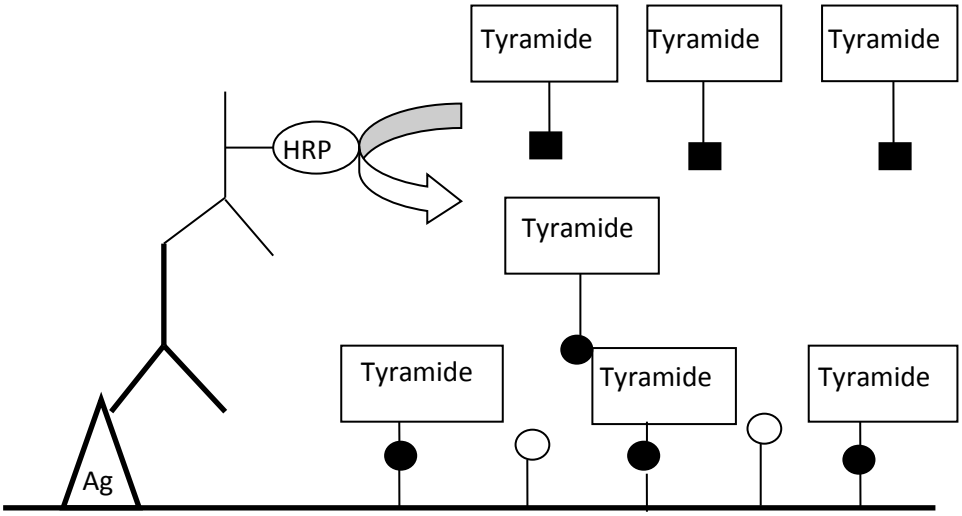

Key:

Target Antigen

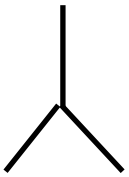

Primary Antibody

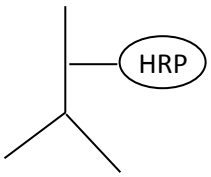

HRP-Conjugated Secondary Antibody

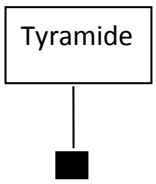

Alexa Fluor 488-labeled tyramide derivative

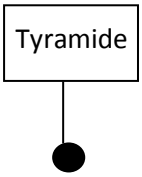

Activated tyramide derivative

Protein tyrosine

6.3.7. NeuN immunohistochemistry

NeuN immunohistochemistry was carried out to check that the HRP kit used in experiments described in section 6.3.5 was viable, using a NeuN primary antibody protocol that had already been optimised in house. L3-L5 DRG sections were blocked with 1% blocking solution (1ml 0.1M PBS, 3µl triton X-100, 30µl goat serum) for 1 hour and then incubated with a rabbit polyclonal anti-NeuN antibody (1:300; Millipore, UK) for 1 hour at 4°C. Following 3 x 10 minute washes with PBS, sections were incubated with a goat anti-rabbit HRP-conjugated secondary antibody (1:100), incubated for 1 hour. Sections were washed for 3 x 10 minutes with PBS before and after 10 minute incubation with tyramide working solution (1:100). Slides were mounted and coverslipped with Fluoromount (Sigma). All incubations took place at room temperature and antibodies were prepared in TTBS.

6.3.8. Image acquisition and analysis

Images of DRGs were captured on a Leica DM4000B fluorescence microscope (TRITC filter: NeuN; FITC filter: GPR55). Images were acquired using SimplePCI software to control a Mamatsu Orca C4692-92 camera. Immunoreactive cells were determined subjectively based on the intensity of staining compared to the background. Cell size analysis was carried out using Image J software.

6.4. Results

6.4.1. TRPV1 immunoreactivity in L3-L5 DRGs

Training in the basic principles of immunohistochemistry was carried out using an optimised TRPV1 immunohistochemistry protocol. Immunohistochemical staining for the TRPV1 channel was detected on small-sized L4 DRG neuronal cell bodies (Figure 6.3A & B). TRPV1 expression was primarily distributed within the cytoplasm and cell membrane of neurones (Figure 6.3B). Omission of the primary antibody for TRPV1 resulted in a lack of staining in DRG sections (Figure 6.3C), confirming the specificity of the primary antibody and of the immunoreactivity observed. These findings are consistent with previous studies that have examined identified TRPV1 expression in DRG neurones (Greffrath et al., 2003, Yu et al., 2008, Zacharova and Palecek, 2009) and also validates my general immunohistochemical technique.

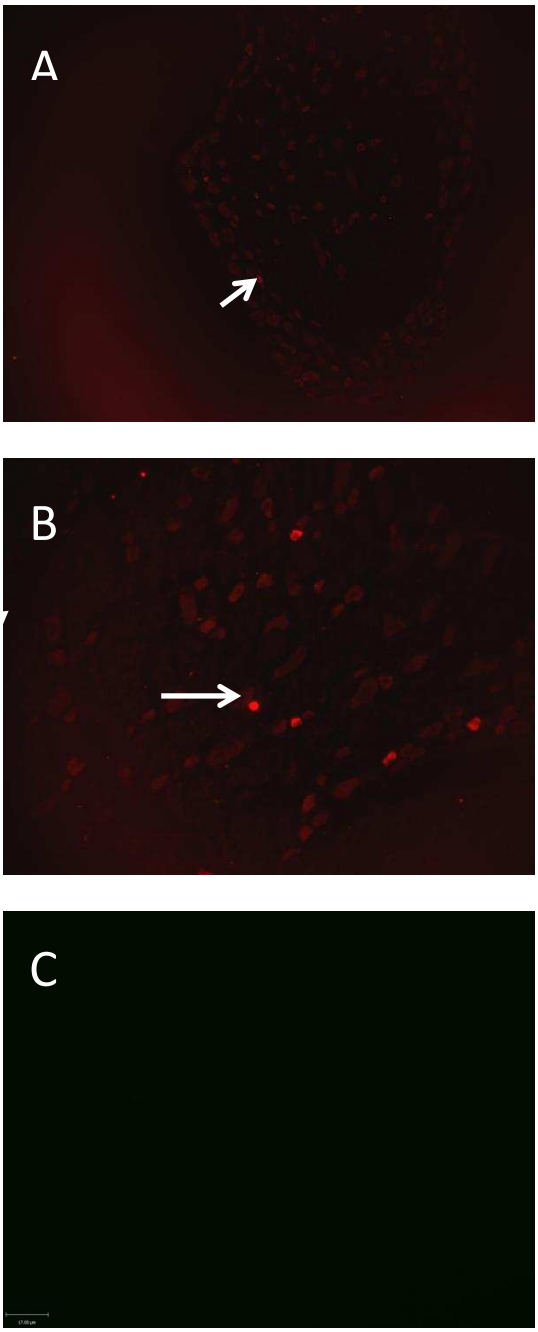

Figure 6.3. TRPV1 immunoreactivity was detected in small sized L4 DRG neurones. (A) A representative L4 DRG section that demonstrates immunoreactivity for TRPV1 was acquired at x10 and (B) x20 magnifications (white arrows). (C) Negative control sections did not demonstrate TRPV1 immunoreactivity.

6.4.2. GPR55 immunoreactivity in L3-L5 DRG neurones and p10 rat spinal cord: ABC method

An immunohistochemistry protocol using the ABC method was developed with the aim of determining whether the GPR55 receptor is expressed in L3-L5 DRG neurone cell bodies. Rat p10 spinal cord was used as a positive control. Immunohistochemical staining for the GPR55 receptor was detected in L3-L5 DRG neuronal cell bodies following incubation with a 1:10000 concentration of the GPR55 primary antibody for 96 hours at 4°C using an ABC method (Figure 6.4A & B). GPR55 was distributed within the cytoplasm and at the cell membrane of small, medium and large neurones. GPR55 did not appear to be expressed in the nucleus. As expected, incubation of the positive control p10 spinal cord sections with the primary antibody for GPR55 resulted in staining (Figure 6.4D) which confirms that the staining protocol is viable. Omission of the primary antibody for GPR55 resulted in a lack of staining in DRG sections (Figure 6.4C) and p10 spinal cord (Figure 6.4E), confirming the specificity of the primary antibody and of the immunoreactivity observed.

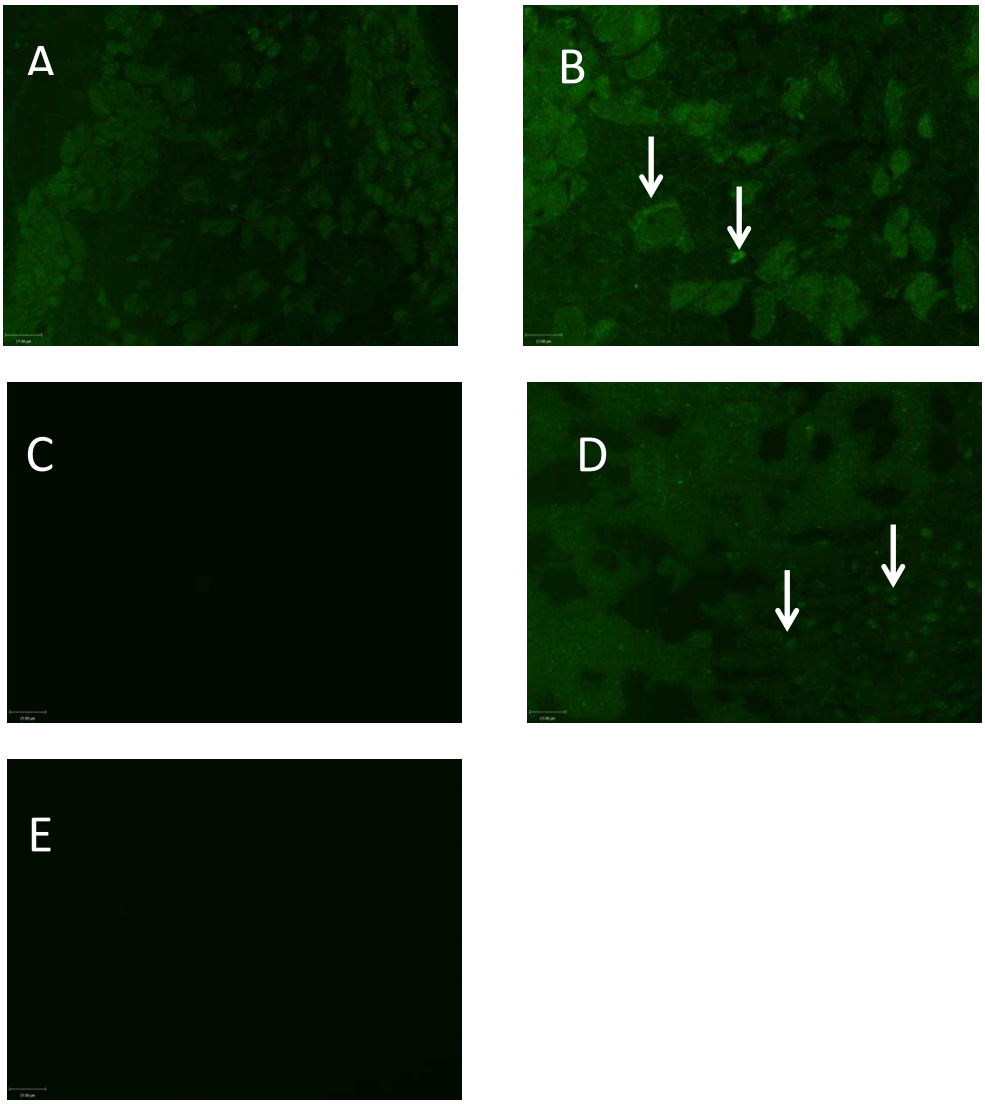

Figure 6.4. GPR55 immunoreactivity was detected in L3-L5 DRG neurones and p10 spinal cord using an ABC method. (A) A representative L3-L5 DRG section that demonstrates immunoreactivity for GPR55 (white arrows) was acquired at x10 and (B) x20 magnifications. (C) L3-L5 DRG sections in which the primary antibody was omitted did not demonstrate staining. (D) A representative p10 spinal cord section showing staining for GPR55 (white arrows) and (E) no staining in the absence of the GPR55 antibody. Scale bar = 17µm.

6.4.3. Optimising the ABC immunohistochemistry staining method: effect of varying GPR55 primary antibody incubation period

A further experiment was conducted with the aim of optimising the GPR55 receptor immunohistochemistry protocol by determining the optimum incubation period for the GPR55 primary antibody. Sections of L3-L5 DRGs were incubated with a 1:10000 concentration of the primary antibody for either 24, 48 or 72 hours at room temperature. However, unexpectedly (given the initial positive staining response observed, see above Figure 6.4) a lack of positive staining was found after incubation with the primary antibody and images of sections looked similar to the negative control sections.

6.4.4. Optimising the ABC immunohistochemistry staining method: effects of varying GPR55 primary antibody concentration

Due to the unexpected absence of staining in the previous experiment, the next logical approach was to determine if increasing the concentration of the GPR55 receptor primary antibody (from 1:10000) would result in the detection of GPR55 immunoreactivity as initially observed (Section 6.4.2. and Figure 6.4). Sections of L3-L5 DRG were incubated with the GPR55 primary antibody at concentrations of 1:5000, 1:2500 or 1:1500 for 48 hours at room temperature. Under these conditions, immunoreactivity was observed at all concentrations of primary antibody (Figure 6.5A - F) but was also present on negative control slides (Figure 6.5G - H) suggesting that the staining observed was not due to GPR55 receptor expression but might be attributed to autofluorescence. Similar encountered issues in the Hathway lab (School of Life Sciences) in experiments using this primary antibody on p10 spinal cord indicated that the detected immunofluorescence may be attributable to autofluorescence.

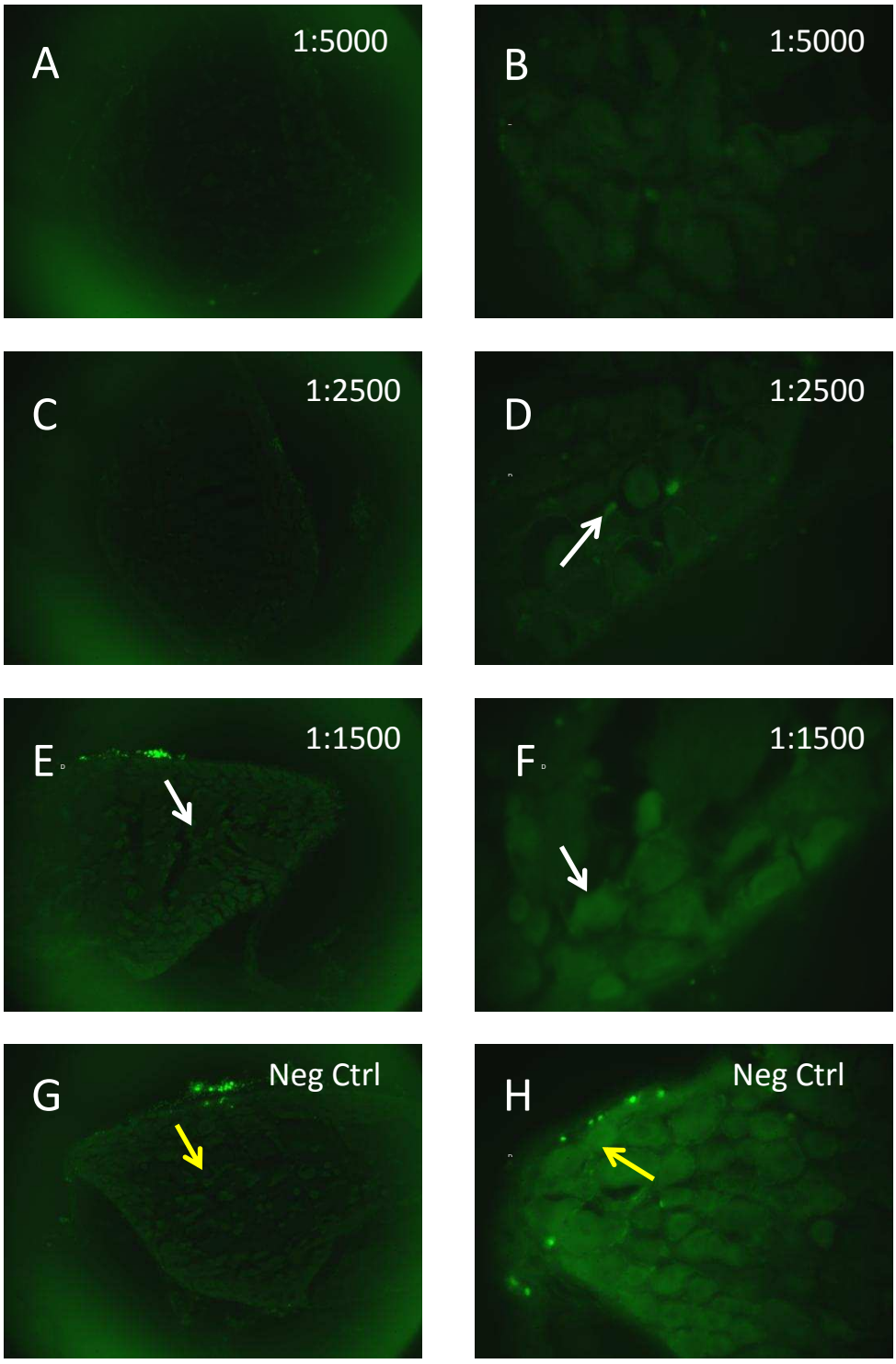

Figure 6.5. Fluorescence was present after incubation of L3-L5 DRG sections. GPR55 primary antibody concentrations of 1:5000 (A-B), 1:2500 (C-D) or 1:1500 (E-F) (white arrows) as well as in negative control sections (G-H) (yellow arrows). Images were acquired at x10 (A, C, E, G) and x20 (B, D, F, H) magnifications.

6.4.5. Determination of the cause of autofluorescence

The next experiment aimed to determine the cause of autofluorescence. To determine whether the secondary antibody steps were the cause, L3-L5 DRG sections were incubated with a 1:2500 concentration of the primary antibody for 48 hours at room temperature and the secondary antibody steps were omitted (Figure 6.6A & B) while the remaining slides were incubated with TTBS instead of the primary antibody but underwent the secondary antibody steps as described above (section 6.3.5). Surprisingly, autofluorescence was encountered under all conditions, and the cause was not identified from this experiment.

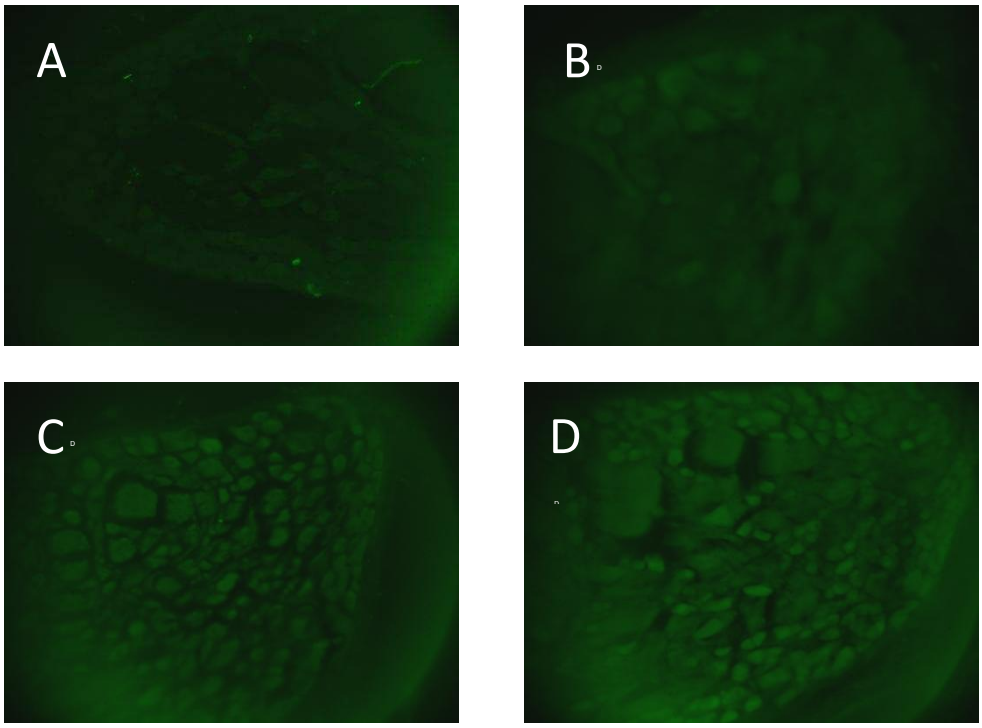

Figure 6.6. Determination of the cause of autofluorescence. L3-L5 DRG neurones were incubated with a 1:2500 concentration of the GPR55 receptor primary antibody and were incubated with TTBS alone during the secondary antibody incubations (A and B). Separate sections were incubated with TTBS alone and underwent incubation with the secondary antibody (C and D).

6.4.6. Establishing the HRP method using a NeuN primary antibody

Given the problems associated with autofluorescence using the ABC method described above, further experiments were undertaken using an HRP approach in an attempt to avoid this issue. Due to the small amount of GPR55 primary antibody available, the HRP staining protocol was tested using a NeuN primary antibody that had been successfully used in our lab previously (Bullock et al., 2014). As expected, L3-L5 DRG neurone cell bodies (all sizes) (Figure 6.7A) and p10 spinal cord (Figure 6.7B) demonstrated NeuN immunoreactivity. Omission of the primary antibody for NeuN resulted in a lack of staining in DRG and spinal cord sections, confirming the specificity of the primary antibody and of the immunoreactivity observed (Figure 6.7C & D). This experiment confirmed that the HRP kit was viable to investigate GPR55 receptor expression on L3-L5 DRG neurones.

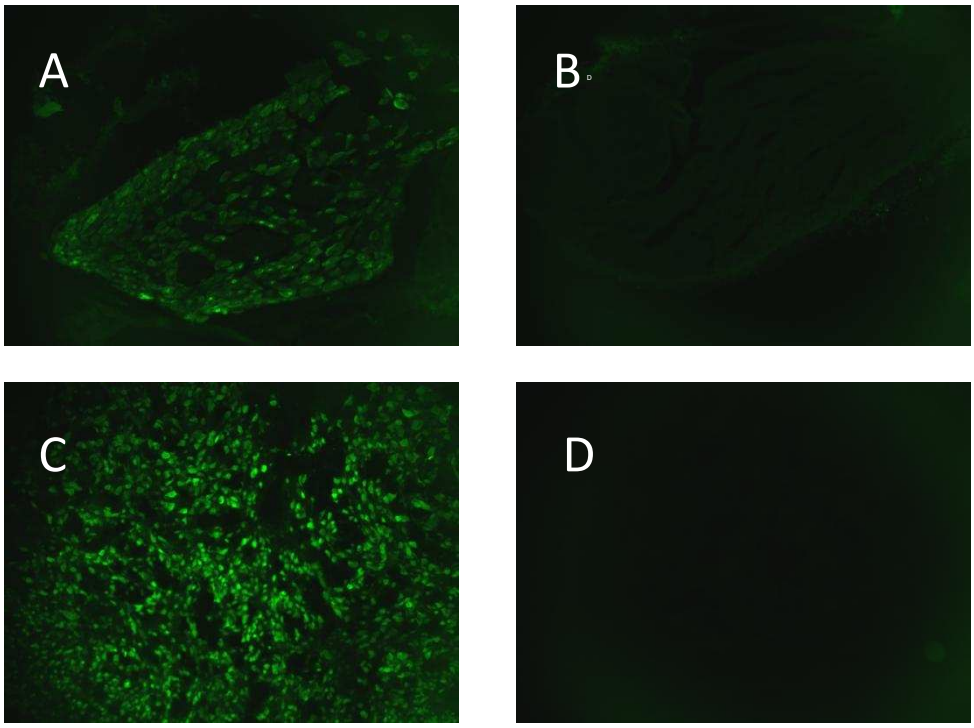

Figure 6.7. NeuN immunoreactivity was detected in L3-L5 DRG and p10 spinal cord. (A) A representative image of a L3-L5 DRG and (C) p10 spinal cord section demonstrating immunoreactivity for NeuN. (B) Negative control L3-L5 DRG and (D) p10 spinal cord sections did not show NeuN immunoreactivity. Images were acquired at a magnification of x10.

6.4.7. Detection of GPR55 immunoreactivity using an HRP method of immunohistochemistry

The HRP method had been used successfully to detect GPR55 expression in p10 spinal cord (Dr Gareth Hathway, personal communication). In initial experiments using the HRP method no GPR55 staining was observed in L3-L5 DRG neurone cell bodies or p10 spinal cord incubated with a 1:1000 concentration of the GPR55 primary antibody for 72 hours at a temperature of 4°C.

The GPR55 receptor immunohistochemistry protocol was repeated using the HRP method, incubating L3-L5 DRG sections with a 1:1000 concentration of the GPR55 primary antibody for 72 hours at room temperature. Consistent with previous initial observations (see section 6.4.2 and figure 6.4) GPR55 receptor immunoreactivity was detected in L3-L5 DRGs (Figure 6.8). In general, GPR55 expression was primarily distributed within the cytoplasm and around the perimeter of some DRG cells (Figure 6.8A & B). GPR55 did not appear to be expressed in the nucleus. GPR55 immunoreactivity appeared to be associated with both large (51.82±1.95µm) and small to medium (23.86±1.24µm) DRG neurones. Despite this, the pattern of staining appeared to differ between the two types of cell; with some small to medium cells exhibiting high levels of immunoreactivity throughout the cytoplasm and some large cells exhibiting immunoreactivity around the perimeter of the cell in what could be satellite glial cells (SGCs) and lower levels within the cytoplasm of the neurone. Omission of the primary antibodies for GPR55 resulted in a lack

of staining in DRG sections, confirming the specificity of the primary antibodies and of the immunoreactivity observed (Figure 6.8 C&D).

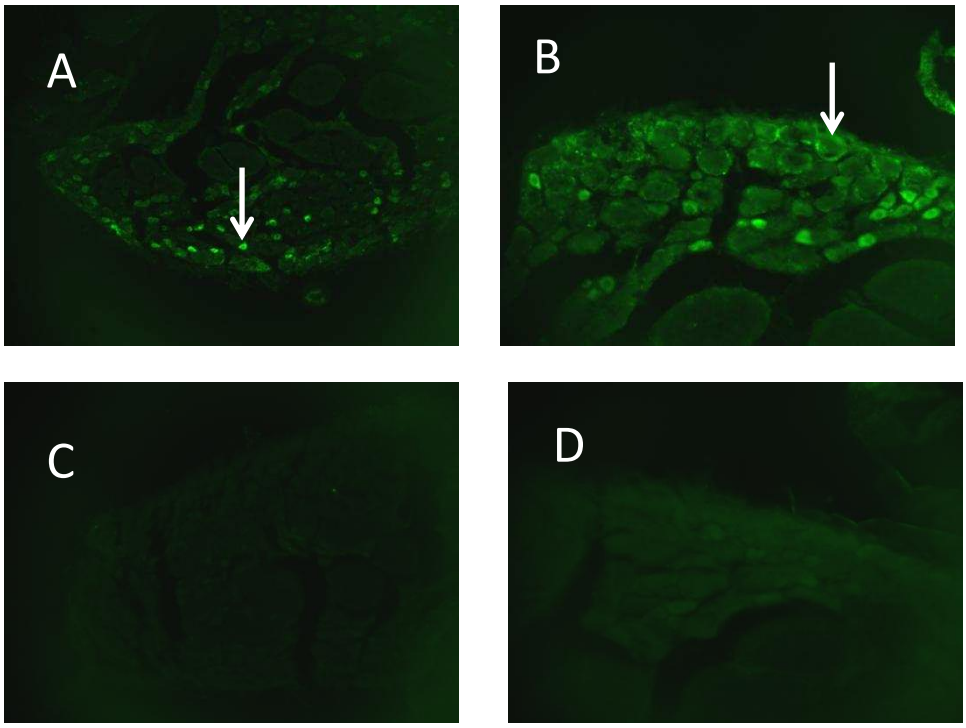

Figure 6.8. GPR55 immunoreactivity was detected in L3-L5 DRGs. (A) A representative L3-L5 DRG section demonstrating immunoreactivity for GPR55 with images acquired at a magnification of x10 and (B) x20 (white arrows). (C) No immunoreactivity was observed on negative control DRG sections with images acquired at a magnification of x10 and (D) x20.

6.5. Discussion

The work outlined in this thesis chapter has demonstrated the expression of the GPR55 receptor in L3-L5 (knee innervating) DRGs from naïve rats. Incubation of rat L3-L5 DRGs with a polyclonal GPR55 receptor primary antibody resulted in immunoreactivity that was associated with both large and medium to small DRG neurones and the included negative controls confirmed the specificity of the observed immunoreactivity.

These data are the first demonstration of GPR55 receptor protein expression in rat DRG neurones and support and extend a previous study demonstrating GPR55 receptor expression in large and small mouse DRG neurones (Lauckner et al., 2008). The Lauckner study is the only other study that investigated the expression of GPR55 in DRGs and reported that the receptor was preferentially expressed in large neurones with low levels in small cells which contrasts with the findings reported here. Differences in the reported expression could be due to species differences (rat vs mouse), differences in DRG levels, GPR55 primary antibody, or immunohistochemistry protocol used. Expression of GPR55 in small and medium sized rat DRG neurones is consistent with the electrophysiological effects of peripheral LPI on both C- and Aδ-fibre knee joint nociceptors reported in chapters 4 and 5. Moreover, this immunohistochemical evidence supports direct effect of LPI on knee joint nociceptor peripheral terminals, although GPR55 receptor immunohistochemistry was not combined with retrograde labelling of knee joint afferents. As such expression by these neurones cannot be unequivocally confirmed.

Initial immunohistochemistry training carried out using a TRPV1 immunohistochemistry protocol optimised in house confirmed the expression of the TRPV1 channel with a distribution consistent with the current literature (Fernihough et al., 2005). These findings meant that I could next investigate GPR55 expression with a GPR55 receptor antibody not previously used on DRGs confident in the validity of my general technique. GPR55 immunoreactivity was initially investigated using an ABC based method and produced encouraging results (described above), although some optimisation was required. These optimisation experiments encountered problems and although GPR55 immunoreactivity was initially detected using the ABC method, subsequent optimisation experiments (varying incubation periods and primary antibody concentrations) all failed to detect GPR55 immunoreactivity in L3-L5 DRG neurones. Fluorescence was present in both sections that had been incubated with the primary antibody and those used as negative control sections not exposed to the primary antibody, an effect thought to be attributed to autofluorescence. The Hathway laboratory had been successful in overcoming the issue of autofluorescence by using a HRP immunohistochemistry protocol. This approach was then adopted for my studies and used successfully, detecting. GPR55 expression in L3-L5 DRG neurones that again ranged from small-, medium- and large- cell diameters (in agreement with earlier experiments using the ABC method). The immunoreactivity associated with large DRG neurones was located around the perimeter of the cell. The appearance of this staining indicated possible expression at the cell membrane and/or expression in SGCs. In the DRG, SGCs wrap completely around sensory neurones, with each neurone being

surrounded by several SGCs (Hanani, 2005). The neurone and its surrounding SGCs are said to form a distinct morphological and functional unit (Hanani, 2005). Published findings indicate that SGCs do not merely provide mechanical support to the neurones as previously thought, but share many functions with CNS glia including being able to receive and transmit chemical signals and are known to express various receptors for neurochemicals (Hanani, 2005). Given these characteristics, SGCs are likely to participate in signal processing and transmission in sensory ganglia and are thought to play a role during chronic pain states (Liu et al., 2012, Warwick and Hanani, 2013). Thus, with this in mind, the possible expression of GPR55 in SGCs of the DRG is intriguing. GPR55 mRNA has been demonstrated in both mouse primary microglia cells and in the immune cell line BV2 and its expression is increased in these cells following exposure to an inflammatory stimulus (Pietr et al., 2009). This increased GPR55 expression during microglia activation suggests a possible involvement in modulating inflammatory signalling. In fact, GPR55 is known to influence the regulation of cytokines during inflammatory hyperalgesia (Staton et al., 2008) SGCs are thought to release cytokines, and thus influence DRG neurones expressing corresponding cytokine receptors. GPR55 may play a role in modulating sensory processing at the level of the DRG by regulating cytokine expression in SGCs. Studies examining GPR55 co-expression with a SGC marker, glial fibrillary acidic protein (GFAP) or glutamine synthetase (GS) (Hanani, 2005) would be required to confirm expression in these important cells.

As discussed above, GPR55 expression in L3-L5 DRG neurones suggests that the electrophysiological effects of LPI reported in chapters 4 and 5 could occur at least in part via a direct activation of GPR55 receptors localised on the peripheral terminal endings of knee joint nociceptors. However, I cannot exclude the possibility that an indirect effect of LPI on knee joint nociceptors was mediated via an activation of non-neuronal cells within the joint. For example mast cells are known to be expressed in both normal (Russell et al., 2012) and inflamed (Schiltz et al., 2002) rat knee joint synovia and the activation of GPR55 expressed by human mast cells inhibits their degranulation and subsequent NGF release (Cantarella et al., 2011). I postulate that these cells could be a non-neuronal site of action of LPI, activation of which could potentially modulate the release of NGF at the level of the synovium (de Lange-Brokaar et al., 2012). This inhibition of NGF release would reduce mast cell degranulation and the release of other pro-nociceptive mediators (histamine, 5-HT) (Lewin et al., 1994). NGF is known to have an important role in joint pain mechanism, including following the development of MIA-induced OA (Ashraf et al., 2013). Intra-articular injection of NGF induces weight bearing asymmetry (Ashraf et al., 2013) suggesting an NGF induced mechanical sensitization of joint nociceptors. Whether activation of GPR55 receptors expressed by mast cells at the level of the joint has the potential to reduce joint nociceptor mechanosensitivity via an inhibition of mast cell mediated NGF release is an intriguing possibility. Moreover whether these effects could account for the electrophysiological response to LPI reported in earlier chapters is unknown.

In summary, the data presented in this chapter identified a novel expression of the GPR55 receptor in DRG neurones that are at the level innervating the knee joint (L3-L5) in naïve rats. These findings suggest that the in vivo electrophysiological effects of LPI presented in chapters 4 and 5 could be mediated at least in part by GPR55 receptors expressed on the peripheral terminals of knee joint afferent nociceptors. However, future work using retrograde labelling would be required to unequivocally localise expression to knee joint innervating nociceptors.

Chapter Seven

General Discussion

7.1. Discussion of findings

Overall, the findings of this thesis highlight a role for the GPR55 receptor in the modulation of joint nociceptor mechanosensitivity and in the inhibition of peripheral sensitization during established OA pain behaviour in the MIA model. These findings provide insight into the potential of GPR55 as a novel analgesic target for joint pain that could have relevance for the treatment of OA knee pain. Electrophysiological studies have demonstrated for the first time that activation of peripheral GPR55 receptors by the putative endogenous ligand LPI inhibited the sensitivity of joint nociceptors to mechanical stimulation under non-pathological (naïve) conditions and in the MIA model of knee OA pain. This demonstration of an anti-nociceptive role of GPR55 on joint nociceptive inputs that is maintained during an arthritis pain state is in agreement with a previous study that used the synthetic agonist O1602 in an acute model of joint inflammation (Schuelert and McDougall, 2011). Blockade of LPI effects by the putative GPR55 antagonist cannabidiol confirmed an involvement of GPR55. LPI's inhibitory effects were partially attenuated by AM281, a CB_1 antagonist that also shows partial agonist activity at GPR55 (Henstridge et al., 2009, Anavi-Goffer et al., 2012) and inhibits LPI-mediated ERK1/2 phosphorylation in hGPR55-HEK293 cells (Anavi-Goffer et al., 2012).

The electrophysiological studies in this thesis demonstrated that joint nociceptors are sensitized in the MIA model at day 14, during established pain behaviour. These findings support those of recent published studies from our

lab (Kelly et al., 2012, Kelly et al., 2013a, Bullock et al., 2014) and others (Schuelert et al., 2010), collectively pointing towards a critical role for aberrant input from the joint in maintaining OA pain. This suggestion is supported by clinical studies that demonstrate the pain relieving effects of i.a. local anaesthetic (Creamer et al., 1996) and of joint replacement surgery (Kosek and Ordeberg, 2000a) and by the attenuation of pain behaviour by interventions that block peripheral nociceptor activity at the level of the joint in animal models of OA (McDougall et al., 2006, Schuelert and McDougall, 2006a, Schuelert and McDougall, 2012, Ashraf et al., 2013, Kelly et al., 2013a).

Candidate chemical mediators, ion channels and receptors that have been suggested to be involved in the maintenance of joint nociceptor sensitization in OA include SP (Ahmed et al., 2012), CGRP (Bullock et al., 2014), BK (Cialdai et al., 2009), NGF (Ashraf et al., 2013), TRPV1 (Puttfarcken et al., 2010, Kelly et al., 2013a), $Na_v1.8$ (Schuelert and McDougall, 2012), and paradoxically the CB_2 receptor (Schuelert et al., 2010). Given recent published data suggesting that GPR55 might have a role in the modulation of nociception (Staton et al., 2008, Breen et al., 2012, Gangadharan et al., 2013) including during acute inflammatory arthritis (Schuelert and McDougall, 2011), the work described in this thesis focused on the role GPR55 in the modulation of joint nociceptor excitability and demonstrated that activation of GPR55 at the level of the knee joint (using LPI) potently inhibited joint nociceptor excitability in control rats and importantly this inhibition was maintained in MIA rats, highlighting a critical novel anti-nociceptive role for GPR55 during experimental OA pain. Findings in untreated and saline rats suggest that

GPR55 receptor activation can regulate the normal level of mechanical sensitivity of joint nociceptors. However the physiological relevance of this suggestion is challenged by the fact that local administration of cannabidiol had no effect on mechanical sensitivity of joint nociceptors in both control and MIA rats. Despite this, the fact that inhibitory effects of GPR55 receptor activation are maintained in the face of joint nociceptor mechanical sensitization in OA rats suggests that further investigation of the potential of GPR55 agonists as a therapeutic strategy in OA for the alleviation of pain during established joint degeneration and pain warrants further investigation.

The work in this thesis demonstrated that semi-local administration of LPI modulated the mechanical sensitivity of joint nociceptors via a mechanism that was abolished by pre-administration of the GPR55 antagonist cannabidiol. These novel findings suggest that the activation of peripheral GPR55 receptors within the joint has the potential to desensitize joint nociceptors to mechanical stimuli. While the desensitizing effects of GPR55 activation corroborate previous findings of GPR55 receptor activation on C-fibre joint nociceptor responses (Schuelert and McDougall, 2011), a direct sensitizing effect for LPI has been observed on cutaneous afferents from naive mice (Gangadharan et al., 2013). This sensitising effect of LPI on cutaneous afferents is in line with previous studies that have identified a pro-nociceptive role for the GPR55 receptor in the CFA-induced model of cutaneous inflammation (Staton et al., 2008), chronic constriction (Breen et al., 2012) and partial nerve injury models (Staton et al., 2008) of neuropathic pain. The identification of an anti-nociceptive role of GPR55 on joint nociceptors with a pro-nociceptive role in

cutaneous pain indicates that the nociceptive role of GPR55 may be tissue-specific (Ross, 2009).

Since the effects of LPI on joint nociceptor mechanosensitivity were studied in vivo it is not known whether the inhibition of joint nociceptor responses occurred via a direct neuronal effect through GPR55 expressed by joint afferents or by GPR55 expressed elsewhere in the joint. A previous study in the mouse has demonstrated GPR55 expression on DRG neurones (Lauckner et al., 2008), however expression in rat DRGs has not previously been reported. The work in this thesis demonstrated that GPR55 receptor protein was expressed in L3-L5 DRG (at the level that innervates the knee joint) in naive rats. Whilst this does not conclusively confirm that functional GPR55 receptors are formed on knee afferent neurones, given the electrophysiological findings presented in this thesis it is a plausible suggestion. That said, expression by other cells of the joint in other tissues (e.g. synovium) cannot be excluded and activation of GPR55 receptors at these sites may contribute to effects of LPI on joint nociceptors in vivo.

The role of the GPR55 receptor as a novel third cannabinoid receptor was initially proposed by GSK and AstraZeneca patents that identified cannabinoid ligands as having affinity and efficacy at the recently cloned GPR55. As a consequence, several studies investigated whether GPR55 was indeed a new member of the cannabinoid receptor family (Petitet et al., 2006, Ryberg et al., 2007, Lauckner et al., 2008, Yin, 2009, Henstridge et al., 2010, Anavi-Goffer

et al., 2012) with endocannabinoids (anandamide, 2-AG), phytocannabinoids (Δ^9-THC, cannabidiol) and synthetic cannabinoids (AM251, O-1602) identified as GPR55 ligands. The pharmacology of cannabinoid ligands at GPR55 is controversial as published studies have produced conflicting findings. Some cannabinoid ligands (e.g. AM251, anandamide, 2-AG, CP55940, O-1602) function as GPR55 agonists and in other studies have no effect. These conflicting findings could be due to the use of different cell lines (HEK293, U2OS) and assays (GTPγS, Ca^{2+} currents, β-arrestin binding, ERK phosphorylation) between groups. The classical cannabinoid receptors and GPR55 exhibit low sequence homology (10-15%) and do not share a common functional fingerprint to enabling ligand binding (Petitet et al., 2006). Given that GPR55 has a unique response profile to cannabinoid ligands, sequence homology and functional fingerprint compared to CB_1 and CB_2 suggests that GPR55 is more accurately defined as an atypical cannabinoid receptor rather than a new member of the cannabinoid receptor family.

7.1.1. Limitations of the work presented

One possible limitation of the work presented in this thesis is the use of LPI in as a GPR55 receptor agonist to investigate the effects of GPR55 activation on joint nociceptor sensitivity. A recent study identified that in GPR55 knockout mice LPI still partially modulated pain behaviour depending on the concentration of LPI and strength or duration of mechanical stimuli (Gangadharan et al., 2013). Further studies have demonstrated that LPI causes the opening of two pore domain mechanogated K^+ channels TREK-1 and

TRAAK. As a consequence, this effect would facilitate membrane hyperpolarization and reduce neuronal excitability. Despite these effects, the inhibitory response to LPI was completely blocked by the GPR55 antagonist cannabidiol. Due to the investigation of GPR55 being at an early stage and the receptor not being fully characterised, the pharmacological tools available to investigate GPR55 function have their limitations. However, on the balance of what has been published to date I chose LPI since most studies were in agreement that LPI is a good candidate as a GPR55 agonist.

Another limitation of this work may relate to the use of AM281 in this thesis to investigate if the effects of LPI on knee joint nociceptor sensitivity were mediated by the CB_1 receptor. Although some studies have found that AM281 has no effect at GPR55 (Kapur et al., 2009), other studies have identified that AM281 can increase intracellular Ca^{2+} concentration (Henstridge et al., 2010) and phosphorylate ERK1/2 (Anavi-Goffer et al., 2012) in hGPR55 expressing HEK293 cells and can inhibit LPI-mediated phosphorylation of ERK1/2 in the same model system in which it functioned as an agonist (Anavi-Goffer et al., 2012). It is possible that AM281 inhibited the LPI-mediated inhibition of knee joint nociceptor mechanical sensitivity by modulating GPR55 making it difficult to conclude definitively that the effect of LPI is mediated by a non-CB_1 receptor mechanism.

Significant difficulties were encountered with establishing a reliable immunohistochemistry protocol. The work involved in attempting to overcome

issues such as autofluorescence and unreliable staining in initial experiments, was time consuming and unfortunately prevented further characterisation of GPR55 receptor expression in L3-L5 DRG neurones and specifically in retrograde labelled knee afferents as well as other tissues of the joint.

7.1.2. Future directions

The findings in this thesis provide the rationale for further investigations into the role of GPR55 in the modulation of joint pain. Further work is required to fully investigate the role of the GPR55 receptor in pathological joint conditions such as OA, to determine whether GPR55 agonists warrant clinical investigation in man. Although the electrophysiological studies in this thesis point towards GPR55 being a novel analgesic target for the treatment of joint pain conditions, a study investigating the effects of i.a. injection of a GPR55 receptor agonist on pain behaviour is required to confirm this. Generation of nociceptor specific GPR55 knock out mice would facilitate further investigations into the role of peripherally expressed GPR55 in the generation of pain behaviour under normal physiological conditions (in naïve mice) or following OA-induction.

Further electrophysiological studies could investigate the effects of LPI on joint afferents in a surgical model of OA (e.g. MNX) to enable an assessment of the generalizability of these findings to OA pain and in a slowly progressing model (e.g. rat low dose MIA model) to assess the role of GPR55 in the

modulation of knee afferent mechanosensitivity during early versus late stage OA pain. Studies investigating GPR55 expression by FG backlabelled knee afferent neurones and the investigation of GPR55 expression in synovia would further understanding of of GPR55 receptor mediate antinociception at the level of the joint. Finally, further, studies examining GPR55 co-expression with a SGC marker, GFAP or GS would be required to confirm expression in these important cells.

7.2. Concluding remarks

Overall, the studies presented in this thesis provide new information regarding the role of the GPR55 receptor in the modulation of knee joint nociceptor mechanosensitivity under non-pathological conditions and in an experimental model of OA. This thesis has identified a novel role for the GPR55 receptor in attenuating nociceptive inputs from the joint, including during established OA pain, and has provided novel insights into the analgesic potential of targeting GPR55 at the level of the joint. The outcomes of this thesis could have direct relevance for future investigations of the clinical utility of GPR55 receptor agonists for the treatment of human joint pain. In addition, understanding the sites and mechanisms of action of GPR55 receptor agonists has important implications for the development of site directed therapies. The outcomes of this thesis support the idea that the GPR55 receptor system may function as an endogenous pain control system at the level of the joint.

References

AGARWAL, N., PACHER, P., TEGEDER, I., AMAYA, F., CONSTANTIN, C. E., BRENNER, G. J., RUBINO, T., MICHALSKI, C. W., MARSICANO, G., MONORY, K., MACKIE, K., MARIAN, C., BATKAI, S., PAROLARO, D., FISCHER, M. J., REEH, P., KUNOS, G., KRESS, M., LUTZ, B., WOOLF, C. J. & KUNER, R. 2007. Cannabinoids mediate analgesia largely via peripheral type 1 cannabinoid receptors in nociceptors. *Nat Neurosci,* 10**,** 870-9.

AHLUWALIA, J., RANG, H. & NAGY, I. 2002a. The putative role of vanilloid receptor-like protein-1 in mediating high threshold noxious heat-sensitivity in rat cultured primary sensory neurons. *Eur J Neurosci,* 16**,** 1483-9.

AHLUWALIA, J., URBAN, L., BEVAN, S., CAPOGNA, M. & NAGY, I. 2002b. Cannabinoid 1 receptors are expressed by nerve growth factor- and glial cell-derived neurotrophic factor-responsive primary sensory neurones. *Neuroscience,* 110**,** 747-53.

AHLUWALIA, J., URBAN, L., CAPOGNA, M., BEVAN, S. & NAGY, I. 2000. Cannabinoid 1 receptors are expressed in nociceptive primary sensory neurons. *Neuroscience,* 100**,** 685-8.

AHMED, A. S., LI, J., ERLANDSSON-HARRIS, H., STARK, A., BAKALKIN, G. & AHMED, M. 2012. Suppression of pain and joint destruction by inhibition of the proteasome system in experimental osteoarthritis. *Pain,* 153**,** 18-26.

AHMED, M., BJURHOLM, A., THEODORSSON, E., SCHULTZBERG, M. & KREICBERGS, A. 1995. Neuropeptide Y- and vasoactive intestinal polypeptide-like immunoreactivity in adjuvant arthritis: effects of capsaicin treatment. *Neuropeptides,* 29**,** 33-43.

AKOPIAN, A. N., SOUSLOVA, V., ENGLAND, S., OKUSE, K., OGATA, N., URE, J., SMITH, A., KERR, B. J., MCMAHON, S. B., BOYCE, S., HILL, R., STANFA, L. C., DICKENSON, A. H. & WOOD, J. N. 1999. The tetrodotoxin-resistant sodium channel SNS has a specialized function in pain pathways. *Nat Neurosci,* 2**,** 541-8.

ALESSANDRI-HABER, N., DINA, O. A., CHEN, X. & LEVINE, J. D. 2009. TRPC1 and TRPC6 channels cooperate with TRPV4 to mediate mechanical hyperalgesia and nociceptor sensitization. *J Neurosci,* 29**,** 6217-28.

ALEXANDER, S. P. & KENDALL, D. A. 2007. The complications of promiscuity: endocannabinoid action and metabolism. *Br J Pharmacol,* 152**,** 602-23.

ALLOUI, A., ZIMMERMANN, K., MAMET, J., DUPRAT, F., NOEL, J., CHEMIN, J., GUY, N., BLONDEAU, N., VOILLEY, N., RUBAT-COUDERT, C., BORSOTTO, M., ROMEY, G., HEURTEAUX, C., REEH, P., ESCHALIER, A. & LAZDUNSKI, M. 2006. TREK-1, a K+ channel involved in polymodal pain perception. *Embo Journal,* 25**,** 2368-2376.

ALOE, L., TUVERI, M. A., CARCASSI, U. & LEVI-MONTALCINI, R. 1992. Nerve growth factor in the synovial fluid of patients with chronic arthritis. *Arthritis Rheum,* 35**,** 351-5.

AMAYA, F., SHIMOSATO, G., KAWASAKI, Y., HASHIMOTO, S., TANAKA, Y., JI, R. R. & TANAKA, M. 2006a. Induction of CB1 cannabinoid receptor by inflammation in primary afferent neurons facilitates antihyperalgesic effect of peripheral CB1 agonist. *Pain,* 124**,** 175-83.

AMAYA, F., WANG, H. B., COSTIGAN, M., ALLCHORNE, A. J., HATCHER, J. P., EGERTON, J., STEAN, T., MORISSET, V., GROSE, D., GUNTHORPE, M. J., CHESSELL, I. P., TATE, S., GREEN, P. J. & WOOLF, C. J. 2006b. The voltage-gated sodium channel Na(v)1.9 is an effector of peripheral inflammatory pain hypersensitivity. *Journal of Neuroscience,* 26**,** 12852-12860.

ANAND, U., OTTO, W. R., SANCHEZ-HERRERA, D., FACER, P., YIANGOU, Y., KORCHEV, Y., BIRCH, R., BENHAM, C., BOUNTRA, C., CHESSELL, I. P. & ANAND, P. 2008.

Cannabinoid receptor CB2 localisation and agonist-mediated inhibition of capsaicin responses in human sensory neurons. *Pain,* 138**,** 667-80.

ANAVI-GOFFER, S., BAILLIE, G., IRVING, A. J., GERTSCH, J., GREIG, I. R., PERTWEE, R. G. & ROSS, R. A. 2012. Modulation of L-alpha-lysophosphatidylinositol/GPR55 mitogen-activated protein kinase (MAPK) signaling by cannabinoids. *J Biol Chem,* 287**,** 91-104.

ANDOH, T., NAGASAWA, T. & KURAISHI, Y. 1996. Expression of tachykinin NK1 receptor mRNA in dorsal root ganglia of the mouse. *Molecular Brain Research,* 35**,** 329-332.

ARDEN, N. & NEVITT, M. C. 2006. Osteoarthritis: Epidemiology. *Best Practice & Research in Clinical Rheumatology,* 20**,** 3-25.

ARENDT-NIELSEN, L., NIE, H., LAURSEN, M. B., LAURSEN, B. S., MADELEINE, P., SIMONSEN, O. H. & GRAVEN-NIELSEN, T. 2010. Sensitization in patients with painful knee osteoarthritis. *Pain,* 149**,** 573-81.

ASHRAF, S., MAPP, P. I., BURSTON, J., BENNETT, A. J., CHAPMAN, V. & WALSH, D. A. 2013. Augmented pain behavioural responses to intra-articular injection of nerve growth factor in two animal models of osteoarthritis. *Annals of the Rheumatic Diseases*.

ASHRAF, S., MAPP, P. I. & WALSH, D. A. 2011a. Contributions of angiogenesis to inflammation, joint damage, and pain in a rat model of osteoarthritis. *Arthritis Rheum,* 63**,** 2700-10.

ASHRAF, S., WIBBERLEY, H., MAPP, P. I., HILL, R., WILSON, D. & WALSH, D. A. 2011b. Increased vascular penetration and nerve growth in the meniscus: a potential source of pain in osteoarthritis. *Annals of the Rheumatic Diseases,* 70**,** 523-9.

ASHRAF, S., WIBBERLEY, H., MAPP, P. I., HILL, R., WILSON, D. & WALSH, D. A. 2011c. Increased vascular penetration and nerve growth in the meniscus: a potential source of pain in osteoarthritis. *Annals of the Rheumatic Diseases,* 70**,** 523-529.

ASO, K., IKEUCHI, M., IZUMI, M., SUGIMURA, N., KATO, T., USHIDA, T. & TANI, T. 2014. Nociceptive phenotype of dorsal root ganglia neurons innervating the subchondral bone in rat knee joints. *Eur J Pain,* 18**,** 174-81.

AVERILL, S., MCMAHON, S. B., CLARY, D. O., REICHARDT, L. F. & PRIESTLEY, J. V. 1995. Immunocytochemical localization of trkA receptors in chemically identified subgroups of adult rat sensory neurons. *Eur J Neurosci,* 7**,** 1484-94.

BALANESCU, A. R., FEIST, E., WOLFRAM, G., DAVIGNON, I., SMITH, M. D., BROWN, M. T. & WEST, C. R. 2013. Efficacy and safety of tanezumab added on to diclofenac sustained release in patients with knee or hip osteoarthritis: a double-blind, placebo-controlled, parallel-group, multicentre phase III randomised clinical trial. *Annals of the Rheumatic Diseases*.

BANDELL, M., STORY, G. M., HWANG, S. W., VISWANATH, V., EID, S. R., PETRUS, M. J., EARLEY, T. J. & PATAPOUTIAN, A. 2004a. Noxious cold ion channel TRPA1 is activated by pungent compounds and bradykinin. *Neuron,* 41**,** 849-857.

BANDELL, M., STORY, G. M., HWANG, S. W., VISWANATH, V., EID, S. R., PETRUS, M. J., EARLEY, T. J. & PATAPOUTIAN, A. 2004b. Noxious cold ion channel TRPA1 is activated by pungent compounds and bradykinin. *Neuron,* 41**,** 849-57.

BAR, K. J., SCHURIGT, U., SCHOLZE, A., SEGOND VON BANCHET, G., STOPFEL, N., BRAUER, R., HALBHUBER, K. J. & SCHAIBLE, H. G. 2004. The expression and localization of somatostatin receptors in dorsal root ganglion neurons of normal and monoarthritic rats. *Neuroscience,* 127**,** 197-206.

BARAKAT-WALTER, I., AFFOLTER, H. U. & DROZ, B. 1991. Expression of substance P and preprotachykinin mRNA by primary sensory neurons in culture:

regulation by factors present in peripheral and central target tissues. *Brain Res Mol Brain Res,* 10**,** 107-14.

BARANN, M., MOLDERINGS, G., BRUSS, M., BONISCH, H., URBAN, B. W. & GOTHERT, M. 2002. Direct inhibition by cannabinoids of human 5-HT3A receptors: probable involvement of an allosteric modulatory site. *Br J Pharmacol,* 137**,** 589-96.

BASBAUM, A. I., BAUTISTA, D. M., SCHERRER, G. & JULIUS, D. 2009. Cellular and molecular mechanisms of pain. *Cell,* 139**,** 267-84.

BASU, P. P., ALOYSIUS, M. M., SHAH, N. J. & BROWN, R. S., JR. 2014. Review article: the endocannabinoid system in liver disease, a potential therapeutic target. *Aliment Pharmacol Ther,* 39**,** 790-801.

BAUTISTA, D. M., SIEMENS, J., GLAZER, J. M., TSURUDA, P. R., BASBAUM, A. I., STUCKY, C. L., JORDT, S. E. & JULIUS, D. 2007. The menthol receptor TRPM8 is the principal detector of environmental cold. *Nature,* 448**,** 204-8.

BELLUCCI, F., MEINI, S., CUCCHI, P., CATALANI, C., NIZZARDO, A., RIVA, A., GUIDELLI, G. M., FERRATA, P., FIORAVANTI, A. & MAGGI, C. A. 2013. Synovial fluid levels of bradykinin correlate with biochemical markers for cartilage degradation and inflammation in knee osteoarthritis. *Osteoarthritis Cartilage,* 21**,** 1774-80.

BENDELE, A. M. 2001. Animal models of osteoarthritis. *J Musculoskelet Neuronal Interact,* 1**,** 363-76.

BENDELE, A. M. & HULMAN, J. F. 1988. Spontaneous Cartilage Degeneration in Guinea-Pigs. *Arthritis Rheum,* 31**,** 561-565.

BINZEN, U., GREFFRATH, W., HENNESSY, S., BAUSEN, M., SAALER-REINHARDT, S. & TREEDE, R. D. 2006. Co-expression of the voltage-gated potassium channel Kv1.4 with transient receptor potential channels (TRPV1 and TRPV2) and the cannabinoid receptor CB1 in rat dorsal root ganglion neurons. *Neuroscience,* 142**,** 527-39.

BLEAKMAN, D., COLMERS, W. F., FOURNIER, A. & MILLER, R. J. 1991. Neuropeptide-Y Inhibits Ca2+ Influx into Cultured Dorsal-Root Ganglion Neurons of the Rat Via a Y2 Receptor. *British Journal of Pharmacology,* 103**,** 1781-1789.

BONDARENKO, A., WALDECK-WEIERMAIR, M., NAGHDI, S., POTESER, M., MALLI, R. & GRAIER, W. F. 2010. GPR55-dependent and -independent ion signalling in response to lysophosphatidylinositol in endothelial cells. *Br J Pharmacol,* 161**,** 308-20.

BOUABOULA, M., BIANCHINI, L., MCKENZIE, F. R., POUYSSEGUR, J. & CASELLAS, P. 1999. Cannabinoid receptor CB1 activates the Na+/H+ exchanger NHE-1 isoform via Gi-mediated mitogen activated protein kinase signaling transduction pathways. *FEBS Lett,* 449**,** 61-5.

BOUABOULA, M., POINOT-CHAZEL, C., BOURRIE, B., CANAT, X., CALANDRA, B., RINALDI-CARMONA, M., LE FUR, G. & CASELLAS, P. 1995. Activation of mitogen-activated protein kinases by stimulation of the central cannabinoid receptor CB1. *Biochem J,* 312 (Pt 2)**,** 637-41.

BOVE, S. E., CALCATERRA, S. L., BROOKER, R. M., HUBER, C. M., GUZMAN, R. E., JUNEAU, P. L., SCHRIER, D. J. & KILGORE, K. S. 2003. Weight bearing as a measure of disease progression and efficacy of anti-inflammatory compounds in a model of monosodium iodoacetate-induced osteoarthritis. *Osteoarthritis and Cartilage,* 11**,** 821-830.

BOWLES, R. D., MATA, B. A., BELL, R. D., MWANGI, T. K., HUEBNER, J. L., KRAUS, V. B. & SETTON, L. A. 2014. In vivo luminescence imaging of NF-kappaB activity and serum cytokine levels predict pain sensitivities in a rodent model of osteoarthritis. *Arthritis Rheumatol,* 66**,** 637-46.

BREEN, C., BROWNJOHN, P. W. & ASHTON, J. C. 2012. The atypical cannabinoid O-1602 increases hind paw sensitisation in the chronic constriction injury model of neuropathic pain. *Neurosci Lett,* 508**,** 119-22.

BREIVIK, H., COLLETT, B., VENTAFRIDDA, V., COHEN, R. & GALLACHER, D. 2006. Survey of chronic pain in Europe: prevalence, impact on daily life, and treatment. *Eur J Pain,* 10**,** 287-333.

BREIVOGEL, C. S., GRIFFIN, G., DI MARZO, V. & MARTIN, B. R. 2001. Evidence for a new G protein-coupled cannabinoid receptor in mouse brain. *Mol Pharmacol,* 60**,** 155-63.

BRIDGES, D., RICE, A. S., EGERTOVA, M., ELPHICK, M. R., WINTER, J. & MICHAEL, G. J. 2003. Localisation of cannabinoid receptor 1 in rat dorsal root ganglion using in situ hybridisation and immunohistochemistry. *Neuroscience,* 119**,** 803-12.

BROWN, A. J. 2007. Novel cannabinoid receptors. *Br J Pharmacol,* 152**,** 567-75.

BRUNDTLAND, G. H. 2003. A WHO Scientific Group on the Burden of Musculoskeletal Conditions at the Start of the New Millennium met in Geneva from 13 to 15 January 2000. *Burden of Musculoskeletal Conditions at the Start of the New Millennium,* 919**,** 1-218.

BULLOCK, C. M., WOOKEY, P., BENNETT, A., MOBASHERI, A., DICKERSON, I. & KELLY, S. 2014. Increased peripheral calcitonin gene-related peptide receptor signalling drives mechanical sensitization of the joint in rat models of osteoarthritis pain. *Arthritis Rheumatol*.

BUSHNELL, M. C. 2006. Representation of pain in the brain. *In:* MCMAHON, S. B. (ed.) *Textbook of pain.* 5 ed.: Churchill Livingstone.

BUTLER, R. K. & FINN, D. P. 2009. Stress-induced analgesia. *Prog Neurobiol,* 88**,** 184-202.

CALIGNANO, A., LA RANA, G., GIUFFRIDA, A. & PIOMELLI, D. 1998. Control of pain initiation by endogenous cannabinoids. *Nature,* 394**,** 277-81.

CALIXTO, J. B., CABRINI, D. A., FERREIRA, J. & CAMPOS, M. M. 2000. Kinins in pain and inflammation. *Pain,* 87**,** 1-5.

CALVO, R. R., MEEGALLA, S. K., PARKS, D. J., PARSONS, W. H., BALLENTINE, S. K., LUBIN, M. L., SCHNEIDER, C., COLBURN, R. W., FLORES, C. M. & PLAYER, M. R. 2012. Discovery of vinylcycloalkyl-substituted benzimidazole TRPM8 antagonists effective in the treatment of cold allodynia. *Bioorganic & Medicinal Chemistry Letters,* 22**,** 1903-1907.

CANTARELLA, G., SCOLLO, M., LEMPEREUR, L., SACCANI-JOTTI, G., BASILE, F. & BERNARDINI, R. 2011. Endocannabinoids inhibit release of nerve growth factor by inflammation-activated mast cells. *Biochem Pharmacol,* 82**,** 380-8.

CAO, Y. Q., MANTYH, P. W., CARLSON, E. J., GILLESPIE, A. M., EPSTEIN, C. J. & BASBAUM, A. I. 1998. Primary afferent tachykinins are required to experience moderate to intense pain. *Nature,* 392**,** 390-4.

CARLTON, S. M. 2001. Peripheral excitatory amino acids. *Curr Opin Pharmacol,* 1**,** 52-6.

CARLTON, S. M. & COGGESHALL, R. E. 2002. Inflammation-induced up-regulation of neurokinin 1 receptors in rat glabrous skin. *Neurosci Lett,* 326**,** 29-32.

CATERINA, M. J., LEFFLER, A., MALMBERG, A. B., MARTIN, W. J., TRAFTON, J., PETERSEN-ZEITZ, K. R., KOLTZENBURG, M., BASBAUM, A. I. & JULIUS, D. 2000. Impaired nociception and pain sensation in mice lacking the capsaicin receptor. *Science,* 288**,** 306-313.

CATERINA, M. J., SCHUMACHER, M. A., TOMINAGA, M., ROSEN, T. A., LEVINE, J. D. & JULIUS, D. 1997. The capsaicin receptor: a heat-activated ion channel in the pain pathway. *Nature,* 389**,** 816-24.

CESARE, P. & MCNAUGHTON, P. 1996a. A novel heat-activated current in nociceptive neurons and its sensitization by bradykinin. *Proceedings of the National Academy of Sciences of the United States of America,* 93**,** 15435-15439.

CESARE, P. & MCNAUGHTON, P. 1996b. A novel heat-activated current in nociceptive neurons and its sensitization by bradykinin. *Proc Natl Acad Sci U S A,* 93**,** 15435-9.

CHEN, S., ZHOU, Y., LI, J., SHAN, L. Q. & FAN, Q. Y. 2012. The effect of bradykinin B2 receptor polymorphisms on the susceptibility and severity of osteoarthritis in a Chinese cohort. *J Biomed Biotechnol,* 2012**,** 597637.

CHENG, J. K. & JI, R. R. 2008. Intracellular signaling in primary sensory neurons and persistent pain. *Neurochemical Research,* 33**,** 1970-1978.

CHEUNG, P. P., GOSSEC, L. & DOUGADOS, M. 2010. What are the best markers for disease progression in osteoarthritis (OA)? *Best Practice & Research in Clinical Rheumatology,* 24**,** 81-92.

CHRISTIANSEN, C. L. & STEVENS-LAPSLEY, J. E. 2010. Weight-bearing asymmetry in relation to measures of impairment and functional mobility for people with knee osteoarthritis. *Arch Phys Med Rehabil,* 91**,** 1524-8.

CHRISTINA, A., MERLIN, N., VIJAYA, C., JAYAPRAKASH, S. & MURUGESH, N. 2004. Daily rhythm of nociception in rats. *J Circadian Rhythms,* 2**,** 2.

CHU, K. L., CHANDRAN, P., JOSHI, S. K., JARVIS, M. F., KYM, P. R. & MCGARAUGHTY, S. 2011. TRPV1-related modulation of spinal neuronal activity and behavior in a rat model of osteoarthritic pain. *Brain Res,* 1369**,** 158-66.

CIALDAI, C., GIULIANI, S., VALENTI, C., TRAMONTANA, M. & MAGGI, C. A. 2009. Effect of Intra-articular 4-(S)-amino-5-(4-{4-[2,4-dichloro-3-(2,4-dimethyl-8-quinolyloxymethyl)phenylsulfo namido]-tetrahydro-2H-4-pyranylcarbonyl} piperazino)-5-oxopentyl](trimethyl)ammonium chloride hydrochloride (MEN16132), a kinin B2 receptor antagonist, on nociceptive response in monosodium iodoacetate-induced experimental osteoarthritis in rats. *Journal of Pharmacology and Experimental Therapeutics,* 331**,** 1025-32.

COGGESHALL, R. E., HONG, K. A. P., LANGFORD, L. A., SCHAIBLE, H. G. & SCHMIDT, R. F. 1983. Discharge Characteristics of Fine Medial Articular Afferents at Rest and during Passive Movements of Inflamed Knee Joints. *Brain Res,* 272**,** 185-188.

COLBURN, R. W., LUBIN, M. L., STONE, D. J., JR., WANG, Y., LAWRENCE, D., D'ANDREA, M. R., BRANDT, M. R., LIU, Y., FLORES, C. M. & QIN, N. 2007. Attenuated cold sensitivity in TRPM8 null mice. *Neuron,* 54**,** 379-86.

COMBE, R., BRAMWELL, S. & FIELD, M. J. 2004. The monosodium iodoacetate model of osteoarthritis: a model of chronic nociceptive pain in rats? *Neurosci Lett,* 370**,** 236-40.

CONAGHAN, P. G., PORCHERET, M., KINGSBURY, S. R., GAMMON, A., SONI, A., HURLEY, M., RAYMAN, M. P., BARLOW, J., HULL, R. G., CUMMING, J., LLEWELYN, K., MOSCOGIURI, F., LYONS, J. & BIRRELL, F. 2014. Impact and therapy of osteoarthritis: the Arthritis Care OA Nation 2012 survey. *Clin Rheumatol*.

COOPER, C., ARDEN, N., JAVAID, K., JUDGE, A., PRIETO-ALHAMBRA, D., HARVEY, N., DENNISON, E. & GRP, M. B. J. R. 2011. Epidemiology and Outcome of Lower Limb Osteoarthritis and Arthroplasty. *Osteoporosis International,* 22**,** 94-94.

COX, J. J., REIMANN, F., NICHOLAS, A. K., THORNTON, G., ROBERTS, E., SPRINGELL, K., KARBANI, G., JAFRI, H., MANNAN, J., RAASHID, Y., AL-GAZALI, L., HAMAMY, H., VALENTE, E. M., GORMAN, S., WILLIAMS, R., MCHALE, D. P., WOOD, J. N., GRIBBLE, F. M. & WOODS, C. G. 2006. An SCN9A channelopathy causes congenital inability to experience pain. *Nature,* 444**,** 894-8.

CRAIG, A. D. 2003. Pain mechanisms: labeled lines versus convergence in central processing. *Annu Rev Neurosci,* 26**,** 1-30.

CRAIG, A. D., HEPPELMANN, B. & SCHAIBLE, H. G. 1988. The projection of the medial and posterior articular nerves of the cat's knee to the spinal cord. *J Comp Neurol,* 276**,** 279-88.

CRAWFORD, R. W., GIE, G. A., LING, R. S. & MURRAY, D. W. 1998. Diagnostic value of intra-articular anaesthetic in primary osteoarthritis of the hip. *Journal of Bone and Joint Surgery-British Volume,* 80**,** 279-81.

CREAMER, P., HUNT, M. & DIEPPE, P. 1996. Pain mechanisms in osteoarthritis of the knee: Effect of intraarticular anesthetic. *Journal of Rheumatology,* 23**,** 1031-1036.

CREAMER, P., LETHBRIDGE-CEJKU, M. & HOCHBERG, M. C. 1998. Where does it hurt? Pain localization in osteoarthritis of the knee. *Osteoarthritis and Cartilage,* 6**,** 318-323.

CUMMINS, T. R., AGLIECO, F., RENGANATHAN, M., HERZOG, R. I., DIB-HAJJ, S. D. & WAXMAN, S. G. 2001. Nav1.3 sodium channels: rapid repriming and slow closed-state inactivation display quantitative differences after expression in a mammalian cell line and in spinal sensory neurons. *J Neurosci,* 21**,** 5952-61.

CUMMINS, T. R., DIB-HAJJ, S. D., BLACK, J. A., AKOPIAN, A. N., WOOD, J. N. & WAXMAN, S. G. 1999. A novel persistent tetrodotoxin-resistant sodium current in SNS-null and wild-type small primary sensory neurons. *J Neurosci,* 19**,** RC43.

DADO, R. J., KATTER, J. T. & GIESLER, G. J., JR. 1994. Spinothalamic and spinohypothalamic tract neurons in the cervical enlargement of rats. II. Responses to innocuous and noxious mechanical and thermal stimuli. *J Neurophysiol,* 71**,** 981-1002.

DAVIS, J. B., GRAY, J., GUNTHORPE, M. J., HATCHER, J. P., DAVEY, P. T., OVEREND, P., HARRIES, M. H., LATCHAM, J., CLAPHAM, C., ATKINSON, K., HUGHES, S. A., RANCE, K., GRAU, E., HARPER, A. J., PUGH, P. L., ROGERS, D. C., BINGHAM, S., RANDALL, A. & SHEARDOWN, S. A. 2000. Vanilloid receptor-1 is essential for inflammatory thermal hyperalgesia. *Nature,* 405**,** 183-187.

DAVIS, K. D. & POPE, G. E. 2002. Noxious cold evokes multiple sensations with distinct time courses. *Pain,* 98**,** 179-85.

DE BIASI, S. & RUSTIONI, A. 1988. Glutamate and substance P coexist in primary afferent terminals in the superficial laminae of spinal cord. *Proc Natl Acad Sci U S A,* 85**,** 7820-4.

DE FELIPE, C. 1988. Altered nociception, analgesia and aggression in mice lacking the substance P receptor. *Nature,* 392**,** 394-397.

DE LANGE-BROKAAR, B. J. E., IOAN-FACSINAY, A., VAN OSCH, G. J. V. M., ZUURMOND, A. M., SCHOONES, J., TOES, R. E. M., HUIZINGA, T. W. J. & KLOPPENBURG, M. 2012. Synovial inflammation, immune cells and their cytokines in osteoarthritis: a review. *Osteoarthritis and Cartilage,* 20**,** 1484-1499.

DECOSTERD, I. & WOOLF, C. J. 2000. Spared nerve injury: an animal model of persistent peripheral neuropathic pain. *Pain,* 87**,** 149-158.

DEVANE, W. A., HANUS, L., BREUER, A., PERTWEE, R. G., STEVENSON, L. A., GRIFFIN, G., GIBSON, D., MANDELBAUM, A., ETINGER, A. & MECHOULAM, R. 1992. Isolation and structure of a brain constituent that binds to the cannabinoid receptor. *Science,* 258**,** 1946-9.

DHAKA, A., MURRAY, A. N., MATHUR, J., EARLEY, T. J., PETRUS, M. J. & PATAPOUTIAN, A. 2007. TRPM8 is required for cold sensation in mice. *Neuron,* 54**,** 371-378.

DI MARZO, V., BISOGNO, T., DE PETROCELLIS, L., MELCK, D., ORLANDO, P., WAGNER, J. A. & KUNOS, G. 1999. Biosynthesis and inactivation of the endocannabinoid 2-arachidonoylglycerol in circulating and tumoral macrophages. *Eur J Biochem,* 264**,** 258-67.

DI PIERO, V., JONES, A. K., IANNOTTI, F., POWELL, M., PERANI, D., LENZI, G. L. & FRACKOWIAK, R. S. 1991. Chronic pain: a PET study of the central effects of percutaneous high cervical cordotomy. *Pain,* 46**,** 9-12.

DIB-HAJJ, S. D., CUMMINS, T. R., BLACK, J. A. & WAXMAN, S. G. 2010. Sodium channels in normal and pathological pain. *Annu Rev Neurosci,* 33**,** 325-47.

DIB-HAJJ, S. D., YANG, Y., BLACK, J. A. & WAXMAN, S. G. 2013. The Na(V)1.7 sodium channel: from molecule to man. *Nat Rev Neurosci,* 14**,** 49-62.

DICKINSON, T. & FLEETWOOD-WALKER, S. M. 1999. VIP and PACAP: very important in pain? *Trends Pharmacol Sci,* 20**,** 324-9.

DINH, T. P., CARPENTER, D., LESLIE, F. M., FREUND, T. F., KATONA, I., SENSI, S. L., KATHURIA, S. & PIOMELLI, D. 2002. Brain monoglyceride lipase participating in endocannabinoid inactivation. *Proc Natl Acad Sci U S A,* 99**,** 10819-24.

DIXON, T., SHAW, M., EBRAHIM, S. & DIEPPE, P. 2004. Trends in hip and knee joint replacement: socioeconomic inequalities and projections of need. *Annals of the Rheumatic Diseases,* 63**,** 825-830.

DJOUHRI, L., FANG, X., OKUSE, K., WOOD, J. N., BERRY, C. M. & LAWSON, S. N. 2003. The TTX-resistant sodium channel Nav1.8 (SNS/PN3): expression and correlation with membrane properties in rat nociceptive primary afferent neurons. *J Physiol,* 550**,** 739-52.

DJOUHRI, L. & LAWSON, S. N. 2004. Abeta-fiber nociceptive primary afferent neurons: a review of incidence and properties in relation to other afferent A-fiber neurons in mammals. *Brain Res Brain Res Rev,* 46**,** 131-45.

DONALDSON, L. F., MCQUEEN, D. S. & SECKL, J. R. 1995. Neuropeptide gene expression and capsaicin-sensitive primary afferents: maintenance and spread of adjuvant arthritis in the rat. *J Physiol,* 486 (Pt 2)**,** 473-82.

DOSTROVSKY 2006. Ascending projection systems. *In:* MCMAHON, S. B. (ed.) *Textbook of pain.* 5 ed.: Churchill Livingstone.

DUNHAM, J. P., KELLY, S. & DONALDSON, L. F. 2008. Inflammation reduces mechanical thresholds in a population of transient receptor potential channel A1-expressing nociceptors in the rat. *Eur J Neurosci,* 27**,** 3151-60.

DYE, S. F., VAUPEL, G. L. & DYE, C. C. 1998. Conscious neurosensory mapping of the internal structures of the human knee without intraarticular anesthesia. *Am J Sports Med,* 26**,** 773-7.

EBINGER, M., SCHMIDT, R. F. & HEPPELMANN, B. 2001. Composition of the medial and posterior articular nerves of the mouse knee joint. *Somatosens Mot Res,* 18**,** 62-5.

EIJKELKAMP, N., LINLEY, J. E., TORRES, J. M., BEE, L., DICKENSON, A. H., GRINGHUIS, M., MINETT, M. S., HONG, G. S., LEE, E., OH, U., ISHIKAWA, Y., ZWARTKUIS, F. J., COX, J. J. & WOOD, J. N. 2013. A role for Piezo2 in EPAC1-dependent mechanical allodynia. *Nat Commun,* 4**,** 1682.

ELMES, S. J., WINYARD, L. A., MEDHURST, S. J., CLAYTON, N. M., WILSON, A. W., KENDALL, D. A. & CHAPMAN, V. 2005. Activation of CB1 and CB2 receptors attenuates the induction and maintenance of inflammatory pain in the rat. *Pain,* 118**,** 327-35.

ENGELI, S. 2012. Central and peripheral cannabinoid receptors as therapeutic targets in the control of food intake and body weight. *Handb Exp Pharmacol***,** 357-81.

FANG, X., DJOUHRI, L., BLACK, J. A., DIB-HAJJ, S. D., WAXMAN, S. G. & LAWSON, S. N. 2002. The presence and role of the tetrodotoxin-resistant sodium channel

Na(v)1.9 (NaN) in nociceptive primary afferent neurons. *J Neurosci,* 22**,** 7425-33.

FELSON, D. T. 2005. The sources of pain in knee osteoarthritis. *Curr Opin Rheumatol,* 17**,** 624-628.

FELSON, D. T., CHAISSON, C. E., HILL, C. L., TOTTERMAN, S. M., GALE, M. E., SKINNER, K. M., KAZIS, L. & GALE, D. R. 2001. The association of bone marrow lesions with pain in knee osteoarthritis. *Ann Intern Med,* 134**,** 541-9.

FELSON, D. T., ZHANG, Y. Q., HANNAN, M. T., NAIMARK, A., WEISSMAN, B. N., ALIABADI, P. & LEVY, D. 1995. The Incidence and Natural-History of Knee Osteoarthritis in the Elderly - the Framingham Osteoarthritis Study. *Arthritis Rheum,* 38**,** 1500-1505.

FERLAND, C. E., LAVERTY, S., BEAUDRY, F. & VACHON, P. 2011. Gait analysis and pain response of two rodent models of osteoarthritis. *Pharmacol Biochem Behav,* 97**,** 603-10.

FERNIHOUGH, J., GENTRY, C., BEVAN, S. & WINTER, J. 2005. Regulation of calcitonin gene-related peptide and TRPV1 in a rat model of osteoarthritis. *Neurosci Lett,* 388**,** 75-80.

FERNIHOUGH, J., GENTRY, C., MALCANGIO, M., FOX, A., REDISKE, J., PELLAS, T., KIDD, B., BEVAN, S. & WINTER, J. 2004. Pain related behaviour in two models of osteoarthritis in the rat knee. *Pain,* 112**,** 83-93.

FERREIRA-GOMES, J., ADAES, S., SARKANDER, J. & CASTRO-LOPES, J. M. 2010. Phenotypic Alterations of Neurons That Innervate Osteoarthritic Joints in Rats. *Arthritis and Rheumatism,* 62**,** 3677-3685.

FERTLEMAN, C. R., BAKER, M. D., PARKER, K. A., MOFFATT, S., ELMSLIE, F. V., ABRAHAMSEN, B., OSTMAN, J., KLUGBAUER, N., WOOD, J. N., GARDINER, R. M. & REES, M. 2006. SCN9A mutations in paroxysmal extreme pain disorder: allelic variants underlie distinct channel defects and phenotypes. *Neuron,* 52**,** 767-74.

FIELDS, H. L. 2006. Central nervous system mechanisms of pain modulation. *In:* MCMAHON, S. B. (ed.) *Textbook of pain.* 5 ed.: Churchill Livingstone.

FORD, L. A., ROELOFS, A. J., ANAVI-GOFFER, S., MOWAT, L., SIMPSON, D. G., IRVING, A. J., ROGERS, M. J., RAJNICEK, A. M. & ROSS, R. A. 2010. A role for L-alpha-lysophosphatidylinositol and GPR55 in the modulation of migration, orientation and polarization of human breast cancer cells. *Br J Pharmacol,* 160**,** 762-71.

FREEMAN, M. A. & WYKE, B. 1967. The innervation of the knee joint. An anatomical and histological study in the cat. *J Anat,* 101**,** 505-32.

FURUYAMA, T., SATO, M., SATO, K., ARAKI, T., INAGAKI, S., TAKAGI, H. & TOHYAMA, M. 1992. Co-expression of glycine receptor beta subunit and GABAA receptor gamma subunit mRNA in the rat dorsal root ganglion cells. *Brain Res Mol Brain Res,* 12**,** 335-8.

GALIEGUE, S., MARY, S., MARCHAND, J., DUSSOSSOY, D., CARRIERE, D., CARAYON, P., BOUABOULA, M., SHIRE, D., LE FUR, G. & CASELLAS, P. 1995. Expression of central and peripheral cannabinoid receptors in human immune tissues and leukocyte subpopulations. *Eur J Biochem,* 232**,** 54-61.

GANGADHARAN, V. & KUNER, R. 2013a. Pain hypersensitivity mechanisms at a glance. *Dis Model Mech,* 6**,** 889-95.

GANGADHARAN, V. & KUNER, R. 2013b. Pain hypersensitivity mechanisms at a glance. *Dis Model Mech,* 6**,** 889-895.

GANGADHARAN, V., SELVARAJ, D., KUREJOVA, M., NJOO, C., GRITSCH, S., SKORICOVA, D., HORSTMANN, H., OFFERMANNS, S., BROWN, A. J., KUNER, T., TAPPE-THEODOR, A. & KUNER, R. 2013. A novel biological role for the

phospholipid lysophosphatidylinositol in nociceptive sensitization via activation of diverse G-protein signalling pathways in sensory nerves in vivo. *Pain*.

GARDNER, E. & LENN, N. J. 1977. Fibers in monkey posterior articular nerves. *Anat Rec,* 187**,** 99-106.

GARNERO, P., ARONSTEIN, W. S., COHEN, S. B., CONAGHAN, P. G., CLINE, G. A., CHRISTIANSEN, C., BEARY, J. F., MEYER, J. M. & BINGHAM, C. O., 3RD 2008. Relationships between biochemical markers of bone and cartilage degradation with radiological progression in patients with knee osteoarthritis receiving risedronate: the Knee Osteoarthritis Structural Arthritis randomized clinical trial. *Osteoarthritis Cartilage,* 16**,** 660-6.

GEORGE, A., KLEINSCHNITZ, C., ZELENKA, M., BRINKHOFF, J., STOLL, G. & SOMMER, C. 2004. Wallerian degeneration after crush or chronic constriction injury of rodent sciatic nerve is associated with a depletion of endoneurial interleukin-10 protein. *Experimental Neurology,* 188**,** 187-191.

GERWIN, N., BENDELE, A. M., GLASSON, S. & CARLSON, C. S. 2010. The OARSI histopathology initiative - recommendations for histological assessments of osteoarthritis in the rat. *Osteoarthritis Cartilage,* 18 Suppl 3**,** S24-34.

GHELARDINI, C., DESAPHY, J. F., MURAGLIA, M., CORBO, F., MATUCCI, R., DIPALMA, A., BERTUCCI, C., PISTOLOZZI, M., NESI, M., NORCINI, M., FRANCHINI, C. & CAMERINO, D. C. 2010. Effects of a new potent analog of tocainide on hNav1.7 sodium channels and in vivo neuropathic pain models. *Neuroscience,* 169**,** 863-73.

GIANG, D. K. A. C., B.F. 1997. Molecular characterization of human and mouse fatty acid amide hydrolase. *Proc. Natl. Acad.,* 94**,** 2238-2242.

GOLD, M. S., LEVINE, J. D. & CORREA, A. M. 1998. Modulation of TTX-R INa by PKC and PKA and their role in PGE2-induced sensitization of rat sensory neurons in vitro. *J Neurosci,* 18**,** 10345-55.

GOMIS, A., MIRALLES, A., SCHMIDT, R. F. & BELMONTE, C. 2007. Nociceptive nerve activity in an experimental model of knee joint osteoarthritis of the guinea pig: effect of intra-articular hyaluronan application. *Pain,* 130**,** 126-36.

GREFFRATH, W., BINZEN, U., SCHWARZ, S. T., SAALER-REINHARDT, S. & TREEDE, R. D. 2003. Co-expression of heat sensitive vanilloid receptor subtypes in rat dorsal root ganglion neurons. *Neuroreport,* 14**,** 2251-5.

GRIGG, P., SCHAIBLE, H. G. & SCHMIDT, R. F. 1986. Mechanical Sensitivity of Group-Iii and Group-Iv Afferents from Posterior Articular Nerve in Normal and Inflamed Cat Knee. *J Neurophysiol,* 55**,** 635-643.

GROTLE, M., HAGEN, K. B., NATVIG, B., DAHL, F. A. & KVIEN, T. K. 2008. Obesity and osteoarthritis in knee, hip and/or hand: An epidemiological study in the general population with 10 years follow-up. *BMC Musculoskelet Disord,* 9.

GRUBB, B. D., BIRRELL, G. J., MCQUEEN, D. S. & IGGO, A. 1991. The role of PGE2 in the sensitization of mechanoreceptors in normal and inflamed ankle joints of the rat. *Exp Brain Res,* 84**,** 383-92.

GUINDON, J. & HOHMANN, A. G. 2009. The endocannabinoid system and pain. *CNS Neurol Disord Drug Targets,* 8**,** 403-21.

GULER, A. D., LEE, H., IIDA, T., SHIMIZU, I., TOMINAGA, M. & CATERINA, M. 2002. Heat-evoked activation of the ion channel, TRPV4. *J Neurosci,* 22**,** 6408-14.

GUTIERREZ, T., FARTHING, J. N., ZVONOK, A. M., MAKRIYANNIS, A. & HOHMANN, A. G. 2007. Activation of peripheral cannabinoid CB1 and CB2 receptors suppresses the maintenance of inflammatory nociception: a comparative analysis. *Br J Pharmacol,* 150**,** 153-63.

GUZMAN, R. E., EVANS, M. G., BOVE, S., MORENKO, B. & KILGORE, K. 2003. Mono-iodoacetate-induced histologic changes in subchondral bone and articular cartilage of rat femorotibial joints: an animal model of osteoarthritis. *Toxicol Pathol,* 31**,** 619-24.

GWILYM, S. E., POLLARD, T. C. B. & CARR, A. J. 2008. Understanding pain in osteoarthritis. *Journal of Bone and Joint Surgery-British Volume,* 90B**,** 280-287.

HAINS, B. C., KLEIN, J. P., SAAB, C. Y., CRANER, M. J., BLACK, J. A. & WAXMAN, S. G. 2003. Upregulation of sodium channel Nav1.3 and functional involvement in neuronal hyperexcitability associated with central neuropathic pain after spinal cord injury. *J Neurosci,* 23**,** 8881-92.

HAMTIAUX, L., HANSOULLE, L., DAUGUET, N., MUCCIOLI, G. G., GALLEZ, B. & LAMBERT, D. M. 2011. Increasing Antiproliferative Properties of Endocannabinoids in N1E-115 Neuroblastoma Cells through Inhibition of Their Metabolism. *PLoS One,* 6.

HAN, C., RUSH, A. M., DIB-HAJJ, S. D., LI, S., XU, Z., WANG, Y., TYRRELL, L., WANG, X., YANG, Y. & WAXMAN, S. G. 2006. Sporadic onset of erythermalgia: a gain-of-function mutation in Nav1.7. *Ann Neurol,* 59**,** 553-8.

HANANI, M. 2005. Satellite glial cells in sensory ganglia: from form to function. *Brain Res Brain Res Rev,* 48**,** 457-76.

HANNAN, M. T., FELSON, D. T. & PINCUS, T. 2000. Analysis of the discordance between radiographic changes and knee pain in osteoarthritis of the knee. *Journal of Rheumatology,* 27**,** 1513-7.

HANUS, L., ABU-LAFI, S., FRIDE, E., BREUER, A., VOGEL, Z., SHALEV, D. E., KUSTANOVICH, I. & MECHOULAM, R. 2001. 2-arachidonyl glyceryl ether, an endogenous agonist of the cannabinoid CB1 receptor. *Proc Natl Acad Sci U S A,* 98**,** 3662-5.

HARPER, A. A. A. L., S.N. 1985. Conduction velocity is related to morphological cell type in rat dorsal root ganglion neurons. *Journal of Physiology,* 359**,** 31-46.

HARVEY, V. L. & DICKENSON, A. H. 2009. Behavioural and electrophysiological characterisation of experimentally induced osteoarthritis and neuropathy in C57Bl/6 mice. *Mol Pain,* 5**,** 18.

HAVERSATH, M., HANKE, J., LANDGRAEBER, S., HERTEN, M., ZILKENS, C., KRAUSPE, R. & JAGER, M. 2013. The distribution of nociceptive innervation in the painful hip: a histological investigation. *Bone Joint J,* 95-B**,** 770-6.

HENDIANI, J. A., WESTLUND, K. N., LAWAND, N., GOEL, N., LISSE, J. & MCNEARNEY, T. 2003. Mechanical sensation and pain thresholds in patients with chronic arthropathies. *J Pain,* 4**,** 203-11.

HENSTRIDGE, C. M., BALENGA, N. A., FORD, L. A., ROSS, R. A., WALDHOER, M. & IRVING, A. J. 2009. The GPR55 ligand L-alpha-lysophosphatidylinositol promotes RhoA-dependent Ca2+ signaling and NFAT activation. *FASEB J,* 23**,** 183-93.

HENSTRIDGE, C. M., BALENGA, N. A. B., SCHRODER, R., KARGL, J. K., PLATZER, W., MARTINI, L., ARTHUR, S., PENMAN, J., WHISTLER, J. L., KOSTENIS, E., WALDHOER, M. & IRVING, A. J. 2010. GPR55 ligands promote receptor coupling to multiple signalling pathways. *British Journal of Pharmacology,* 160**,** 604-614.

HEPPELMANN, B., JUST, S. & PAWLAK, M. 2000. Galanin influences the mechanosensitivity of sensory endings in the rat knee joint. *European Journal of Neuroscience,* 12**,** 1567-1572.

HEPPELMANN, B. & PAWLAK, M. 1997a. Inhibitory effect of somatostatin on the mechanosensitivity of articular afferents in normal and inflamed knee joints of the rat. *Pain,* 73**,** 377-382.

HEPPELMANN, B. & PAWLAK, M. 1997b. Sensitisation of articular afferents in normal and inflamed knee joints by substance P in the rat. *Neuroscience Letters,* 223**,** 97-100.

HILDEBRAND, C., OQVIST, G., BRAX, L. & TUISKU, F. 1991. Anatomy of the rat knee joint and fibre composition of a major articular nerve. *Anat Rec,* 229**,** 545-55.

HILL, C. L., GALE, D. G., CHAISSON, C. E., SKINNER, K., KAZIS, L., GALE, M. E. & FELSON, D. T. 2001. Knee effusions, popliteal cysts, and synovial thickening: association with knee pain in osteoarthritis. *Journal of Rheumatology,* 28**,** 1330-7.

HILL, R. G. 2000. NK1 (substance P) receptor antagonists- why are they not analgesia in humans. *Trends in Pharmcological Science,* 21**,** 244-246.

HILLARD, C. J. & JARRAHIAN, A. 2003. Cellular accumulation of anandamide: consensus and controversy. *Br J Pharmacol,* 140**,** 802-8.

HODGKIN, A. L. & HUXLEY, A. F. 1952. A quantitative description of membrane current and its application to conduction and excitation in nerve. *J Physiol,* 117**,** 500-44.

HOHMANN, A. G. & HERKENHAM, M. 1999. Localization of central cannabinoid CB1 receptor messenger RNA in neuronal subpopulations of rat dorsal root ganglia: a double-label in situ hybridization study. *Neuroscience,* 90**,** 923-31.

HOLZER, P. 1998. Neurogenic vasodilatation and plasma leakage in the skin. *Gen Pharmacol,* 30**,** 5-11.

HORNER, G. & DELLON, A. L. 1994. Innervation of the human knee joint and implications for surgery. *Clin Orthop Relat Res***,** 221-6.

HOWLETT, A. C., BARTH, F., BONNER, T. I., CABRAL, G., CASELLAS, P., DEVANE, W. A., FELDER, C. C., HERKENHAM, M., MACKIE, K., MARTIN, B. R., MECHOULAM, R. & PERTWEE, R. G. 2002. International Union of Pharmacology. XXVII. Classification of cannabinoid receptors. *Pharmacol Rev,* 54**,** 161-202.

HOWLETT, A. C., BREIVOGEL, C. S., CHILDERS, S. R., DEADWYLER, S. A., HAMPSON, R. E. & PORRINO, L. J. 2004. Cannabinoid physiology and pharmacology: 30 years of progress. *Neuropharmacology,* 47 Suppl 1**,** 345-58.

HUANG, L., RAMIREZ, J. C., FRAMPTON, G. A., GOLDEN, L. E., QUINN, M. A., PAE, H. Y., HORVAT, D., LIANG, L. J. & DEMORROW, S. 2011. Anandamide exerts its antiproliferative actions on cholangiocarcinoma by activation of the GPR55 receptor. *Laboratory Investigation,* 91**,** 1007-1017.

HUCHO, T. & LEVINE, J. D. 2007. Signaling pathways in sensitization: toward a nociceptor cell biology. *Neuron,* 55**,** 365-76.

HULSE, R. P., WYNICK, D. & DONALDSON, L. F. 2011. Activation of the galanin receptor 2 in the periphery reverses nerve injury-induced allodynia. *Mol Pain,* 7**,** 26.

HUNT, S. P. & MANTYH, P. W. 2001. The molecular dynamics of pain control. *Nat Rev Neurosci,* 2**,** 83-91.

HUNTER, D. J., MCDOUGALL, J. J. & KEEFE, F. J. 2008. The symptoms of osteoarthritis and the genesis of pain. *Rheum Dis Clin North Am,* 34**,** 623-43.

HUNTER, D. J., MCDOUGALL, J. J. & KEEFE, F. J. 2009. The symptoms of osteoarthritis and the genesis of pain. *Med Clin North Am,* 93**,** 83-100, xi.

IANNONE, F., DE BARI, C., DELL'ACCIO, F., COVELLI, M., PATELLA, V., LO BIANCO, G. & LAPADULA, G. 2002. Increased expression of nerve growth factor (NGF) and high affinity NGF receptor (p140 TrkA) in human osteoarthritic chondrocytes. *Rheumatology (Oxford),* 41**,** 1413-8.

IVANAVICIUS, S. P., BALL, A. D., HEAPY, C. G., WESTWOOD, F. R., MURRAY, F. & READ, S. J. 2007. Structural pathology in a rodent model of osteoarthritis is associated with neuropathic pain: Increased expression of ATF-3 and pharmacological characterisation. *Pain,* 128**,** 272-282.

IVANAVICIUS, S. P., BLAKE, D. R., CHESSELL, I. P. & MAPP, P. I. 2004. Isolectin B4 binding neurons are not present in the rat knee joint. *Neuroscience,* 128**,** 555-60.

JANIG, W. 1996. Neurobiology of visceral afferent neurons: neuroanatomy, functions, organ regulations and sensations. *Biol Psychol,* 42**,** 29-51.

JHAVERI, M. D., SAGAR, D. R., ELMES, S. J., KENDALL, D. A. & CHAPMAN, V. 2007. Cannabinoid CB2 receptor-mediated anti-nociception in models of acute and chronic pain. *Mol Neurobiol,* 36**,** 26-35.

JIN, X. H., UYAMA, T., WANG, J., OKAMOTO, Y., TONAI, T. & UEDA, N. 2009. cDNA cloning and characterization of human and mouse Ca(2+)-independent phosphatidylethanolamine N-acyltransferases. *Biochim Biophys Acta,* 1791**,** 32-8.

JOHANEK, L. M. & SIMONE, D. A. 2004. Activation of peripheral cannabinoid receptors attenuates cutaneous hyperalgesia produced by a heat injury. *Pain,* 109**,** 432-42.

JOHANNSON, H., SJOLANDER, P. AND SOJKA, P. 1991. Receptors in the knee joint ligaments and their role in biomechanics of the joint. *CRC Critical Reviews in Biomedical Engineering,* 18**,** 341-368.

JOHNS, D. G., BEHM, D.J., WALKER, D.J., AO, Z., SHAPLAND, E.M., DANIELS, D.A., RIDDICK, M., DOWELL, STATON, P.C., GREEN, P., SHABON, U., BAO, W., AIYAR, N., YUE, T-L., BROWN, A.J., MORRISON, A.D. AND DOUGLAS, S.A. 2007. The novel endocannabinoid receptor GPR55 is activated by atypical cannabinoids but does not mediate their vasodilator effects. . *Br. J. Pharmacol.,* 152**,** 825-831.

JULIUS, D. 2013. TRP Channels and Pain. *Annual Review of Cell and Developmental Biology, Vol 29,* 29**,** 355-384.

JULIUS, D. & BASBAUM, A. I. 2001. Molecular mechanisms of nociception. *Nature,* 413**,** 203-10.

KALFF, K. M., EL MOUEDDEN, M., VAN EGMOND, J., VEENING, J., JOOSTEN, L., SCHEFFER, G. J., MEERT, T. & VISSERS, K. 2010. Pre-treatment with capsaicin in a rat osteoarthritis model reduces the symptoms of pain and bone damage induced by monosodium iodoacetate. *Eur J Pharmacol,* 641**,** 108-13.

KANAAN, S. A., POOLE, S., SAADE, N. E., JABBUR, S. & SAFIEH-GARABEDIAN, B. 1998. Interleukin-10 reduces the endotoxin-induced hyperalgesia in mice. *Journal of Neuroimmunology,* 86**,** 142-150.

KAPLAN, B. L. 2013. The role of CB1 in immune modulation by cannabinoids. *Pharmacol Ther,* 137**,** 365-74.

KAPUR, A., ZHAO, P., SHARIR, H., BAI, Y., CARON, M. G., BARAK, L. S. & ABOOD, M. E. 2009. Atypical responsiveness of the orphan receptor GPR55 to cannabinoid ligands. *J Biol Chem,* 284**,** 29817-27.

KASHIBA, H., NISHIGORI, A. & UEDA, Y. 1992. Expression of Galanin in Rat Primary Sensory Afferents after Moxibustion to the Skin. *American Journal of Chinese Medicine,* 20**,** 103-114.

KAUFMAN, G. N., ZAOUTER, C., VALTEAU, B., SIROIS, P. & MOLDOVAN, F. 2011. Nociceptive tolerance is improved by bradykinin receptor B1 antagonism and joint morphology is protected by both endothelin type A and bradykinin receptor B1 antagonism in a surgical model of osteoarthritis. *Arthritis Res Ther,* 13.

KELLGREN, J. H. & SAMUEL, E. P. 1950. The Sensitivity and Innervation of the Articular Capsule. *Journal of Bone and Joint Surgery-British Volume,* 32**,** 84-92.

KELLY, S., CHAPMAN, R. J., WOODHAMS, S., SAGAR, D. R., TURNER, J., BURSTON, J. J., BULLOCK, C., PATON, K., HUANG, J., WONG, A., MCWILLIAMS, D. F., OKINE, B. N., BARRETT, D. A., HATHWAY, G. J., WALSH, D. A. & CHAPMAN, V. 2013a. Increased function of pronociceptive TRPV1 at the level of the joint in a rat model of osteoarthritis pain. *Annals of the Rheumatic Diseases*.

KELLY, S., DOBSON, K. L. & HARRIS, J. 2013b. Spinal nociceptive reflexes are sensitized in the monosodium iodoacetate model of osteoarthritis pain in the rat. *Osteoarthritis and Cartilage,* 21**,** 1327-1335.

KELLY, S. & DONALDSON, L. F. 2008. Peripheral cannabinoid CB1 receptors inhibit evoked responses of nociceptive neurones in vivo. *Eur J Pharmacol,* 586**,** 160-3.

KELLY, S., DUNHAM, J. P., MURRAY, F., READ, S., DONALDSON, L. F. & LAWSON, S. N. 2012. Spontaneous firing in C-fibers and increased mechanical sensitivity in A-fibers of knee joint-associated mechanoreceptive primary afferent neurones during MIA-induced osteoarthritis in the rat. *Osteoarthritis Cartilage,* 20**,** 305-13.

KELLY, S., JHAVERI, M. D., SAGAR, D. R., KENDALL, D. A. & CHAPMAN, V. 2003. Activation of peripheral cannabinoid CB1 receptors inhibits mechanically evoked responses of spinal neurons in noninflamed rats and rats with hindpaw inflammation. *Eur J Neurosci,* 18**,** 2239-43.

KESSLER, F., HABELT, C., AVERBECK, B., REEH, P. W. & KRESS, M. 1999. Heat-induced release of CGRP from isolated rat skin and effects of bradykinin and the protein kinase C activator PMA. *Pain,* 83**,** 289-295.

KIDD, B. L. 2006. Osteoarthritis and joint pain. *Pain,* 123**,** 6-9.

KIDD, B. L. & URBAN, L. A. 2001. Mechanisms of inflammatory pain. *Br J Anaesth,* 87**,** 3-11.

KIM, S. E., COSTE, B., CHADHA, A., COOK, B. & PATAPOUTIAN, A. 2012. The role of Drosophila Piezo in mechanical nociception. *Nature,* 483**,** 209-12.

KIRSCHSTEIN, T., BUSSELBERG, D. & TREEDE, R. D. 1997. Coexpression of heat-evoked and capsaicin-evoked inward currents in acutely dissociated rat dorsal root ganglion neurons. *Neuroscience Letters,* 231**,** 33-36.

KLEINSCHNITZ, C., BRINKHOFF, J., ZELENKA, M., SOMMER, C. & STOLL, G. 2004. The extent of cytokine induction in peripheral nerve lesions depends on the mode of injury and NMDA receptor signaling. *Journal of Neuroimmunology,* 149**,** 77-83.

KNOWLTON, W. M., BIFOLCK-FISHER, A., BAUTISTA, D. M. & MCKEMY, D. D. 2010. TRPM8, but not TRPA1, is required for neural and behavioral responses to acute noxious cold temperatures and cold-mimetics in vivo. *Pain,* 150**,** 340-50.

KOBAYASHI, K., FUKUOKA, T., OBATA, K., YAMANAKA, H., DAI, Y., TOKUNAGA, A. & NOGUCHI, K. 2005. Distinct expression of TRPM8, TRPA1, and TRPV1 mRNAs in rat primary afferent neurons with adelta/c-fibers and colocalization with trk receptors. *J Comp Neurol,* 493**,** 596-606.

KOBAYASHI, K., YAMANAKA, H. & NOGUCHI, K. 2013. Expression of ATP receptors in the rat dorsal root ganglion and spinal cord. *Anat Sci Int,* 88**,** 10-6.

KOSEK, E. & ORDEBERG, G. 2000a. Abnormalities of somatosensory perception in patients with painful osteoarthritis normalize following successful treatment. *Eur J Pain,* 4**,** 229-38.

KOSEK, E. & ORDEBERG, G. 2000b. Lack of pressure pain modulation by heterotopic noxious conditioning stimulation in patients with painful osteoarthritis before, but not following, surgical pain relief. *Pain,* 88**,** 69-78.

KOSUWON, W., SIRICHATIWAPEE, W., WISANUYOTIN, T., JEERAVIPOOLVARN, P. & LAUPATTARAKASEM, W. 2010. Efficacy of symptomatic control of knee osteoarthritis with 0.0125% of capsaicin versus placebo. *J Med Assoc Thai,* 93**,** 1188-95.

KRAS, J. V., DONG, L. & WINKELSTEIN, B. A. 2013. The Prostaglandin E2 Receptor, EP2, Is Upregulated in the Dorsal Root Ganglion After Painful Cervical Facet Joint Injury in the Rat. *Spine,* 38**,** 217-222.

KREMEYER, B., LOPERA, F., COX, J. J., MOMIN, A., RUGIERO, F., MARSH, S., WOODS, C. G., JONES, N. G., PATERSON, K. J., FRICKER, F. R., VILLEGAS, A., ACOSTA, N., PINEDA-TRUJILLO, N. G., RAMIREZ, J. D., ZEA, J., BURLEY, M. W., BEDOYA, G., BENNETT, D. L., WOOD, J. N. & RUIZ-LINARES, A. 2010. A gain-of-function mutation in TRPA1 causes familial episodic pain syndrome. *Neuron,* 66**,** 671-80.

KRESS, M., RODL, J. & REEH, P. W. 1996. Stable analogues of cyclic AMP but not cyclic GMP sensitize unmyelinated primary afferents in rat skin to heat stimulation but not to inflammatory mediators, in vitro. *Neuroscience,* 74**,** 609-617.

KUL-PANZA, E. & BERKER, N. 2006. Pedobarographic findings in patients with knee osteoarthritis. *Am J Phys Med Rehabil,* 85**,** 228-33.

KWAN, K. Y., ALLCHORNE, A. J., VOLLRATH, M. A., CHRISTENSEN, A. P., ZHANG, D. S., WOOLF, C. J. & COREY, D. P. 2006. TRPA1 contributes to cold, mechanical, and chemical nociception but is not essential for hair-cell transduction. *Neuron,* 50**,** 277-89.

LA PORTA, C., BURA, S. A., ARACIL-FERNANDEZ, A., MANZANARES, J. & MALDONADO, R. 2013. Role of CB1 and CB2 cannabinoid receptors in the development of joint pain induced by monosodium iodoacetate. *Pain,* 154**,** 160-74.

LAI, J., GOLD, M. S., KIM, C. S., BIAN, D., OSSIPOV, M. H., HUNTER, J. C. & PORRECA, F. 2002. Inhibition of neuropathic pain by decreased expression of the tetrodotoxin-resistant sodium channel, NaV1.8. *Pain,* 95**,** 143-52.

LANE, N. E., BRANDT, K., HAWKER, G., PEEVA, E., SCHREYER, E., TSUJI, W. & HOCHBERG, M. C. 2011. OARSI-FDA initiative: defining the disease state of osteoarthritis. *Osteoarthritis Cartilage,* 19**,** 478-82.

LANE, N. E., SCHNITZER, T. J., BIRBARA, C. A., MOKHTARANI, M., SHELTON, D. L., SMITH, M. D. & BROWN, M. T. 2010. Tanezumab for the Treatment of Pain from Osteoarthritis of the Knee. *New England Journal of Medicine,* 363**,** 1521-1531.

LANGFORD, L. A. & SCHMIDT, R. F. 1983. Afferent and efferent axons in the medial and posterior articular nerves of the cat. *Anat Rec,* 206**,** 71-8.

LASSEN, N. A., INGVAR, D. H. & SKINHOJ, E. 1978. Brain function and blood flow. *Sci Am,* 239**,** 62-71.

LAUCKNER, J. E., JENSEN, J. B., CHEN, H. Y., LU, H. C., HILLE, B. & MACKIE, K. 2008. GPR55 is a cannabinoid receptor that increases intracellular calcium and inhibits M current. *Proc Natl Acad Sci U S A,* 105**,** 2699-704.

LAWSON, S. N. 2005. The Peripheral Sensory Nervous System: Dorsal Root Ganglion Neurons. *Peripheral Neuropathy.* 4 ed.

LAWSON, S. N., CREPPS, B. A. & PERL, E. R. 1997. Relationship of substance P to afferent characteristics of dorsal root ganglion neurones in guinea-pig. *J Physiol,* 505 (Pt 1)**,** 177-91.

LEE, C. J., LABRAKAKIS, C., JOSEPH, D. J. & MACDERMOTT, A. B. 2004. Functional similarities and differences of AMPA and kainate receptors expressed by cultured rat sensory neurons. *Neuroscience,* 129**,** 35-48.

LEFFLER, A., LINTE, R. M., NAU, C., REEH, P. & BABES, A. 2007. A high-threshold heat-activated channel in cultured rat dorsal root ganglion neurons resembles TRPV2 and is blocked by gadolinium. *European Journal of Neuroscience,* 26**,** 12-22.

LEWIN, G. R., RUEFF, A. & MENDELL, L. M. 1994. Peripheral and central mechanisms of NGF-induced hyperalgesia. *Eur J Neurosci,* 6**,** 1903-12.

LEWIS, T. 1938. Study of Somatic Pain. *Br Med J,* 1**,** 321-5.

LI, K., FICHNA, J., SCHICHO, R., SAUR, D., BASHASHATI, M., MACKIE, K., LI, Y., ZIMMER, A., GOKE, B., SHARKEY, K. A. & STORR, M. 2013. A role for O-1602 and G protein-coupled receptor GPR55 in the control of colonic motility in mice. *Neuropharmacology,* 71**,** 255-63.

LI, L., HASAN, R. & ZHANG, X. 2014. The basal thermal sensitivity of the TRPV1 ion channel is determined by PKCbetaII. *J Neurosci,* 34**,** 8246-58.

LI, Y., JIANG, J. M., YANG, D. H., WANG, F. L. & MAO, Z. X. 2009. [Determination of the concentrations of interleukin-18 and other cytokines in the synovial fluid in patients with osteoarthritis]. *Nan Fang Yi Ke Da Xue Xue Bao,* 29**,** 729-31.

LIGHT, A. R. 1993. *Peripheral Sensory Systems.* Philidelphia: W.B. Saunders.

LIGHT, A. R. & PERL, E. R. 1979. Reexamination of the dorsal root projection to the spinal dorsal horn including observations on the differential termination of coarse and fine fibers. *J Comp Neurol,* 186**,** 117-31.

LIGHT, A. R., TREVINO, D. L. & PERL, E. R. 1979. Morphological features of functionally defined neurons in the marginal zone and substantia gelatinosa of the spinal dorsal horn. *J Comp Neurol,* 186**,** 151-71.

LINHART, O., OBREJA, O. & KRESS, M. 2003. The inflammatory mediators serotonin, prostaglandin E2 and bradykinin evoke calcium influx in rat sensory neurons. *Neuroscience,* 118**,** 69-74.

LIU, F. Y., SUN, Y. N., WANG, F. T., LI, Q., SU, L., ZHAO, Z. F., MENG, X. L., ZHAO, H., WU, X., SUN, Q., XING, G. G. & WAN, Y. 2012. Activation of satellite glial cells in lumbar dorsal root ganglia contributes to neuropathic pain after spinal nerve ligation. *Brain Res,* 1427**,** 65-77.

LIU, H. X. A. H., T. 2002. Participation of galanin in pain processing at the spinal level. *Trends Pharmacol. Sci,* .23**,** 468.

LIU, M. & WOOD, J. N. 2011. The roles of sodium channels in nociception: implications for mechanisms of neuropathic pain. *Pain Med,* 12 Suppl 3**,** S93-9.

LIU, P., OKUN, A., REN, J. Y., GUO, R. C., OSSIPOV, M. H., XIE, J., KING, T. & PORRECA, F. 2011. Ongoing pain in the MIA model of osteoarthritis. *Neuroscience Letters,* 493**,** 72-75.

LOESER, J. D. & TREEDE, R. D. 2008. The Kyoto protocol of IASP Basic Pain Terminology. *Pain,* 137**,** 473-7.

LOHMANDER, L. S., DE VERDIER, M. G., ROLLOF, J., NILSSON, P. M. & ENGSTROM, G. 2009. Incidence of severe knee and hip osteoarthritis in relation to different measures of body mass: a population-based prospective cohort study. *Annals of the Rheumatic Diseases,* 68**,** 490-496.

LOZA, E., ABASOLO, L., JOVER, J. A., CARMONA, L. & GRP, E. S. 2008. Burden of disease across chronic diseases: A health survey that measured prevalence, function, and quality of life. *Journal of Rheumatology,* 35**,** 159-165.

MA, W., CHABOT, J. G., POWELL, K. J., JHAMANDAS, K., DICKERSON, I. M. & QUIRION, R. 2003. Localization and modulation of calcitonin gene-related peptide-

receptor component protein-immunoreactive cells in the rat central and peripheral nervous systems. *Neuroscience,* 120**,** 677-94.

MAINGRET, F., PATEL, A. J., LESAGE, F., LAZDUNSKI, M. & HONORE, E. 2000. Lysophospholipids open the two-pore domain mechano-gated K(+) channels TREK-1 and TRAAK. *J Biol Chem,* 275**,** 10128-33.

MALCANGIO, M., GETTING, S. J., GRIST, J., CUNNINGHAM, J. R., BRADBURY, E. J., CHARBEL ISSA, P., LEVER, I. J., PEZET, S. & PERRETTI, M. 2002. A novel control mechanism based on GDNF modulation of somatostatin release from sensory neurones. *FASEB J,* 16**,** 730-2.

MALFAIT, A. M. & SCHNITZER, T. J. 2013. Towards a mechanism-based approach to pain management in osteoarthritis. *Nature Reviews Rheumatology,* 9**,** 654-64.

MANTYH, P. W. 2014. The neurobiology of skeletal pain. *Eur J Neurosci,* 39**,** 508-19.

MANTYH, P. W., ROGERS, S. D., HONORE, P., ALLEN, B. J., GHILARDI, J. R., LI, J., DAUGHTERS, R. S., LAPPI, D. A., WILEY, R. G. & SIMONE, D. A. 1997. Inhibition of hyperalgesia by ablation of lamina I spinal neurons expressing the substance P receptor. *Science,* 278**,** 275-9.

MAPP, P. I., SAGAR, D. R., ASHRAF, S., BURSTON, J. J., SURI, S., CHAPMAN, V. & WALSH, D. A. 2013. Differences in structural and pain phenotypes in the sodium monoiodoacetate and meniscal transection models of osteoarthritis. *Osteoarthritis and Cartilage,* 21**,** 1336-1345.

MARINOZZI, G., FERRANTE, F., GAUDIO, E., RICCI, A. & AMENTA, F. 1991. Intrinsic innervation of the rat knee joint articular capsule and ligaments. *Acta Anat (Basel),* 141**,** 8-14.

MASON, R. M., CHAMBERS, M. G., FLANNELLY, J., GAFFEN, J. D., DUDHIA, J. & BAYLISS, M. T. 2001. The STR/ort mouse and its use as a model of osteoarthritis. *Osteoarthritis and Cartilage,* 9**,** 85-91.

MATSUDA, L. A., LOLAIT, S. J., BROWNSTEIN, M. J., YOUNG, A. C. & BONNER, T. I. 1990. Structure of a cannabinoid receptor and functional expression of the cloned cDNA. *Nature,* 346**,** 561-4.

MCCALLUM, J. B., WU, H. E., TANG, Q., KWOK, W. M. & HOGAN, Q. H. 2011. Subtype-specific reduction of voltage-gated calcium current in medium-sized dorsal root ganglion neurons after painful peripheral nerve injury. *Neuroscience,* 179**,** 244-55.

MCDOUGALL, J. J. 2006. Arthritis and pain. Neurogenic origin of joint pain. *Arthritis Res Ther,* 8**,** 220.

MCDOUGALL, J. J. 2011. Peripheral analgesia: Hitting pain where it hurts. *Biochim Biophys Acta,* 1812**,** 459-67.

MCDOUGALL, J. J., ANDRUSKI, B., SCHUELERT, N., HALLGRIMSSON, B. & MATYAS, J. R. 2009. Unravelling the relationship between age, nociception and joint destruction in naturally occurring osteoarthritis of Dunkin Hartley guinea pigs. *Pain,* 141**,** 222-232.

MCDOUGALL, J. J., HANESCH, U., PAWLAK, M. & SCHMIDT, R. F. 2001. Participation of NK1 receptors in nociceptin-induced modulation of rat knee joint mechanosensitivity. *Exp Brain Res,* 137**,** 249-53.

MCDOUGALL, J. J. & LINTON, P. 2012. Neurophysiology of arthritis pain. *Curr Pain Headache Rep,* 16**,** 485-91.

MCDOUGALL, J. J., SCHUELERT, N. & BOWYER, J. 2010. Cathepsin K inhibition reduces CTXII levels and joint pain in the guinea pig model of spontaneous osteoarthritis. *Osteoarthritis and Cartilage,* 18**,** 1355-1357.

MCDOUGALL, J. J., WATKINS, L. & LI, Z. 2006. Vasoactive intestinal peptide (VIP) is a modulator of joint pain in a rat model of osteoarthritis. *Pain,* 123**,** 98-105.

MCGLONE, F. & REILLY, D. 2010. The cutaneous sensory system. *Neurosci Biobehav Rev,* 34**,** 148-59.

MCKEMY, D. D., NEUHAUSSER, W. M. & JULIUS, D. 2002. Identification of a cold receptor reveals a general role for TRP channels in thermosensation. *Nature,* 416**,** 52-8.

MCQUEEN, D. S., IGGO, A., BIRRELL, G. J. & GRUBB, B. D. 1991. Effects of paracetamol and aspirin on neural activity of joint mechanonociceptors in adjuvant arthritis. *Br J Pharmacol,* 104**,** 178-82.

MECHOULAM, R., BRAUN, P. & GAONI, Y. 1967. A stereospecific synthesis of (-)-delta 1- and (-)-delta 1(6)-tetrahydrocannabinols. *J Am Chem Soc,* 89**,** 4552-4.

MEIR, A., GINSBURG, S., BUTKEVICH, A., KACHALSKY, S. G., KAISERMAN, I., AHDUT, R., DEMIRGOREN, S. & RAHAMIMOFF, R. 1999. Ion channels in presynaptic nerve terminals and control of transmitter release. *Physiol Rev,* 79**,** 1019-88.

MESSIER, S. P. 1994. Osteoarthritis of the knee and associated factors of age and obesity: effects on gait. *Med Sci Sports Exerc,* 26**,** 1446-52.

MEYER, R. A., DAVIS, K. D., COHEN, R. H., TREEDE, R. D. & CAMPBELL, J. N. 1991. Mechanically insensitive afferents (MIAs) in cutaneous nerves of monkey. *Brain Res,* 561**,** 252-61.

MICHAELIS, M., HABLER, H. J. & JAENIG, W. 1996. Silent afferents: a separate class of primary afferents? *Clin Exp Pharmacol Physiol,* 23**,** 99-105.

MILLAN, M. J. 2002. Descending control of pain. *Prog Neurobiol,* 66**,** 355-474.

MILNER, J. M., PATEL, A., DAVIDSON, R. K., SWINGLER, T. E., DESILETS, A., YOUNG, D. A., KELSO, E. B., DONELL, S. T., CAWSTON, T. E., CLARK, I. M., FERRELL, W. R., PLEVIN, R., LOCKHART, J. C., LEDUC, R. & ROWAN, A. D. 2010. Matriptase Is a Novel Initiator of Cartilage Matrix Degradation in Osteoarthritis. *Arthritis Rheum,* 62**,** 1955-1966.

MOGIL, J. S. 2009. Animal models of pain: progress and challenges. *Nat Rev Neurosci,* 10**,** 283-94.

MULDERRY, P. K. & LINDSAY, R. M. 1990. Rat dorsal root ganglion neurons in culture express vasoactive intestinal polypeptide (VIP) independently of nerve growth factor. *Neurosci Lett,* 108**,** 314-20.

MUNRO, S., THOMAS, K. L. & ABU-SHAAR, M. 1993. Molecular characterization of a peripheral receptor for cannabinoids. *Nature,* 365**,** 61-5.

NACKLEY, A. G., SUPLITA, R. L., 2ND & HOHMANN, A. G. 2003. A peripheral cannabinoid mechanism suppresses spinal fos protein expression and pain behavior in a rat model of inflammation. *Neuroscience,* 117**,** 659-70.

NEOGI, T., FELSON, D., NIU, J. B., NEVITT, M., LEWIS, C. E., ALIABADI, P., SACK, B., TORNER, J., BRADLEY, L. & ZHANG, Y. Q. 2009. Association between radiographic features of knee osteoarthritis and pain: results from two cohort studies. *Br Med J,* 339.

NEUGEBAUER, V., HAN, J. S., ADWANIKAR, H., FU, Y. & JI, G. 2007. Techniques for assessing knee joint pain in arthritis. *Mol Pain,* 3**,** 8.

NEUGEBAUER, V., LUCKE, T., GRUBB, B. & SCHAIBLE, H. G. 1994. The involvement of N-methyl-D-aspartate (NMDA) and non-NMDA receptors in the responsiveness of rat spinal neurons with input from the chronically inflamed ankle. *Neurosci Lett,* 170**,** 237-40.

NEUGEBAUER, V., LUCKE, T. & SCHAIBLE, H. G. 1993a. Differential effects of N-methyl-D-aspartate (NMDA) and non-NMDA receptor antagonists on the responses of rat spinal neurons with joint input. *Neurosci Lett,* 155**,** 29-32.

NEUGEBAUER, V., LUCKE, T. & SCHAIBLE, H. G. 1993b. N-methyl-D-aspartate (NMDA) and non-NMDA receptor antagonists block the hyperexcitability of dorsal

horn neurons during development of acute arthritis in rat's knee joint. *J Neurophysiol,* 70**,** 1365-77.

NEUGEBAUER, V., RUMENAPP, P. & SCHAIBLE, H. G. 1996. Calcitonin gene-related peptide is involved in the spinal processing of mechanosensory input from the rat's knee joint and in the generation and maintenance of hyperexcitability of dorsal horn neurons during development of acute inflammation. *Neuroscience,* 71**,** 1095-1109.

NEUGEBAUER, V., SCHAIBLE, H. G. & SCHMIDT, R. F. 1989. Sensitization of articular afferents to mechanical stimuli by bradykinin. *Pflugers Arch,* 415**,** 330-5.

NOEL, J., ZIMMERMANN, K., BUSSEROLLES, J., DEVAL, E., ALLOUI, A., DIOCHOT, S., GUY, N., BORSOTTO, M., REEH, P., ESCHALIER, A. & LAZDUNSKI, M. 2009. The mechano-activated K+ channels TRAAK and TREK-1 control both warm and cold perception. *EMBO J,* 28**,** 1308-18.

NOGUCHI, K., SENBA, E., MORITA, Y., SATO, M. & TOHYAMA, M. 1990. Co-Expression of Alpha-Cgrp and Beta-Cgrp Messenger-Rnas in the Rat Dorsal-Root Ganglion-Cells. *Neuroscience Letters,* 108**,** 1-5.

NUESCH, E., DIEPPE, P., REICHENBACH, S., WILLIAMS, S., IFF, S. & JUNI, P. 2011. All cause and disease specific mortality in patients with knee or hip osteoarthritis: population based cohort study. *Br Med J,* 342.

O'CONNOR, B. L. & WOODBURY, P. 1982. The primary articular nerves to the dog knee. *J Anat,* 134**,** 563-72.

OBARA, Y., UENO, S., YANAGIHATA, Y. & NAKAHATA, N. 2011. Lysophosphatidylinositol causes neurite retraction via GPR55, G13 and RhoA in PC12 cells. *PLoS One,* 6**,** e24284.

OFFERTALER, L., MO, F. M., BATKAI, S., LIU, J., BEGG, M., RAZDAN, R. K., MARTIN, B. R., BUKOSKI, R. D. & KUNOS, G. 2003. Selective ligands and cellular effectors of a G protein-coupled endothelial cannabinoid receptor. *Mol Pharmacol,* 63**,** 699-705.

OGBONNA, A. C., CLARK, A. K., GENTRY, C., HOBBS, C. & MALCANGIO, M. 2013. Pain-like behaviour and spinal changes in the monosodium iodoacetate model of osteoarthritis in C57Bl/6 mice. *Eur J Pain,* 17**,** 514-26.

OKA, S., KIMURA, S., TOSHIDA, T., OTA, R., YAMASHITA, A. & SUGIURA, T. 2010. Lysophosphatidylinositol induces rapid phosphorylation of p38 mitogen-activated protein kinase and activating transcription factor 2 in HEK293 cells expressing GPR55 and IM-9 lymphoblastoid cells. *Journal of Biochemistry,* 147**,** 671-678.

OKA, S., NAKAJIMA, K., YAMASHITA, A., KISHIMOTO, S. & SUGIURA, T. 2007. Identification of GPR55 as a lysophosphatidylinositol receptor. *Biochemical and Biophysical Research Communications,* 362**,** 928-934.

OKA, S., TOSHIDA, T., MARUYAMA, K., NAKAJIMA, K., YAMASHITA, A. AND SUGIURA, T. 2009. 2-Arachidonoyl-sn-glycerol-3-phosphoinositol: A possible natural ligand for GPR55. *J. Biochem.,* 145**,** 13-20.

OKUN, A., LIU, P., DAVIS, P., REN, J., REMENIUK, B., BRION, T., OSSIPOV, M. H., XIE, J., DUSSOR, G. O., KING, T. & PORRECA, F. 2012. Afferent drive elicits ongoing pain in a model of advanced osteoarthritis. *Pain,* 153**,** 924-33.

ORITA, S., ISHIKAWA, T., MIYAGI, M., OCHIAI, N., INOUE, G., EGUCHI, Y., KAMODA, H., ARAI, G., TOYONE, T., AOKI, Y., KUBO, T., TAKAHASHI, K. & OHTORI, S. 2011. Pain-related sensory innervation in monoiodoacetate-induced osteoarthritis in rat knees that gradually develops neuronal injury in addition to inflammatory pain. *BMC Musculoskelet Disord,* 12**,** 134.

OSHITA, K., INOUE, A., TANG, H. B., NAKATA, Y., KAWAMOTO, M. & YUGE, O. 2005. CB1 cannabinoid receptor stimulation modulates transient receptor

potential vanilloid receptor 1 activities in calcium influx and substance P release in cultured rat dorsal root ganglion cells. *Journal of Pharmacological Sciences,* 97**,** 377-385.

PATRICK HARTY, T. & WAXMAN, S. G. 2007. Inactivation properties of sodium channel Nav1.8 maintain action potential amplitude in small DRG neurons in the context of depolarization. *Mol Pain,* 3**,** 12.

PELLETIER, J. P., MARTEL-PELLETIER, J. & ABRAMSON, S. B. 2001. Osteoarthritis, an inflammatory disease: potential implication for the selection of new therapeutic targets. *Arthritis Rheum,* 44**,** 1237-47.

PEREIRA, D., PELETEIRO, B., ARAUJO, J., BRANCO, J., SANTOS, R. A. & RAMOS, E. 2011. The effect of osteoarthritis definition on prevalence and incidence estimates: a systematic review. *Osteoarthritis and Cartilage,* 19**,** 1270-1285.

PEREZ-GOMEZ, E., ANDRADAS, C., FLORES, J. M., QUINTANILLA, M., PARAMIO, J. M., GUZMAN, M. & SANCHEZ, C. 2013. The orphan receptor GPR55 drives skin carcinogenesis and is upregulated in human squamous cell carcinomas. *Oncogene,* 32**,** 2534-2542.

PERTWEE, R. G. 1997. Pharmacology of cannabinoid CB1 and CB2 receptors. *Pharmacol Ther,* 74**,** 129-80.

PERTWEE, R. G. 2001. Cannabinoid Receptors and Pain.

PETITET, F., DONLAN, M. & MICHEL, A. 2006. GPR55 as a new cannabinoid receptor: Still a long way to prove it. *Chemical Biology & Drug Design,* 67**,** 252-253.

PETTERSSON, L. M., SUNDLER, F. & DANIELSEN, N. 2002. Expression of orphanin FQ/nociceptin and its receptor in rat peripheral ganglia and spinal cord. *Brain Res,* 945**,** 266-75.

PIETR, M., KOZELA, E., LEVY, R., RIMMERMAN, N., LIN, Y. H., STELLA, N., VOGEL, Z. & JUKNAT, A. 2009. Differential changes in GPR55 during microglial cell activation. *FEBS Lett,* 583**,** 2071-6.

PINEIRO, R., MAFFUCCI, T. & FALASCA, M. 2011. The putative cannabinoid receptor GPR55 defines a novel autocrine loop in cancer cell proliferation. *Oncogene,* 30**,** 142-152.

PIOMELLI, D. 2001. The ligand that came from within. *Trends Pharmacol Sci,* 22**,** 17-9.

POMONIS, J. D., BOULET, J. M., GOTTSHALL, S. L., PHILLIPS, S., SELLERS, R., BUNTON, T. & WALKER, K. 2005a. Development and pharmacological characterization of a rat model of osteoarthritis pain. *Pain,* 114**,** 339-46.

POMONIS, J. D., BOULET, J. M., GOTTSHALL, S. L., PHILLIPS, S., SELLERS, R., BUNTON, T. & WALKER, K. 2005b. Development and pharmacological characterization of a rat model of osteoarthritis pain. *Pain,* 114**,** 339-346.

POTENZIERI, C., BRINK, T. S., PACHARINSAK, C. & SIMONE, D. A. 2008. Cannabinoid modulation of cutaneous Adelta nociceptors during inflammation. *J Neurophysiol,* 100**,** 2794-806.

PRITZKER, K. P. 1994. Animal models for osteoarthritis: processes, problems and prospects. *Annals of the Rheumatic Diseases,* 53**,** 406-20.

PROSKE, U., SCHAIBLE, H. G. & SCHMIDT, R. F. 1988. Joint receptors and kinaesthesia. *Exp Brain Res,* 72**,** 219-24.

PULICHINO, A. M., ROWLAND, S., WU, T., CLARK, P., XU, D., MATHIEU, M. C., RIENDEAU, D. & AUDOLY, L. P. 2006. Prostacyclin antagonism reduces pain and inflammation in rodent models of hyperalgesia and chronic arthritis. *Journal of Pharmacology and Experimental Therapeutics,* 319**,** 1043-50.

PUTTFARCKEN, P. S., HAN, P., JOSHI, S. K., NEELANDS, T. R., GAUVIN, D. M., BAKER, S. J., LEWIS, L. G., BIANCHI, B. R., MIKUSA, J. P., KOENIG, J. R., PERNER, R. J., KORT, M. E., HONORE, P., FALTYNEK, C. R., KYM, P. R. & REILLY, R. M. 2010. A-995662 [(R)-8-(4-methyl-5-(4-(trifluoromethyl)phenyl)oxazol-2-ylamino)-

1,2,3,4-tetrahydr onaphthalen-2-ol], a novel, selective TRPV1 receptor antagonist, reduces spinal release of glutamate and CGRP in a rat knee joint pain model. *Pain,* 150**,** 319-26.

QUARTILHO, A., MATA, H. P., IBRAHIM, M. M., VANDERAH, T. W., PORRECA, F., MAKRIYANNIS, A. & MALAN, T. P., JR. 2003. Inhibition of inflammatory hyperalgesia by activation of peripheral CB2 cannabinoid receptors. *Anesthesiology,* 99**,** 955-60.

QUICK, K., ZHAO, J., EIJKELKAMP, N., LINLEY, J. E., RUGIERO, F., COX, J. J., RAOUF, R., GRINGHUIS, M., SEXTON, J. E., ABRAMOWITZ, J., TAYLOR, R., FORGE, A., ASHMORE, J., KIRKWOOD, N., KROS, C. J., RICHARDSON, G. P., FREICHEL, M., FLOCKERZI, V., BIRNBAUMER, L. & WOOD, J. N. 2012. TRPC3 and TRPC6 are essential for normal mechanotransduction in subsets of sensory neurons and cochlear hair cells. *Open Biol,* 2**,** 120068.

REID, G. & FLONTA, M. L. 2001. Physiology - Cold current in thermoreceptive neurons. *Nature,* 413**,** 480-480.

REMADEVI, R. & SZALLISI, A. 2008. Adlea (ALGRX-4975), an injectable capsaicin (TRPV1 receptor agonist) formulation for longlasting pain relief. *IDrugs,* 11**,** 120-32.

REXED, B. 1952. The cytoarchitectonic organization of the spinal cord in the cat. *J Comp Neurol,* 96**,** 414-95.

RICHARDSON, D., PEARSON, R. G., KURIAN, N., LATIF, M. L., GARLE, M. J., BARRETT, D. A., KENDALL, D. A., SCAMMELL, B. E., REEVE, A. J. & CHAPMAN, V. 2008. Characterisation of the cannabinoid receptor system in synovial tissue and fluid in patients with osteoarthritis and rheumatoid arthritis. *Arthritis Res Ther,* 10.

RICHARDSON, J. D., KILO, S. & HARGREAVES, K. M. 1998. Cannabinoids reduce hyperalgesia and inflammation via interaction with peripheral CB1 receptors. *Pain,* 75**,** 111-9.

RICHARDSON, J. D. & VASKO, M. R. 2002. Cellular mechanisms of neurogenic inflammation. *J Pharmacol Exp Ther,* 302**,** 839-45.

RICHTER, F., NATURA, G., EBBINGHAUS, M., VON BANCHET, G. S., HENSELLEK, S., KONIG, C., BRAUER, R. & SCHAIBLE, H. G. 2012. Interleukin-17 Sensitizes Joint Nociceptors to Mechanical Stimuli and Contributes to Arthritic Pain Through Neuronal Interleukin-17 Receptors in Rodents. *Arthritis Rheum,* 64**,** 4125-4134.

ROMERO, A., GONZALEZ-CUELLO, A., LAORDEN, M. L., CAMPILLO, A., VASCONCELOS, N., ROMERO-ALEJO, E. & PUIG, M. M. 2012. Effects of surgery and/or remifentanil administration on the expression of pERK1/2, c-Fos and dynorphin in the dorsal root ganglia in mice. *Naunyn-Schmiedebergs Archives of Pharmacology,* 385**,** 397-409.

ROSS, H. R., GILMORE, A. J. & CONNOR, M. 2009. Inhibition of human recombinant T-type calcium channels by the endocannabinoid N-arachidonoyl dopamine. *Br J Pharmacol,* 156**,** 740-50.

ROSS, R. A. 2009. The enigmatic pharmacology of GPR55. *Trends Pharmacol Sci,* 30**,** 156-63.

ROSS, R. A., COUTTS, A. A., MCFARLANE, S. M., ANAVI-GOFFER, S., IRVING, A. J., PERTWEE, R. G., MACEWAN, D. J. & SCOTT, R. H. 2001. Actions of cannabinoid receptor ligands on rat cultured sensory neurones: implications for antinociception. *Neuropharmacology,* 40**,** 221-32.

RUSSELL, F. A., SCHUELERT, N., VELDHOEN, V. E., HOLLENBERG, M. D. & MCDOUGALL, J. J. 2012. Activation of PAR(2) receptors sensitizes primary

afferents and causes leukocyte rolling and adherence in the rat knee joint. *Br J Pharmacol,* 167**,** 1665-78.

RYBERG, E., LARSSON, N., SJOGREN, S., HJORTH, S., HERMANSSON, N. O., LEONOVA, J., ELEBRING, T., NILSSON, K., DRMOTA, T. & GREASLEY, P. J. 2007. The orphan receptor GPR55 is a novel cannabinoid receptor. *Br J Pharmacol,* 152**,** 1092-101.

SAGAR, D. R., ASHRAF, S., XU, L., BURSTON, J. J., MENHINICK, M. R., POULTER, C. L., BENNETT, A. J., WALSH, D. A. & CHAPMAN, V. 2013. Osteoprotegerin reduces the development of pain behaviour and joint pathology in a model of osteoarthritis. *Annals of the Rheumatic Diseases*.

SAGAR, D. R., BURSTON, J. J., HATHWAY, G. J., WOODHAMS, S. G., PEARSON, R. G., BENNETT, A. J., KENDALL, D. A., SCAMMELL, B. E. & CHAPMAN, V. 2011. The contribution of spinal glial cells to chronic pain behaviour in the monosodium iodoacetate model of osteoarthritic pain. *Mol Pain,* 7**,** 88.

SAGAR, D. R., KELLY, S., MILLNS, P. J., O'SHAUGHNESSEY, C. T., KENDALL, D. A. & CHAPMAN, V. 2005. Inhibitory effects of CB1 and CB2 receptor agonists on responses of DRG neurons and dorsal horn neurons in neuropathic rats. *Eur J Neurosci,* 22**,** 371-9.

SAGAR, D. R., STANIASZEK, L. E., OKINE, B. N., WOODHAMS, S., NORRIS, L. M., PEARSON, R. G., GARLE, M. J., ALEXANDER, S. P., BENNETT, A. J., BARRETT, D. A., KENDALL, D. A., SCAMMELL, B. E. & CHAPMAN, V. 2010. Tonic modulation of spinal hyperexcitability by the endocannabinoid receptor system in a rat model of osteoarthritis pain. *Arthritis Rheum,* 62**,** 3666-76.

SALO, P. T. & THERIAULT, E. 1997. Number, distribution and neuropeptide content of rat knee joint afferents. *J Anat,* 190 (Pt 4)**,** 515-22.

SALO, P. T., THERIAULT, E. & WILEY, R. G. 1997. Selective ablation of rat knee joint innervation with injected immunotoxin: a potential new model for the study of neuropathic arthritis. *J Orthop Res,* 15**,** 622-8.

SANDELL, L. J. & AIGNER, T. 2001. Articular cartilage and changes in arthritis. An introduction: cell biology of osteoarthritis. *Arthritis Res,* 3**,** 107-13.

SATO, A. & SCHMIDT, R. F. 1973. Somatosympathetic reflexes: afferent fibers, central pathways, discharge characteristics. *Physiol Rev,* 53**,** 916-47.

SATO, K., KIYAMA, H., PARK, H. T. & TOHYAMA, M. 1993. AMPA, KA and NMDA receptors are expressed in the rat DRG neurones. *Neuroreport,* 4**,** 1263-5.

SAWZDARGO, M., NGUYEN, T., LEE, D. K., LYNCH, K. R., CHENG, R., HENG, H. H., GEORGE, S. R. & O'DOWD, B. F. 1999. Identification and cloning of three novel human G protein-coupled receptor genes GPR52, PsiGPR53 and GPR55: GPR55 is extensively expressed in human brain. *Brain Res Mol Brain Res,* 64**,** 193-8.

SAXLER, G., LOER, F., SKUMAVC, M., PFORTNER, J. & HANESCH, U. 2007. Localization of SP- and CGRP-immunopositive nerve fibers in the hip joint of patients with painful osteoarthritis and of patients with painless failed total hip arthroplasties. *European Journal of Pain,* 11**,** 67-74.

SCHAIBLE, H. G., EBERSBERGER, A. & VON BANCHET, G. S. 2002. Mechanisms of pain in arthritis. *Ann N Y Acad Sci,* 966**,** 343-54.

SCHAIBLE, H. G. & GRUBB, B. D. 1993. Afferent and spinal mechanisms of joint pain. *Pain,* 55**,** 5-54.

SCHAIBLE, H. G., RICHTER, F., EBERSBERGER, A., BOETTGER, M. K., VANEGAS, H., NATURA, G., VAZQUEZ, E. & SEGOND VON BANCHET, G. 2009. Joint pain. *Exp Brain Res,* 196**,** 153-62.

SCHAIBLE, H. G., SCHMELZ, M. & TEGEDER, I. 2006. Pathophysiology and treatment of pain in joint disease. *Adv Drug Deliv Rev,* 58**,** 323-42.

SCHAIBLE, H. G. & SCHMIDT, R. F. 1983a. Activation of groups III and IV sensory units in medial articular nerve by local mechanical stimulation of knee joint. *J Neurophysiol,* 49**,** 35-44.

SCHAIBLE, H. G. & SCHMIDT, R. F. 1983b. Responses of fine medial articular nerve afferents to passive movements of knee joints. *J Neurophysiol,* 49**,** 1118-26.

SCHAIBLE, H. G. & SCHMIDT, R. F. 1985. Effects of an experimental arthritis on the sensory properties of fine articular afferent units. *J Neurophysiol,* 54**,** 1109-22.

SCHAIBLE, H. G. & SCHMIDT, R. F. 1986. Discharge characteristics of receptors with fine afferents from normal and inflamed joints: influence of analgesics and prostaglandins. *Agents Actions Suppl,* 19**,** 99-117.

SCHAIBLE, H. G. & SCHMIDT, R. F. 1988a. Excitation and sensitization of fine articular afferents from cat's knee joint by prostaglandin E2. *J Physiol,* 403**,** 91-104.

SCHAIBLE, H. G. & SCHMIDT, R. F. 1988b. Time course of mechanosensitivity changes in articular afferents during a developing experimental arthritis. *J Neurophysiol,* 60**,** 2180-95.

SCHAIBLE, H. G., SCHMIDT, R. F. & WILLIS, W. D. 1987. Convergent inputs from articular, cutaneous and muscle receptors onto ascending tract cells in the cat spinal cord. *Exp Brain Res,* 66**,** 479-88.

SCHEPELMANN, K., MESSLINGER, K., SCHAIBLE, H. G. & SCHMIDT, R. F. 1992. Inflammatory mediators and nociception in the joint: excitation and sensitization of slowly conducting afferent fibers of cat's knee by prostaglandin I2. *Neuroscience,* 50**,** 237-47.

SCHILTZ, C., LIOTE, F., PRUDHOMMEAUX, F., MEUNIER, A., CHAMPY, R., CALLEBERT, J. & BARDIN, T. 2002. Monosodium urate monohydrate crystal-induced inflammation in vivo - Quantitative histomorphometric analysis of cellular events. *Arthritis Rheum,* 46**,** 1643-1650.

SCHMIDT, R. F. 1996. The articular polymodal nociceptor in health and disease. *Prog Brain Res,* 113**,** 53-81.

SCHUELERT, N., JOHNSON, M. P., OSKINS, J. L., JASSAL, K., CHAMBERS, M. G. & MCDOUGALL, J. J. 2011. Local application of the endocannabinoid hydrolysis inhibitor URB597 reduces nociception in spontaneous and chemically induced models of osteoarthritis. *Pain,* 152**,** 975-81.

SCHUELERT, N. & MCDOUGALL, J. J. 2006a. Electrophysiological evidence that the vasoactive intestinal peptide receptor antagonist VIP6-28 reduces nociception in an animal model of osteoarthritis. *Osteoarthritis Cartilage,* 14**,** 1155-62.

SCHUELERT, N. & MCDOUGALL, J. J. 2006b. Electrophysiological evidence that the vasoactive intestinal peptide receptor antagonist VIP6-28 reduces nociception in an animal model of osteoarthritis. *Osteoarthritis and Cartilage,* 14**,** 1155-1162.

SCHUELERT, N. & MCDOUGALL, J. J. 2008. Cannabinoid-mediated antinociception is enhanced in rat osteoarthritic knees. *Arthritis Rheum,* 58**,** 145-153.

SCHUELERT, N. & MCDOUGALL, J. J. 2009. Grading of monosodium iodoacetate-induced osteoarthritis reveals a concentration-dependent sensitization of nociceptors in the knee joint of the rat. *Neurosci Lett,* 465**,** 184-8.

SCHUELERT, N. & MCDOUGALL, J. J. 2011. The abnormal cannabidiol analogue O-1602 reduces nociception in a rat model of acute arthritis via the putative cannabinoid receptor GPR55. *Neurosci Lett,* 500**,** 72-6.

SCHUELERT, N. & MCDOUGALL, J. J. 2012. Involvement of Nav 1.8 sodium ion channels in the transduction of mechanical pain in a rodent model of osteoarthritis. *Arthritis Res Ther,* 14**,** R5.

SCHUELERT, N., ZHANG, C., MOGG, A. J., BROAD, L. M., HEPBURN, D. L., NISENBAUM, E. S., JOHNSON, M. P. & MCDOUGALL, J. J. 2010. Paradoxical effects of the cannabinoid CB2 receptor agonist GW405833 on rat osteoarthritic knee joint pain. *Osteoarthritis Cartilage,* 18**,** 1536-43.

SCOTT, D. 2006. Osteoarthritis of the hip. *Clin Evid (Online),* 2006.

SEABROOK, G. R., BOWERY, B. J., HEAVENS, R., BROWN, N., FORD, H., SIRINATHSINGHI, D. J. S., BORKOWSKI, J. A., HESS, J. F., STRADER, C. D. & HILL, R. G. 1997. Expression of B-1 and B-2 bradykinin receptor mRNA and their functional roles in sympathetic ganglia and sensory dorsal root ganglia neurones from wild-type and B-2 receptor knockout mice. *Neuropharmacology,* 36**,** 1009-1017.

SEGOND VON BANCHET, G., PETERSEN, M. & HEPPELMANN, B. 1996. Bradykinin receptors in cultured rat dorsal root ganglion cells: influence of length of time in culture. *Neuroscience,* 75**,** 1211-8.

SHARIR, H. & ABOOD, M. E. 2010. Pharmacological characterization of GPR55, a putative cannabinoid receptor. *Pharmacol Ther,* 126**,** 301-13.

SHARIR, H., CONSOLE-BRAM, L., MUNDY, C., POPOFF, S. N., KAPUR, A. & ABOOD, M. E. 2012. The endocannabinoids anandamide and virodhamine modulate the activity of the candidate cannabinoid receptor GPR55. *J Neuroimmune Pharmacol,* 7**,** 856-65.

SHARMA, L., KAPOOR, D. & ISSA, S. 2006. Epidemiology of osteoarthritis: an update. *Curr Opin Rheumatol,* 18**,** 147-156.

SHARMA, L., SONG, J., FELSON, D. T., CAHUE, S., SHAMIYEH, E. & DUNLOP, D. D. 2001. The role of knee alignment in disease progression and functional decline in knee osteoarthritis. *Jama-Journal of the American Medical Association,* 286**,** 188-195.

SKOGLUND, S. 1956. Anatomical and physiological studies of knee joint innervation in the cat. *Acta Physiol Scand Suppl,* 36**,** 1-101.

SLUKA, K. A. & WESTLUND, K. N. 1993. Behavioral and immunohistochemical changes in an experimental arthritis model in rats. *Pain,* 55**,** 367-77.

SMITH, G. D., GUNTHORPE, J., KELSELL, R. E., HAYES, P. D., REILLY, P., FACER, P., WRIGHT, J. E., JERMAN, J. C., WALHIN, J. P., OOI, L., EGERTON, J., CHARLES, K. J., SMART, D., RANDALL, A. D., ANAND, P. & DAVIS, J. B. 2002. TRPV3 is a temperature-sensitive vanilloid receptor-like protein. *Nature,* 418**,** 186-190.

SNIJDELAAR, D. G., DIRKSEN, R., SLAPPENDEL, R. & CRUL, B. J. 2000. Substance P. *Eur J Pain,* 4**,** 121-35.

SOUTHALL, M. D. & VASKO, M. R. 2001. Prostaglandin receptor subtypes, EP3C and EP4, mediate the prostaglandin E2-induced cAMP production and sensitization of sensory neurons. *J Biol Chem,* 276**,** 16083-91.

SPIERINGS, E. L., FIDELHOLTZ, J., WOLFRAM, G., SMITH, M. D., BROWN, M. T. & WEST, C. R. 2013. A phase III placebo- and oxycodone-controlled study of tanezumab in adults with osteoarthritis pain of the hip or knee. *Pain,* 154**,** 1603-12.

STATON, P. C., HATCHER, J. P., WALKER, D. J., MORRISON, A. D., SHAPLAND, E. M., HUGHES, J. P., CHONG, E., MANDER, P. K., GREEN, P. J., BILLINTON, A., FULLEYLOVE, M., LANCASTER, H. C., SMITH, J. C., BAILEY, L. T., WISE, A., BROWN, A. J., RICHARDSON, J. C. & CHESSELL, I. P. 2008. The putative cannabinoid receptor GPR55 plays a role in mechanical hyperalgesia associated with inflammatory and neuropathic pain. *Pain,* 139**,** 225-36.

STOYANOVA, I., DANDOV, A., LAZAROV, N. & CHOUCHKOV, C. 1998. GABA- and glutamate-immunoreactivity in sensory ganglia of cat: a quantitative analysis. *Arch Physiol Biochem,* 106**,** 362-9.

STRICKLAND, I. T., MARTINDALE, J. C., WOODHAMS, P. L., REEVE, A. J., CHESSELL, I. P. & MCQUEEN, D. S. 2008. Changes in the expression of NaV1.7, NaV1.8 and NaV1.9 in a distinct population of dorsal root ganglia innervating the rat knee joint in a model of chronic inflammatory joint pain. *Eur J Pain,* 12**,** 564-72.

SUOKAS, A. K., WALSH, D. A., MCWILLIAMS, D. F., CONDON, L., MORETON, B., WYLDE, V., ARENDT-NIELSEN, L. & ZHANG, W. 2012. Quantitative sensory testing in painful osteoarthritis: a systematic review and meta-analysis. *Osteoarthritis Cartilage,* 20**,** 1075-85.

SURI, S., GILL, S. E., DE CAMIN, S. M., WILSON, D., MCWILLIAMS, D. F. & WALSH, D. A. 2007. Neurovascular invasion at the osteochondral junction and in osteophytes in osteoarthritis. *Annals of the Rheumatic Diseases,* 66**,** 1423-1428.

TABUCHI, K., SUZUKI, M., MIZUNO, A. & HARA, A. 2005. Hearing impairment in TRPV4 knockout mice. *Neurosci Lett,* 382**,** 304-8.

TAIWO, Y. O., BJERKNES, L. K., GOETZL, E. J. & LEVINE, J. D. 1989. Mediation of Primary Afferent Peripheral Hyperalgesia by the Camp 2nd Messenger System. *Neuroscience,* 32**,** 577-580.

TAIWO, Y. O. & LEVINE, J. D. 1991. Further Confirmation of the Role of Adenyl-Cyclase and of Camp-Dependent Protein-Kinase in Primary Afferent Hyperalgesia. *Neuroscience,* 44**,** 131-135.

TALLEY, E. M., SOLORZANO, G., LEI, Q. B., KIM, D. & BAYLISS, D. A. 2001. CNS distribution of members of the two-pore-domain (KCNK) potassium channel family. *Journal of Neuroscience,* 21**,** 7491-7505.

TAMURA, R., NEMOTO, T., MARUTA, T., ONIZUKA, S., YANAGITA, T., WADA, A., MURAKAMI, M. & TSUNEYOSHI, I. 2014. Up-regulation of NaV1.7 sodium channels expression by tumor necrosis factor-alpha in cultured bovine adrenal chromaffin cells and rat dorsal root ganglion neurons. *Anesth Analg,* 118**,** 318-24.

THAKUR, M., RAHMAN, W., HOBBS, C., DICKENSON, A. H. & BENNETT, D. L. 2012. Characterisation of a peripheral neuropathic component of the rat monoiodoacetate model of osteoarthritis. *PLoS One,* 7**,** e33730.

TINDELL, A. G., KELSO, E. B., FERRELL, W. R., LOCKHART, J. C., WALSH, D. A., DUNNING, L. & MCINNES, I. B. 2012. Correlation of protease-activated receptor-2 expression and synovitis in rheumatoid and osteoarthritis. *Rheumatology International,* 32**,** 3077-86.

TODD, A. J. 2002. Anatomy of primary afferents and projection neurones in the rat spinal dorsal horn with particular emphasis on substance P and the neurokinin 1 receptor. *Exp Physiol,* 87**,** 245-9.

TODD, A. J. 2010. Neuronal circuitry for pain processing in the dorsal horn. *Nat Rev Neurosci,* 11**,** 823-36.

TOMINAGA, M., CATERINA, M. J., MALMBERG, A. B., ROSEN, T. A., GILBERT, H., SKINNER, K., RAUMANN, B. E., BASBAUM, A. I. & JULIUS, D. 1998. The cloned capsaicin receptor integrates multiple pain-producing stimuli. *Neuron,* 21**,** 531-543.

TRACEY, I. & MANTYH, P. W. 2007. The cerebral signature for pain perception and its modulation. *Neuron,* 55**,** 377-91.

TREEDE, R. D., MEYER, R. A. & CAMPBELL, J. N. 1998. Myelinated mechanically insensitive afferents from monkey hairy skin: heat-response properties. *J Neurophysiol,* 80**,** 1082-93.

TRUMBLE, T. N., BILLINGHURST, C. & MCILWRAITH, W. 2004. Correlation of prostaglandin E-2 concentrations in synovial fluid with ground reaction forces and clinical variables for pain or inflammation in dogs with

osteoarthritis induced by transection of the cranial cruciate ligament. *American Journal of Veterinary Research,* 65**,** 1269-1275.

VALDES, A. M., DE WILDE, G., DOHERTY, S. A., LORIES, R. J., VAUGHN, F. L., LASLETT, L. L., MACIEWICZ, R. A., SONI, A., HART, D. J., ZHANG, W., MUIR, K. R., DENNISON, E. M., WHEELER, M., LEAVERTON, P., COOPER, C., SPECTOR, T. D., CICUTTINI, F. M., CHAPMAN, V., JONES, G., ARDEN, N. K. & DOHERTY, M. 2011. The Ile585Val TRPV1 variant is involved in risk of painful knee osteoarthritis. *Annals of the Rheumatic Diseases,* 70**,** 1556-61.

VALDES, A. M. & SPECTOR, T. D. 2010. The clinical relevance of genetic susceptibility to osteoarthritis. *Best Practice & Research in Clinical Rheumatology,* 24**,** 3-14.

VALLBO, A., OLAUSSON, H., WESSBERG, J. & NORRSELL, U. 1993. A system of unmyelinated afferents for innocuous mechanoreception in the human skin. *Brain Res,* 628**,** 301-4.

VINCENT, T. L., WILLIAMS, R. O., MACIEWICZ, R., SILMAN, A., GARSIDE, P. & WORKING, A. R. U. A. M. 2012. Mapping pathogenesis of arthritis through small animal models. *Rheumatology,* 51**,** 1931-1941.

VONSY, J. L., GHANDEHARI, J. & DICKENSON, A. H. 2009. Differential analgesic effects of morphine and gabapentin on behavioural measures of pain and disability in a model of osteoarthritis pain in rats. *Eur J Pain,* 13**,** 786-93.

WALDECK-WEIERMAIR, M., ZORATTI, C., OSIBOW, K., BALENGA, N., GOESSNITZER, E., WALDHOER, M., MALLI, R. & GRAIER, W. F. 2008. Integrin clustering enables anandamide-induced Ca2+ signaling in endothelial cells via GPR55 by protection against CB1-receptor-triggered repression. *J Cell Sci,* 121**,** 1704-17.

WALL, P. A. M., R. 2006. *Textbook of Pain*, Churchill Livingstone.

WALL, P. D. 1967. The laminar organization of dorsal horn and effects of descending impulses. *J Physiol,* 188**,** 403-23.

WANG, H. B., EHNERT, C., BRENNER, G. J. & WOOLF, C. J. 2006a. Bradykinin and peripheral sensitization. *Biological Chemistry,* 387**,** 11-14.

WANG, P. H. M., CENEDEZE, M. A., PESQUERO, J. B., PACHECO-SILVA, A. & CAMARA, N. O. S. 2006b. Influence of bradykinin B1 and B2 receptors in the immune response triggered by renal ischemia-reperfusion injury. *International Immunopharmacology,* 6**,** 1960-1965.

WARWICK, R. A. & HANANI, M. 2013. The contribution of satellite glial cells to chemotherapy-induced neuropathic pain. *European Journal of Pain,* 17**,** 571-580.

WHYTE, L. S., RYBERG, E., SIMS, N. A., RIDGE, S. A., MACKIE, K., GREASLEY, P. J., ROSS, R. A. & ROGERS, M. J. 2009. The putative cannabinoid receptor GPR55 affects osteoclast function in vitro and bone mass in vivo. *Proc Natl Acad Sci U S A,* 106**,** 16511-6.

WIBERG, M., WESTMAN, J. & BLOMQVIST, A. 1987. Somatosensory projection to the mesencephalon: an anatomical study in the monkey. *J Comp Neurol,* 264**,** 92-117.

WIELAND, H. A., MICHAELIS, M., KIRSCHBAUM, B. J. & RUDOLPHI, K. A. 2005. Osteoarthritis - an untreatable disease? *Nat Rev Drug Discov,* 4**,** 331-44.

WOOD, J. N. & EIJKELKAMP, N. 2012. Noxious mechanosensation - molecules and circuits. *Curr Opin Pharmacol,* 12**,** 4-8.

WOOLF, C. J. 2011. Central sensitization: implications for the diagnosis and treatment of pain. *Pain,* 152**,** S2-15.

WU, D. F., CHANDRA, D., MCMAHON, T., WANG, D., DADGAR, J., KHARAZIA, V. N., LIANG, Y. J., WAXMAN, S. G., DIB-HAJJ, S. D. & MESSING, R. O. 2012. PKCepsilon phosphorylation of the sodium channel NaV1.8 increases channel

function and produces mechanical hyperalgesia in mice. *J Clin Invest,* 122**,** 1306-15.

WU, Q. & HENRY, J. L. 2010. Changes in Abeta non-nociceptive primary sensory neurons in a rat model of osteoarthritis pain. *Mol Pain,* 6**,** 37.

WYLDE, V., HEWLETT, S., LEARMONTH, I. D. & DIEPPE, P. 2011. Persistent pain after joint replacement: prevalence, sensory qualities, and postoperative determinants. *Pain,* 152**,** 566-72.

XU, H. X., RAMSEY, I. S., KOTECHA, S. A., MORAN, M. M., CHONG, J. H. A., LAWSON, D., GE, P., LILLY, J., SILOS-SANTIAGO, I., XIE, Y., DISTEFANO, P. S., CURTIS, R. & CLAPHAM, D. E. 2002. TRPV3 is a calcium-permeable temperature-sensitive cation channel. *Nature,* 418**,** 181-186.

YIN, H., CHU, A., LI, W., WANG, B., SHELTON, F., OTERO, F., NGUYEN, D.G., CALDWELL, J.S. AND CHEN, Y.A.. 2009. Lipid G protein-coupled Receptor ligand identification using β-arrestin PathHunterTM assay. *J. Biol. Chem,* 284**,** 12328-12338.

YU, J., DELIU, E., ZHANG, X. Q., HOFFMAN, N. E., CARTER, R. L., GRISANTI, L. A., BRAILOIU, G. C., MADESH, M., CHEUNG, J. Y., FORCE, T., ABOOD, M. E., KOCH, W. J., TILLEY, D. G. & BRAILOIU, E. 2013. Differential activation of cultured neonatal cardiomyocytes by plasmalemmal versus intracellular G protein-coupled receptor 55. *J Biol Chem,* 288**,** 22481-92.

YU, L., YANG, F., LUO, H., LIU, F. Y., HAN, J. S., XING, G. G. & WAN, Y. 2008. The role of TRPV1 in different subtypes of dorsal root ganglion neurons in rat chronic inflammatory nociception induced by complete Freund's adjuvant. *Mol Pain,* 4**,** 61.

YU, X. H., ZHANG, E. T., CRAIG, A. D., SHIGEMOTO, R., RIBEIRO-DA-SILVA, A. & DE KONINCK, Y. 1999. NK-1 receptor immunoreactivity in distinct morphological types of lamina I neurons of the primate spinal cord. *J Neurosci,* 19**,** 3545-55.

YUDIN, Y. & ROHACS, T. 2012. Regulation of TRPM8 channel activity. *Molecular and Cellular Endocrinology,* 353**,** 68-74.

ZACHAROVA, G. & PALECEK, J. 2009. Parvalbumin and TRPV1 receptor expression in dorsal root ganglion neurons after acute peripheral inflammation. *Physiol Res,* 58**,** 305-9.